

## **Abstract**

WENDISCH, BERTRAM PETER. Development of Disc Shaped Fiberwebs with Circumferential Fiber Orientation. (Under the Direction of Dr. Helmut H. Hergeth and Dr. Abdel-Fattah M. Seyam.)

Current fiberweb forming systems such as carding, air-lay, wet-lay, and carding and cross-lapping do not provide positive control over the fiber orientation. In these systems, several trials with different process parameters are conducted until fiber orientation with close values to the desired level is achieved.

The main purpose of this research is to develop a new device for the formation of disc shaped fiberwebs with desired fiber orientation using an electrostatic field. To achieve the goal of the research, a new device was designed and built. The device consists of fiber dispensing system, turning disc with speed controller (which was used as a fiber collection surface), high voltage supply for creation of an electrostatic field, fiber lay-down mechanism, and two electrodes. Full description of the device and its components are provided. Additionally, a set of experimental trials with full factorial statistical design was conducted to study the influence of electrostatic potential, distance between the two electrodes, fiber collecting disc rotational speed, and the diameter of fiber lay-down rod and their interactions on the percent number of fiber in the circumferential direction, which was chosen to demonstrate the control of fiber orientation as a target direction. Image analysis was used to measure the fiber orientation distribution. The orientation distribution data was measured in number of fibers as well as percentage for individual ranges of ten degree intervals over 90°.

Experimentation with the new device showed that the fiber alignment in circumferential direction (other directions are possible) is achievable with the correct levels of the independent parameters (field potential, distance between the two electrodes, disc rotational speed, and the rod diameter). Moreover, statistical analysis of the data revealed that there is significant influence of the main effects

and their first order interactions (distance \* disc speed and potential \* disc speed) on circumferential fiber orientation.

While the device is believed to be capable of handling any type of fibers, trials with carbon fibers were not successful due to matting and cling of these fibers. Additional refinements are required to allow handling of fine fibers and form fiberwebs with high thickness a matter that make the device more acceptable commercially. Proposed solutions to such problems are provided.

Possible applications of disc shaped fiberwebs with controlled fiber orientation are seen in the industrial fields of carbon fiber reinforced brake discs for planes and passenger cars as well as grinding, cutting and sanding pads. An introductory market review for the use of the developed technology as carbon fiber brake discs was undertaken in order to evaluate the economic value of the presented innovation. From the market review study, it can be concluded that the innovation may be successfully marketable if technical problems can be solved, which is the primarily task for future research. While the technology promises great value for the textile industry, additional financial and cost effectiveness concepts need to be provided in order to evaluate the competitiveness of the technology compared to existing products.

# **DEVELOPMENT OF DISC SHAPED FIBERWEBS WITH CIRCUMFERENTIAL FIBER ORIENTATION**

by  
**BERTRAM WENDISCH**

A thesis submitted to the Graduate Faculty of  
North Carolina State University  
in partial fulfillment of the  
requirements of the degree of  
Master of Science

**TEXTILES**

Raleigh

2006

**APPROVED BY:**

---

---

Co-Chair of Advisory Committee

---

Co-Chair of Advisory Committee

## **Biography**

Bertram Wendisch was born in Dresden, Germany on April 14, 1981. He received his Diploma in Textile Technology from the Department of Textile and Apparel Technology of the Niederrhein University of Applied Sciences in Germany in 2004. Directly after graduation from Niederrhein University he joined the College of Textiles at North Carolina State University to pursue his M.S. program in Textile Management and Technology.

## Acknowledgments

I would like to extend my sincere thanks to the German Academic Exchange Service (DAAD) for their financial support during my studies at North Carolina State University. Additional thanks are due to the National Textile Center for providing additional research fund for building the device and my financial support.

Many thanks are due to Dr. A.M. Seyam for initiating the equipment concepts, his contribution in the design of equipments, planning of experiments at the University of Massachusetts Dartmouth and North Carolina State University, and his guidance regarding thesis writing.

Many thanks to Dr. H.H. Hergeth for his contribution and advice on the market analysis of carbon fiber brake discs as well as his advising throughout my studies at North Carolina State University.

I would like to thank Dr. P. Banks-Lee for her support and encouragement throughout my study program.

Thanks to Dr. Yong Kim of the University of Massachusetts Dartmouth, College of Engineering for providing access to the flocking laboratory at the Department of Textile Science and for his contribution in device modification and planning of experiments.

Sincere thanks to Mr. Hai Bui of the machine shop at the College of Textile and Mr. Larry DuFour of the Precision Machine Shop at North Carolina State University for their help in building the equipment.

# Table of Content

<b>List of Figures</b>	<b>vii</b>
<b>List of Tables</b>	<b>xvii</b>
<b>List of Equations</b>	<b>xxi</b>
<b>1. Introduction</b>	<b>1</b>
<b>2. Literature Review</b>	<b>6</b>
2.1. Application of Electrostatic in Textiles	6
2.2. Electrostatic Principle	7
2.3. Development of Nonwovens with Controlled Fiber Orientation	12
2.4. Carbon Fiber Brake Disc	14
2.4.1. Conventional Brake Systems	14
2.4.2. Why Carbon Fiber Brake Disc?	16
2.4.3. Fiber Based Composites: Basic Concept and Advantages	17
2.4.4. Carbon Fiber Composite Brakes	19
2.5. Summary	23
<b>3. Research Objectives</b>	<b>24</b>
<b>4. Equipment Development</b>	<b>27</b>
4.1. Electrostatic Field Electrodes	28
4.2. Fiber Dispensing System	30

<b>4.3.</b>	<b>Fiber Collecting System</b>	<b>32</b>
<b>4.4.</b>	<b>Fiber Lay-Down Mechanism</b>	<b>36</b>
<b>4.5</b>	<b>Problems and Solutions</b>	<b>38</b>
4.5.1	Fiber Dispenser	38
4.5.2	Motor Protection	42
4.5.3	Electrostatic Field Formation and Uniformity	43
4.5.4.	Fiber Lay-Down	45
<b>5.</b>	<b><i>Experimental Work</i></b>	<b>47</b>
<b>5.1</b>	<b>Experimental Design</b>	<b>47</b>
<b>5.2</b>	<b>Sample Collection Method</b>	<b>52</b>
<b>5.3</b>	<b>Fiberwebs with Circumferential and z-Directional Fiber Orientation</b>	<b>54</b>
<b>5.4</b>	<b>Problems</b>	<b>55</b>
5.4.1	Carbon Fiber Separation	56
5.4.2	Web Thickness	56
5.4.3	Environmental Conditions	58
<b>5.5</b>	<b>Measurement of Fiber Orientation</b>	<b>59</b>
<b>5.6</b>	<b>Statistical Analysis</b>	<b>63</b>
<b>6.</b>	<b><i>Results and Discussion</i></b>	<b>64</b>
<b>6.1</b>	<b>Distance between the two electrodes</b>	<b>66</b>
<b>6.2</b>	<b>Electrostatic Potential</b>	<b>73</b>

6.3	Disc Rotational Speed _____	80
6.4	Rod Diameter _____	86
6.5	Interaction between Parameters _____	92
6.6	Summary _____	94
<b>7.</b>	<b><i>Carbon Fiber Brake Disc – A Introductory Market Study</i></b> _____	<b>97</b>
7.1	Why Market Study on Carbon Fiber Brake Discs? _____	98
7.2	Competitive Analysis _____	99
7.3	Market Potential _____	101
7.3.1	Market Estimation _____	105
7.3.2	Target Costing _____	107
<b>8.</b>	<b><i>Conclusion</i></b> _____	<b>109</b>
8.1	Technical Feasibility _____	109
8.2	Market _____	110
<b>9.</b>	<b><i>Future Work</i></b> _____	<b>111</b>
<b>10.</b>	<b><i>Bibliography</i></b> _____	<b>112</b>
	<b><i>Appendix I: Fiber Distribution Data Tables</i></b> _____	<b>117</b>
	<b><i>Appendix II: Fiber Distribution Histograms</i></b> _____	<b>145</b>
	<b><i>Appendix III: First Order Interaction Graphs</i></b> _____	<b>253</b>

## List of Figures

Figure 1: Like charges repel (left) and unlike charges attract (right) [6]	7
Figure 2: Two flat and parallel electrodes separated by a distance $d$ [6]	9
Figure 3: Flocking setup – 1 fibrous substrate; 2 bonding agent; 3 flocks; 4 dosage device; 5 electrodes; 6 opposite electrodes grounded; 7 electrostatic suction; 8 pneumatic suction [23]	10
Figure 4: Vacuum Conveyor Belt Table System [34]	13
Figure 5: Different Design of brake discs [18]	15
Figure 6: Basic mechanics of composite action [29]	17
Figure 7: Fiber diameter versus fiber tensile strength [2]	18
Figure 8: Ribbon-wrapped brake disc [42]	19
Figure 9: Thickness differences of the carbon ribbon layer (15) due to the wrapping process and a corresponding perform cross-sectional shape (11) to overcome these difficulties [42]	20
Figure 10: Needle punching process of fibrous performs to achieve z-directional fiber orientation to improve de-lamination properties [35]	20
Figure 11: Some fibers will be oriented in z-direction (66) due to the penetrating barbed needles (14), resulting in improved de-lamination properties of the resulting composite material [35]	21
Figure 12: Curved braid apparatus for forming helical flat ribbon structures [28]	22
Figure 13: Schematic drawing of the lay-down process of the fibers	25
Figure 14: Equipment to form disc shaped fiberwebs with circumferential fiber orientation	27
Figure 15: Non-uniform and uniform field line formation (red) depending on dimension and position of the electrostatic field electrodes (grey)	28
Figure 16: Fiber dispenser (side view)	30
Figure 17: Fiber dispenser (bottom view)	31
Figure 18: Fiber collecting disc	32
Figure 19: Engineering drawing of the fiber collecting device including fiber lay-down mechanism (top view) (dimensions in millimeter)	33
Figure 20: Speed of the disc, corresponding to the scale shown on the motor controller	34
Figure 21: Belt transmission and carbon brushes	34

Figure 22: Dimensions of the fiber collecting disc	35
Figure 23: Collected fibers on the plate	36
Figure 24: Tube and height adjustment of the tube	36
Figure 25: Engineering drawing of the fiber lay-down tube and height adjustment mechanism (side view) (dimensions in millimeter)	37
Figure 26: Tube can be swung for better access to the disc and fiberweb after web formation is completed (e.g. remove web)	38
Figure 27: "Hand- Shaker" from MAAG Flockmaschinen as a fiber dispenser	39
Figure 28: New fiber dispenser with electrode and stand	40
Figure 29: Conical brush and box design (dimensions in millimeter)	41
Figure 30: The motor is mounted very close to the electrode	42
Figure 31: Modified setup of the motor and fiber dispenser	43
Figure 32: Fiber agglomeration due to local irregularities of the electrostatic field	44
Figure 33: Some metal parts were replaced by plastic materials	44
Figure 34: Original design of the lay-down tube with a diameter of 20mm	45
Figure 35: Schematic showing the effect of lay-down rod diameter on the fiber lay-down characteristics	45
Figure 36: Modified design of the lay-down tube, which can carry all rod sizes up to $\varnothing 10\text{mm}$	46
Figure 37: Sample placement on collecting disc	52
Figure 38: Sample placement (grey) on the collecting disc (dimensions in millimeter)	53
Figure 39: Picture showing the z-directional ("standing") fibers	55
Figure 40: Carbon fibers cannot be treated with the current technology available	56
Figure 41 (a): The rod (patterned) does not touch the adhesive layer (grey), therefore the fiber (red) will not be re-oriented, resulting in an unsuccessful lay-down process (b). (c): If the rod is in touch with the adhesive layer, the chance of successful fiber re-orientation is higher (d).	57
Figure 42: Baush & Lomb Monozoom-7 light microscope with monitor and video printer	59
Figure 43: Magnified image of a collected sample	60
Figure 44: Schematic of the sample and the locations the magnified photographs were taken for fiber counting	61

Figure 45: Fiber angle measurement _____	61
Figure 46: Percent number of fibers at 5° corresponding to the electrostatic field distance _____	66
Figure 47: Fiber distribution histogram depending on the electrostatic field distance at 50rpm disc speed / 10kV electrostatic potential / 20mm lay-down rod _____	69
Figure 48: Fiber distribution histogram depending on the electrostatic field distance at 13rpm disc speed / 10kV electrostatic potential / 20mm lay-down rod _____	70
Figure 49: Fiber distribution histogram depending on the electrostatic field distance at 50rpm disc speed / 50kV electrostatic potential / 20mm lay-down rod _____	71
Figure 50: Fiber distribution histogram depending on the electrostatic field distance at 13rpm disc speed / 50kV electrostatic potential / 20mm lay-down rod _____	72
Figure 51: Percent number of fibers at 5° corresponding to the electric potential _____	73
Figure 52: Fibers need to hit the collecting disc perpendicularly in order to get circumferentially oriented after lay-down _____	75
Figure 53: Fiber distribution histogram depending on the potential applied at 50rpm disc speed / 30cm electrode distance / 20mm lay-down rod _____	76
Figure 54: Fiber distribution histogram depending on the potential applied at 50rpm disc speed / 20cm electrode distance / 20mm lay-down rod _____	77
Figure 55: Fiber distribution histogram depending on the potential applied at 50rpm disc speed / 10cm electrode distance / 20mm lay-down rod _____	78
Figure 56: Fiber distribution histogram depending on the potential applied at 13rpm disc speed / 30cm electrode distance / 20mm lay-down rod _____	79
Figure 57: Percent number of fibers at 5° corresponding to the disc rotational speed _____	80
Figure 58: Fiber distribution histogram depending on the fiber collecting disc speed at 30cm electrode distance / 10kV electrostatic potential / 20mm lay-down rod _____	82
Figure 59: Fiber distribution histogram depending on the fiber collecting disc speed at 30cm electrode distance / 50kV electrostatic potential / 20mm lay-down rod _____	83
Figure 60: Fiber distribution histogram depending on the fiber collecting disc speed at 10cm electrode distance / 10kV electrostatic potential / 20mm lay-down rod _____	84
Figure 61: Fiber distribution histogram depending on the fiber collecting disc speed at 10cm electrode distance / 50kV electrostatic potential / 20mm lay-down rod _____	85
Figure 62: Percent number of fibers at 5° corresponding to the rod diameter _____	86
Figure 63: Fiber distribution histogram depending on the fiber lay-down rod diameter at 30cm electrode distance / 10kV electrostatic potential / 50rpm disc speed _____	88

Figure 64: Fiber distribution histogram depending on the fiber lay-down rod diameter at 10cm electrode distance / 10kV electrostatic potential / 50rpm disc speed \_\_\_\_\_ 89

Figure 65: Fiber distribution histogram depending on the fiber lay-down rod diameter at 30cm electrode distance / 50kV electrostatic potential / 50rpm disc speed \_\_\_\_\_ 90

Figure 66: Fiber distribution histogram depending on the fiber lay-down rod diameter at 10cm electrode distance / 50kV electrostatic potential / 50rpm disc speed \_\_\_\_\_ 91

Figure 67: Percent number of fibers at 5° corresponding to the interaction of disc rotational speed and distance \_\_\_\_\_ 93

Figure 68: Percent number of fibers at 5° corresponding to the interaction of distance and potential \_\_\_\_\_ 94

Figure 69: Stage-Gate-Model according to Robert Cooper [8] \_\_\_\_\_ 97

Figure 70: Distribution depending on disc AAspeed at 10cm electrode distance / 10kV electrostatic potential / 20mm lay-down rod \_\_\_\_\_ 145

Figure 71: Distribution depending on disc speed at 10cm electrode distance / 20kV electrostatic potential / 20mm lay-down rod \_\_\_\_\_ 146

Figure 72: Distribution depending on disc speed at 10cm electrode distance / 50kV electrostatic potential / 20mm lay-down rod \_\_\_\_\_ 147

Figure 73: Distribution depending on disc speed at 20cm electrode distance / 10kV electrostatic potential / 20mm lay-down rod \_\_\_\_\_ 148

Figure 74: Distribution depending on disc speed at 20cm electrode distance / 20kV electrostatic potential / 20mm lay-down rod \_\_\_\_\_ 149

Figure 75: Distribution depending on disc speed at 20cm electrode distance / 50kV electrostatic potential / 20mm lay-down rod \_\_\_\_\_ 150

Figure 76: Distribution depending on disc speed at 30cm electrode distance / 10kV electrostatic potential / 20mm lay-down rod \_\_\_\_\_ 151

Figure 77: Distribution depending on disc speed at 30cm electrode distance / 20kV electrostatic potential / 20mm lay-down rod \_\_\_\_\_ 152

Figure 78: Distribution depending on disc speed at 30cm electrode distance / 50kV electrostatic potential / 20mm lay-down rod \_\_\_\_\_ 153

Figure 79: Distribution depending on disc speed at 10cm electrode distance / 10kV electrostatic potential / 9.4mm lay-down rod \_\_\_\_\_ 154

Figure 80: Distribution depending on disc speed at 10cm electrode distance / 20kV electrostatic potential / 9.4mm lay-down rod \_\_\_\_\_ 155

Figure 81: Distribution depending on disc speed at 10cm electrode distance / 50kV electrostatic potential / 9.4mm lay-down rod \_\_\_\_\_ 156

Figure 82: Distribution depending on disc speed at 20cm electrode distance / 10kV electrostatic potential / 9.4mm lay-down rod \_\_\_\_\_ 157

Figure 83: Distribution depending on disc speed at 20cm electrode distance / 20kV electrostatic potential / 9.4mm lay-down rod \_\_\_\_\_ 158

Figure 84: Distribution depending on disc speed at 20cm electrode distance / 50kV electrostatic potential / 9.4mm lay-down rod \_\_\_\_\_ 159

Figure 85: Distribution depending on disc speed at 30cm electrode distance / 10kV electrostatic potential / 9.4mm lay-down rod \_\_\_\_\_ 160

Figure 86: Distribution depending on disc speed at 30cm electrode distance / 20kV electrostatic potential / 9.4mm lay-down rod \_\_\_\_\_ 161

Figure 87: Distribution depending on disc speed at 30cm electrode distance / 50kV electrostatic potential / 9.4mm lay-down rod \_\_\_\_\_ 162

Figure 88: Distribution depending on disc speed at 10cm electrode distance / 10kV electrostatic potential / 4.76mm lay-down rod \_\_\_\_\_ 163

Figure 89: Distribution depending on disc speed at 10cm electrode distance / 20kV electrostatic potential / 4.76mm lay-down rod \_\_\_\_\_ 164

Figure 90: Distribution depending on disc speed at 10cm electrode distance / 50kV electrostatic potential / 4.76mm lay-down rod \_\_\_\_\_ 165

Figure 91: Distribution depending on disc speed at 20cm electrode distance / 10kV electrostatic potential / 4.76mm lay-down rod \_\_\_\_\_ 166

Figure 92: Distribution depending on disc speed at 20cm electrode distance / 20kV electrostatic potential / 4.76mm lay-down rod \_\_\_\_\_ 167

Figure 93: Distribution depending on disc speed at 20cm electrode distance / 50kV electrostatic potential / 4.76mm lay-down rod \_\_\_\_\_ 168

Figure 94: Distribution depending on disc speed at 30cm electrode distance / 10kV electrostatic potential / 4.76mm lay-down rod \_\_\_\_\_ 169

Figure 95: Distribution depending on disc speed at 30cm electrode distance / 20kV electrostatic potential / 4.76mm lay-down rod \_\_\_\_\_ 170

Figure 96: Distribution depending on disc speed at 30cm electrode distance / 50kV electrostatic potential / 4.76mm lay-down rod \_\_\_\_\_ 171

Figure 97: Distribution depending on distance at 13rpm disc speed / 10kV electrostatic potential / 20mm lay-down rod \_\_\_\_\_ 172

Figure 98: Distribution depending on distance at 23.5rpm disc speed / 10kV electrostatic potential / 20mm lay-down rod \_\_\_\_\_ 173

Figure 99: Distribution depending on distance at 50rpm disc speed / 10kV electrostatic potential / 20mm lay-down rod	174
Figure 100: Distribution depending on distance at 13rpm disc speed / 20kV electrostatic potential / 20mm lay-down rod	175
Figure 101: Distribution depending on distance at 23.5rpm disc speed / 20kV electrostatic potential / 20mm lay-down rod	176
Figure 102: Distribution depending on distance at 50rpm disc speed / 20kV electrostatic potential / 20mm lay-down rod	177
Figure 103: Distribution depending on distance at 13rpm disc speed / 50kV electrostatic potential / 20mm lay-down rod	178
Figure 104: Distribution depending on distance at 23.5rpm disc speed / 50kV electrostatic potential / 20mm lay-down rod	179
Figure 105: Distribution depending on distance at 50rpm disc speed / 50kV electrostatic potential / 20mm lay-down rod	180
Figure 106: Distribution depending on distance at 13rpm disc speed / 10kV electrostatic potential / 9.4mm lay-down rod	181
Figure 107: Distribution depending on distance at 23.5rpm disc speed / 10kV electrostatic potential / 9.4mm lay-down rod	182
Figure 108: Distribution depending on distance at 50rpm disc speed / 10kV electrostatic potential / 9.4mm lay-down rod	183
Figure 109: Distribution depending on distance at 13rpm disc speed / 20kV electrostatic potential / 9.4mm lay-down rod	184
Figure 110: Distribution depending on distance at 23.5rpm disc speed / 20kV electrostatic potential / 9.4mm lay-down rod	185
Figure 111: Distribution depending on distance at 50rpm disc speed / 20kV electrostatic potential / 9.4mm lay-down rod	186
Figure 112: Distribution depending on distance at 13rpm disc speed / 50kV electrostatic potential / 9.4mm lay-down rod	187
Figure 113: Distribution depending on distance at 23.5rpm disc speed / 50kV electrostatic potential / 9.4mm lay-down rod	188
Figure 114: Distribution depending on distance at 50rpm disc speed / 50kV electrostatic potential / 9.4mm lay-down rod	189
Figure 115: Distribution depending on distance at 13rpm disc speed / 10kV electrostatic potential / 4.76mm lay-down rod	190

Figure 116: Distribution depending on distance at 23.5rpm disc speed / 10kV electrostatic potential / 4.76mm lay-down rod	191
Figure 117: Distribution depending on distance at 50rpm disc speed / 10kV electrostatic potential / 4.76mm lay-down rod	192
Figure 118: Distribution depending on distance at 13rpm disc speed / 20kV electrostatic potential / 4.76mm lay-down rod	193
Figure 119: Distribution depending on distance at 23.5rpm disc speed / 20kV electrostatic potential / 4.76mm lay-down rod	194
Figure 120: Distribution depending on distance at 50rpm disc speed / 20kV electrostatic potential / 4.76mm lay-down rod	195
Figure 121: Distribution depending on distance at 13rpm disc speed / 50kV electrostatic potential / 4.76mm lay-down rod	196
Figure 122: Distribution depending on distance at 23.5rpm disc speed / 50kV electrostatic potential / 4.76mm lay-down rod	197
Figure 123: Distribution depending on distance at 50rpm disc speed / 50kV electrostatic potential / 4.76mm lay-down rod	198
Figure 124: Distribution depending on potential at 13rpm disc speed / 10cm electrode distance / 20mm lay-down rod	199
Figure 125: Distribution depending on potential at 23.5rpm disc speed / 10cm electrode distance / 20mm lay-down rod	200
Figure 126: Distribution depending on potential at 50rpm disc speed / 10cm electrode distance / 20mm lay-down rod	201
Figure 127: Distribution depending on potential at 13rpm disc speed / 20cm electrode distance / 20mm lay-down rod	202
Figure 128: Distribution depending on potential at 23.5rpm disc speed / 20cm electrode distance / 20mm lay-down rod	203
Figure 129: Distribution depending on potential at 50rpm disc speed / 20cm electrode distance / 20mm lay-down rod	204
Figure 130: Distribution depending on potential at 13rpm disc speed / 30cm electrode distance / 20mm lay-down rod	205
Figure 131: Distribution depending on potential at 23.5rpm disc speed / 30cm electrode distance / 20mm lay-down rod	206
Figure 132: Distribution depending on potential at 50rpm disc speed / 30cm electrode distance / 20mm lay-down rod	207

Figure 133: Distribution depending on potential at 13rpm disc speed / 10cm electrode distance / 9.4mm lay-down rod \_\_\_\_\_ 208

Figure 134: Distribution depending on potential at 23.5rpm disc speed / 10cm electrode distance / 9.4mm lay-down rod \_\_\_\_\_ 209

Figure 135: Distribution depending on potential at 50rpm disc speed / 10cm electrode distance / 9.4mm lay-down rod \_\_\_\_\_ 210

Figure 136: Distribution depending on potential at 13rpm disc speed / 20cm electrode distance / 9.4mm lay-down rod \_\_\_\_\_ 211

Figure 137: Distribution depending on potential at 23.5rpm disc speed / 20cm electrode distance / 9.4mm lay-down rod \_\_\_\_\_ 212

Figure 138: Distribution depending on potential at 50rpm disc speed / 20cm electrode distance / 9.4mm lay-down rod \_\_\_\_\_ 213

Figure 139: Distribution depending on potential at 13rpm disc speed / 30cm electrode distance / 9.4mm lay-down rod \_\_\_\_\_ 214

Figure 140: Distribution depending on potential at 23.5rpm disc speed / 30cm electrode distance / 9.4mm lay-down rod \_\_\_\_\_ 215

Figure 141: Distribution depending on potential at 50rpm disc speed / 30cm electrode distance / 9.4mm lay-down rod \_\_\_\_\_ 216

Figure 142: Distribution depending on potential at 13rpm disc speed / 10cm electrode distance / 4.76mm lay-down rod \_\_\_\_\_ 217

Figure 143: Distribution depending on potential at 23.5rpm disc speed / 10cm electrode distance / 4.76mm lay-down rod \_\_\_\_\_ 218

Figure 144: Distribution depending on potential at 50rpm disc speed / 10cm electrode distance / 4.76mm lay-down rod \_\_\_\_\_ 219

Figure 145: Distribution depending on potential at 13rpm disc speed / 20cm electrode distance / 4.76mm lay-down rod \_\_\_\_\_ 220

Figure 146: Distribution depending on potential at 23.5rpm disc speed / 20cm electrode distance / 4.76mm lay-down rod \_\_\_\_\_ 221

Figure 147: Distribution depending on potential at 50rpm disc speed / 20cm electrode distance / 4.76mm lay-down rod \_\_\_\_\_ 222

Figure 148: Distribution depending on potential at 13rpm disc speed / 30cm electrode distance / 4.76mm lay-down rod \_\_\_\_\_ 223

Figure 149: Distribution depending on potential at 23.5rpm disc speed / 30cm electrode distance / 4.76mm lay-down rod \_\_\_\_\_ 224

- Figure 150: Distribution depending on potential at 50rpm disc speed / 30cm electrode distance / 4.76mm lay-down rod \_\_\_\_\_ 225
- Figure 151: Distribution depending on rod diameter at 10cm electrode distance / 10kV electrostatic potential / 13rpm disc speed \_\_\_\_\_ 226
- Figure 152: Distribution depending on rod diameter at 10cm electrode distance / 10kV electrostatic potential / 23.5rpm disc speed \_\_\_\_\_ 227
- Figure 153: Distribution depending on rod diameter at 10cm electrode distance / 10kV electrostatic potential / 50rpm disc speed \_\_\_\_\_ 228
- Figure 154: Distribution depending on rod diameter at 10cm electrode distance / 20kV electrostatic potential / 13rpm disc speed \_\_\_\_\_ 229
- Figure 155: Distribution depending on rod diameter at 10cm electrode distance / 20kV electrostatic potential / 23.5rpm disc speed \_\_\_\_\_ 230
- Figure 156: Distribution depending on rod diameter at 10cm electrode distance / 20kV electrostatic potential / 50rpm disc speed \_\_\_\_\_ 231
- Figure 157: Distribution depending on rod diameter at 10cm electrode distance / 50kV electrostatic potential / 13rpm disc speed \_\_\_\_\_ 232
- Figure 158: Distribution depending on rod diameter at 10cm electrode distance / 50kV electrostatic potential / 23.5rpm disc speed \_\_\_\_\_ 233
- Figure 159: Distribution depending on rod diameter at 10cm electrode distance / 50kV electrostatic potential / 50rpm disc speed \_\_\_\_\_ 234
- Figure 160: Distribution depending on rod diameter at 20cm electrode distance / 10kV electrostatic potential / 13rpm disc speed \_\_\_\_\_ 235
- Figure 161: Distribution depending on rod diameter at 20cm electrode distance / 10kV electrostatic potential / 23.5rpm disc speed \_\_\_\_\_ 236
- Figure 162: Distribution depending on rod diameter at 20cm electrode distance / 10kV electrostatic potential / 50rpm disc speed \_\_\_\_\_ 237
- Figure 163: Distribution depending on rod diameter at 20cm electrode distance / 20kV electrostatic potential / 13rpm disc speed \_\_\_\_\_ 238
- Figure 164: Distribution depending on rod diameter at 20cm electrode distance / 20kV electrostatic potential / 23.5rpm disc speed \_\_\_\_\_ 239
- Figure 165: Distribution depending on rod diameter at 20cm electrode distance / 20kV electrostatic potential / 50rpm disc speed \_\_\_\_\_ 240
- Figure 166: Distribution depending on rod diameter at 20cm electrode distance / 50kV electrostatic potential / 13rpm disc speed \_\_\_\_\_ 241

Figure 167: Distribution depending on rod diameter at 20cm electrode distance / 50kV electrostatic potential / 23.5rpm disc speed \_\_\_\_\_ 242

Figure 168: Distribution depending on rod diameter at 20cm electrode distance / 50kV electrostatic potential / 50rpm disc speed \_\_\_\_\_ 243

Figure 169: Distribution depending on rod diameter at 30cm electrode distance / 10kV electrostatic potential / 13rpm disc speed \_\_\_\_\_ 244

Figure 170: Distribution depending on rod diameter at 30cm electrode distance / 10kV electrostatic potential / 23.5rpm disc speed \_\_\_\_\_ 245

Figure 171: Distribution depending on rod diameter at 30cm electrode distance / 10kV electrostatic potential / 50rpm disc speed \_\_\_\_\_ 246

Figure 172: Distribution depending on rod diameter at 30cm electrode distance / 20kV electrostatic potential / 13rpm disc speed \_\_\_\_\_ 247

Figure 173: Distribution depending on rod diameter at 30cm electrode distance / 20kV electrostatic potential / 23.5rpm disc speed \_\_\_\_\_ 248

Figure 174: Distribution depending on rod diameter at 30cm electrode distance / 20kV electrostatic potential / 50rpm disc speed \_\_\_\_\_ 249

Figure 175: Distribution depending on rod diameter at 30cm electrode distance / 50kV electrostatic potential / 13rpm disc speed \_\_\_\_\_ 250

Figure 176: Distribution depending on rod diameter at 30cm electrode distance / 50kV electrostatic potential / 23.5rpm disc speed \_\_\_\_\_ 251

Figure 177: Distribution depending on rod diameter at 30cm electrode distance / 50kV electrostatic potential / 50rpm disc speed \_\_\_\_\_ 252

Figure 178: Percent number of fibers at 5° corresponding to the interaction of distance and potential \_\_\_\_\_ 253

Figure 179: Percent number of fibers at 5° corresponding to the interaction of distance and rod diameter \_\_\_\_\_ 254

Figure 180: Percent number of fibers at 5° corresponding to the interaction of potential and rod diameter \_\_\_\_\_ 255

Figure 181: Percent number of fibers at 5° corresponding to the interaction of disc rotational speed and rod diameter \_\_\_\_\_ 256

## List of Tables

<i>Table 1: Conductivity (<math>\chi</math>) of three different Polyamid samples treated with different finishes and conditioned at different levels of relative humidity [23]</i>	11
<i>Table 2: Design of Experiments for <math>\varnothing</math> 20mm lay-down rod</i>	49
<i>Table 3: Design of Experiments for <math>\varnothing</math> 9.4mm lay-down rod</i>	50
<i>Table 4: Design of Experiments for <math>\varnothing</math> 4.76mm lay-down rod</i>	51
<i>Table 5: Design of Experiments for samples with circumferential and z-directional fiber orientation</i>	54
<i>Table 6: Example of fiber orientation distribution data</i>	62
<i>Table 7: General Linear Model (GLM) procedure of the factorial ANOVA</i>	65
<i>Table 8: Sample numbers and their corresponding parameters sorted from the highest to lowest "percent number of fibers at 5°"</i>	95
<i>Table 9: Selection of different brake disc prizes</i>	100
<i>Table 10: Overview on the development of the number of passenger cars and the associated costs from 1985 to 2004 [40] (Fixed costs include: insurance, license, registration, taxes, depreciation, and finance charges; passenger cars do not include other 2-axle 4-tire vehicles like Pick-Ups, SUVs and Minivans) combined with population and income data [38, 39]</i>	102
<i>Table 11: Personal Consumption Expenditures on Transportation by Subcategory in current \$ millions (Repair and Rental includes greasing, washing, parking, storage, and leasing) [40]</i>	103
<i>Table 12: Passenger car sales and U.S. as well as world motor vehicle production (Note: passenger cars do not include Pick-Ups, SUVs and Minivans) [40]</i>	105
<i>Table 13: Annual sales and market shares of light trucks and automobiles in 2003 [40]</i>	106
<i>Table 14: Cost estimate</i>	107
<i>Table 15: Fiber distribution data table for sample number 1</i>	117
<i>Table 16: Fiber distribution data table for sample number 3</i>	117
<i>Table 17: Fiber distribution data table for sample number 5</i>	118
<i>Table 18: Fiber distribution data table for sample number 6</i>	118
<i>Table 19: Fiber distribution data table for sample number 7</i>	118
<i>Table 20: Fiber distribution data table for sample number 8</i>	119
<i>Table 21: Fiber distribution data table for sample number 9</i>	119

<i>Table 22: Fiber distribution data table for sample number 10</i>	119
<i>Table 23: Fiber distribution data table for sample number 11</i>	120
<i>Table 24: Fiber distribution data table for sample number 12</i>	120
<i>Table 25: Fiber distribution data table for sample number 13</i>	120
<i>Table 26: Fiber distribution data table for sample number 14</i>	121
<i>Table 27: Fiber distribution data table for sample number 21</i>	121
<i>Table 28: Fiber distribution data table for sample number 22</i>	121
<i>Table 29: Fiber distribution data table for sample number 23</i>	122
<i>Table 30: Fiber distribution data table for sample number 24</i>	122
<i>Table 31: Fiber distribution data table for sample number 25</i>	122
<i>Table 32: Fiber distribution data table for sample number 26</i>	123
<i>Table 33: Fiber distribution data table for sample number 27</i>	123
<i>Table 34: Fiber distribution data table for sample number 28</i>	123
<i>Table 35: Fiber distribution data table for sample number 29</i>	124
<i>Table 36: Fiber distribution data table for sample number 30</i>	124
<i>Table 37: Fiber distribution data table for sample number 31</i>	124
<i>Table 38: Fiber distribution data table for sample number 32</i>	125
<i>Table 39: Fiber distribution data table for sample number 33</i>	125
<i>Table 40: Fiber distribution data table for sample number 34</i>	125
<i>Table 41: Fiber distribution data table for sample number 35</i>	126
<i>Table 42: Fiber distribution data table for sample number 40</i>	126
<i>Table 43: Fiber distribution data table for sample number 41</i>	126
<i>Table 44: Fiber distribution data table for sample number 42</i>	127
<i>Table 45: Fiber distribution data table for sample number 43</i>	127
<i>Table 46: Fiber distribution data table for sample number 44</i>	127

<i>Table 47: Fiber distribution data table for sample number 45</i>	128
<i>Table 48: Fiber distribution data table for sample number 46</i>	128
<i>Table 49: Fiber distribution data table for sample number 47</i>	128
<i>Table 50: Fiber distribution data table for sample number 48</i>	129
<i>Table 51: Fiber distribution data table for sample number 49</i>	129
<i>Table 52: Fiber distribution data table for sample number 50</i>	129
<i>Table 53: Fiber distribution data table for sample number 51</i>	130
<i>Table 54: Fiber distribution data table for sample number 52</i>	130
<i>Table 55: Fiber distribution data table for sample number 53</i>	130
<i>Table 56: Fiber distribution data table for sample number 54</i>	131
<i>Table 57: Fiber distribution data table for sample number 55</i>	131
<i>Table 58: Fiber distribution data table for sample number 56</i>	131
<i>Table 59: Fiber distribution data table for sample number 57</i>	132
<i>Table 60: Fiber distribution data table for sample number 58</i>	132
<i>Table 61: Fiber distribution data table for sample number 59</i>	132
<i>Table 62: Fiber distribution data table for sample number 60</i>	133
<i>Table 63: Fiber distribution data table for sample number 61</i>	133
<i>Table 64: Fiber distribution data table for sample number 62</i>	133
<i>Table 65: Fiber distribution data table for sample number 63</i>	134
<i>Table 66: Fiber distribution data table for sample number 64</i>	134
<i>Table 67: Fiber distribution data table for sample number 65</i>	134
<i>Table 68: Fiber distribution data table for sample number 66</i>	135
<i>Table 69: Fiber distribution data table for sample number 70</i>	135
<i>Table 70: Fiber distribution data table for sample number 71</i>	135
<i>Table 71: Fiber distribution data table for sample number 72</i>	136

<i>Table 72: Fiber distribution data table for sample number 73</i>	136
<i>Table 73: Fiber distribution data table for sample number 74</i>	136
<i>Table 74: Fiber distribution data table for sample number 75</i>	137
<i>Table 75: Fiber distribution data table for sample number 76</i>	137
<i>Table 76: Fiber distribution data table for sample number 77</i>	137
<i>Table 77: Fiber distribution data table for sample number 78</i>	138
<i>Table 78: Fiber distribution data table for sample number 79</i>	138
<i>Table 79: Fiber distribution data table for sample number 80</i>	138
<i>Table 80: Fiber distribution data table for sample number 81</i>	139
<i>Table 81: Fiber distribution data table for sample number 82</i>	139
<i>Table 82: Fiber distribution data table for sample number 83</i>	139
<i>Table 83: Fiber distribution data table for sample number 84</i>	140
<i>Table 84: Fiber distribution data table for sample number 85</i>	140
<i>Table 85: Fiber distribution data table for sample number 86</i>	140
<i>Table 86: Fiber distribution data table for sample number 87</i>	141
<i>Table 87: Fiber distribution data table for sample number 88</i>	141
<i>Table 88: Fiber distribution data table for sample number 89</i>	141
<i>Table 89: Fiber distribution data table for sample number 90</i>	142
<i>Table 90: Fiber distribution data table for sample number 91</i>	142
<i>Table 91: Fiber distribution data table for sample number 92</i>	142
<i>Table 92: Fiber distribution data table for sample number 93</i>	143
<i>Table 93: Fiber distribution data table for sample number 95</i>	143
<i>Table 94: Fiber distribution data table for sample number 96</i>	143
<i>Table 95: Fiber distribution data table for sample number 97</i>	144

## List of Equations

Equation 1: The force between two charges increases linearly with each of the two charges (~ means proportional to) [6] \_\_\_\_\_ 7

Equation 2: The magnitude of the force falls off quadratically when the two charges are separated (~ means proportional to) [3, 6, 13, 15] \_\_\_\_\_ 7

Equation 3: Coulomb's law [3, 6, 13, 15] \_\_\_\_\_ 8

Equation 4: Permittivity of free space [3, 6, 13, 15] \_\_\_\_\_ 8

Equation 5: Calculating the electric field ( $E$  in  $\text{kV/cm}$ ) for the case of two parallel electrodes with a certain distance ( $d$  in  $\text{cm}$ ) and given electric potential ( $U$  in  $\text{kV}$ ) [6] \_\_\_\_\_ 9

Equation 6: The total charge ( $Q$ ) of the capacitor [6] \_\_\_\_\_ 9

Equation 7: Capacitance of the capacitor [6] \_\_\_\_\_ 9

## 1. Introduction

Traditional fiberweb forming processes such as carding, carding and cross-lapping, wet-lay and air-lay do not provide full positive control over fiber orientation. The final fiber orientation distribution is critical for fabric properties like strength, pore-size and bending behavior to name a few. The fiber orientation distribution using traditional processes can only be controlled by the maintenance of a consistent process up to a certain extent. Due to the lack of active and positive fiber orientation distribution control, it is not possible to accurately design fabric properties.

Carding process provides fiber orientation mostly in machine direction (MD). Fibers are not fully straight and possess leading and tailing hooks. Generally nonwovens from carded fiberwebs suffer from lack of strength in the cross machine direction (CD). Machine manufacturers introduce attachments to get carded fiberwebs with some orientation in CD to improve CD strength of nonwovens from carded fiberwebs. The overall control over fiber orientation is not, however, good enough to precisely engineer nonwoven fabrics from such webs. In most cases fabric weight has to be increased to achieve certain properties [4, 30].

To improve MD/CD strength, carded and cross-lapped webs were developed. Combining carded webs with carded and cross-lapped webs provided better balance between MD and CD strength. Several carding machines and cross-lappers are required to achieve such orientation. In spite of these improvements, the fiber orientation is still not fully controlled with one main orientation (in case of carded webs) or two main orientations (in case of combining carded webs with carded and cross-lapped webs) [30]. Air-lay and wet-lay processes produce fiberwebs with random orientation. While such orientation is required in certain applications, other applications require specific fiber orientation [1, 36].

Three dimensional (3-D) weaving processes are capable of producing shaped products with three main orientations in x-, y-, and z-directions. This process

provides positive control over the three main orientations. Other fiber orientation in the x-y plane and parallel planes is possible and can be combined with the three main directions. The advantage of 3-D weaving structure is the prevention of the de-lamination due to integrating the structure layers with the z-direction fibers/yarns. The process is, however, very slow and the hardware is complex and expensive.

If a nonwoven process could be developed to provide fiberwebs with fully controlled fiber orientation in different desired directions, the disadvantages of existing nonwoven fiberweb forming systems and 3-D weaving process could be eliminated.

Motivated by the need of fiberwebs with controlled fiber orientation, a team from North Carolina State University and the University of Massachusetts Dartmouth developed a new process in which fiber orientation is controlled by electrostatic forces. Initial data, which was recently published, proved that indeed the new technology is capable of controlling fiber orientation. Current equipment is capable of producing fiberwebs with any desired orientation in x-y plane and z-direction [34].

This thesis presents research of a novel technology, which can be used to produce disc shaped fiberwebs with desired fiber orientation using the concept of electrostatic field. A new device was designed and built to achieve this objective. The circumferential fiber orientation is the focus of this study. Fiber orientation in different directions could be achieved using the equipment with variation in design of electrodes and fiber dispensing systems. The device consists of the following parts:

- Fiber dispensing system
- Turning disc with speed controller, which also acts as fiber collecting surface,
- Electrostatic field electrodes and high voltage power supply, as well as

- Fiber lay-down mechanism.

In addition to the actual design and manufacturing process of the device, a set of experimental trials with full factorial statistical design was performed to study the effect of process parameters and their interactions on the fiber orientation in circumferential direction. These parameters are:

- Electrostatic field strength, which is determined by electrostatic potential and the distance between the electrodes,
- Fiber collecting disc rotational speed, and
- Diameter of the fiber lay-down rod.

Image analysis and Analysis of Variance (ANOVA) was used to measure the fiber orientation and analyze the data obtained by the experiments to determine the best parameter combination(s) that lead to circumferential fiber orientation. It was found that using the correct settings for potential, electrode distance, fiber collecting disc rotational speed and fiber lay-down rod diameter the desired circumferential fiber orientation can be achieved. The statistical analysis revealed that there is a strong interaction between the electrode distance, disc rotational speed and potential, meaning that correct settings of these three parameters have significant influence on the fiber orientation.

The design of the equipment was done considering highest flexibility to provide a wide range of processing parameters and easily change them. Therefore a wide range of fibrous raw material can be processed using this device. However, initial experiments with fine carbon fibers in the range of 7 $\mu$ m in diameter revealed some problems of the fiber dispensing system, which need to be optimized if processing such fine fibers is desired. If it is additionally desired to achieve other fiber orientation distributions than circumferential, the device can be upgraded and used for further research.

Disc shaped fiberwebs with controlled orientation are currently used in industrial applications such as:

1. Carbon fiber composite brake rotor discs for passenger cars, planes, and space shuttle and
2. Reinforcement structures for rotational grinding, cutting and sanding pads or discs.

Rotor brake systems from carbon fiber composites have great performance in the racing car industry. If it would be possible to produce carbon fiber brake discs competitively compared to brake systems currently used in the passenger and commercial vehicle industry, an interesting business opportunity could arise. Currently materials for rotors in passenger cars are high performance steels and grey-cast iron components [17 – 20]. Carbon fiber reinforced materials are not seen in the passenger car market except for an extremely expensive brake introduced by companies SGL Carbon AG and Dr.-Ing. h.c. F. Porsche AG [21, 22].

This thesis presents the development of equipment, which may allow fully automated production of disc shaped fiberwebs with controlled fiber orientation and therefore eliminate the following disadvantages of the “Porsche brake disc”:

- The fibers are randomly incorporated in the matrix. Since the applied load on the brake disc is in circumferential direction, and fibers can only take load along their axis, these rotors do not fully use the technical potential of carbon fiber reinforced composite rotors. If the fiber orientation distribution is specifically controlled e.g. fibers are aligned in circumferential orientation, meaning in load direction, the composite material could have better performance compared to composites with random fiber orientation [7].
- The rotor needs to be manufactured in a fully automated process in order to limit manufacturing costs to a competitive level. The “Porsche brake disc” is much too expensive due to high manufacturing cost as a result of manual

labor needed for the fabrication and machining [32]. The cost needs to be lowered in order to find a wide application in regular passenger cars.

An introductory market study for the use of the developed system as carbon fiber brake discs was carried out and disclosed some business opportunities, which makes it worthwhile to expand the research in the area of carbon fiber reinforced brake discs with controlled fiber orientation. For successful marketing of the technology, future research is necessary in the area of processing carbon fibers using the device and increasing the maximum possible web thickness the device can handle. Additional cost benefit analysis need to be provided in order to evaluate the competitiveness of the technology.

Alternative applications of composites with controlled fiber orientation, other than carbon fiber brake discs, are generally seen in all devices or machine parts, that are exposed to high stresses, for example during rotation. Grinding, cutting and sanding pads or discs are examples for such parts. The reinforcement of these pads are a key parameter for the stability and therefore for the lifetime of the product. Improvements in the reinforcing structure of grinding and sanding pads have direct influence on their specific application and performance.

## 2. Literature Review

This chapter provides background and reviews previous research publications that deal with:

- The electrostatic principle and its application in textiles,
- Control of fiber orientation distribution in nonwovens using electrostatic field, and
- Conventional brake systems, as well as advantages of introducing carbon fiber brake discs into the automotive market.

There is no literature available regarding formation of disc shaped fiberwebs with controlled fiber orientation, where electrostatic forces for fiber alignment were used. The electrostatic phenomenon was, however, studied and extensively reviewed in numerous textile areas such as flocking and electrospinning of microfibers and nanofibers.

### ***2.1. Application of Electrostatic in Textiles***

The concept of electrostatic or the electrostatic phenomenon is used in various industrial fields and applications such as powder coating technology [16], the basic concept of the cathode ray tube [24] and the electrostatic precipitator [31].

In textiles electrostatics is used in:

- Flocking to create three dimensional fabrics [23],
- Electrospinning to usually create fibers in the micro and nanometer range with low fiber diameter to provide high surface area [27] and
- Fabric Filtration to create electrostatic attraction forces that are used to increase the filtration efficiency of fabrics [10]

## 2.2. Electrostatic Principle

The electrostatic phenomenon is based primarily on the observation that like charge bodies repel and unlike charge bodies attract, as indicated in Figure 1 [3, 6, 13, 15]:

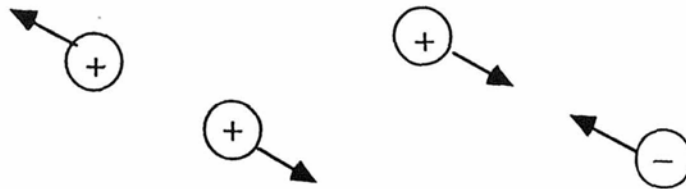


**Figure 1: Like charges repel (left) and unlike charges attract (right) [6]**

The force between the two charge bodies ( $F_{1/2}$ ) is observed to increase linearly with each of the two charges ( $q_1$  and  $q_2$ ) [3, 6, 13, 15]:

$$F_{1/2} \sim q_1 q_2$$

**Equation 1: The force between two charges increases linearly with each of the two charges (~ means proportional to) [6]**

The magnitude of the force is inversely proportional to the quadratic distance between the two bodies. Then the force expression can be further written as

$$F_{1/2} \sim \frac{q_1 q_2}{r^2}$$

where  $r$  is the distance between the two charged bodies.

**Equation 2: The magnitude of the force falls off quadratically when the two charges are separated (~ means proportional to) [3, 6, 13, 15]**

The constant of proportionality in this force expression depends on the units chosen to express the other quantities. For SI units, with charge in coulombs and distance in meters, the force expression becomes

$$F_{1/2} = \frac{q_1 q_2}{4\pi\epsilon_0 r^2}$$

**Equation 3: Coulomb's law [3, 6, 13, 15]**

The constant  $\epsilon_0$ , is known as the permittivity of free space, which is denoted in Farads per Meter (F/m) and has the value

$$\epsilon_0 = 8.854 \times 10^{-12} \text{ F/m}$$

**Equation 4: Permittivity of free space [3, 6, 13, 15]**

“The classical foundational basis of electrostatic charging is the Coulomb interaction, which defines the kinematics and dynamics of charge separation and subsequent charge holding”[6]. Coulomb interaction determines the configurations of charge stability, “the thresholds of sudden charge rearrangements and breakdowns, the effects of charge correlations” (electrostatic ordering, Coulomb blockade, etc.), and electrostatic instabilities and gradual charge leaking processes [6].

To mathematically explain electrostatic fields, Laplace's Law, which is a partial differential equation, named after its discoverer Pierre-Simon Laplace, needs to be considered. The solution of Laplace's Law is important in the fields of electromagnetism, astronomy and fluid dynamics, since it describes the behavior of electric, gravitational and fluid dynamics [3]. Laplace's Law is a simplification of the Poisson equation, which gives the electrostatic potential in terms of the volume charge density [3]. In regions where there is no net charge density, Poisson's equation simplifies to Laplace's equation [3].

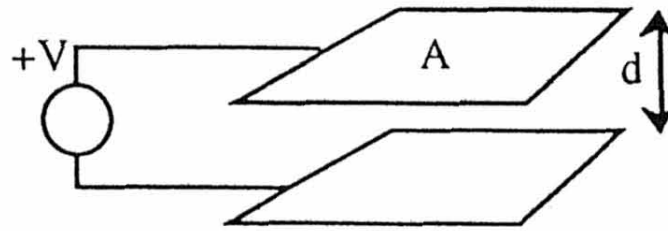


**Figure 2: Two flat and parallel electrodes separated by a distance  $d$  [6]**

In case of two flat, parallel electrodes, the electric field can be calculated using the following equation, which can be derived from Laplace's Law for the specific case shown in Figure 2 [3, 6, 13, 15]:

$$E = \frac{U}{d}$$

**Equation 5: Calculating the electric field ( $E$  in kV/cm) for the case of two parallel electrodes with a certain distance ( $d$  in cm) and given electric potential ( $U$  in kV) [6]**

The total charge on a plate is calculated by using Gauss's law over a volume that encloses the plate, giving the total charge on the electrode as

$$Q = \iint \frac{\epsilon V}{d} dS = \frac{\epsilon A}{d} V$$

**Equation 6: The total charge ( $Q$ ) of the capacitor [6]**

Note that the charge is linearly related to the voltage in this example. The constant of proportionality is defined as the capacitance of the device [3, 6, 13, 15]:

$$C = \frac{\epsilon A}{d}$$

**Equation 7: Capacitance of the capacitor [6]**

The capacitance is a measure of the amount of charge that can be stored on an electrode for a given voltage. Much of electrostatics can be explained by considering how such a capacitor behaves as its dimensions are changed, or the dielectric constant varies [3].

The principle of electrostatic can be applied in textiles, for example in flocking. Figure 3 shows a schematic of possible flocking setup. The electrostatic field produces both the acceleration of the flocks and their orientation. A typical number for the electrostatic field strength in flocking is 3kV/cm [23].

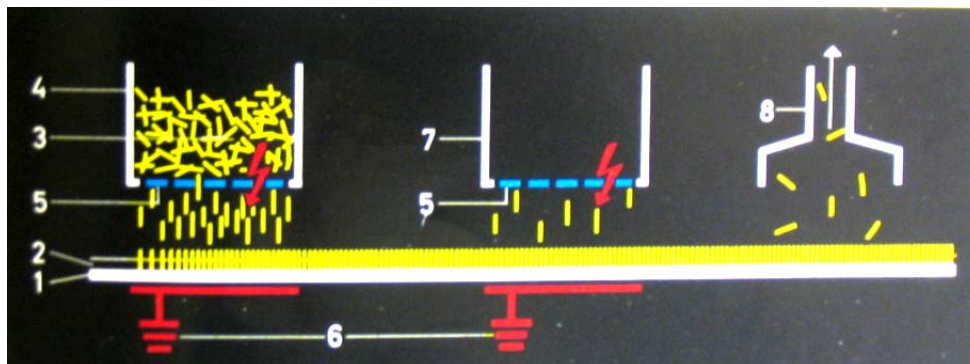


**Figure 3: Flocking setup – 1 fibrous substrate; 2 bonding agent; 3 flocks; 4 dosage device; 5 electrodes; 6 opposite electrodes grounded; 7 electrostatic suction; 8 pneumatic suction [23]**

The fibers penetrate with high velocity and in strict orientation into the binder film. The flocks can be applied to the fibrous substrate either in the direction of or against the force of gravity. In the latter case it is easier to control the amount of flocks and also to remove excess flocks [23].

The conductivity of the flocks is critical for flock orientation within the electrostatic field and discharging of the flock once it hit the grounded plate (ability to change polarity). Rapid discharging is important since flock particles, which are not retained by the bonding agent, need to be immediately rejected and turned back to the fiber dispensing electrode to be charged again. The ability of flock particles to be charged is therefore extremely important for the quality of the flocked product. The chargeability on the other hand is relying on environmental conditions, especially the humidity [23].

**Table 1: Conductivity ( $\chi$ ) of three different Polyamid samples treated with different finishes and conditioned at different levels of relative humidity [23]**

Sample	Conditioned at 20°C; 40% relative humidity		Conditioned at 20°C; 65% relative humidity	
	$\chi [(\Omega \cdot \text{cm})^{-1}]$	Ability to change polarity	$\chi [(\Omega \cdot \text{cm})^{-1}]$	Ability to change polarity
Polyamid I	$1.7 \cdot 10^{-9}$	good	$1.7 \cdot 10^{-8}$	poor
Polyamid II	$5.0 \cdot 10^{-11}$	good	$5.0 \cdot 10^{-10}$	good
Polyamid III	$1.2 \cdot 10^{-13}$	poor	$1.2 \cdot 10^{-11}$	poor

Table 1 shows that a change in humidity has tremendous effect on the ability to change polarity. On the other hand the table shows that the conductive treatment is also important in order to get good flocking results, since not all finishes lead to good chargeability of the flock. In general flocks should possess a conductivity of  $10^{-10} (\Omega \cdot \text{cm})^{-1}$  or more. The conductivity of Polyamid flocks is lower than  $10^{-13} (\Omega \cdot \text{cm})^{-1}$ , which makes it necessary to increase the conductivity considerably by appropriate finish treatments [23].

These findings are also supported by Brokmeier [5] and Tanasescu [37] who stated that conditioning the flock is critical in order to achieve good flocking results, since it is the moisture absorbed by the flock finish which transports the electric charge. Thus a change in moisture results in considerable change in flock conductivity. The amount of moisture to be absorbed by the flock must exactly match flock material and its finish to achieve good results in flocking. The moisture change from the location of flock conditioning and flocking process is also critical. Depending on the material, finish and environmental conditions, a reasonable conditioned flock can get useless if the environmental conditions in the actual flocking apparatus are not appropriate. To prevent this, flocking under controlled environmental conditions is suggested (e.g. enclose the flocking apparatus in a climate chamber) [5, 37].

### ***2.3. Development of Nonwovens with Controlled Fiber Orientation***

The lack of obtaining fiberwebs with desired fiber orientation using existing fiberweb forming systems (such as carding, carding and cross-lapping, wet-lay and air-lay) have prompted a research team from North Carolina State University and the University of Massachusetts Dartmouth to develop new technology [34]. The new technology is based on using electrostatic field to orient the fibers at specific desired directions.

To form fiberwebs with fibers laid in a plane and a controlled fiber orientation distribution (FOD), appropriate equipment was developed using several sets of electrodes and fiber feed stations for fiber orientation in desired direction. The system controls the fiber orientation with respect to a reference direction (e.g. machine direction). Every set of electrodes and feed determine one direction for fibers fed by that set. This system is termed as “Vacuum Conveyor Belt Table System” and shown in Figure 4 [34].

In the Vacuum Conveyor Belt Table System the fibers are fed by a stream delivery system and aspirator with high voltage. The fibers are fed to the orienting zone of two electrodes. A conveyor belt with air suction is used as fiber receiver and fiberweb holding mechanism. To form nonwoven fiberwebs with engineered fiber orientation distribution, the fiber stream delivery and electrostatic orienting zones are arranged in accordance with the desired FOD on a vacuum conveyor belt table [34].

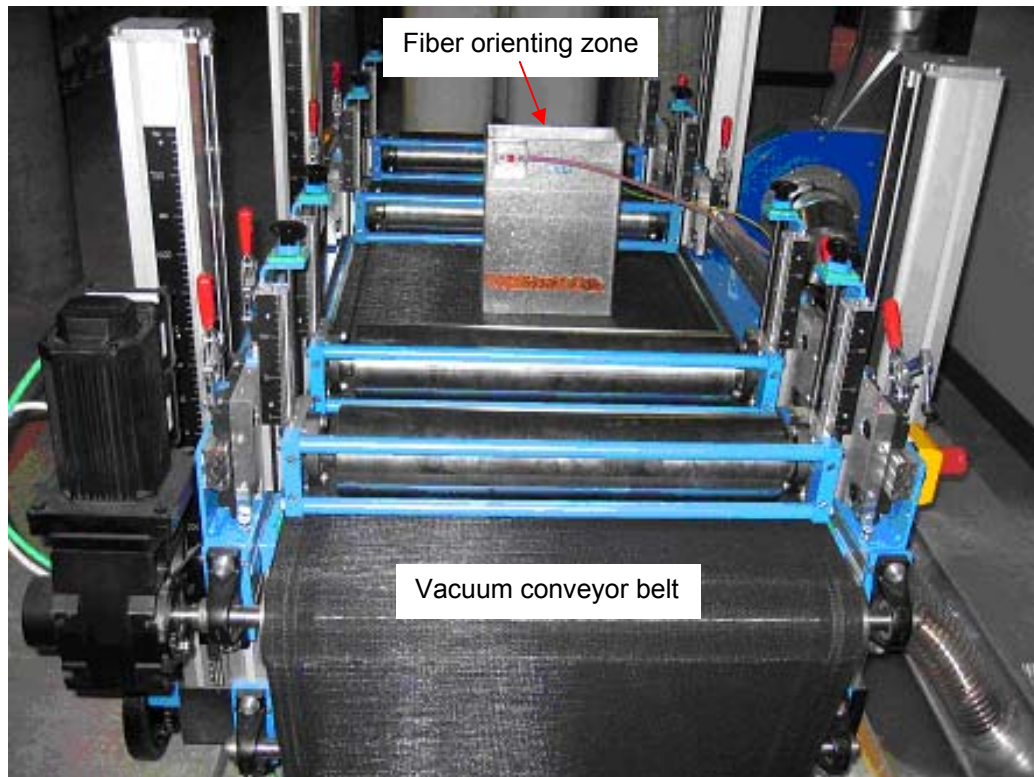


**Figure 4: Vacuum Conveyor Belt Table System [34]**

The predetermined FOD web is formed on the vacuum conveyor belt table by orienting zone geometry, nipping feed roll setting, vacuum pressure and conveyor belt speed [34]. Different electrode geometries and arrangement can fabricate webs with specific FOD as desired.

The proposed process can positively control fiber orientation and fiber orientation distribution using electrostatic forces. Current methods in industry for web formation can only control fiber orientation passively. Therefore the Vacuum Conveyor Belt Table System allows the specific design of nonwovens with specific properties such as strength, pore size and bending behavior [34].

## **2.4. Carbon Fiber Brake Disc**

As mentioned earlier, carbon fiber brake disc for passenger cars and commercial vehicles is a potential application, where the developed equipment, described in this thesis, is beneficial. This section will address the following issues:

- Overview regarding current brake disc technology.
- Why the use of carbon fiber brake discs is beneficial?

The analysis is done considering the introduction of carbon fiber brake discs into the automotive market. Chapter 7, page 97 provides an introductory market analysis for carbon fiber brake discs.

### **2.4.1. Conventional Brake Systems**

The brake disc is a device for slowing or stopping the rotation of a wheel. A brake disc, usually made of cast iron, is connected to the wheel or the axle. To stop the wheel, friction material in the form of brake pads is forced mechanically, hydraulically or pneumatically against both sides of the disc. Friction causes the disc and the attached wheel to slow or stop [17 – 20].

The design of the disc itself can vary. Figure 5 shows examples of drilled, slotted and combinations of drilled and slotted brake disc designs [18]. The slots and holes are designed to improve braking efficiency and reliability. The purpose of the slots and holes is to aid the brake pads in cleaning and wiping the discs surface of dust (e.g. dust from the brake pads) and water which may reduce the braking efficiency. Secondly the holes are drilled to reduce the weight of the unsprung masses.

On the other hand, slotted brake discs wear out brake pads faster than discs with a plain surface, since the edges of the slots are extremely aggressive [17 – 20].

The “Power Star” brake disc design shown in Figure 5 is an attempt to decrease the negative effect of damaging the brake pads due to sharp edged slots. The recessed parabolic grooves and radial slots are specifically designed to prevent brake pads from damage [18].

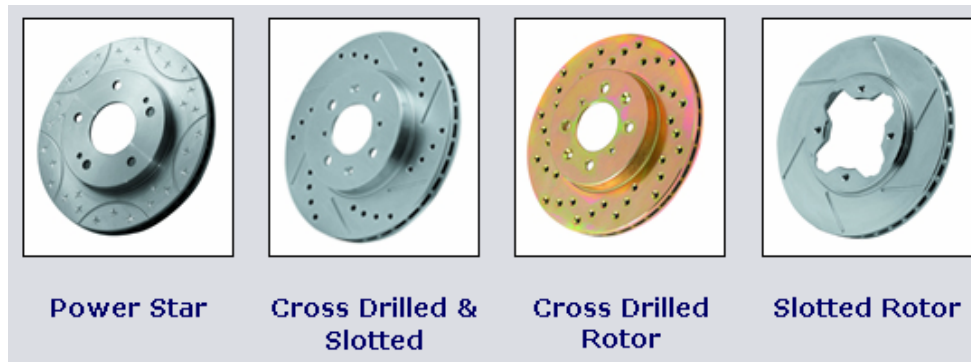


**Figure 5: Different Design of brake discs [18]**

Cast iron brake discs can be severely damaged and temporarily or permanently lose their braking ability due to high temperatures. Especially when driving down hills, drivers often apply low braking forces over a long time, meaning that the brake pads are only lightly touching the rotor, which generates high temperature, but low braking force. Excessive heat can cause the brake disc metal to soften and reshape (warping) [17, 19 – 21].

To reduce disc temperature many brake discs are hollow, like the examples shown in Figure 5. These discs are actually made of two friction surfaces joined together by fins or equivalent. The gaps between the “two discs” allow air flow through the disc when the disc is rotating; resulting in some kind of “active cooling” (also termed as “ventilated” disc design). Many high performance brake discs today are designed in such a way, including the Porsche Ceramic Composite Brake (see next section for more details) [17 – 21].

### 2.4.2. Why Carbon Fiber Brake Disc?

The use of carbon fiber brake discs is not new. They show great performance in the motor sports industry, for high speed trains and aircrafts. Recently the company Dr. Ing. h.c. F. Porsche AG introduced the first carbon brake disc for passenger cars that is commercially available for the Porsche 911 Carrera S and Porsche 911 Carrera 4S. The product name is Porsche Ceramic Composite Brake (PCCB) and it costs 14,000.00€ (www.porsche.com retrieved March 1, 2006).

This brake system was developed together with SGL Carbon AG. The material the brake disc is made of is carbon fiber reinforced ceramic silicon carbide composite [22]. The brake disc is formed by incorporating fibrous materials and matrix in specific disc shaped performs. The fibrous material is preferably pre-impregnated short carbon fiber. From patent literature it can be inferred that fiber orientation distribution is not specifically controlled [14, 32].

The advantages of the brake disc system include [22]:

- “Higher and consistent frictional coefficient than traditional materials” (grey-cast iron components), “making them independent from temperature and weather conditions” such as humidity.
- Weight reduction (about 65% compared to traditional grey-cast iron components), “reduces the weight of the suspension and results in a reduction of unsprung masses with a further improvement of shock absorber response and behavior”, which in the end increases safety and reliability of the vehicle.
- “Can last the lifetime of a car” (due to non-iron based surfaces, which avoid corrosion and temperature independence of the composite material, both of which increase the life span of the brake disc).

The disadvantages of the brake system include [32]:

- High cost, mainly due to non-automated production processes and highly priced materials.
- The reinforcing carbon fibers are randomly incorporated, since the production process does not allow fiber orientation control [32], which means that their reinforcing potential is not fully utilized, since fibers can only take the maximum stress along the direction of their axis [7]. In case of brake discs, fibers need to be in circumferentially oriented in order to optimally withstand the applied load, which is in circumferential direction during braking [32]. While this orientation seems to be important, there is no published work to support it. Fiber orientation in other direction(s) may be essential for the performance of brake discs.

### 2.4.3. Fiber Based Composites: Basic Concept and Advantages

The basic concept of fiber based composite materials can be demonstrated by a simple illustration, considering a composite beam consisting of two identical parts (see Figure 6). In case (a) of Figure 6 both parts behave separately and move freely relative to each other at the interface. In Figure 6 (b) both parts are constrained to act together. The longitudinal slip in (a) does not occur in (b). It is demonstrated “that case (b) is twice as strong and four times as stiff as case (a)” [29].

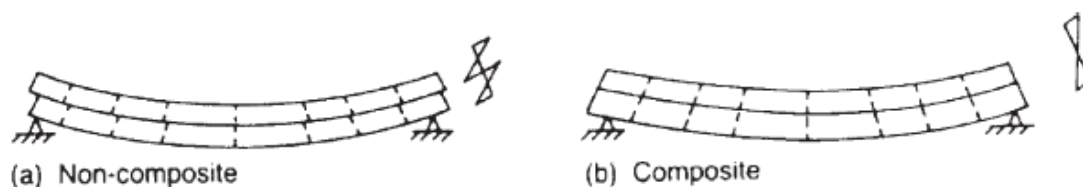
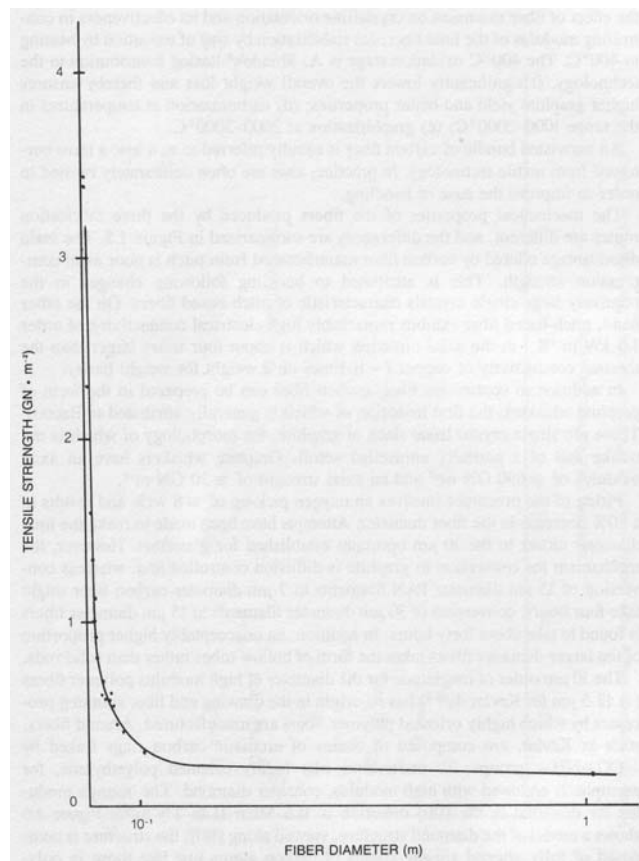


Figure 6: Basic mechanics of composite action [29]

The demonstrated concept for composites can be generally applied for all kind of composites like steel/ concrete composites, but also for fiber reinforced composites with polymeric, ceramic or metal matrix [2, 29].

Ashbee [2] showed that the fiber diameter determines its mechanical properties like tensile strength, but also the mechanical behavior of the composite material. The strength for example of glass fibers exponentially increases with decreasing diameter of the fiber (see Figure 7) [2].



**Figure 7: Fiber diameter versus fiber tensile strength [2]**

The specific strength of materials increases when decreasing the size e.g. the diameter. Mechanical properties of fibers are considerably improved compared to their mechanical properties in bulk form [12, 29].

Carbon fiber composites, especially those with polymeric matrix, have become important for providing advanced materials for aerospace, automobile, sporting

goods and other applications, particularly due to their excellent mechanical and physical properties like high strength, high modulus and low density, which result in a more favorable weight to strength ratio and improved temperature resistance compared to metals [7].

#### 2.4.4. Carbon Fiber Composite Brakes

Literature review disclosed several publications that deal with the development of carbon fiber composite brakes [14, 21, 22, 28, 35, 42].

Goodyear Aerospace Corporation (inventor: Robert L. Zarembka) filed a patent in 1978 disclosing a carbon fiber ribbon that is wrapped around a disc using a certain form to create a carbon fiber brake disc surface (see Figure 8) [42].

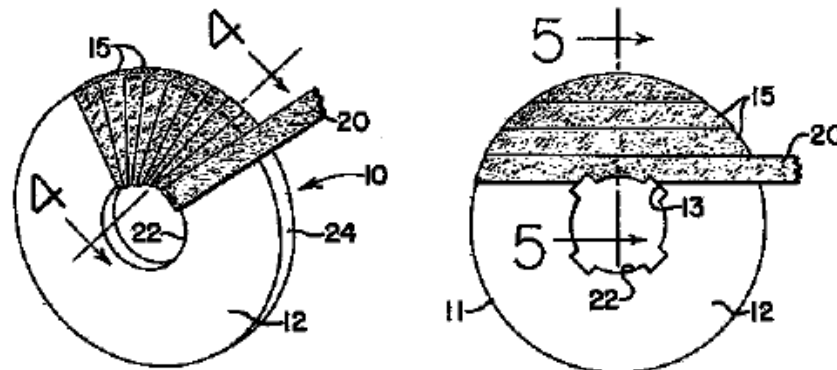


Figure 8: Ribbon-wrapped brake disc [42]

Different wrapping scenarios are presented as indicated in Figure 8 and Figure 9. To overcome differences in the thickness of the carbon fiber material due to the wrapping process, several suggestions were made as examples which are shown in Figure 9 [42]. The wrapping technique is, however, limit the fiber orientation. For example circumferential fiber orientation seems difficult to achieve.

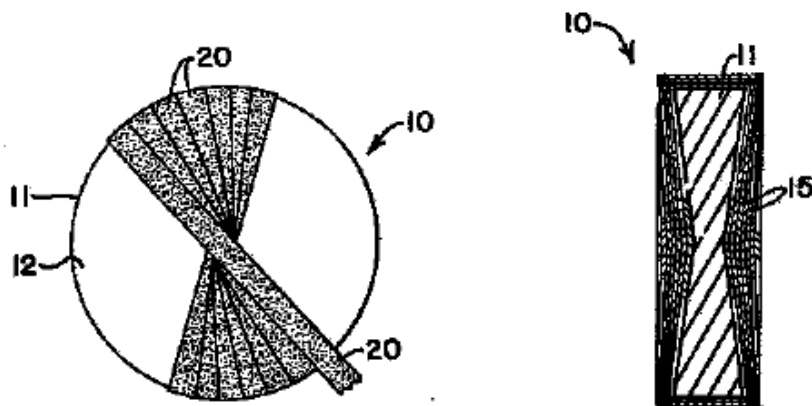


Figure 9: Thickness differences of the carbon ribbon layer (15) due to the wrapping process and a corresponding perform cross-sectional shape (11) to overcome these difficulties [42]

The B.F. Goodrich Company (process inventors: Philip William Sheehan, Ronnie Sze-Heng Liew) provides an additional z-directional fiber orientation to prevent delamination of the disc. To achieve the z-directional fiber orientation a needle punching process follows the web forming process as indicated by Figure 10 and Figure 11:

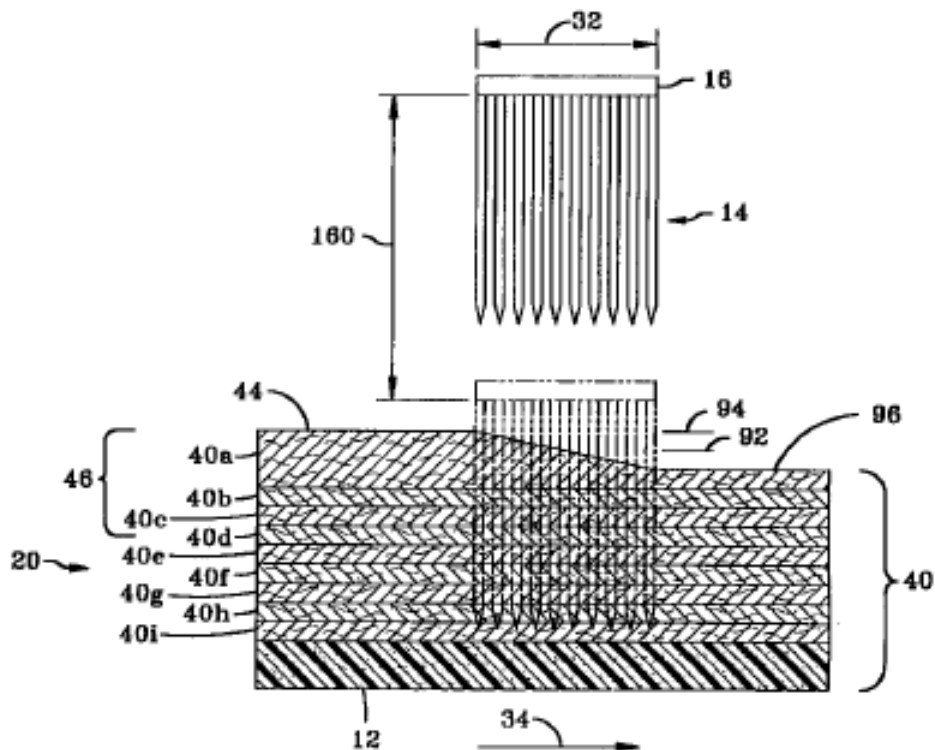
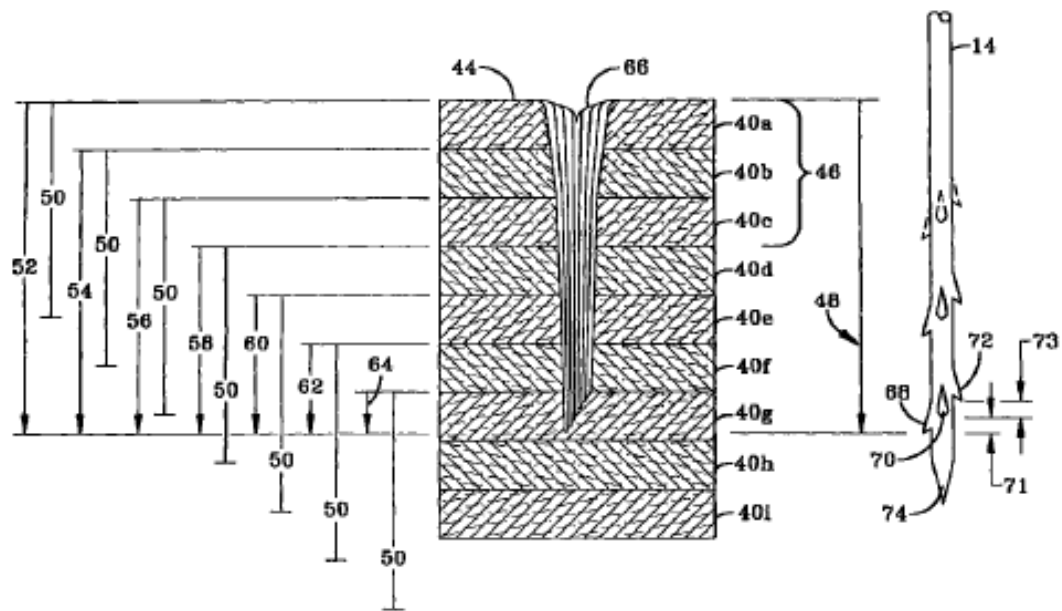


Figure 10: Needle punching process of fibrous performs to achieve z-directional fiber orientation to improve de-lamination properties [35]



**Figure 11: Some fibers will be oriented in z-direction (66) due to the penetrating barbed needles (14), resulting in improved de-lamination properties of the resulting composite material [35]**

The fibrous substrate, which is needle punched, can be manufactured using known web formation processes. These processes, as it was stated earlier, lack specific control of fiber orientation distribution. The patent does not favor a specific process, nor does it discuss the web formation process [35].

The resulting carbon fiber brake disc is primarily used for aircraft brake systems, which are much more complex than brake systems for regular passenger cars. Since aircraft brake systems undergo extremely high stresses, resistance against de-lamination of the brake disc can be improved by z-directional fibers [35].

Weakening of the carbon fibers due to the needle punching process is seen as a significant disadvantage of the process [26]. Another disadvantage is the lack of specific fiber orientation control. Needle punching re-orientates some carbon fibers from their in-plane direction into the z-direction, which also leads to fibers oriented between these two distinct orientations, which do not contribute to the nonwoven composite structure in terms of composite mechanical properties. Specific fiber orientation distribution control e.g. due to electrostatic field may improve final web

and composite properties due to positive control over fiber orientation (in-plane and in z-direction).

B.F. Goodrich Company also patented a braiding process (inventors: Edward L. Morris, John A. Hasler, Hans-Adolf Lange), which might be used for the production of preforms for carbon fiber reinforced brake discs. The pull-out and take-up apparatus of a braiding machine is designed to form flat curves or helices as shown in Figure 12 [28].

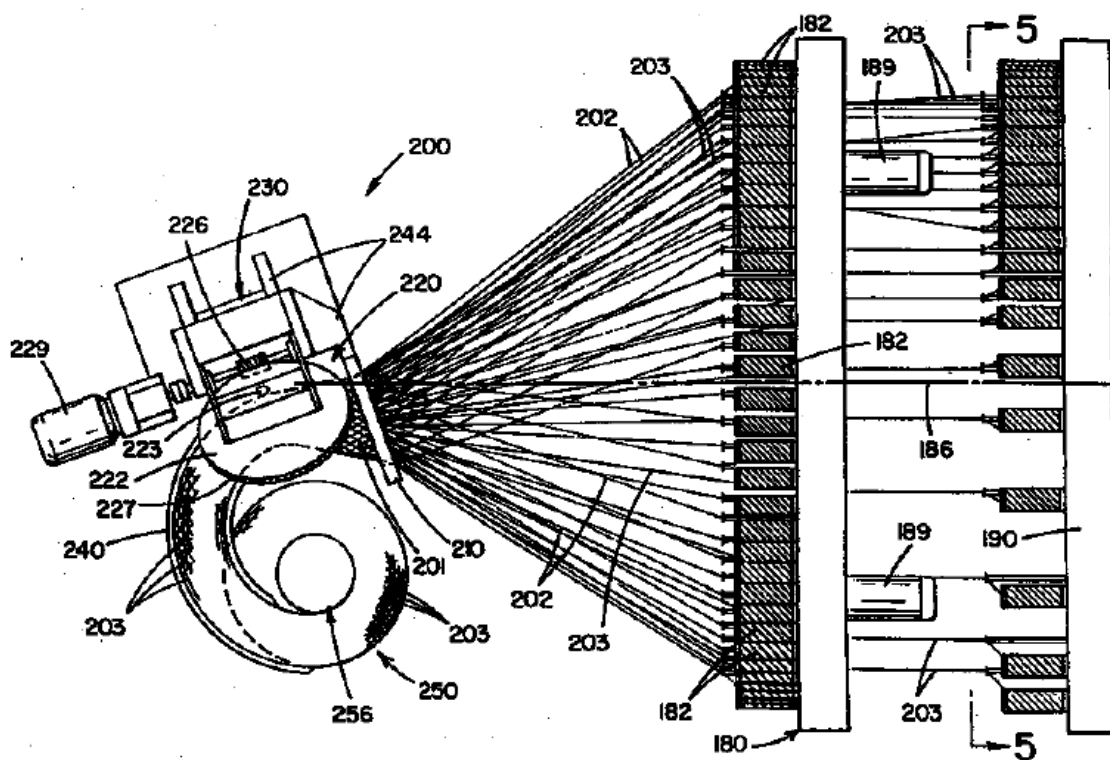


Figure 12: Curved braid apparatus for forming helical flat ribbon structures [28]

The excellent drapability of braided structures supports the forming process of the helical ribbon [28]. This process is, however, slow and requires expensive technology.

As aforementioned, companies SGL Carbon Group and Dr. Ing. h.c. F. Porsche AG introduced the first carbon fiber reinforced brake disc for passenger cars [21, 22]. Advantages and disadvantages were already discussed (see section 2.4.2,

page 16). Neither the Porsche disc, nor the other presented composite brake discs do have positive control of fiber orientation in multi-direction including z-direction and circumferential direction. It seems that there is a need to develop a process for the production of reinforcing fiber structures with controlled multi-directions including z- and circumferential directions.

## **2.5. Summary**

From the reviewed material it can be concluded that there is a technical need for technology to specifically control fiber orientation distribution (e.g. for circumferential oriented fiberwebs of disc shape). While literature review showed that some success has been achieved in developing technologies for producing disc brakes from carbon fiber based composites, a full control over multi-direction fiber orientation is yet to be seen. On the other hand potential applications can be targeted. Therefore the purpose of this work is to design and build equipment which is capable of producing disc shaped fiberwebs with controlled fiber orientation, in order to address business opportunities in potential markets, mainly carbon fiber brake discs. This could be done by extending the work done by Seyam et al [34] which dealt with producing plate form fiberwebs with controlled fiber orientation.

### 3. Research Objectives

The main goal of this research is to design and build a device that is capable of forming disc shaped fiberwebs with circumferential fiber orientation. Other fiber directions could be done. The circumferential direction was selected since none of the previous publications could achieve such orientation. The fiber alignment is achieved by electrostatic forces. The device consists of four main parts, namely:

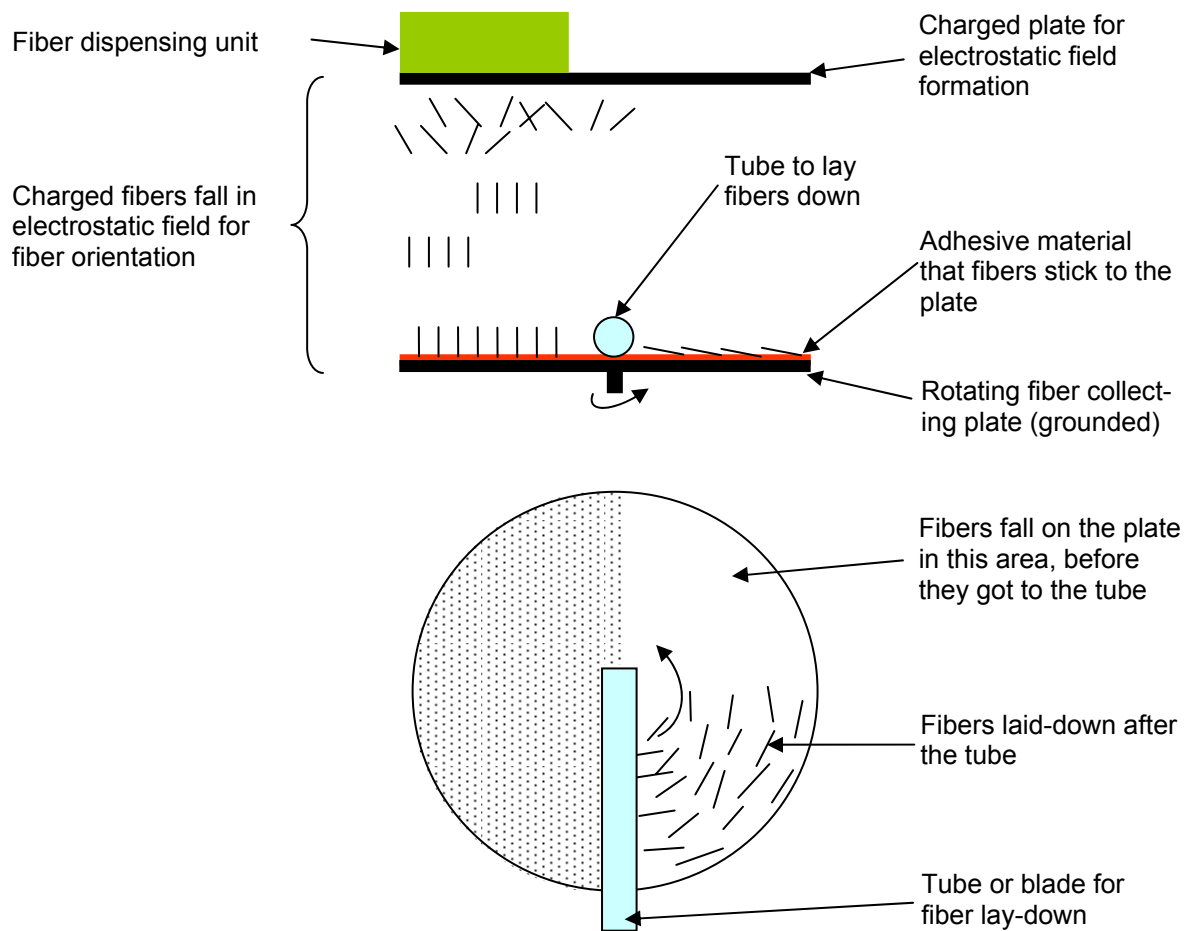
1. positive and negative electrodes to create the electrostatic field
2. fiber dispensing system
3. fiber collecting system
4. fiber lay-down mechanism.

Figure 13 schematically shows the concept of the device and its main parts. After the fibers are dispensed into the electrostatic field region, they become aligned by electrostatic forces and hit the collecting plate perpendicularly or at angles close to  $90^\circ$ . Once the fibers hit the grounded collecting plate, they will be discharged and should bounce back to the charged fiber dispenser. To prevent this, the grounded plate is evenly covered with a thin adhesive layer, which in a fully developed system can also act as composite matrix. After anchoring the fibers they will be laid-down, since the collecting plate is turning under a lay-down tube, that pushes the fibers to lay-down in the plane of the collecting surface.

Knowledge gained from flocking processes was helpful in the successful design and manufacture of the device. In particular the electrostatic field formation using electrodes and fiber dispensing units were similar to those used in flocking with modification in shape and parts to orient the fiber parallel to the collecting surface plane and circumferentially into a disc shaped fiberweb.

The developed device could be used in several industrial fields. It should be generally possible to produce fiberwebs with nearly all kind of fiber materials like

Polyester, Polyamid, Carbon or even Viscose to achieve a wide range of applications as long as disc shaped products are used and fibers can be charged.



**Figure 13: Schematic drawing of the lay-down process of the fibers**

The specific objectives of this work, used to achieve the main goal and demonstrate the capability of the newly developed device are:

1. Design and manufacturing of appropriate equipment to produce disc shaped fiberwebs with circumferential fiber orientation as described above,
2. Testing and initial optimization of the equipment and
3. Run experiments to reveal the influence of the process parameters and the correct blend of their values, which lead to circumferential fiber orientation of the web. The process parameters selected for the study are:
  - a. electric field strength, which is controlled by
    - i. distance between the two electrodes and
    - ii. applied electrical potential
  - b. rotational speed of the collecting disc, and
  - c. the diameter of the lay-down rod.

## 4. Equipment Development

This chapter describes the equipment, which was designed and manufactured in the context of this work.

As stated earlier, the equipment, which is shown in Figure 14, consists of:

1. Electrostatic Field Electrodes
2. Fiber Dispensing System
3. Fiber Collecting System
4. Fiber Lay-Down Mechanism

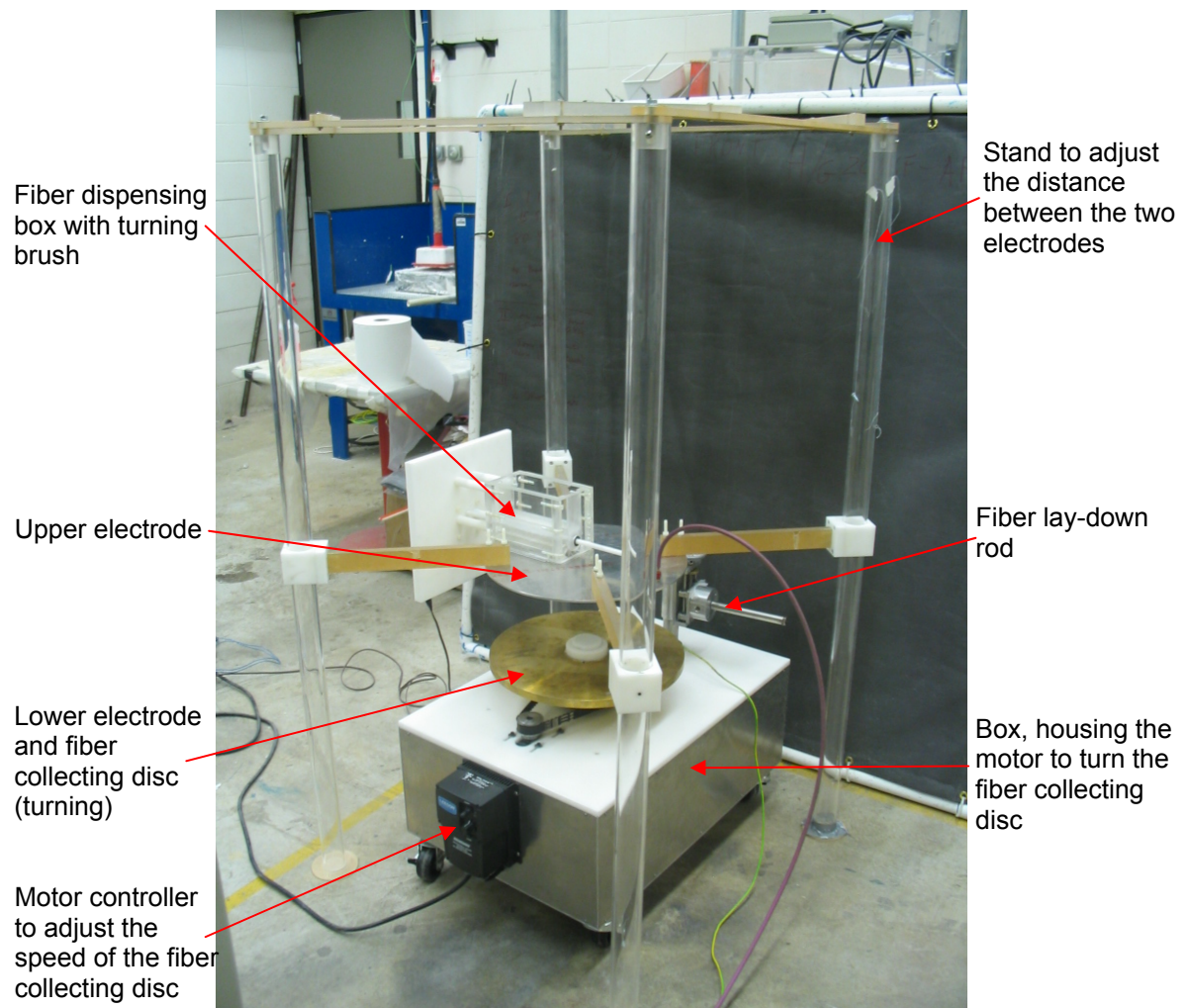


**Figure 14: Equipment to form disc shaped fiberwebs with circumferential fiber orientation**

### 4.1. *Electrostatic Field Electrodes*

The self-aligning effect of conductive (or charged) fibers in electrostatic fields is a well known concept, which is widely used in industry (e.g. flocking industry). Fibers will orient themselves longitudinally along electrostatic field lines. Electrostatic field development occurs due to electrical potential differences between two electrodes. The resulting field strength is a function of the electrode distance and the difference between the electrical potential of the two electrodes.

The electrostatic field electrode design was done considering uniform field line formation that fibers can be collected at angles close to  $90^\circ$  and the form of the fiberweb which is disc shaped. Therefore the dimensions of both electrodes need to be equal size discs. Additionally, positioning of both electrodes is critical for uniform field line formation (see Figure 15).

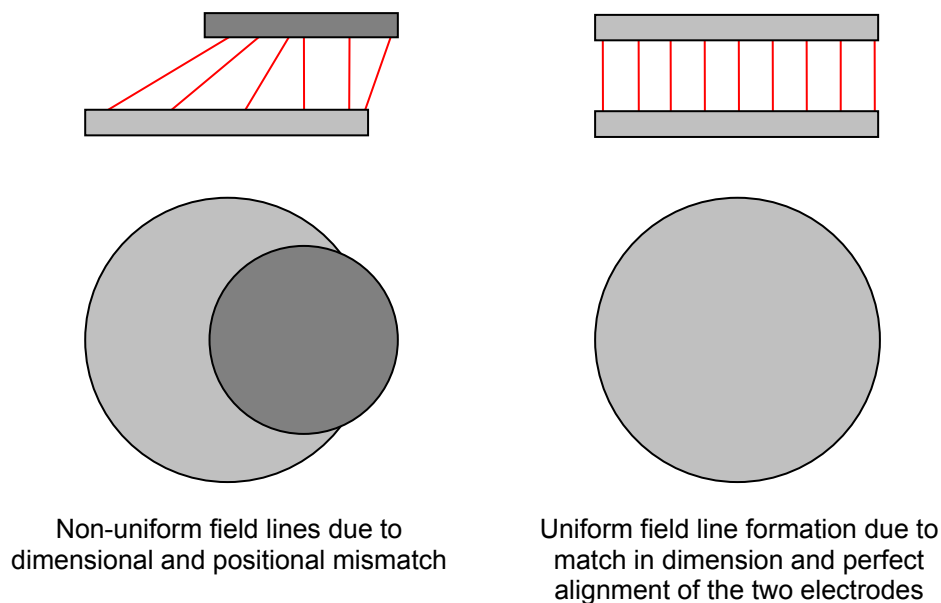


**Figure 15: Non-uniform and uniform field line formation (red) depending on dimension and position of the electrostatic field electrodes (grey)**

The dimensions and the alignment of the position of the electrodes are even more critical since both electrodes have additional functions in this research:

1. The upper electrode also serves as fiber dispensing unit (segment of this electrode is perforated to allow fiber dispensing from the fiber storage box, see Figure 16)
2. The lower electrode also serves as fiber collecting surface

Since the lower electrode is also acting as the fiber collector, the electrodes need to be circular in order to produce disc shaped fiberwebs with circumferential fiber orientation.

### **Electrode specifications:**

- Electrode diameter: 400mm
- Electrode material:
  - Upper (fiber dispensing) electrode: Aluminum
  - Lower (fiber collecting) electrode: Brass
- Distance between electrodes: adjustable up to 1,000mm
- Electrostatic potential:
  - Upper (fiber dispensing) electrode is charged using a special high voltage power supply from Maag Flockmaschinen which is used in flocking and available at the Department of Textile Sciences, College of Engineering, University of Massachusetts, Dartmouth
  - Lower (fiber collecting) electrode is grounded by carbon brushes, since the electrode is turning during fiber collection (see section 4.3, page 32)

The electrode materials were chosen due to their electrical conductivity. Aluminum is more conductive than regular steel and additionally easier to machine and shape. Since the fiber collecting disc needs to turn, a design needed to allow grounding the disc while it is turning. A setup of spring-loaded carbon brushes was used to achieve secure grounding of the disc. Brass was chosen as a material since it has even better conductivity than Aluminum and to provide maximum safety in grounding the disc when it is turning.

The dimensions for the electrode diameter and the electrode distance were chosen in order to achieve high flexibility when working with the equipment, especially for future experiments and to target brake as well as cutting, grinding and sanding pad dimensions that are currently used in industry.

## 4.2. *Fiber Dispensing System*

Fibers need to be opened, individualized and fed into the electrostatic field for alignment. Bundles or clumps of fibers are more difficult to align and are disadvantageous for web formation as well as web uniformity, and final product performance. Therefore the objectives of the fiber dispensing unit can be summarized as follows:

- Opening of fiber bundles,
- feeding separated fibers continuously into the electrostatic field and
- apply electric potential to the fibers for fiber alignment in the electrostatic field.

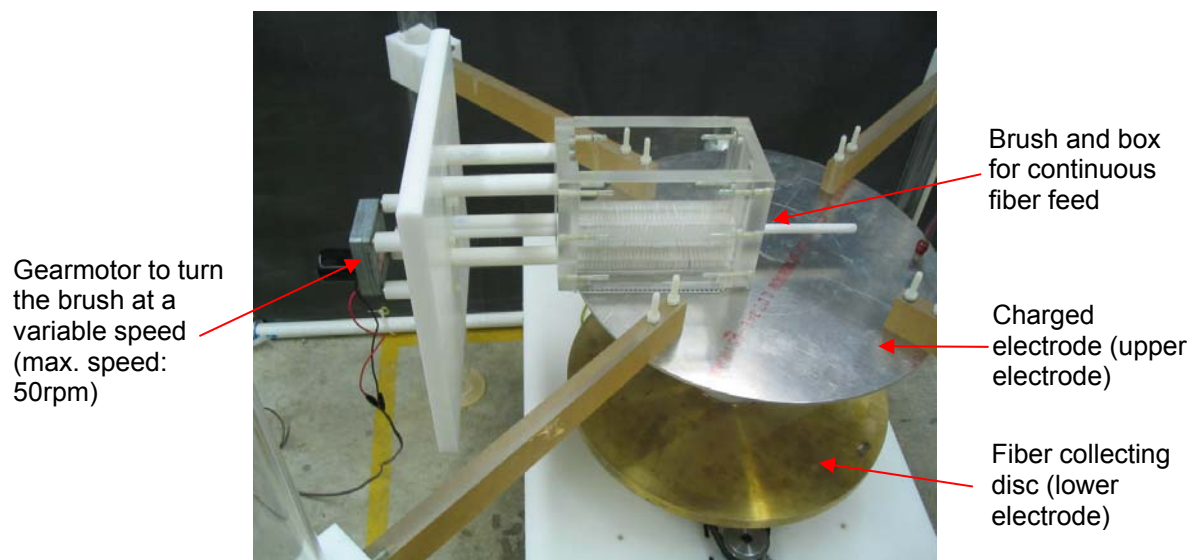


**Figure 16: Fiber dispenser (side view)**

The fibers are opened and fed by a turning brush and screen setup (see Figure 16 and Figure 17). The brush has lines of bristles along its axis, which take fibers from the storage box and pushes them through the screen. Since the bristles penetrate the screen holes slightly (~1mm), the fibers are “mechanically forced” to leave the screen to fall into the electrostatic field. The speed of the brush is variable and can be adjusted up to 50rpm, which increases the flexibility of the fiber dispensing unit in individualizing and feeding fibers into the electrostatic field. The brush is driven by a dedicated small motor (see Figure 16).

When the fibers touch the screen they are automatically charged, since the screen is directly connected to the upper electrode.



**Figure 17: Fiber dispenser (bottom view)**

The parameters determining the amount and uniformity of fibers fed into the electrostatic field are:

1. Amount and distribution of fibers in the box,
2. Brush speed,
3. Brush design (number, length and position of bristles) and
4. Screen type (hole dimension and distribution).

### 4.3. Fiber Collecting System

In Section 4.1 the collecting disc was already presented as one electrode of the electrostatic field. The fiber collecting plate can collect fibers perpendicularly due to uniform field lines created between the two electrodes (see also Figure 15).

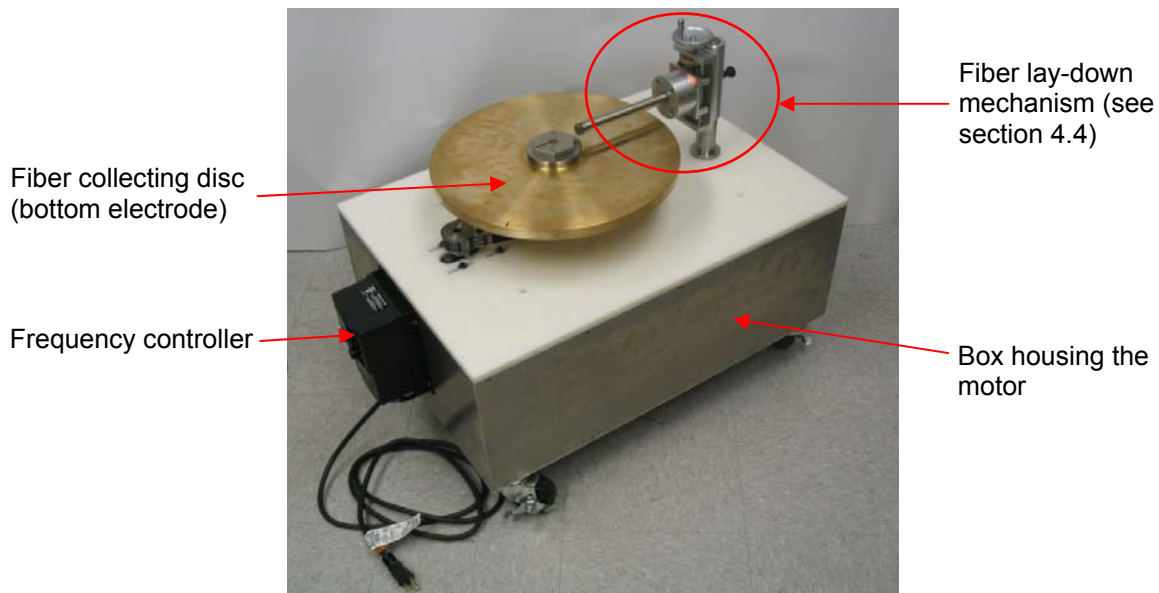


**Figure 18: Fiber collecting disc**

The disc itself is driven by a frequency controlled gear motor. To change the speed of the motor, a belt transmission with timing belt and pulleys was installed (see Figure 19 and Figure 21).

It was thought that relatively low disc speeds are necessary to assure correct fiber web forming. High speeds could cause problems in aligning fibers but also during fiber collection, since radial forces increase with disc rotational speed. Therefore the design was done assuring a maximum speed of the disc of approximately 50 rpm, which can be adjusted using the control knob at the frequency controller. However, the experiments carried out found that a high rotational speed leads to better fiber alignment and that the optimum rotational speed is probably above 50rpm (more details are provided in section 6.3, page 80).

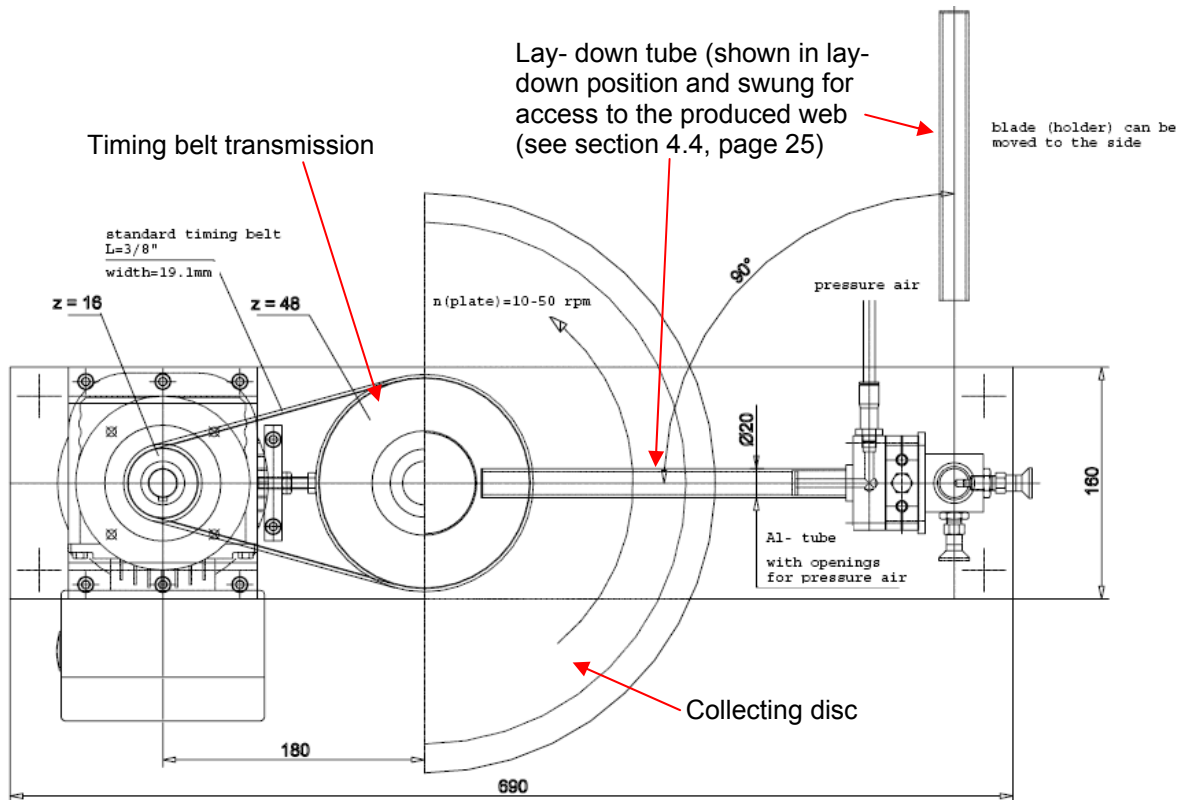


**Figure 19: Engineering drawing of the fiber collecting device including fiber lay-down mechanism (top view) (dimensions in millimeter)**

A diagram of the fiber collecting disc speed corresponding to the scale shown at the control knob (provided by supplier) of the frequency controller is given in Figure 20.

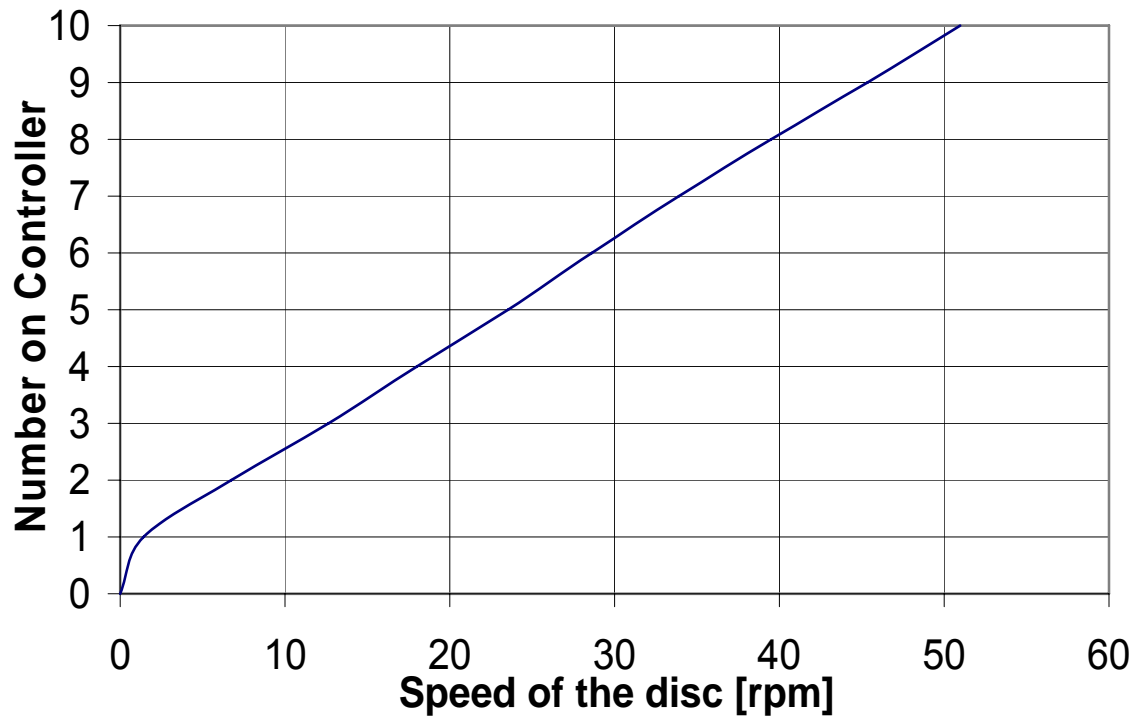


**Figure 20: Speed of the disc, corresponding to the scale shown on the motor controller**

The following image shows details of the belt transmission and the setup of the carbon brushes, which apply the electrostatic potential on the disc:

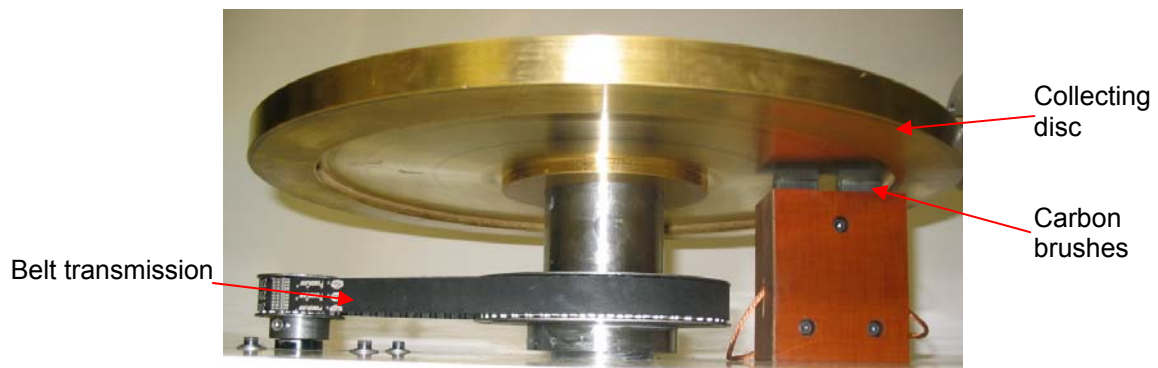


**Figure 21: Belt transmission and carbon brushes**

**Specifications:**

- Motor: DC Gear Motor-1/17 HP, 150 RPM
- Controller: Leeson Speedmaster® Washguard® Model 174107.00 (manufacturer: Leeson Electric Corporation)
- Belt transmission:  $z_1= 16$ ;  $z_2= 48$  ( $z_1/z_2= 0.33$ )
- Collecting disc
  - Inner diameter: 90 mm
  - Outer diameter: 400 mm
  - Maximum possible web area:  $119301.981 \text{ mm}^2$  ( $\sim 0.12 \text{ m}^2$ )

The relatively large outer diameter would allow producing brake discs for regular passenger cars (see Figure 22). The small inner diameter on the other hand could still allow the production of cutting, grinding and sanding pads. Therefore the disc dimensions were chosen to broaden the field of possible applications of the equipment.

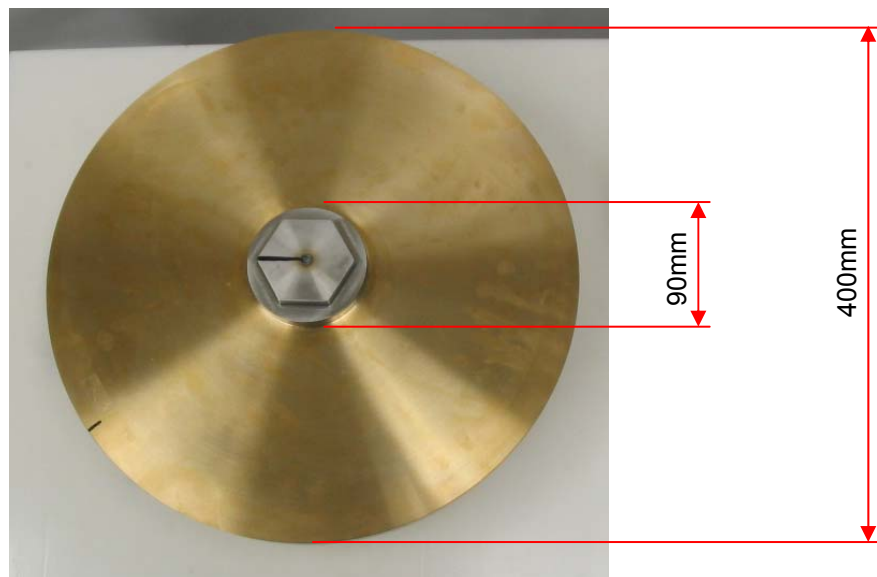


**Figure 22: Dimensions of the fiber collecting disc**

Figure 23 shows an image of fibers dispensed on the collecting disc. The fibers are standing upright, because of the still present electrostatic field. As soon as the

field is removed, the fibers will randomly fall down, when no adhesive layer is present on the disc surface.

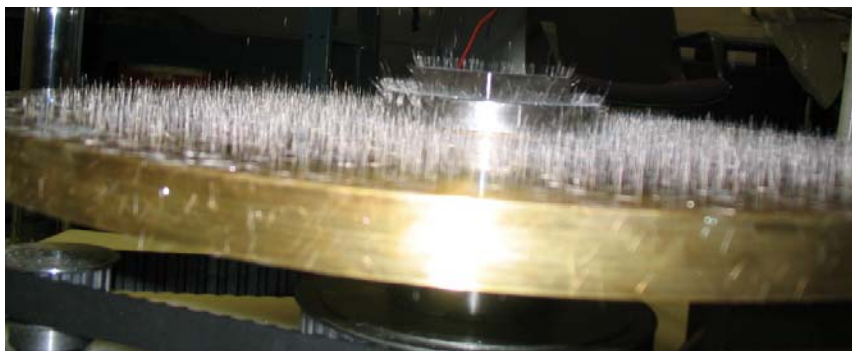


Figure 23: Collected fibers on the plate

#### 4.4. Fiber Lay-Down Mechanism

In order to achieve circumferential fiber orientation, the perpendicularly collected fibers, which are supported by adhesive, need to be re-oriented. The fiber re-orientation is done using a lay-down tube or rod (see Figure 24 and Figure 25).

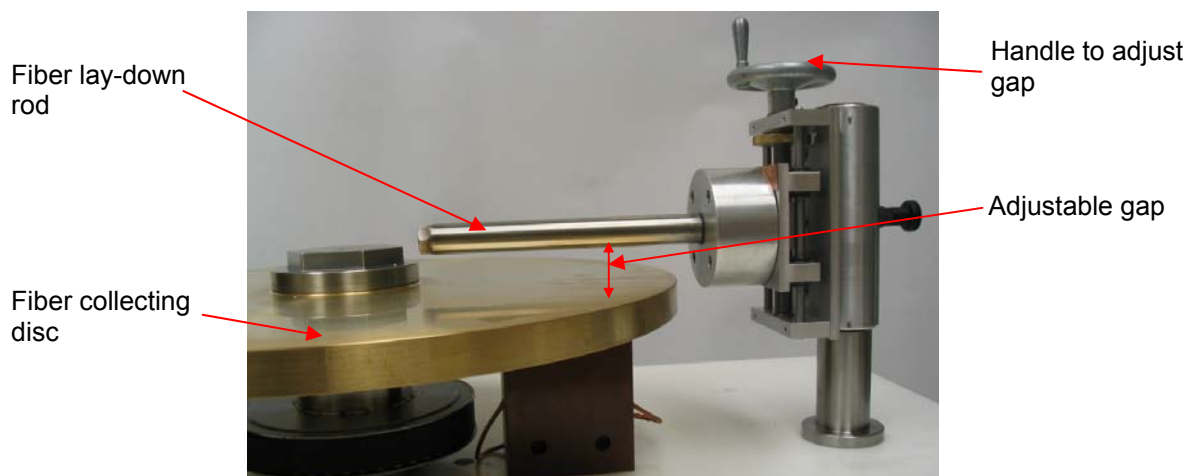
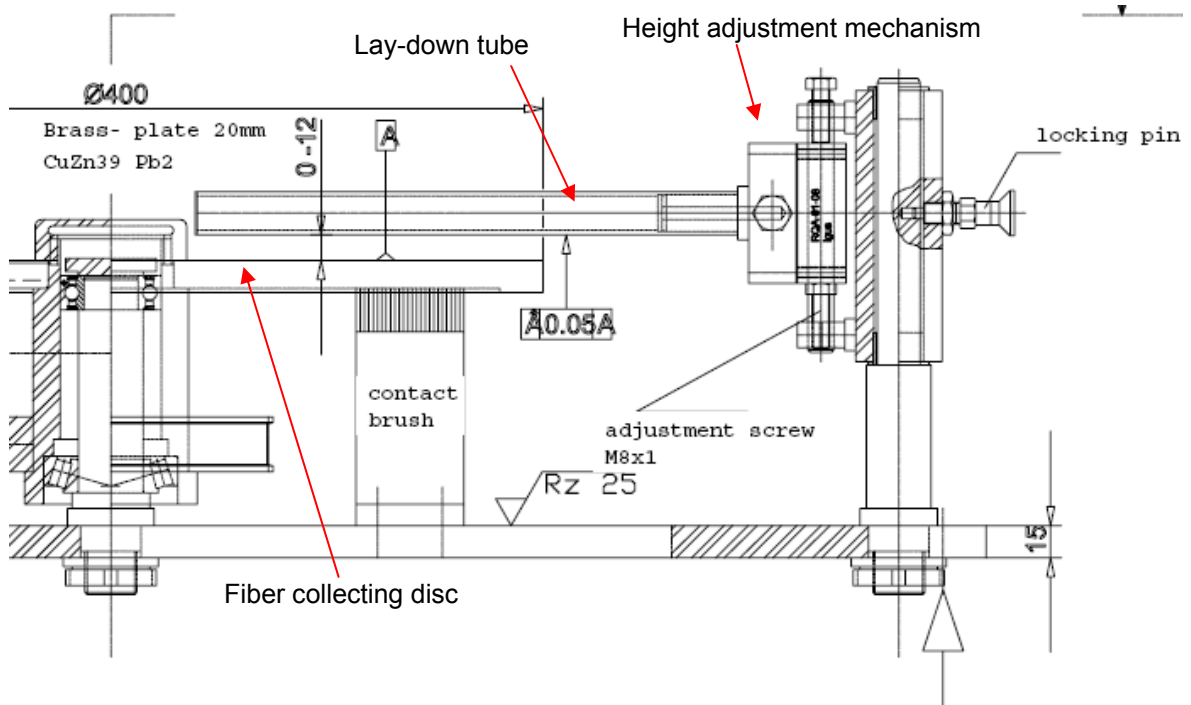


Figure 24: Tube and height adjustment of the tube

The tube itself remains static at a certain adjustable distance above the disc during fiber lay-down. The fibers, which are perpendicularly standing on the surface of the

disc, are moving under the tube and therefore being laid-down, when the gap between the plate and the tube is smaller than the fiber length. The adhesive must not be totally dry at the moment of lay-down.



**Figure 25: Engineering drawing of the fiber lay-down tube and height adjustment mechanism (side view) (dimensions in millimeter)**

The handle shown in Figure 24 controls the distance between the fiber collecting disc and the lay-down rod by moving the rod up or down through rotating the handle manually (see also Figure 25). The manual control of the lay-down rod could be automated if the system was to be upgraded.

For more convenient access to the produced web, the lay-down rod is designed to swing the tube away from the fiber collecting disc (see Figure 26 and Figure 19).



**Figure 26: Tube can be swung for better access to the disc and fiberweb after web formation is completed (e.g. remove web)**

## ***4.5 Problems and Solutions***

During the experiments several problems were experienced. These problems are detailed in the following sections. Beside the actual problem description, solutions which were applied or a possible solution, which can be realized in future research, are provided.

### **4.5.1 Fiber Dispenser**

The original plan was to use a fiber dispensing device from MAAG Flockmaschinen (see Figure 27). This “Hand-Shaker” has the disadvantage that all fiber dispensing parameters cannot be controlled. Initial experiments revealed that it is impossible to work with this device, since parameters regarding the fiber dispersion cannot be kept at a constant level. The second disadvantage was that this device does not allow uniform field line formation (see also Figure 15) due to dimension and shape mismatch with the fiber collecting disc as discussed earlier.

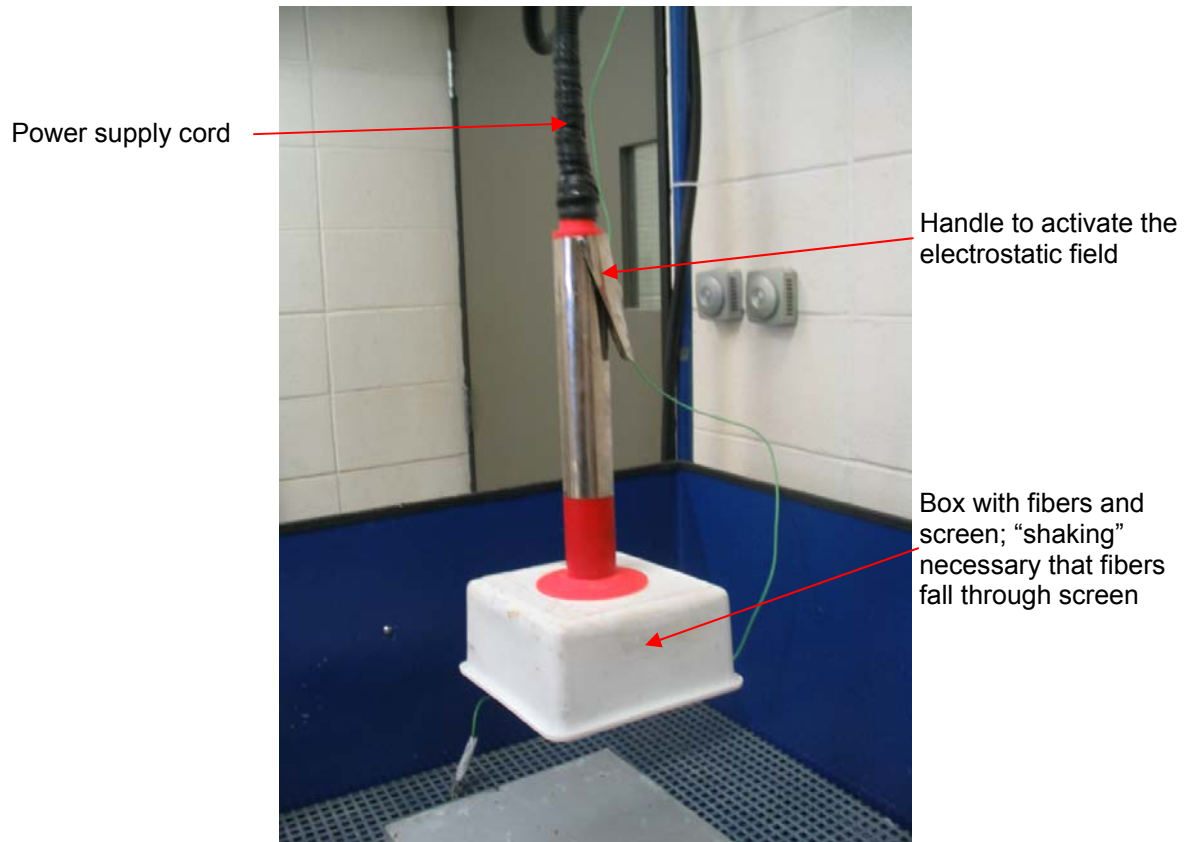


**Figure 27: "Hand- Shaker" from MAAG Flockmaschinen as a fiber dispenser**

The design of a more appropriate device to dispense the fibers into the electrostatic field was necessary. It was decided to design a dedicated new fiber dispenser with features as those used in flocking technology and which used cylindrical brushes to dose the amount of fibers which fall into the electrostatic field. Figure 28 shows the new fiber dispenser with corresponding electrode (see also section 4.2, page 27) and stand, which allows adjustment of the height of the electrode and dispenser.

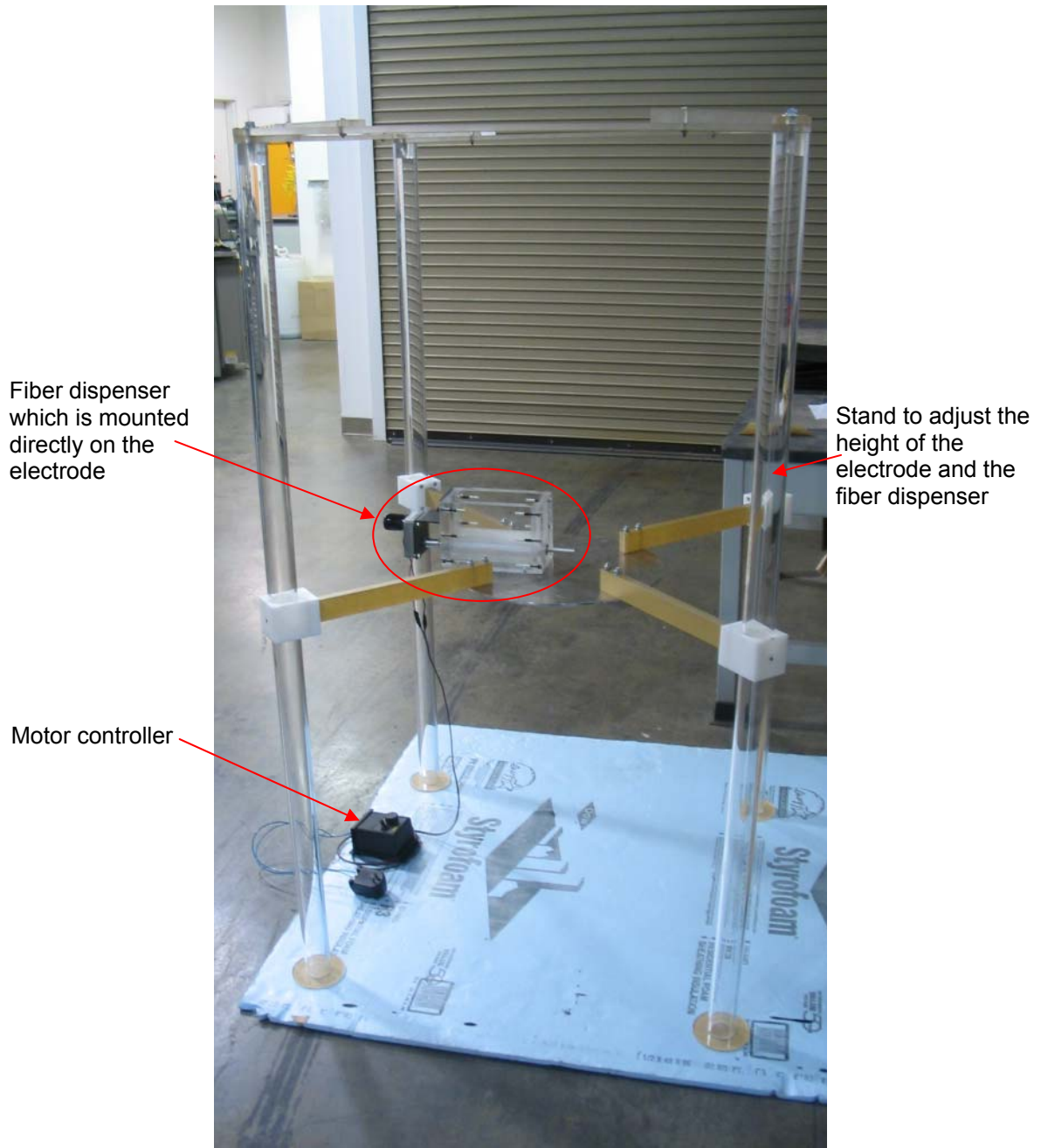


**Figure 28: New fiber dispenser with electrode and stand**

However, during experimentation some problems with the fiber dispenser occurred which can be summarized as follows:

1. discharge over the small motor which turns the brush (detailed described in section 4.5.2, page 42)

2. some minor electrostatic field irregularities around the screen (detailed described in section 4.5.3, page 43)
3. it is not possible to dispense carbon fibers (detailed described in section 5.4.1, page 56)

In order to produce disc shaped fiberwebs with equal fiber density, it is required to have a different fiber feed rate that is proportional to the disc radius. This can be solved by using a conical brush. For simplicity of the design and for the first experiments it was decided not to use a conical setup, since the focus was on fiber orientation at this stage. Therefore the fiberwebs, which the current machine setup can produce, have different densities: high density near the center of the disc and low densities away from the center of the disc. The design for a conical setup was done and can be realized (see Figure 29).

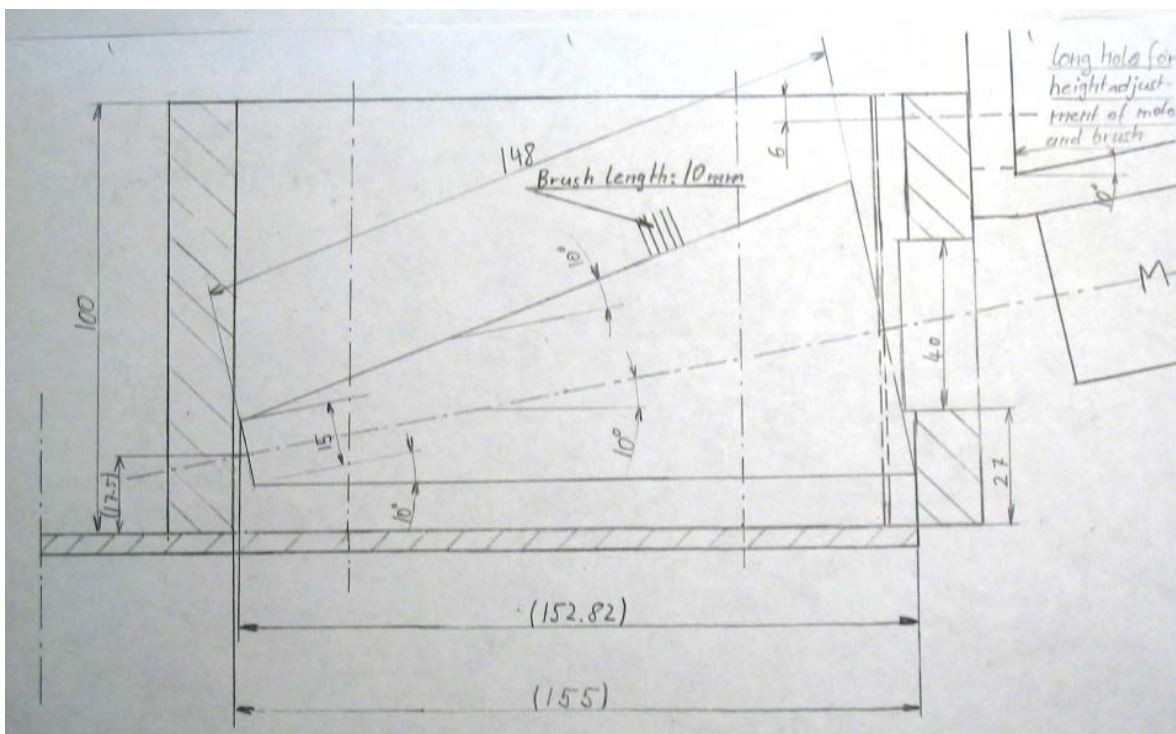
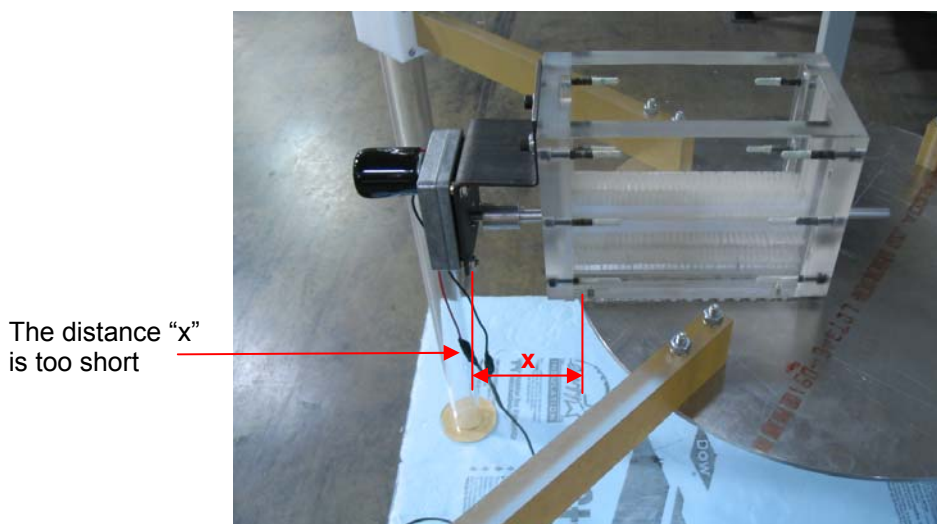


Figure 29: Conical brush and box design (dimensions in millimeter)

### 4.5.2 Motor Protection

Since the motor is mounted very close to the electrode and is connected to the electric ground through its wires, some discharge happened when the applied potential on the electrode exceeded 23kV.



**Figure 30: The motor is mounted very close to the electrode**

The problem was solved by (see Figure 31):

- increasing the distance between the motor and the electrode,
- replacing the aluminum shaft which turns the brush with a non-conductive material (plastic) and
- installing a plastic plate between the electrode and the motor to protect the motor from the electrostatic field.

With these modifications, it was possible to increase the potential of the electrode up to ~55kV, since there is no conductive connection between the motor and the fiber dispenser which provided some kind of electrostatic field protection.

The experiments showed that a lower potential leads to better fiber orientation (see chapter 6). This means that there is no need to further modify the equipment to increase the maximum possible potential of the electrode.

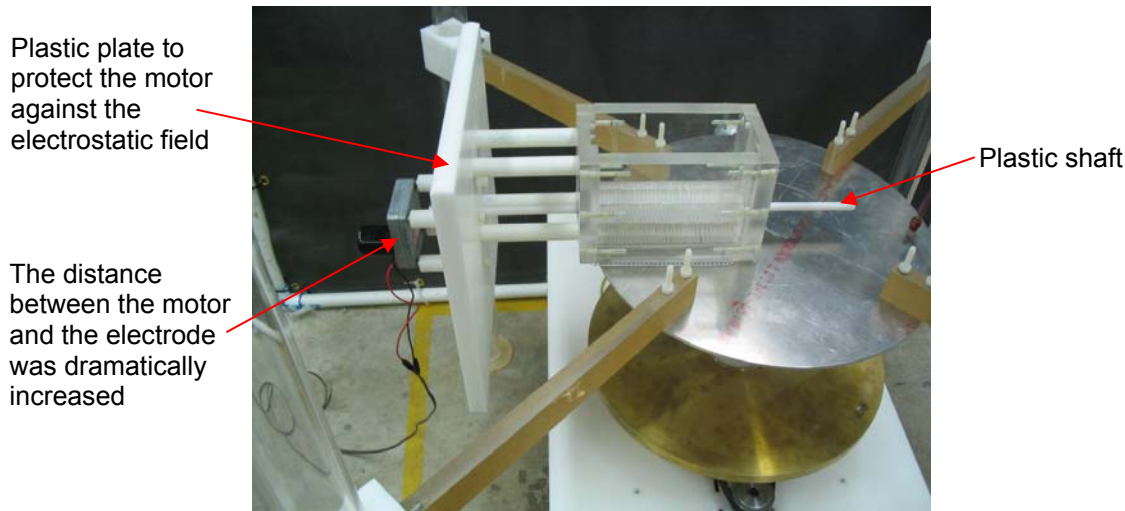


**Figure 31: Modified setup of the motor and fiber dispenser**

### 4.5.3 Electrostatic Field Formation and Uniformity

As it was explained before, there were tremendous irregularities in the electrostatic field when the “Hand Shaker” shown in Figure 27 was used for fiber dispersion. After developing the new fiber dispenser, which was done in accordance to the requirements stated in section 4.1, page 28, an almost uniform electrostatic field could be developed.

However, some minor irregularities were still present:

1. Some fibers were collected at the cap of the fiber collecting disc, since it was made out of metal and therefore locally increased the field strength, because of the lower distance to the upper electrode (see Figure 32).
2. Some fibers were agglomerated at the edges of the slot of the upper electrode (which is covered by the screen of the fiber dispenser) due to the sharp edges of the slot (see Figure 32).

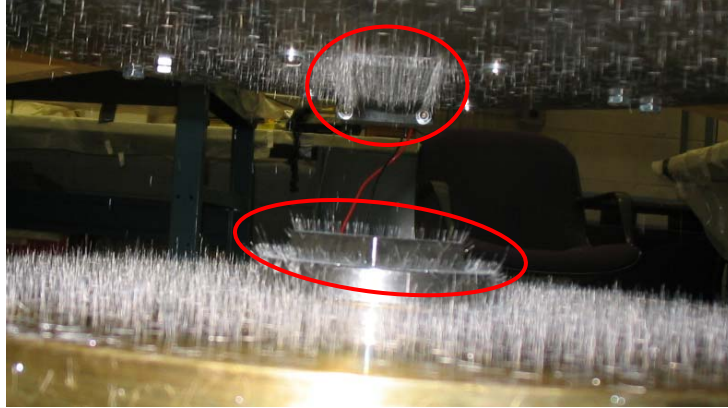


**Figure 32: Fiber agglomeration due to local irregularities of the electrostatic field**

The problems could be solved by:

1. Replacing the metal cap by a cap made out of plastic,
2. rounding the sharp edges of the slot and
3. additionally, all metal screws which were in contact with the electrode were replaced by plastic screws.

With these three changes, the field uniformity was satisfactory and the fiber agglomeration at the slot and at the cap could be reduced to an acceptable minimum.

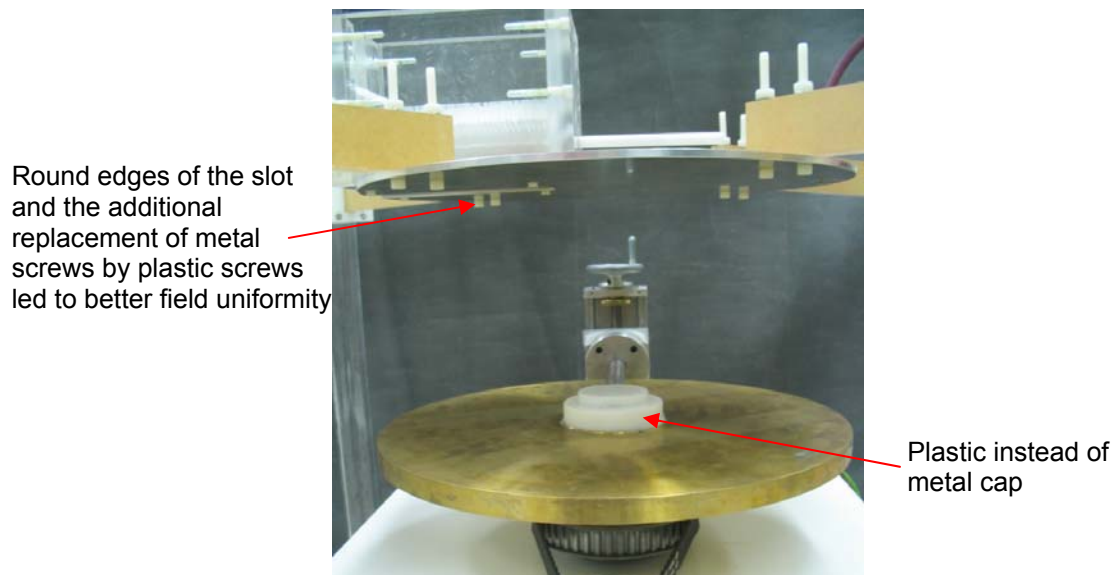


**Figure 33: Some metal parts were replaced by plastic materials**

#### 4.5.4. Fiber Lay-Down

The fibers hit the collecting disc perpendicularly or in an angle close to  $90^\circ$  to the disc surface and are then re-oriented by a lay-down tube. The diameter of the lay-down tube may have an influence on the lay-down characteristics, since these characteristics are depending on the relationship between the fiber length and the rod diameter (curvature). The original design provided a 20mm diameter rod.

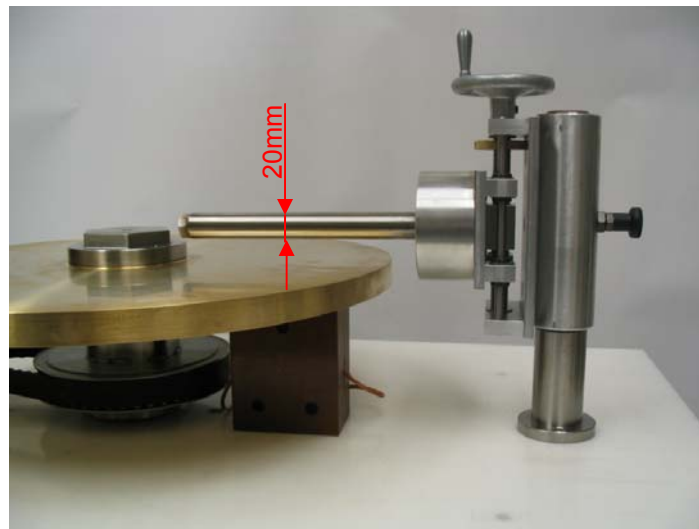


**Figure 34: Original design of the lay-down tube with a diameter of 20mm**

The assumption was that a smaller rod probably could have better lay-down characteristics, since the fiber length was only 5mm (see Figure 35). The lay-down system was re-designed to allow the change of the lay-down rod.

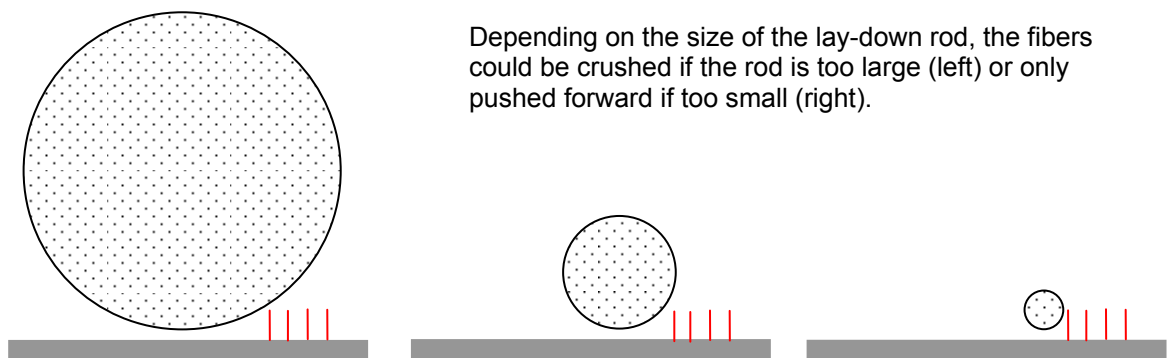


**Figure 35: Schematic showing the effect of lay-down rod diameter on the fiber lay-down characteristics**



**Figure 36: Modified design of the lay-down tube, which can carry all rod sizes up to  $\text{Ø}10\text{mm}$**

Generally it would be better if the lay-down rod could be used as a roller. Since there are different velocities depending on the radius of the disc, the roller needed to be divided into segments or needed to be conical with correct dimensions to match disc surface speed. In this work none of these options were investigated.

Since it was found that no significant differences in the lay-down characteristics of the fibers could be observed between the use of an  $\text{Ø}4.76\text{mm}$  rod or an  $\text{Ø}20\text{mm}$  rod, this does not mean that problems, when using extremely larger rods, can occur (see Figure 35 left). The design parameters of a cone that provides matching surface speed of the collecting disc are:

- small diameter: 15.6mm
- large diameter: 69.46mm
- length: 152.6mm
- cone angle:  $20^\circ$

At this stage it is not clear if a diameter of  $\sim 70\text{mm}$  would cause problems in the fiber lay-down of 5mm long fibers (see also Figure 35). This leads to the suggestion that different design parameters of the lay-down rod need to be investigated.

## 5. Experimental Work

The previous chapter described the equipment which was built to achieve the objective to design and build disc shaped fiberwebs with circumferential fiber orientation. This chapter addresses experimental runs designed to answer the following questions:

1. What experiments were carried out and which parameters were studied?
2. What was the sample collection method?
3. What could be learned from the experiments in order to design and improve the equipment? (see also section 4.5, page 38)
4. What future research needs to be conducted to improve the equipment and processing conditions? (see also chapter 9, page 111)
5. How the obtained samples were analyzed?

### 5.1 *Experimental Design*

To answer the above questions, sets of experimental runs were conducted with independent parameters that are believed to influence the web formation and fiber orientation. The following list includes the independent variables studied along with their values:

- Electric field strength
  - Distance of the electrodes ( $h_1=10\text{cm}$ ;  $h_2=20\text{cm}$ ;  $h_3=30\text{cm}$ )
  - Applied electrical potential ( $V_1=10\text{kV}$ ;  $V_2=20\text{kV}$ ;  $V_3=50\text{kV}$ )
- Rotational speed of the collecting disc ( $v_1=13\text{rpm}$ ;  $v_2=23.5\text{rpm}$ ;  $v_3=50\text{rpm}$ )
- The diameter of the lay-down rod ( $d_1=4.76\text{mm}$ ;  $d_2=9.4\text{mm}$ ;  $d_3=20\text{mm}$ )

The following parameters were kept constant for all runs conducted:

- Fiber dispensing parameters:
  - Fiber type: Polyamid; 15den;  $\text{Ø}=0.04315\text{mm}$ ; 5mm long (aspect ratio: 116)
  - Amount of Fibers in the fiber dispenser per sample: 0.5g
  - Brush rotational speed: 50rpm
  - Screen (round holes with  $\text{Ø } 3.175\text{mm}$ ; 40% open area, Aluminum)
- Sample placement procedure (described later)
- Fiber lay-down method: the distance between the lay-down rod and the turning disc was gradually decreased while the disc was turning; resulting in a “step wise” lay-down process of the fibers until a good contact between the rod and the fiberweb was established.

In all, 81 runs were performed (3x3x3x3). This constituted a full experimental design of the four parameters studied. Table 2 – Table 4 show the details of each run. The sample number is not sequential since sample had to be discarded on the initial trial. The Histogram Tables in Appendix I use the same numbers as indicated on the tables.

All experimental runs were carried out at the flocking laboratory of the Department of Textile Sciences, College of Engineering, University of Massachusetts, Dartmouth. The laboratory temperature and humidity were not controlled. This fact influences the experiments, which is more clearly described in sections 5.4.3, page 58 and 6, page 64.

Table 2: Design of Experiments for Ø 20mm lay-down rod

Design of Experiments for Ø 20mm lay-down rod				
Field Strength [kV/cm]	Distance [cm]	Potential [kV]	Disc Rotational Speed [rpm]	Sample Number
1,00	10	10	13	8
1,00	10	10	23,50	9
1,00	10	10	50	10
2,00	10	20	13	7
2,00	10	20	23,50	5
2,00	10	20	50	6
5,00	10	50	13	34
5,00	10	50	23,50	35
5,00	10	50	50	33
0,50	20	10	13	11
0,50	20	10	23,50	3
0,50	20	10	50	12
1,00	20	20	13	14
1,00	20	20	23,50	1
1,00	20	20	50	13
2,50	20	50	13	31
2,50	20	50	23,50	30
2,50	20	50	50	32
0,33	30	10	13	26
0,33	30	10	23,50	29
0,33	30	10	50	23
0,67	30	20	13	27
0,67	30	20	23,50	21
0,67	30	20	50	24
1,67	30	50	13	22
1,67	30	50	23,50	25
1,67	30	50	50	28

Table 3: Design of Experiments for Ø 9.4mm lay-down rod

Design of Experiments for Ø9.4mm lay-down rod				
Field Strength [kV/cm]	Distance [cm]	Potential [kV]	Disc Rotational Speed [rpm]	Sample Number
1,00	10	10	13	96
1,00	10	10	23,50	93
1,00	10	10	50	90
2,00	10	20	13	92
2,00	10	20	23,50	89
2,00	10	20	50	97
5,00	10	50	13	88
5,00	10	50	23,50	95
5,00	10	50	50	91
0,50	20	10	13	85
0,50	20	10	23,50	80
0,50	20	10	50	83
1,00	20	20	13	86
1,00	20	20	23,50	82
1,00	20	20	50	79
2,50	20	50	13	81
2,50	20	50	23,50	84
2,50	20	50	50	87
0,33	30	10	13	76
0,33	30	10	23,50	73
0,33	30	10	50	70
0,67	30	20	13	74
0,67	30	20	23,50	71
0,67	30	20	50	77
1,67	30	50	13	78
1,67	30	50	23,50	75
1,67	30	50	50	72

Table 4: Design of Experiments for Ø 4.76mm lay-down rod

Design of Experiments for Ø4.76mm Lay-Down Rod				
Field Strength [kV/cm]	Distance [cm]	Potential [kV]	Disc Rotational Speed [rpm]	Sample Number
1,00	10	10	13	42
1,00	10	10	23,50	48
1,00	10	10	50	45
2,00	10	20	13	43
2,00	10	20	23,50	40
2,00	10	20	50	47
5,00	10	50	13	46
5,00	10	50	23,50	44
5,00	10	50	50	41
0,50	20	10	13	52
0,50	20	10	23,50	49
0,50	20	10	50	55
1,00	20	20	13	57
1,00	20	20	23,50	54
1,00	20	20	50	51
2,50	20	50	13	50
2,50	20	50	23,50	56
2,50	20	50	50	53
0,33	30	10	13	63
0,33	30	10	23,50	66
0,33	30	10	50	60
0,67	30	20	13	65
0,67	30	20	23,50	59
0,67	30	20	50	62
1,67	30	50	13	61
1,67	30	50	23,50	64
1,67	30	50	50	58

## 5.2 Sample Collection Method

Since the only response is the fiber orientation, it was decided to form a small sample. The following steps were taken to ensure consistency and proper handling of the samples:

1. The fibers were collected at an exact position.
2. The lay-down method, described earlier, was followed.
3. The sample had to be carefully handled without disturbing the orientation.
4. The fiber orientation evaluation was conducted at North Carolina State University laboratories.

It was decided to use a sticky surface of address labels as a mean to anchor the fibers to the collecting surface. The labels were placed on the collecting disc with the sticky side on top (see Figure 37), so that fibers falling onto the sticky surface would be held and could be laid-down by the rod. The label itself was attached to the collecting disc, using a thin double sided tape.

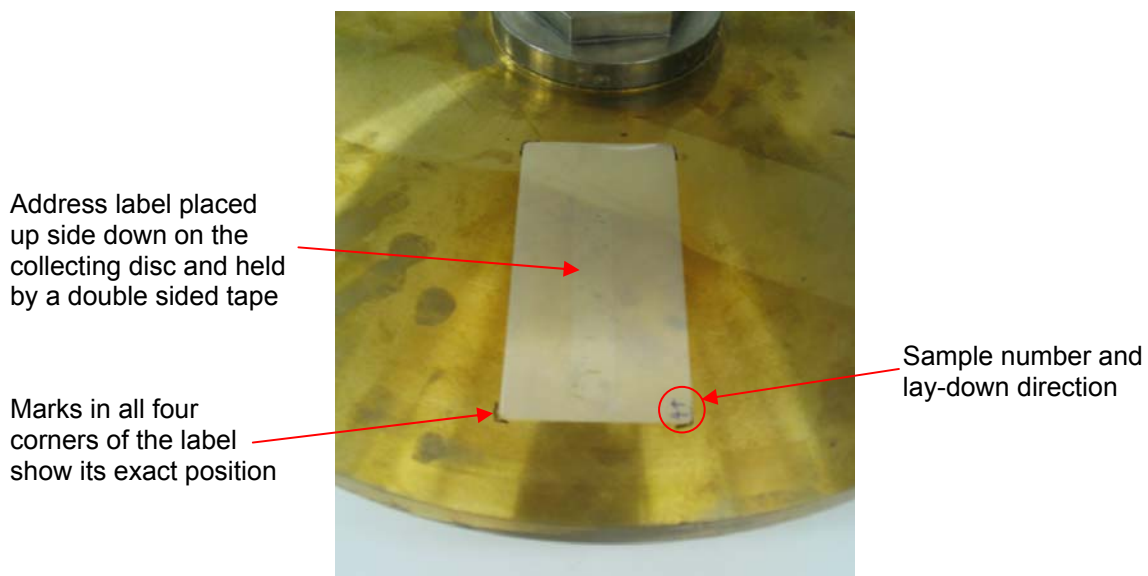
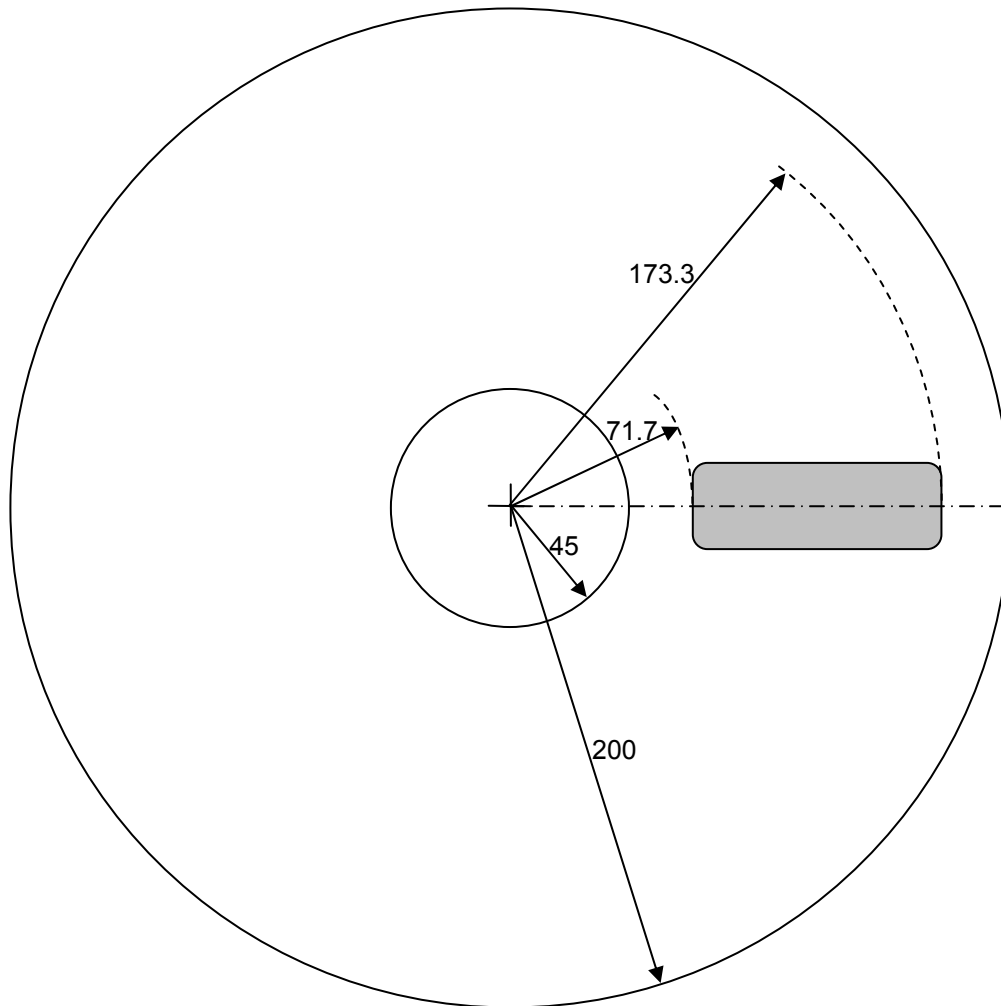


Figure 37: Sample placement on collecting disc

To ensure that each sample was collected at the same position, marks were drawn on the disc to show the position of the label. The location of the label on the collecting disc can be seen in Figure 38.



**Figure 38: Sample placement (grey) on the collecting disc (dimensions in millimeter)**

The label dimensions are as follows:

- length: 4in (101.6mm)
- width: 2in (50.8mm)
- area: 8sqin (5161.28mm<sup>2</sup>).

All samples were labeled at the same corner with a unique number and the direction of fiber lay-down for exact identification of each sample (see Figure 37) was recorded after they were retrieved from the disc.

### **5.3 Fiberwebs with Circumferential and z-Directional Fiber Orientation**

In the course of this work a special series of experiments were carried out. Table 5 shows the Design of Experiments for eight samples with z-directional fiber orientation. These samples have fibers oriented in the circumferential direction and fibers perpendicular to the collecting surface (z-direction).

**Table 5: Design of Experiments for samples with circumferential and z-directional fiber orientation**

<b>Design of Experiments for samples with z-directional fiber orientation</b>				
<b>Field Strength [kV/cm]</b>	<b>Distance [cm]</b>	<b>Potential [kV]</b>	<b>Disc Rotational Speed [rpm]</b>	<b>Sample Number</b>
1,00	10	10	13	102
1,00	10	10	50	104
5,00	10	50	13	103
5,00	10	50	50	101
0,33	30	10	13	107
0,33	30	10	50	105
1,67	30	50	13	106
1,67	30	50	50	108

**Sample preparation:**

1. Fibers were dispensed and laid-down as described before.
2. After the fiber lay-down, an approximate equal amount of fibers with exactly the same process parameters was dispensed. The fibers were left in the z-direction without laying-down.

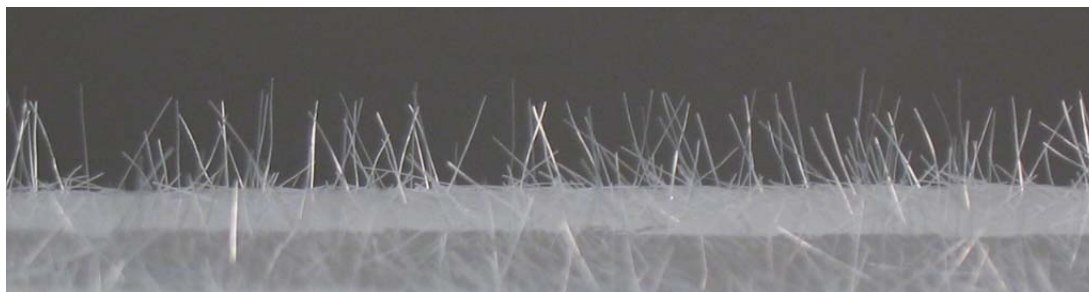


**Figure 39: Picture showing the z-directional (“standing”) fibers**

These samples show that it is possible to align fibers in circumferential direction and in z-direction using the developed equipment. This demonstrates the flexibility of the apparatus which could be highly beneficial, especially in widening the field of applications and to customize properties of fiberwebs. Other fiber orientation in different directions could be produced with modification of electrostatic field direction through appropriate design of electrodes and fiber dispensing systems.

## **5.4 Problems**

During the experiments a variety of problems appeared. These problems are addressed in the following sections.

### 5.4.1 Carbon Fiber Separation

In chapter 1, page 1 the application of carbon fiber brake discs for passenger cars was mentioned as one field where the developed device could be used. Therefore experiments with carbon fibers were carried out. Unfortunately the fiber dispenser was not able to separate the carbon fibers and feed them into the electrostatic field. Turning the brush of the fiber dispenser led to carbon fiber entanglement with the bristles of the brush and carbon fiber agglomeration between the lines of bristles.

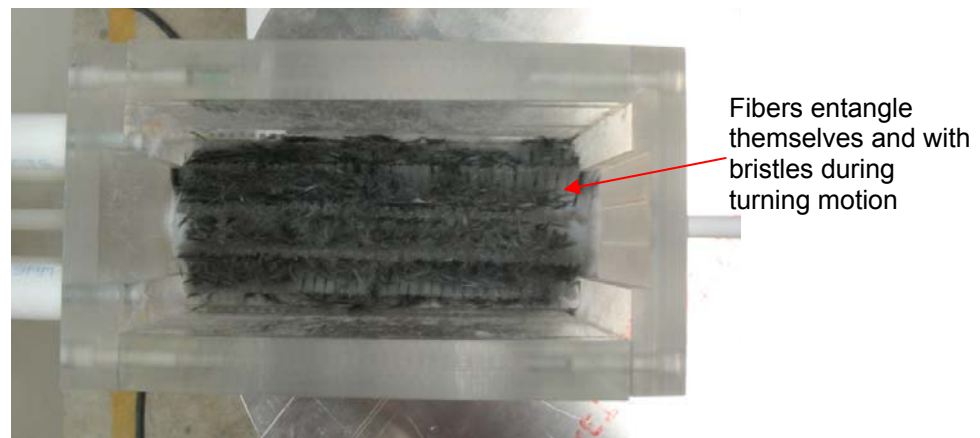


**Figure 40: Carbon fibers cannot be treated with the current technology available**

It is assumed that the fineness of the carbon fibers is too high (diameter too small) causing the individual fibers to stick together due to the extremely high surface area. Further research is needed to allow carbon fiber separation. A different fiber dispensing system using an aspirator, tow of individualized filaments, and a cutting system may resolve this issue.

### 5.4.2 Web Thickness

Major problems are seen in the area of building up a significant web thickness. The fiber lay-down rod (or even if it might be possible to use a segmented or conical roller) needs to touch and press on the fiber collecting disc in order to

“really” re-orient the fibers. If the rod is not physically touching the disc, the fiber re-orientation may be unsuccessful, depending on the type of adhesive and the bending rigidity of the fiber.

These two parameters, type of adhesive and the fiber bending rigidity, may cause fiber bounce back. Bounce back means that fibers may return to their original positions after the lay-down rod passes the fibers. Since the fiber is sticking with a portion of its length into the adhesive layer (called “fiber root”), this small portion needs to be re-oriented in order to successfully re-orient the whole fiber, and set it in the plane (or parallel plane) of the collecting surface.

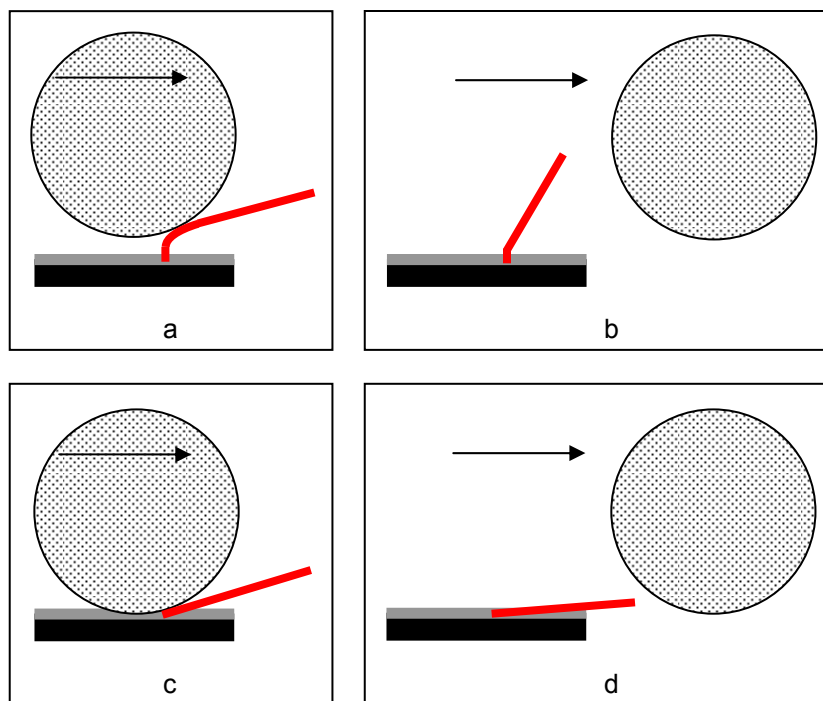


**Figure 41 (a): The rod (patterned) does not touch the adhesive layer (grey), therefore the fiber (red) will not be re-oriented, resulting in an unsuccessful lay-down process (b). (c): If the rod is in touch with the adhesive layer, the chance of successful fiber re-orientation is higher (d).**

During the experiments no problem was posed from the rod touching the adhesive layer and the fiber collecting disc, since the adhesive layer of the labels was extremely small.

### 5.4.3 Environmental Conditions

The outside climate changed dramatically during the days the experiments were carried out. Also, it was not possible to control temperature and humidity in the lab. The change in humidity had huge impact on the characteristics of the fiber movement in the electrostatic field. Since the moisture content in the surrounding air determines the ability of the fiber to be charged by the electrode, differences in humidity lead to variations in fiber behavior in the electrostatic field [20].

Usually when a charged fiber hits the collecting disc it is discharged and should bounce back to the upper electrode if it does not stick to the disc. In the experiments carried out for this work, this effect was not seen; except on one day as a result in climate change. The effect of fiber movement back to the upper electrode resulted in a much higher fiber density on the sticky surface of the label (the collected samples), because fibers moved up and down in the electrostatic field until they found rest on the sticky label.

Generally, this effect is not problematic, since in a fully developed system the whole surface is coated with adhesive material which holds the fibers down. For the interpretation of the data obtained from the experiments, the effect described above must be considered, because it eliminates the total number of fibers as a means of comparing different samples. Note: the effect has no influence on the fiber orientation, only on the fiber density.

Furthermore the experiments showed that low field strength, meaning a high distance between the electrodes and/or low potential, leads to better fiber orientation on the plate. On the other hand low field strength means that the fibers are moving slower from the upper electrode to the collecting disc and are therefore more subject to be blown away by slight air movement in the room, e.g. when a person is walking near the experimental setup. It was observed that a higher number of fibers were blown away when the field strength was low, compared to

experiments with high field strength. Again: this effect has no influence on the fiber orientation of the collected samples, only on the fiber density.

It is suggested to enclose the experimental setup with a plastic foil so that the fiber loss due to air movement can be eliminated.

### **5.5 Measurement of Fiber Orientation**

As already mentioned in section 5.2 page 53 the samples were collected on labels (4" x 2"). These labels were placed under light microscopy to capture magnified images of the samples.



**Figure 42: Baush & Lomb Monozoom-7 light microscope with monitor and video printer**

The Baush & Lomb Monozoom-7 Light Microscope with monitor and video printer, available at the Physical Testing Lab, College of Textiles, North Carolina State

University (see Figure 42), was used for this purpose. Such a magnified photograph is shown in Figure 43.

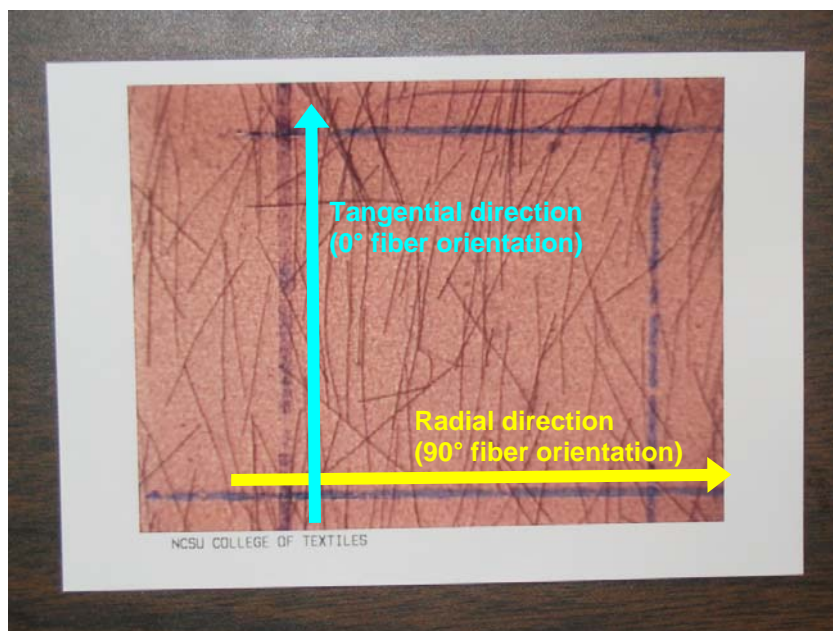


**Figure 43: Magnified image of a collected sample**

The blue square on the image represents 1cm<sup>2</sup> in real size. A transparent plastic foil with the square drawn on the sample was placed on the location where the image should be taken in a way that the lines of the square were in radial and tangential direction of the collecting disc respectively (see Figure 43). In this way, the angle of each fiber within the square could be measured with respect to 0° tangential (circumferential) direction.

From each sample (label), three different images were taken as illustrated in Figure 44.

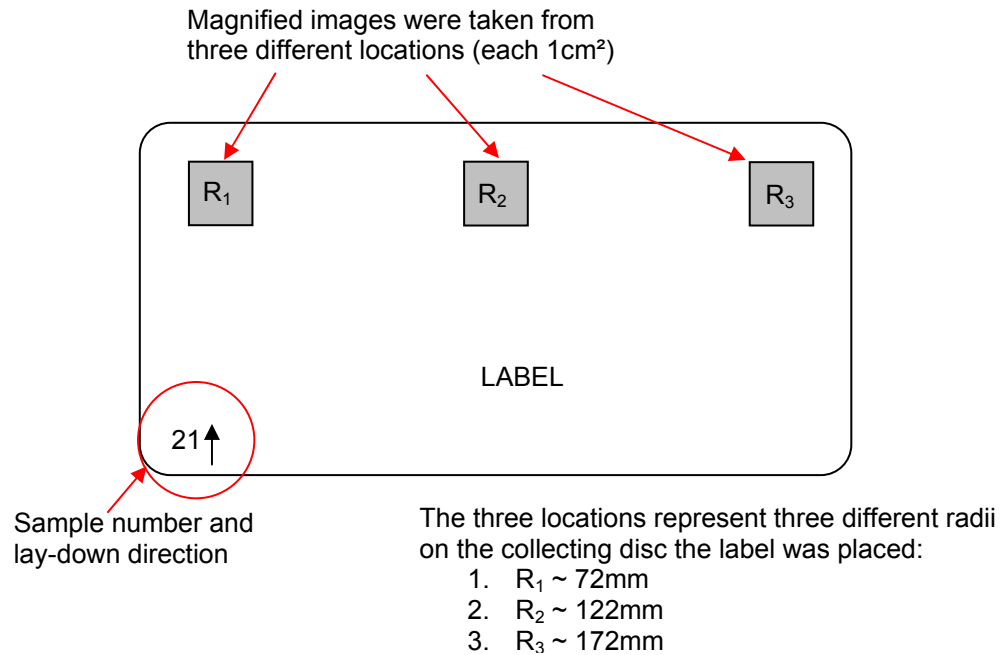


**Figure 44: Schematic of the sample and the locations the magnified photographs were taken for fiber counting**

The fibers were considered to be in the 1cm<sup>2</sup> square area when the center (middle) of the fiber was in the area. The angle was measured between 0° (circumferential direction) and the tangent of the fiber at its center (see Figure 45).

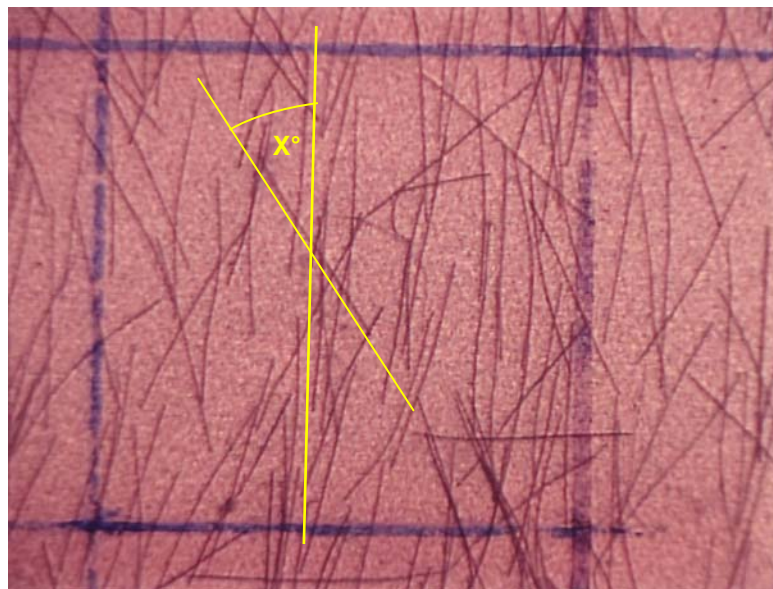


**Figure 45: Fiber angle measurement**

Each fiber within the 1cm<sup>2</sup> area was assigned to a specific class according to the following classification:

- $0^\circ \dots \leq 10^\circ$ , in the following termed as  $5^\circ$
- $< 10^\circ \dots \leq 20^\circ$ , in the following termed as  $15^\circ$
- $< 20^\circ \dots \leq 30^\circ$ , in the following termed as  $25^\circ$
- $< 30^\circ \dots \leq 40^\circ$ , in the following termed as  $35^\circ$
- $< 40^\circ \dots \leq 50^\circ$ , in the following termed as  $45^\circ$
- $< 50^\circ \dots \leq 60^\circ$ , in the following termed as  $55^\circ$
- $< 60^\circ \dots \leq 70^\circ$ , in the following termed as  $65^\circ$
- $< 70^\circ \dots \leq 80^\circ$ , in the following termed as  $75^\circ$
- $< 80^\circ \dots \leq 90^\circ$ , in the following termed as  $85^\circ$

where  $0^\circ$  means circumferential direction and  $90^\circ$  means radial direction of the fibers.

The data for each sample was then collected in the form of tables with the following format:

**Table 6: Example of fiber orientation distribution data**

<b>Sample Number: 1</b>					
<b>Angle</b>	<b>Radius [mm]</b>			<b>Number of Fibers</b>	<b>% Number of Fibers</b>
	<b>~72</b>	<b>~122</b>	<b>~172</b>		
$0^\circ \dots \leq 10^\circ$ ( $5^\circ$ )	15	8	6	<b>29</b>	<b>33.33</b>
$< 10^\circ \dots \leq 20^\circ$ ( $15^\circ$ )	4	6	8	<b>18</b>	<b>20.69</b>
$< 20^\circ \dots \leq 30^\circ$ ( $25^\circ$ )	6	4	3	<b>13</b>	<b>14.94</b>
$< 30^\circ \dots \leq 40^\circ$ ( $35^\circ$ )	8	0	2	<b>10</b>	<b>11.49</b>
$< 40^\circ \dots \leq 50^\circ$ ( $45^\circ$ )	2	5	1	<b>8</b>	<b>9.20</b>
$< 50^\circ \dots \leq 60^\circ$ ( $55^\circ$ )	0	1	1	<b>2</b>	<b>2.30</b>
$< 60^\circ \dots \leq 70^\circ$ ( $65^\circ$ )	2	1	0	<b>3</b>	<b>3.45</b>
$< 70^\circ \dots \leq 80^\circ$ ( $75^\circ$ )	1	1	0	<b>2</b>	<b>2.30</b>
$< 80^\circ \dots \leq 90^\circ$ ( $85^\circ$ )	1	1	0	<b>2</b>	<b>2.30</b>
<b>Total</b>	<b>39</b>	<b>27</b>	<b>21</b>	<b>87</b>	<b>100</b>

Data tables for all samples can be found in Appendix I: Fiber Distribution Data Tables, page 117.

## **5.6 Statistical Analysis**

The obtained data were analyzed using factorial Analysis of Variance (ANOVA). SAS 9.1.3 was used to perform the ANOVA with the following settings:

- Independent variables:
  - Disc rotational speed
  - Electrode distance
  - Electrostatic potential
  - Lay-down rod diameter
- Dependent variable: percent number of fibers at 5°
- The standard model with effects up to three way interactions was performed.
- Plots for the dependent observed means (percent number of fibers at 5°) for the main effects and two way interactions were drawn.
- Significance level: 0.05
- The analysis considered all 81 runs.

## 6. Results and Discussion

The following sections summarize the data obtained from the experiments and will provide information to interpret the different parameters, which were studied:

1. electrostatic field distance ( $h_1=10\text{cm}$ ;  $h_2=20\text{cm}$ ;  $h_3=30\text{cm}$ )
2. applied electrical potential on electrode ( $V_1=10\text{kV}$ ;  $V_2=20\text{kV}$ ;  $V_3=50\text{kV}$ )
3. collecting disc rotational speed ( $v_1=13\text{rpm}$ ;  $v_2=23.5\text{rpm}$ ;  $v_3=50\text{rpm}$ )
4. diameter of lay-down rod ( $d_1=4.76\text{mm}$ ;  $d_2=9.4\text{mm}$ ;  $d_3=20\text{mm}$ )

Graphs of the parameters with significant effect are shown in this chapter, however all graphs are included in Appendix II: Fiber Distribution Histograms, page 145.

As it was explained before in section 5.4.3, page 58, the data cannot be interpreted using the total number of fibers, since the number of fibers in each collected sample is not constant. However, the percent number of fibers can be used for comparison, to eliminate the differences in number of fiber collected in each sample. The samples which are affected by the “climate effect” are the samples collected on Wednesday January 18, 2006: samples 21-35 and samples 40-48.

To support the conclusions obtained from the observation of the histograms, a factorial Analysis of Variance (ANOVA) was performed, which statistically confirms observed trends from the histograms. Since the target of the developed equipment is to produce disc shaped fiberwebs with circumferential orientation, only the “percent number of fiber”-values from the first class of the fiber distribution ( $0^\circ \dots \leq \pm 10^\circ$  or  $5^\circ$ ) were considered as a response when performing the ANOVA analysis. The different sections below show the effects of the parameters studied and their interactions on the “percent number of fibers at  $5^\circ$ ”. The results of General Linear Model (GLM) procedure are summarized in Table 7 and will be referred to in the corresponding sections:

The GLM Procedure					
Class Level Information					
Class	Levels	Values			
Rod_Diameter__mm_	3	4.76	9.4	20	
Distance__cm_	3	10	20	30	
Potential__kv_	3	10	20	50	
Disc_velocity__rpm_	3	13	23.5	50	
Number of Observations Read		81			
Number of Observations Used		81			
14:32 Saturday, March 18, 2006					
The GLM Procedure					
Dependent Variable: __Number_of_Fibers_at_5_degrees % Number of Fibers at 5 degrees					
Source	DF	Sum of Squares	Mean Square	F Value	Pr > F
Model	64	7582.861027	118.482204	4.70	0.0006
Error	16	403.744814	25.234051		
Corrected Total	80	7986.605841			
R-Square	Coeff Var	Root MSE	__Number_of_Fibers_at_5_degrees Mean		
0.949447	16.95306	5.023351	29.63093		
Source	DF	Type III SS	Mean Square	F Value	Pr > F
Disc_velocity__rpm_	2	2886.736098	1443.368049	57.20	<.0001
Distance__cm_	2	322.029948	161.014974	6.38	0.0092
Potential__kv_	2	1430.238479	715.119240	28.34	<.0001
Rod_Diameter__mm_	2	218.902545	109.451272	4.34	0.0313
Distance_*Disc_Veloc	4	363.641328	90.910332	3.60	0.0281
Potential*Disc_Veloc	4	734.333738	183.583434	7.28	0.0015
Rod_Diame*Disc_Veloc	4	152.594366	38.148591	1.51	0.2458
Distance_*Potential_	4	39.256140	9.814035	0.39	0.8135
Rod_Diame*Distance__	4	186.677949	46.669487	1.85	0.1688
Rod_Diame*Potential_	4	216.811308	54.202827	2.15	0.1219
Distan*Potent*Disc_V	8	238.965275	29.870659	1.18	0.3667
Rod_Di*Distan*Disc_V	8	164.799467	20.599933	0.82	0.5993
Rod_Di*Potent*Disc_V	8	295.953631	36.994204	1.47	0.2446
Rod_Di*Distan*Potent	8	331.920757	41.490095	1.64	0.1890

**Table 7: General Linear Model (GLM) procedure of the factorial ANOVA**

When interpreting the ANOVA results in the following sections, 95% confidence interval is assumed, meaning that parameters or the interaction between parameters can be interpreted as statistically significant for forming fiberwebs with circumferential fiber distribution, when the corresponding p-value (see “Pr>F” column in Table 7) is lower than 0.05.

The graphs, which are shown in the following sections, for the main effects and first order interactions, are generated from all 81 runs. Although, the ANOVA

analysis does not consider the whole fiber distribution, the fiber distribution histograms are still important when evaluating the obtained data.

### 6.1 *Distance between the two electrodes*

Looking at Table 7, the p-value for “Distance” is 0.0092, meaning that the distance between the two electrodes is statistically significant for forming fiberwebs with circumferential fiber orientation.

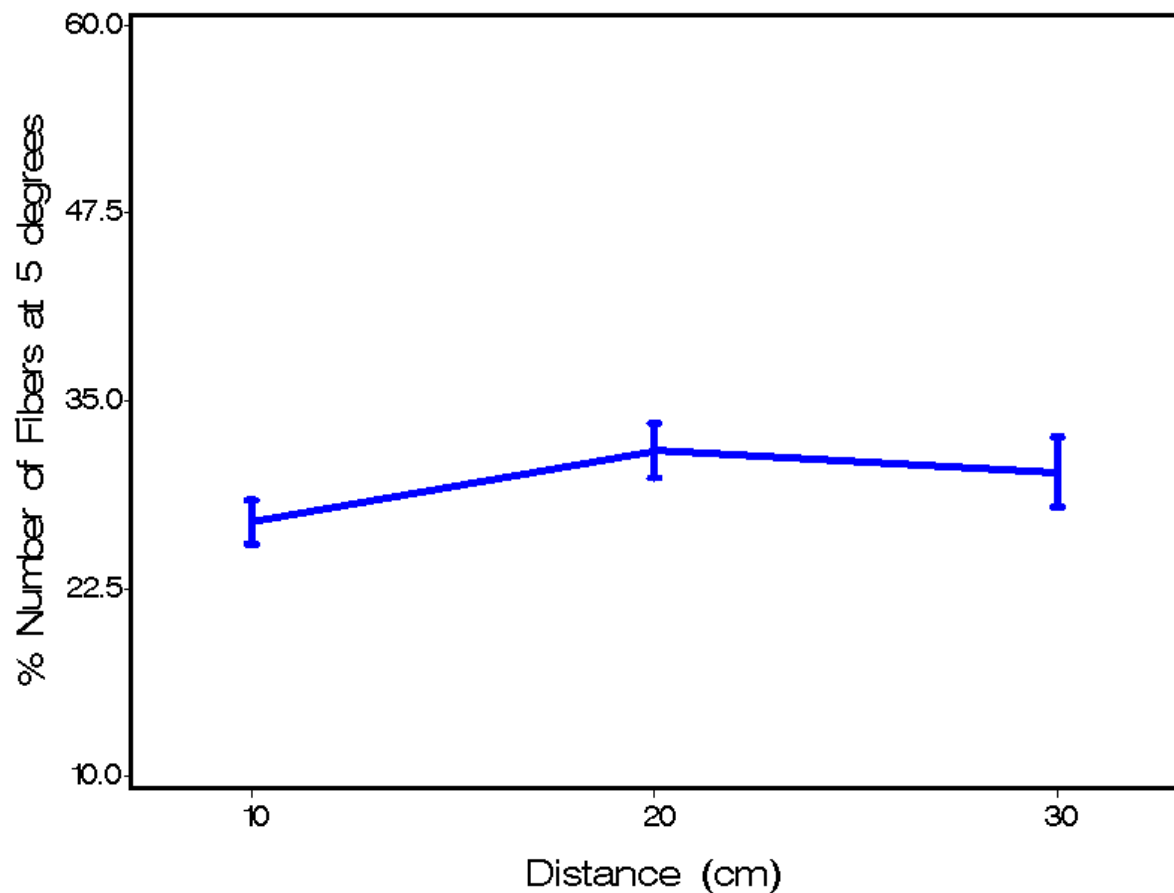


**Figure 46: Percent number of fibers at 5° corresponding to the electrostatic field distance**

Figure 46 shows that a higher electrostatic field distance supports a better fiber orientation in circumferential direction. The optimal distance seems to be around

20cm, since the “percent number of fibers at 5°” falls slightly when increasing the distance beyond 20cm.

When looking at the fiber orientation distribution diagrams, the same trend can be seen. Figure 47 clearly shows that high field distances support good fiber orientation in circumferential direction. Other parameters shown in Figure 47 are also highly supporting circumferential orientations (low potential; high disc rotational speed), as will be discussed in the next sections.

The other levels of potential and disc rotational speed caused the distance effect on fiber orientation to behave differently than the trend seen in Figure 47. Figure 48 shows the fiber orientation distribution at a very low disc rotational speed, and low potential, which promoted fiber orientation in circumferential direction. It can be observed that the better fiber orientation distribution is achieved with 20cm as compared to 30cm electrostatic field distance. The same is true for the data of Figure 49 where the disc rotational speed is high (promotes target orientation) and the potential is also high (disrupt desired orientation). These observations support the previous conclusion that the optimal value of the electrostatic field distance is around 20cm.

When both parameters (disc rotational speed and electrostatic potential) are set at disadvantageous levels, as shown in Figure 50, the desired fiber orientation distribution was not achieved for any of the three distances.

It can also be concluded from the p-value and from the fiber distribution observation that the electrostatic field distance is important for achieving the desired circumferential fiber orientation, but not as important as other parameters. Comparing the p-values, the disc rotational speed and the electrostatic potential are much more important for good fiber orientation in circumferential direction, than the distance.

However, a distance around 20cm is beneficial to circumferential fiber orientation. A higher distance between the two electrodes means lower field strengths at

constant potential. Since the field strength determines the velocity of the fibers during their movement from the fiber dispensing electrode to the fiber collecting electrode, lower field strength leads to lower velocities of the fibers. It seems that a low velocity supports fiber orientation in the electrostatic field, since the fibers have more time for orientation in the electrostatic field. It also seems that any increase in the distance between electrodes beyond 20cm did not improve the fiber orientation in the circumferential direction, since 20cm provided enough time for the fibers to orient themselves in the field direction.

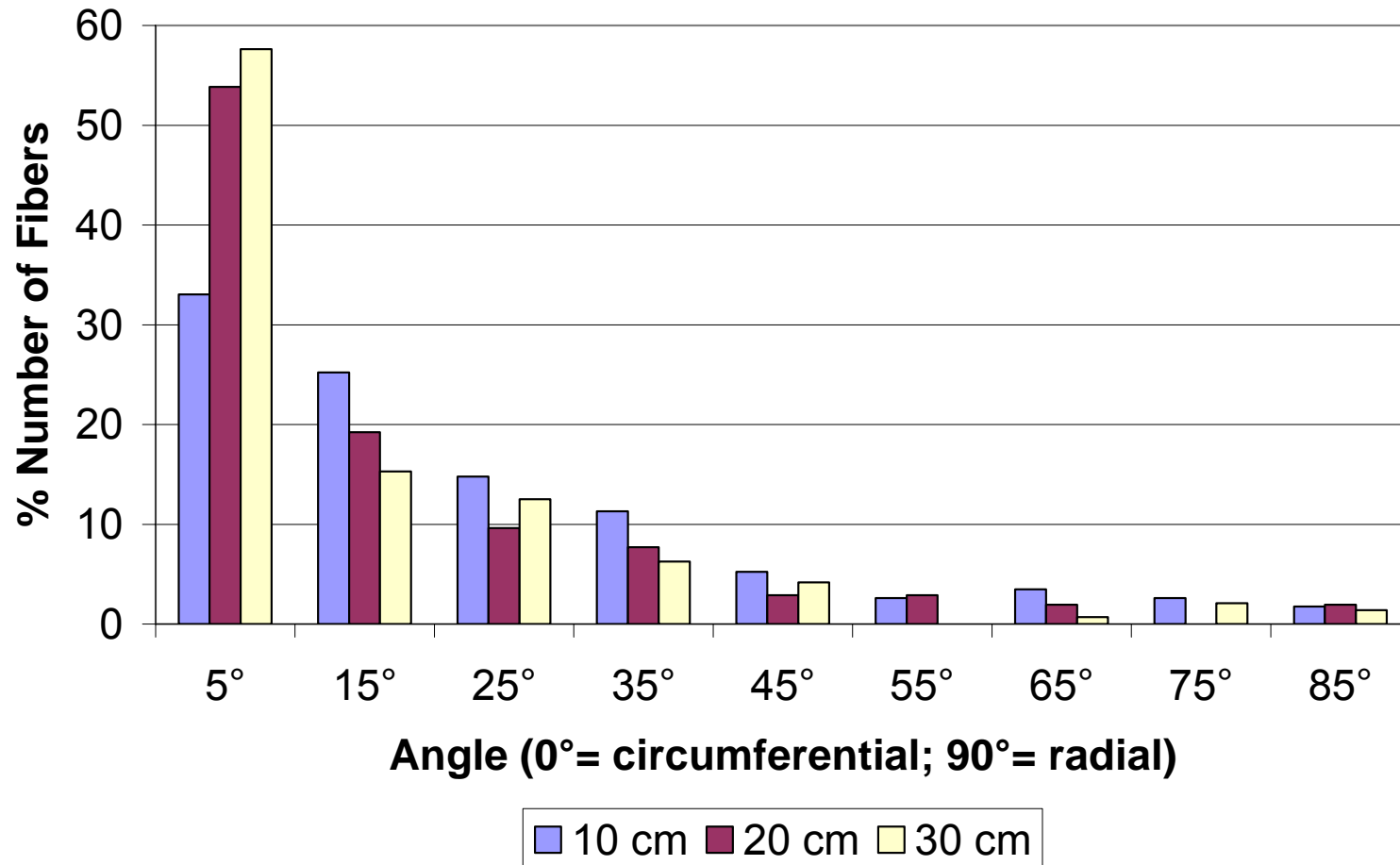


Figure 47: Fiber distribution histogram depending on the electrostatic field distance at 50rpm disc speed / 10kV electrostatic potential / 20mm lay-down rod

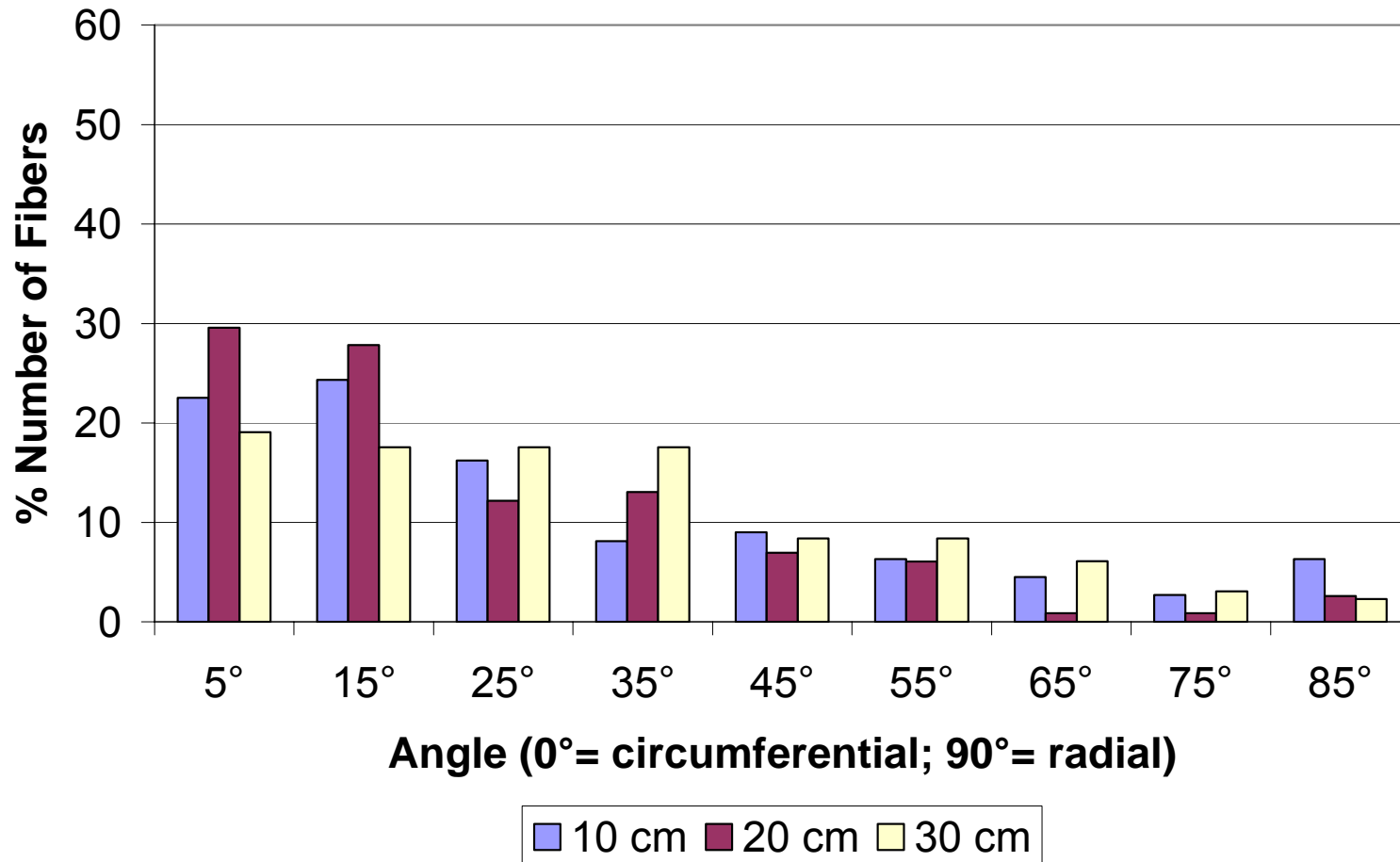


Figure 48: Fiber distribution histogram depending on the electrostatic field distance at 13rpm disc speed / 10kV electrostatic potential / 20mm lay-down rod

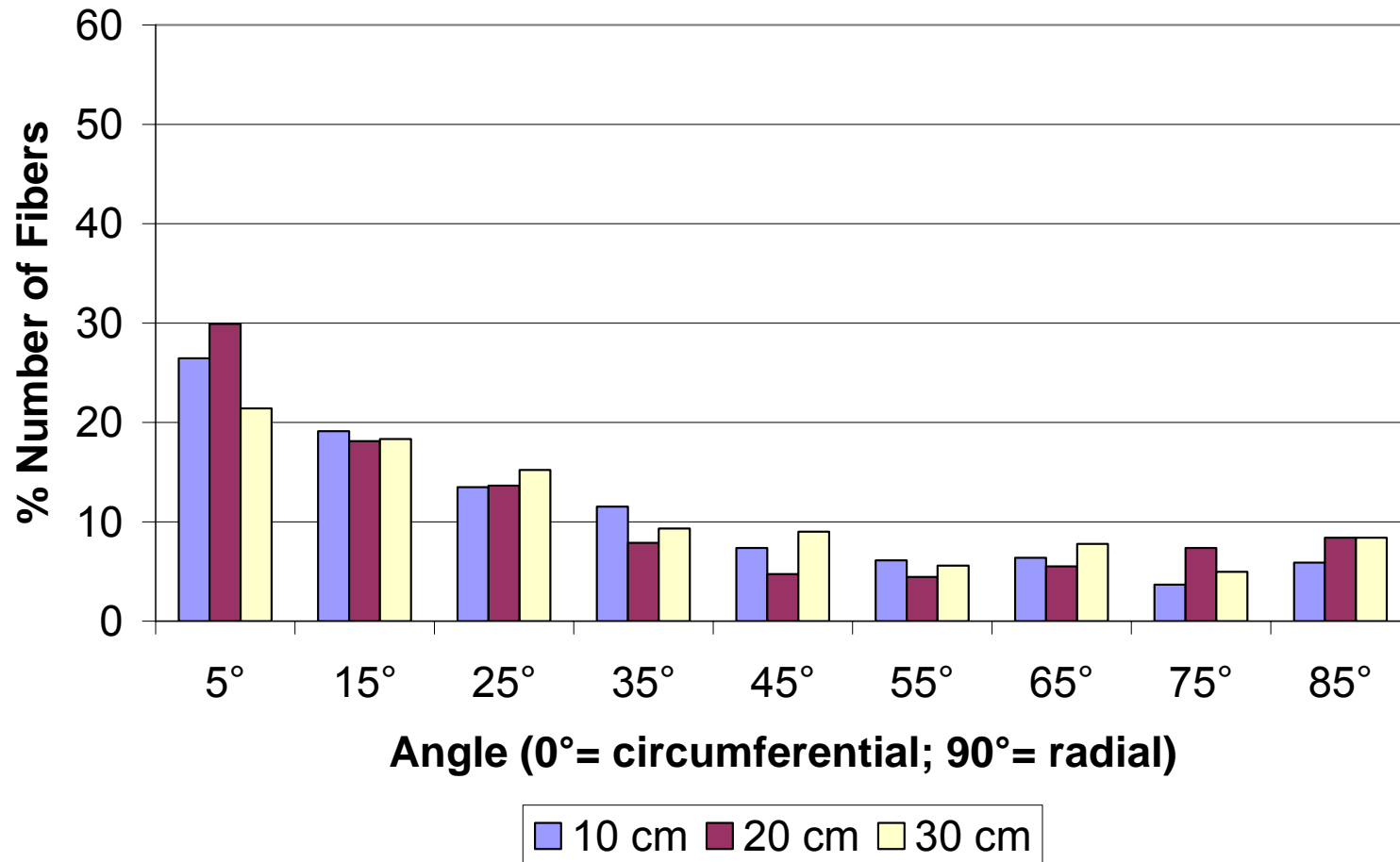


Figure 49: Fiber distribution histogram depending on the electrostatic field distance at 50rpm disc speed / 50kV electrostatic potential / 20mm lay-down rod

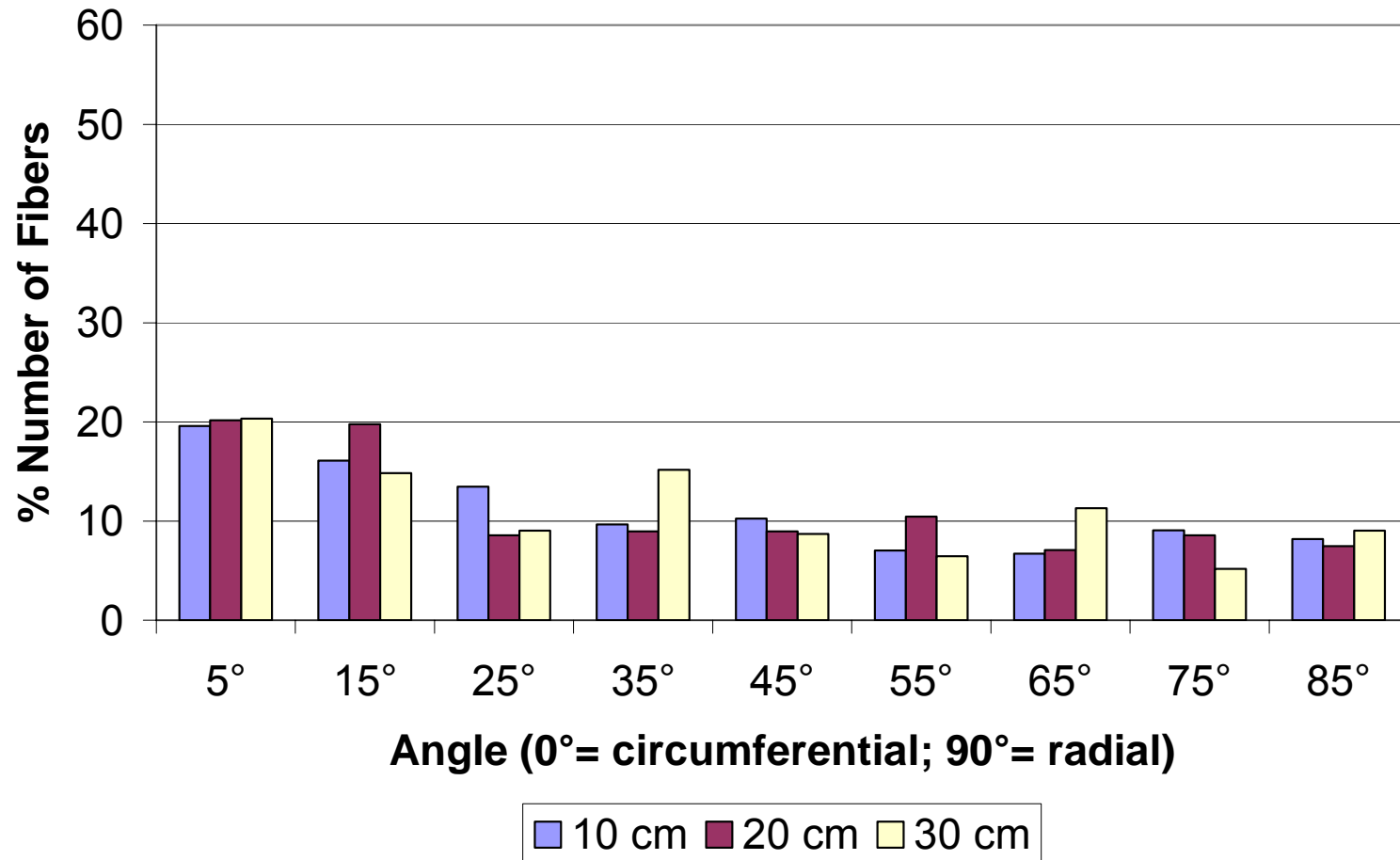
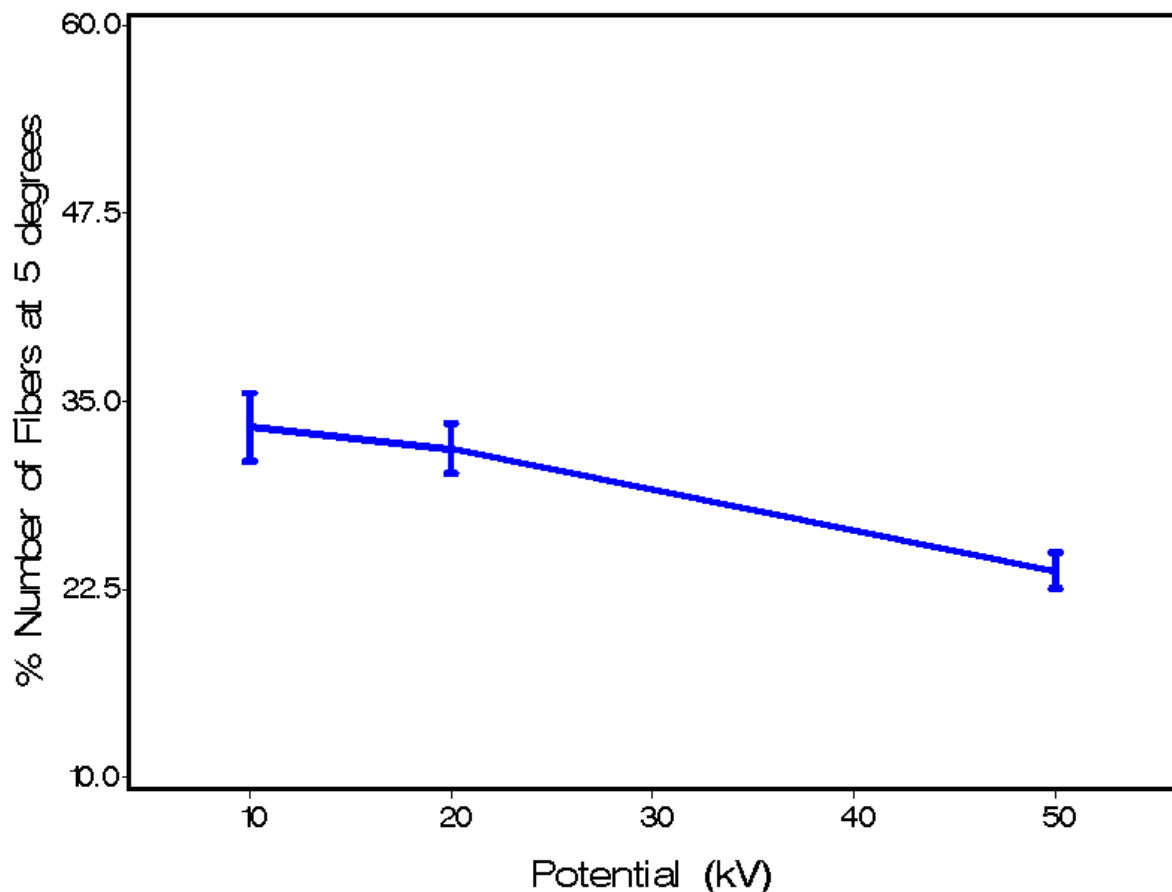


Figure 50: Fiber distribution histogram depending on the electrostatic field distance at 13rpm disc speed / 50kV electrostatic potential / 20mm lay-down rod

## 6.2 Electrostatic Potential

The p-value of the main effect of the electrostatic potential is  $<0.0001$ , meaning that the electrostatic potential definitely has a significant impact on the fiber orientation, since the p-value is so low. This is supported by the data of Figure 51.



**Figure 51: Percent number of fibers at 5° corresponding to the electric potential**

From Figure 51 it can be observed that lower electrostatic potential is beneficial for circumferential fiber orientation of the fiberweb as compared to the higher levels used. Clearly 10kV can be stated as the best value for the potential. It can be furthermore assumed that a decrease of the potential below 10kV will not enhance the overall fiber distribution much, since the rate of percent number of fibers at 5° is decreasing as the potential is decreasing.

As mentioned in the previous section, the potential has a higher influence on the fiber orientation than the electrode distance, which can be illustrated by the p-value ( $<0.0001$  for the potential and  $0.0092$  for the distance), but also when comparing Figure 46 and Figure 51. The difference in “percent number of fibers at  $5^\circ$ ” from highest to lowest is higher for the effect of potential ( $\sim 11\%$ ) than for distance ( $\sim 6\%$ ).

Further evidence can be seen when observing the fiber orientation distribution represented by histograms. The effect of electrostatic potential on fiber orientation in circumferential direction can best be shown by Figure 53. Clearly the target fiber orientation distribution can be best accomplished by using a potential of 10kV. When reducing the distance from 30cm in Figure 53 to 20cm in Figure 54, but keeping disc rotational speed constant at 50rpm, it can be observed that the fiber orientation distribution with 10kV exhibits the best target fiber orientation. Dramatic change in fiber orientation distribution can be observed when further lowering the distance (see Figure 55) to 10cm. Almost no effect of the potential on fiber orientation can be observed when operating with low distances around 10cm. The fiber distributions are not meeting the desired target for all levels of potential studied, compared to the fiber distribution shown with higher field distances (Figure 53 and Figure 54).

The influence of disc rotational speed can be seen from Figure 56. While the distance is at a favorable level of 30cm, the fiber distribution is not satisfactory at any potential level.

As discussed earlier, lower electrostatic field strengths (and therefore lower potential) enhance fiber orientation in the electrostatic field, because fibers have more time for orientation. The probability that fibers hit the collecting disc perpendicularly increases when the fibers have more time to orient in the electrostatic field, which can be supported by the findings of Gabler [11], who also stated that low field strengths leads to perpendicular standing fibers on the substrate [11]. Since the fibers can only be circumferentially oriented when they

are standing at an angle close to  $90^\circ$  on the collecting disc, low field strengths support circumferential orientation. Higher field strengths will randomize the fiber orientation, because the fibers hit the fiber collecting disc more randomly. Tilted fibers (not perpendicularly to the collecting surface) will not achieve circumferential fiber orientation as indicated in Figure 52.

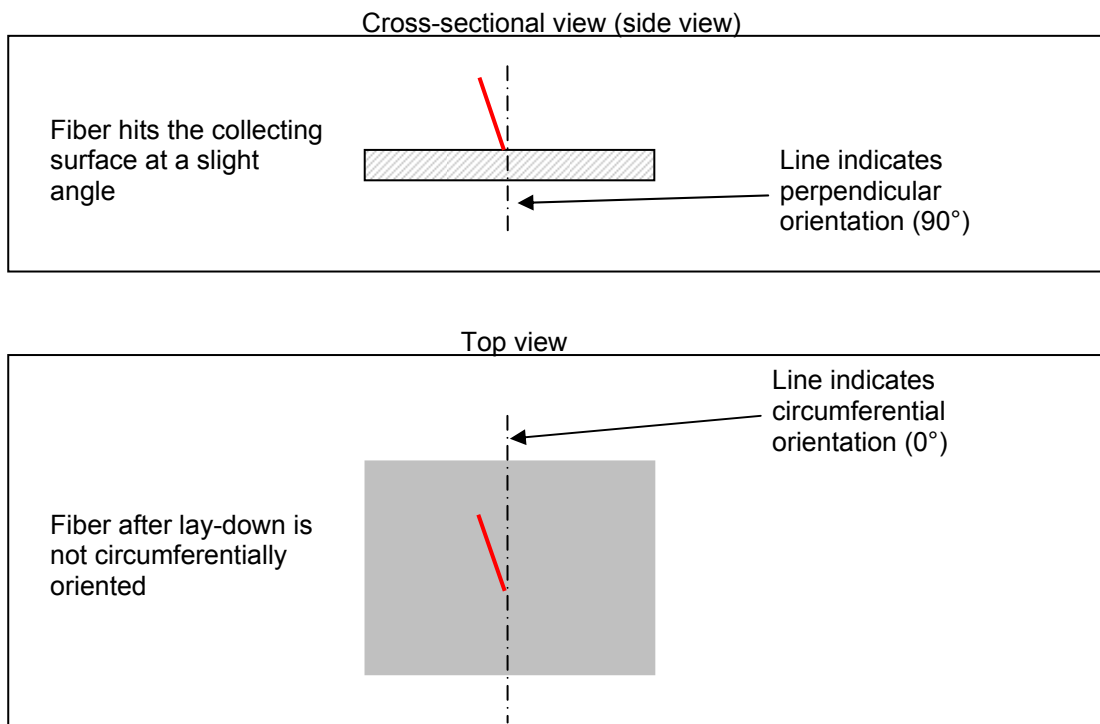


**Figure 52: Fibers need to hit the collecting disc perpendicularly in order to get circumferentially oriented after lay-down**

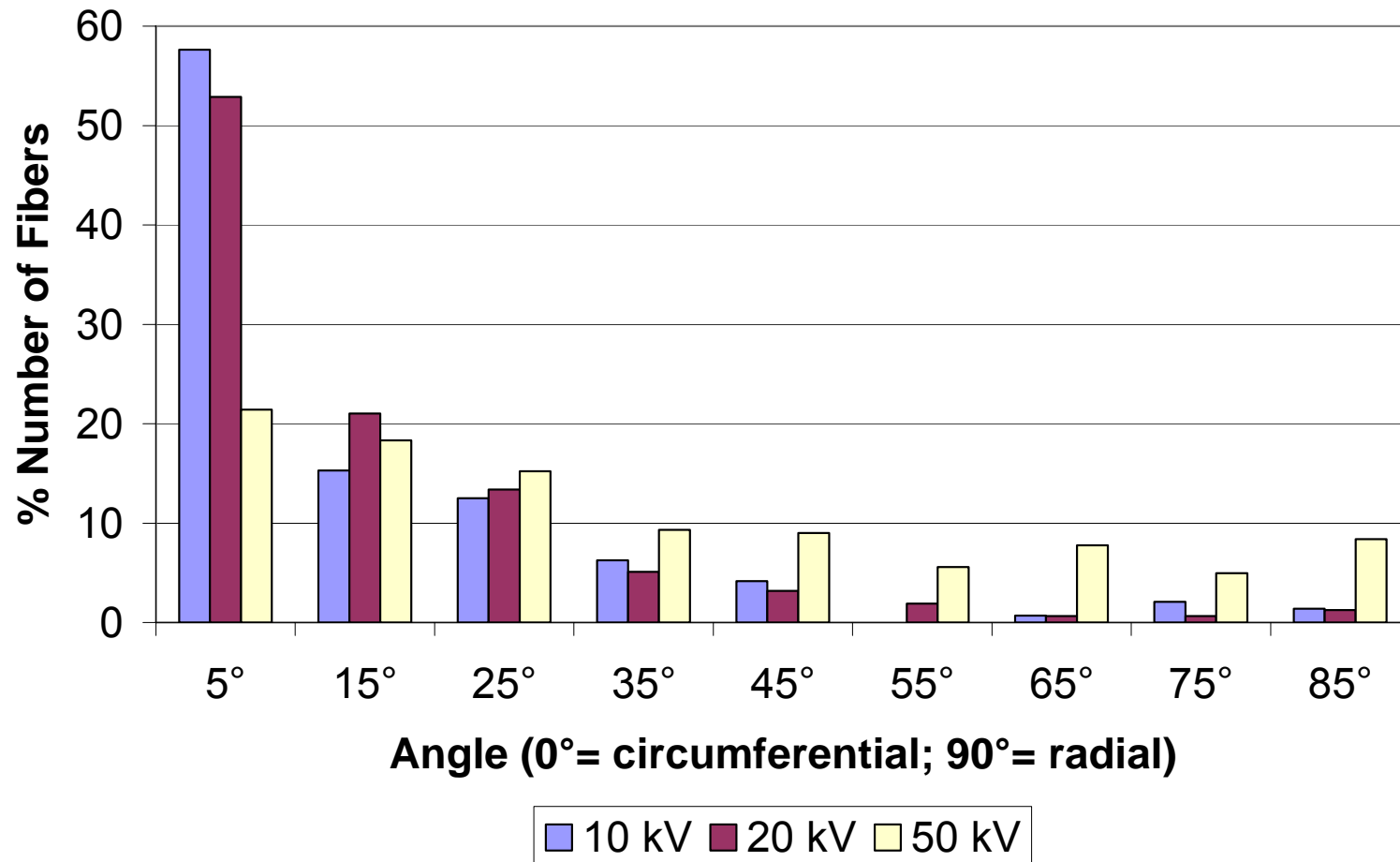


Figure 53: Fiber distribution histogram depending on the potential applied at 50rpm disc speed / 30cm electrode distance / 20mm lay-down rod

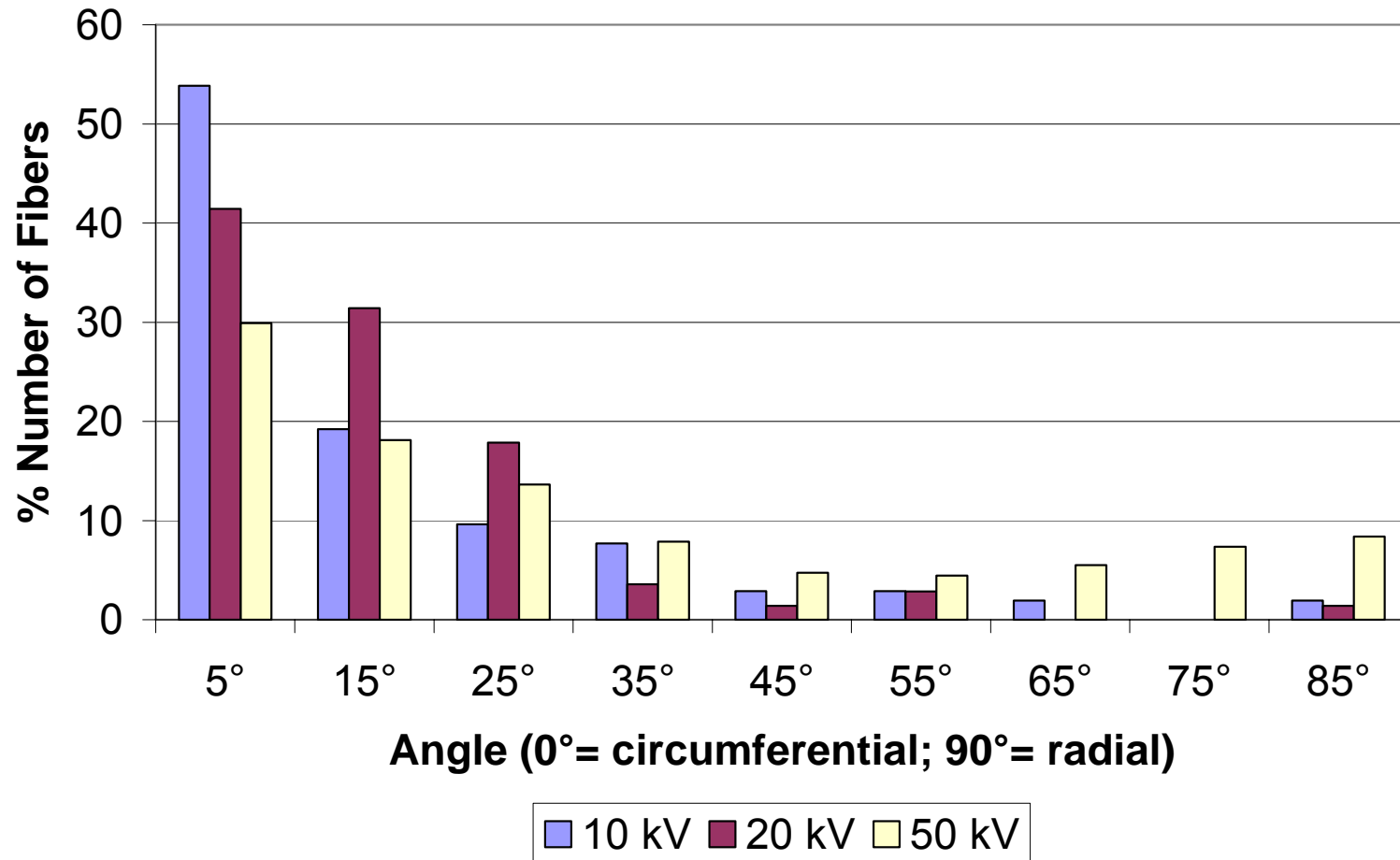


Figure 54: Fiber distribution histogram depending on the potential applied at 50rpm disc speed / 20cm electrode distance / 20mm lay-down rod

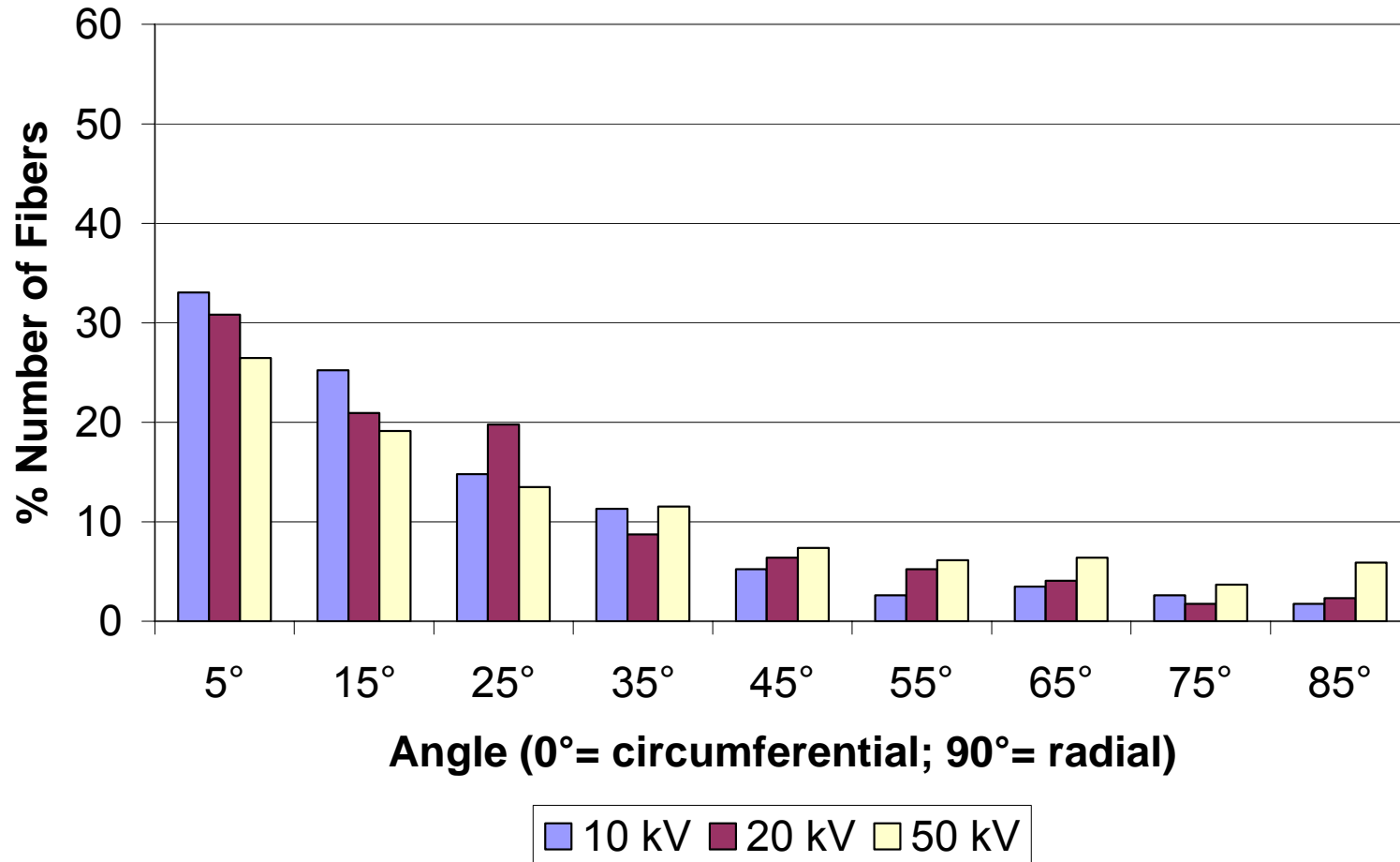


Figure 55: Fiber distribution histogram depending on the potential applied at 50rpm disc speed / 10cm electrode distance / 20mm lay-down rod

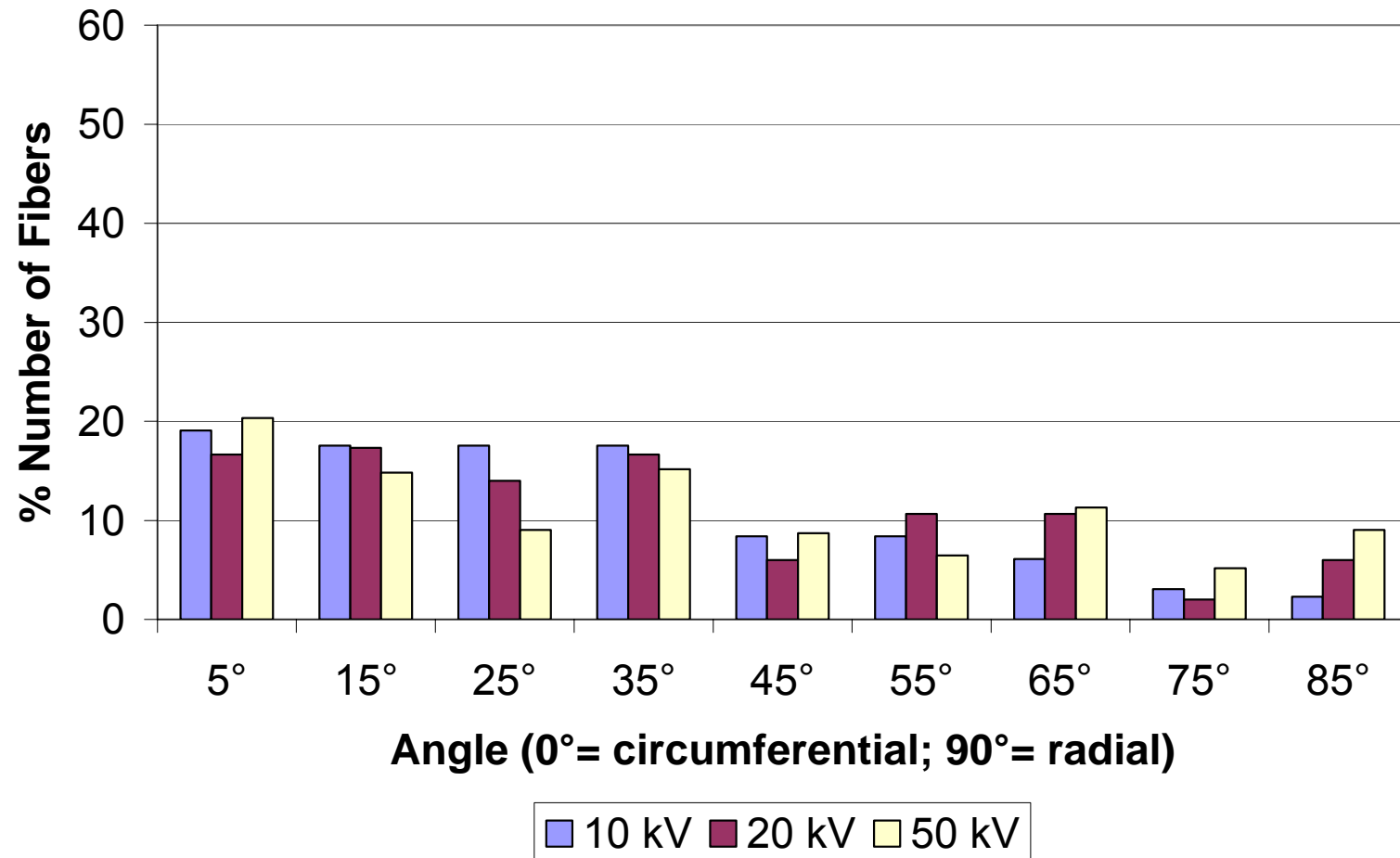
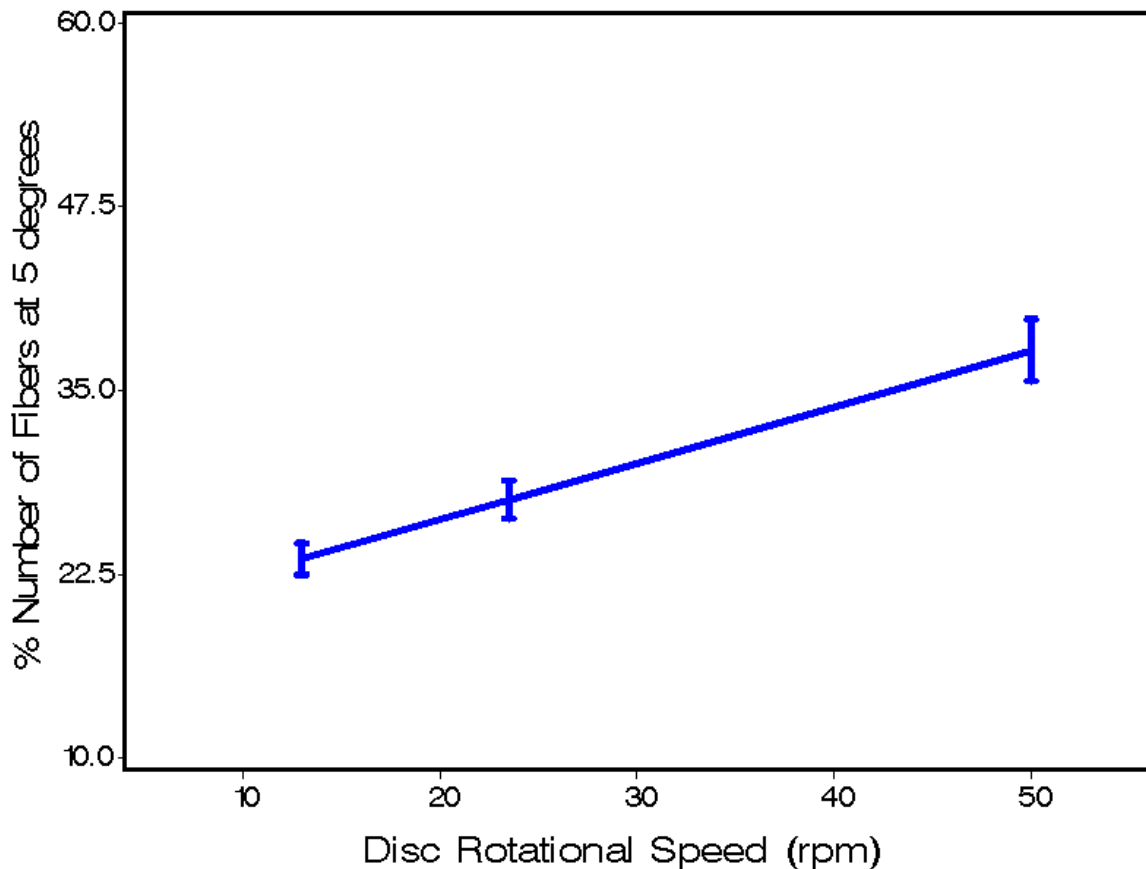


Figure 56: Fiber distribution histogram depending on the potential applied at 13rpm disc speed / 30cm electrode distance / 20mm lay-down rod

### 6.3 *Disc Rotational Speed*

Table 7 depicts that the p-value of the disc rotational speed is  $<0.0001$ . As mentioned before, such a low value indicates a strong dependence of the circumferential fiber orientation on the disc rotational speed. This is obvious from the plot of disc rotational speed versus percent number of fibers at  $5^\circ$  (Figure 57).



**Figure 57: Percent number of fibers at  $5^\circ$  corresponding to the disc rotational speed**

The continuous increase of percent number of fibers at  $5^\circ$  with the increase in disc rotational speed, for the range implemented in this study, leads to the conclusion that higher speeds may promote fiber orientation in the desired circumferential direction. The current machine design does not, however, allow higher disc rotational speeds. Changing the timing belt pulleys is generally an easy way to increase the maximum disc speed and is therefore suggested for future research.

In the previous section the importance of the disc rotational speed was already stated, which could be verified with the p-value of Table 7. The histograms of fiber orientation distribution also support this conclusion.

Figure 58 clearly indicates that 50rpm promotes more circumferential fiber orientation than lower disc speeds. Electrostatic potential and distance between electrodes were both at levels which support circumferential fiber orientation (10kV and 30cm). At other levels of potential and distance, the effect of disc speed is not significant as can be seen from Figure 59, Figure 60 and Figure 61. While the percent number of fibers at 5° is dramatically reduced in Figure 59 – Figure 61 as compared to Figure 58, the percent number of fibers at 5° increases with the disc rotational speed regardless of the other independent parameters levels.

At this stage of research it is not fully understood why higher disc velocities support circumferential fiber orientation and why the dependence is so strong. It is assumed that the “quality” of grounding the collecting disc by carbon brushes is not as good for low disc rotational speeds as for higher disc rotational speeds. The dependence of grounding the collecting disc on the disc rotational speed can be verified by appropriate setup of measurement instruments (e.g. measuring electrostatic field strength during operation of the equipment).

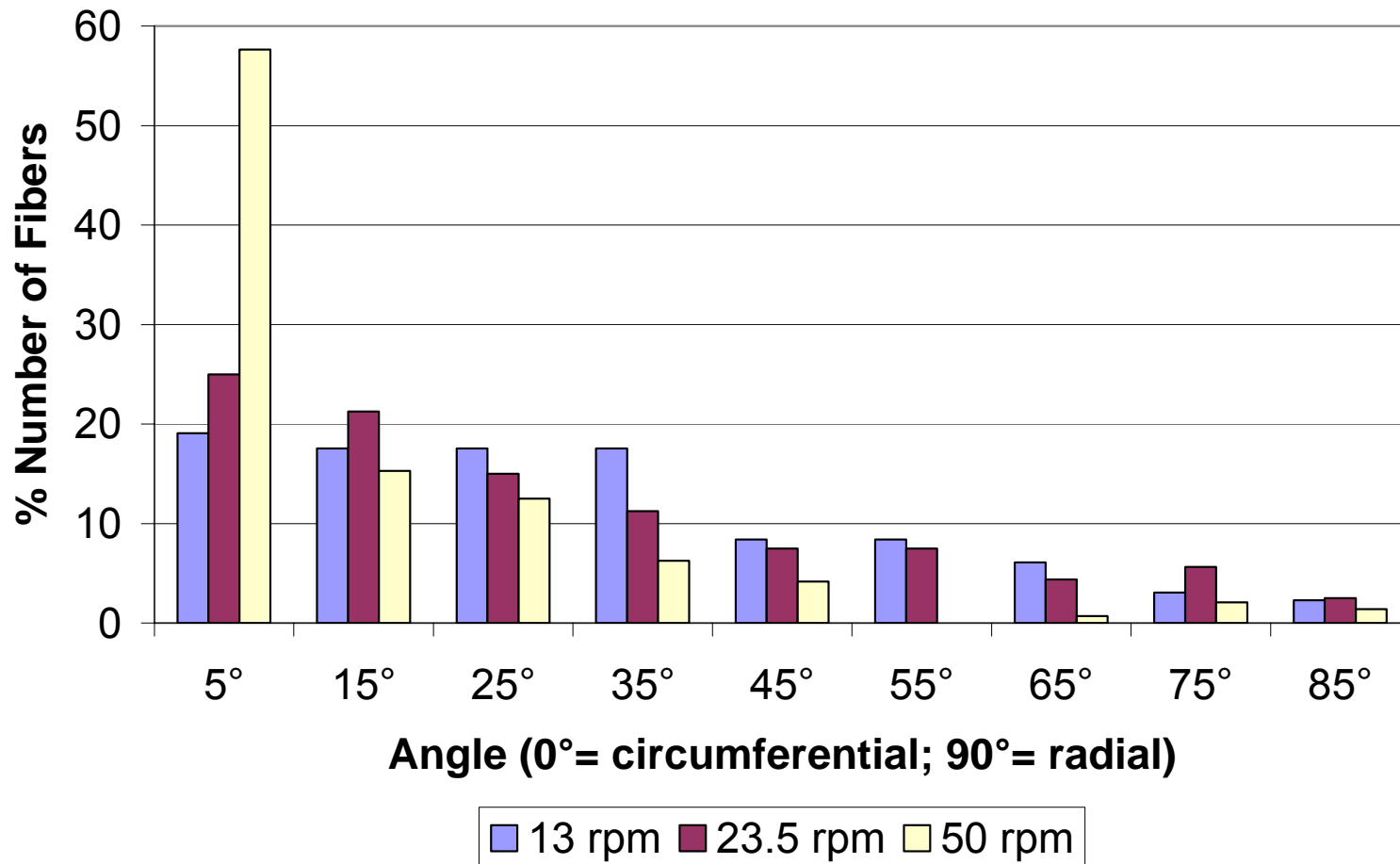


Figure 58: Fiber distribution histogram depending on the fiber collecting disc speed at 30cm electrode distance / 10kV electrostatic potential / 20mm lay-down rod

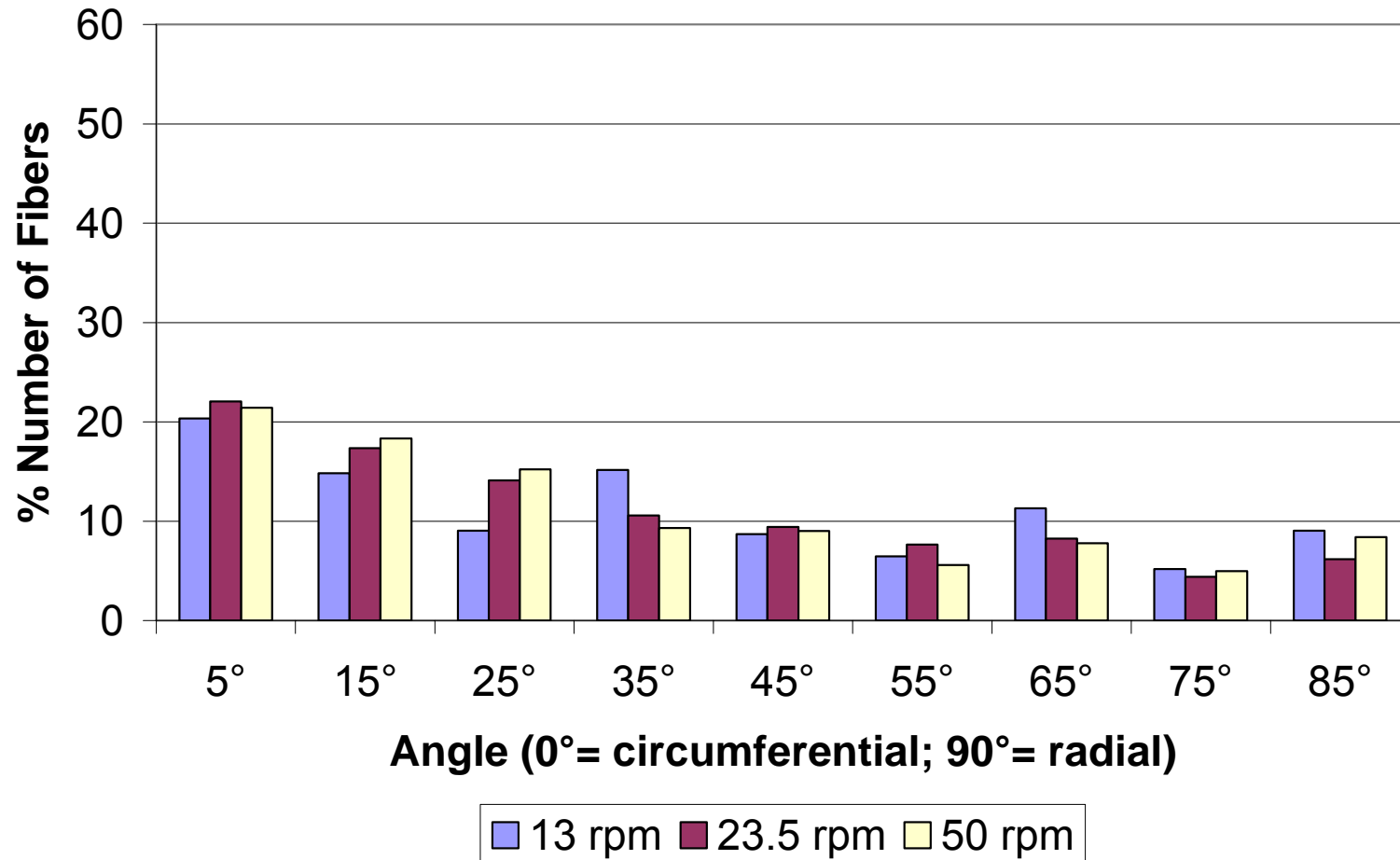


Figure 59: Fiber distribution histogram depending on the fiber collecting disc speed at 30cm electrode distance / 50kV electrostatic potential / 20mm lay-down rod

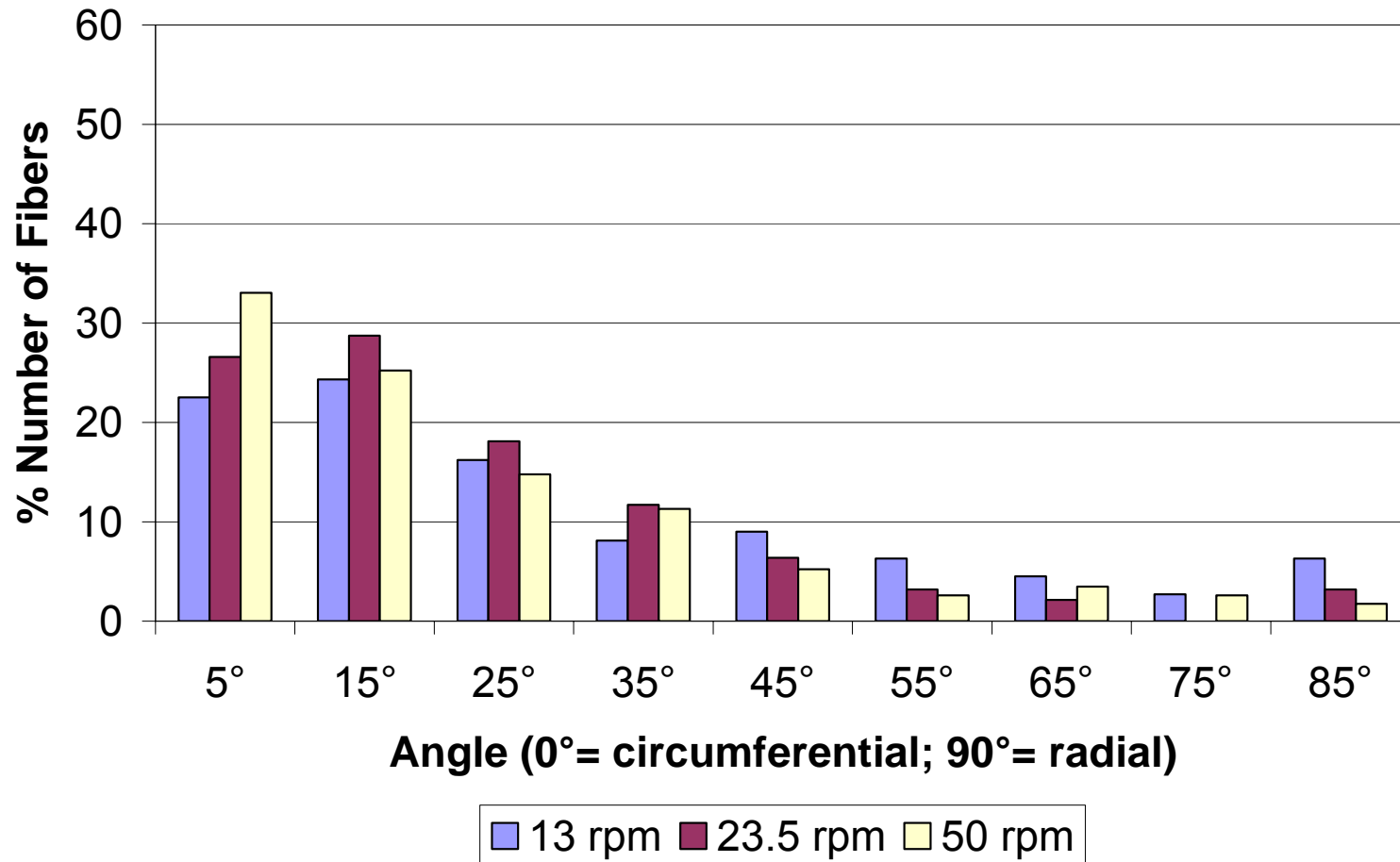


Figure 60: Fiber distribution histogram depending on the fiber collecting disc speed at 10cm electrode distance / 10kV electrostatic potential / 20mm lay-down rod

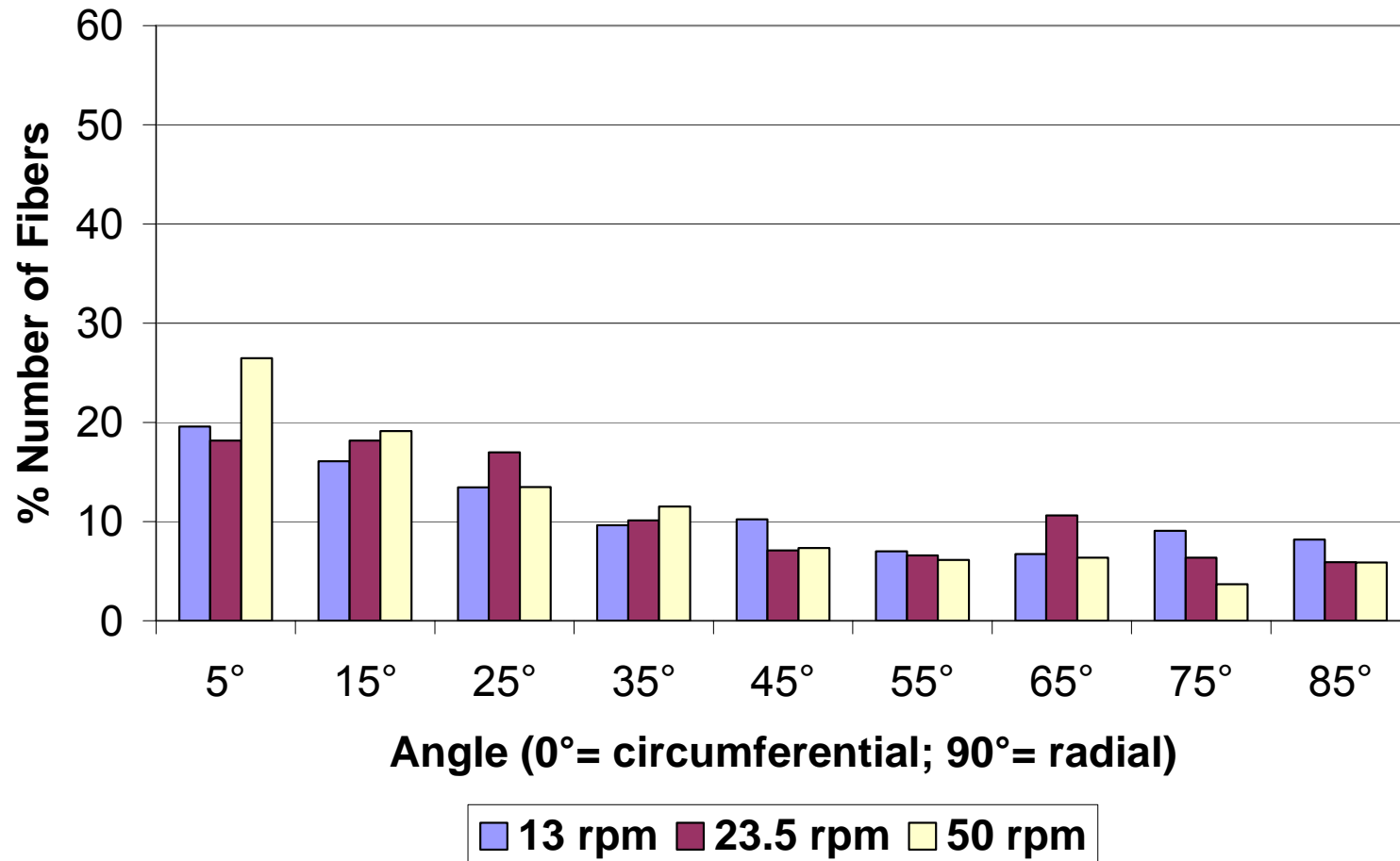


Figure 61: Fiber distribution histogram depending on the fiber collecting disc speed at 10cm electrode distance / 50kV electrostatic potential / 20mm lay-down rod

## 6.4 Rod Diameter

The p-value for the rod diameter according to Table 7 is 0.0313. Considering a 95% confidence level, this p-value leads to the conclusion that the rod diameter has influence on the fiber orientation distribution. Compared to the other parameters discussed in previous sections, the rod diameter has the lowest impact.

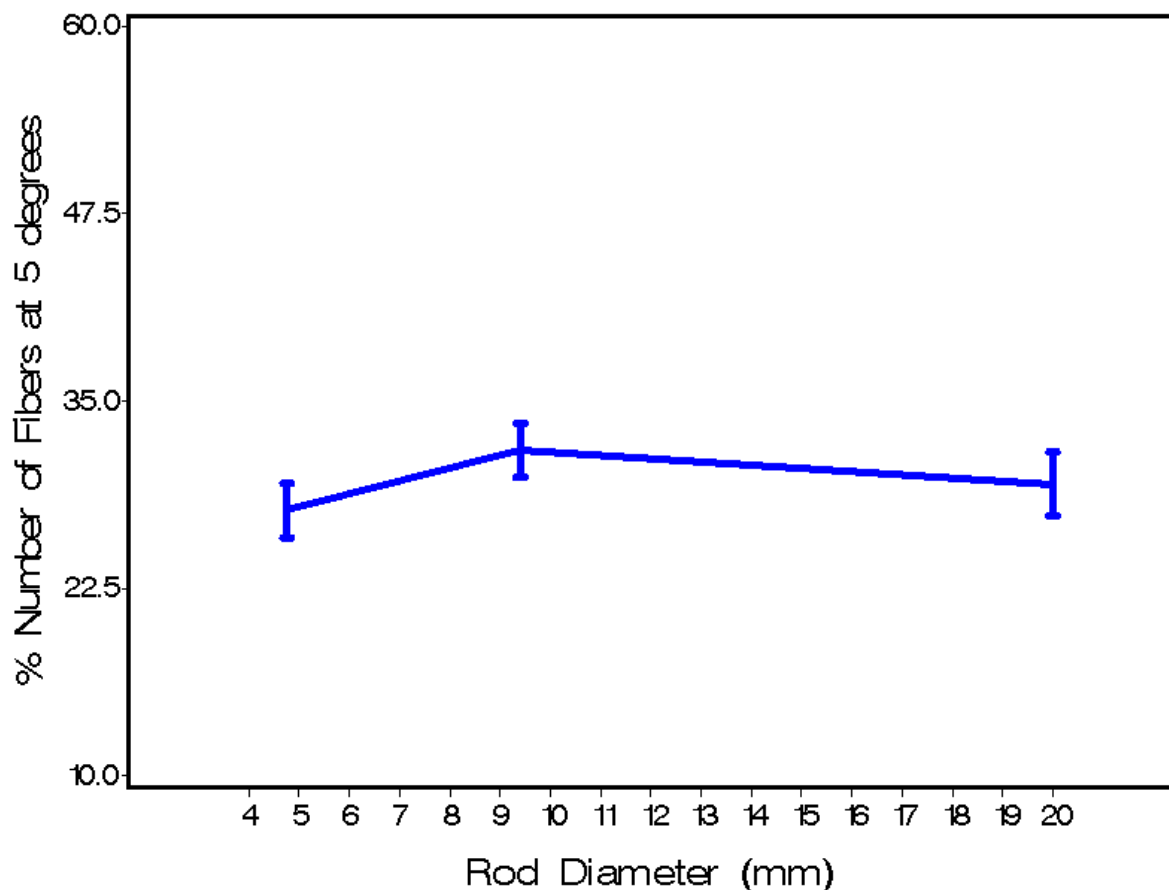


Figure 62: Percent number of fibers at 5° corresponding to the rod diameter

The medium rod diameter ( $\varnothing 9.4\text{mm}$ ) produces the highest “percent number of fibers at 5°” (see Figure 62).

When observing the fiber orientation distribution diagrams, no clear trend can be found. Figure 63 shows the 20mm rod is the optimum, provided that all other parameters are at their optimal values (electrode distance=30cm; potential=10kV;

disc rotational speed=50rpm). For electrode distance of 10cm, potential of 10kV and disc rotational speed of 50rpm, the 9.4mm and 4.76mm rods show the best results (see Figure 64). The 4.76mm rod seems to be good at an electrode distance of 30cm, potential of 50kV and disc rotational speed of 50rpm (see Figure 65). 4.76mm and 20mm rod almost seems to be equal for a setup of electrode distance of 10cm, potential of 50kV and disc rotational speed of 50rpm (see Figure 66).

The fiber lay-down method described in section 5.1, page 47 was applied for all 81 runs. It is believed that other fiber lay-down techniques may lead to different fiber orientation distribution. One technique proposed for future work is that the lay-down rod should touch the surface of the fiber collecting disc as the fiberweb is being formed. The design should allow the rod to rise as the fiberweb thickness increases.

Since the interaction of the rod diameter with any other parameter is statistically not significant (see Table 7) and no clear trend can be observed from the fiber orientation distribution histograms as well as Figure 62, it is seen that the diameter of the lay-down rod does not have an important role in deciding the fiber orientation distribution as compared to the other main effects. It is assumed that the fiber lay-down method described in section 5.1, page 47 allows using differently sized rods without significantly changing the lay-down characteristics. Since the distance between the rod and the collecting disc surface is gradually decreased, the actual diameter is not important in the range the rod diameter was studied. As mentioned before, the significance of the rod diameter is highly depending on the lay-down method and changing this method may lead to increased significance of the rod diameter.

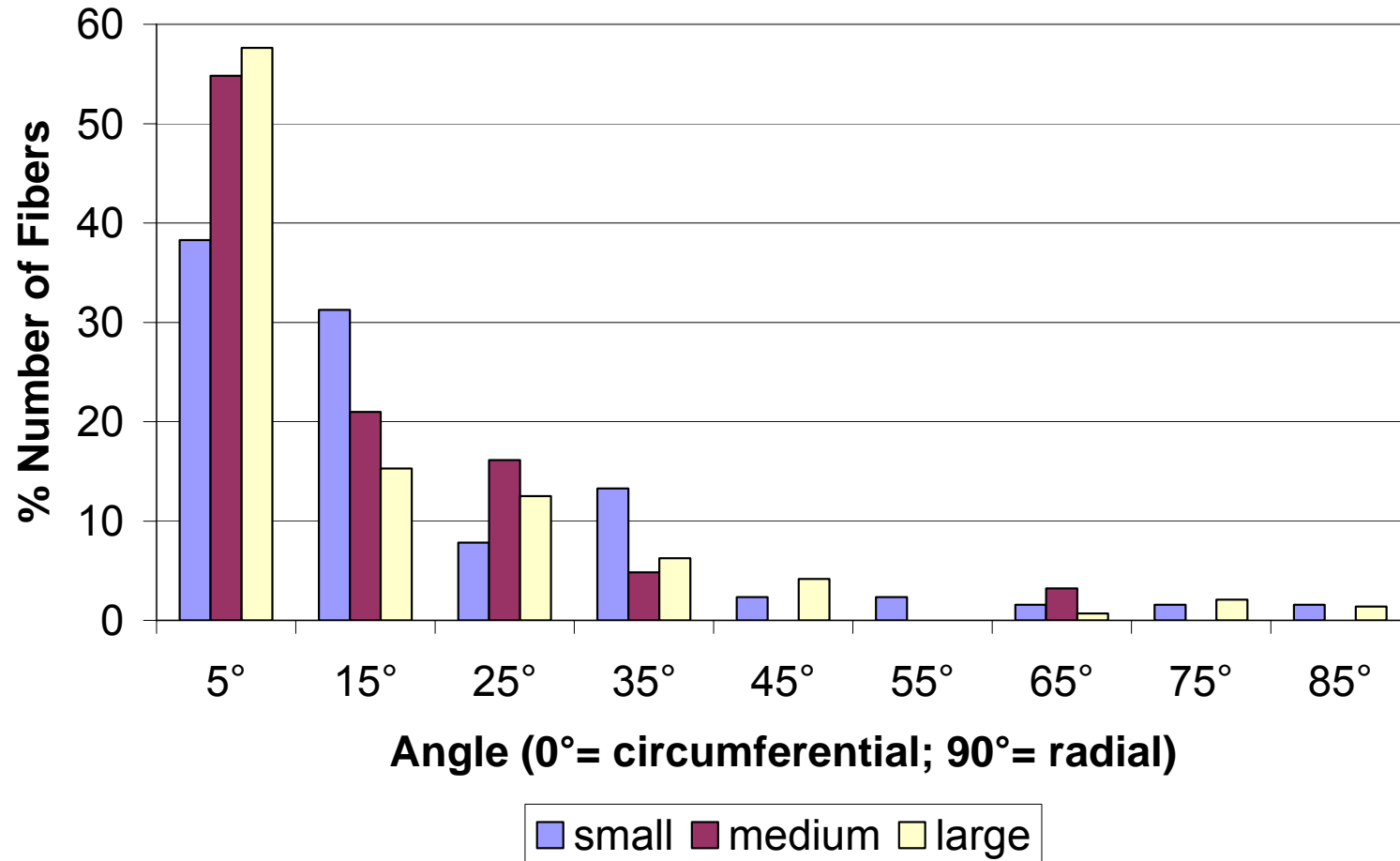


Figure 63: Fiber distribution histogram depending on the fiber lay-down rod diameter at 30cm electrode distance / 10kV electrostatic potential / 50rpm disc speed

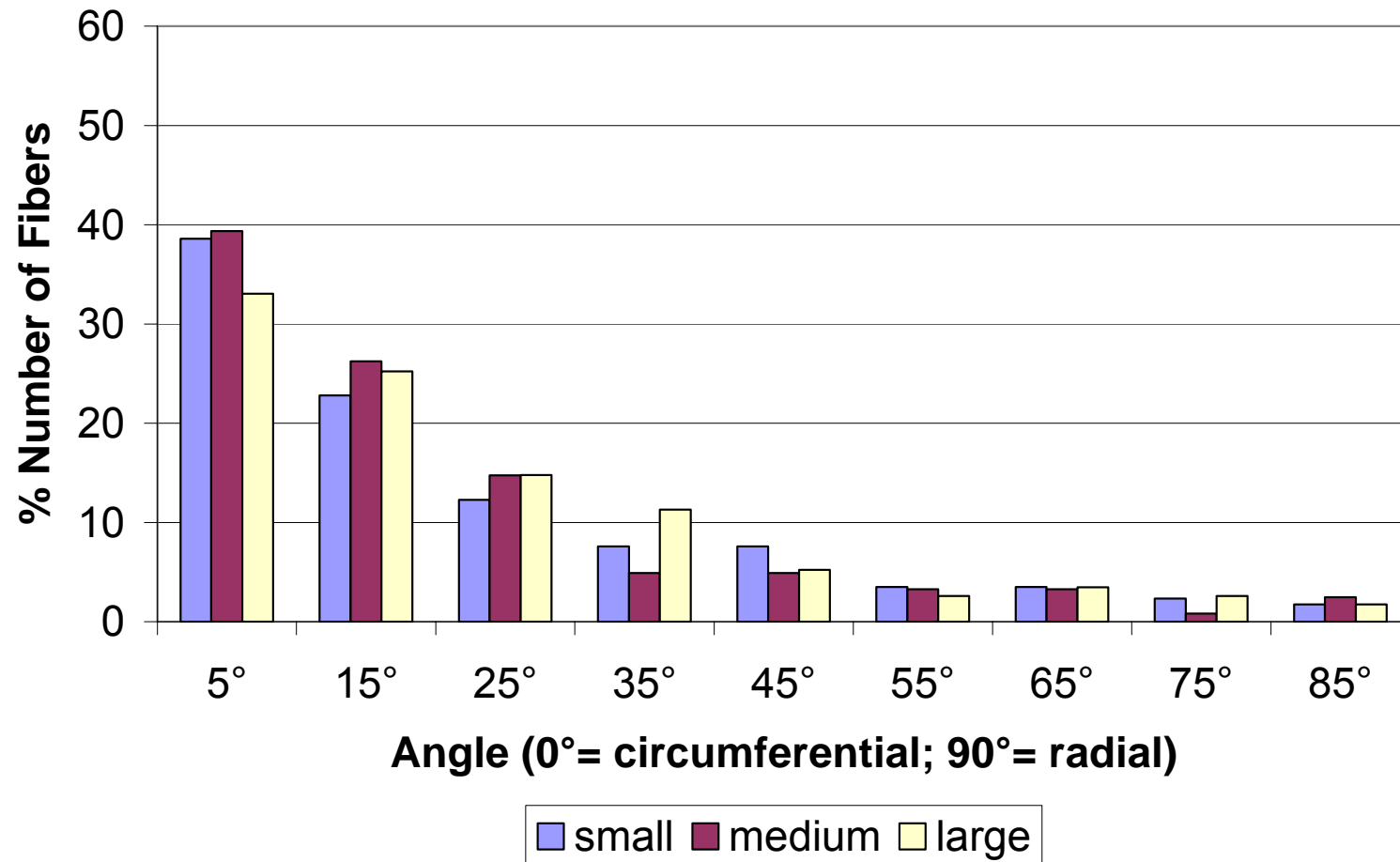


Figure 64: Fiber distribution histogram depending on the fiber lay-down rod diameter at 10cm electrode distance / 10kV electrostatic potential / 50rpm disc speed

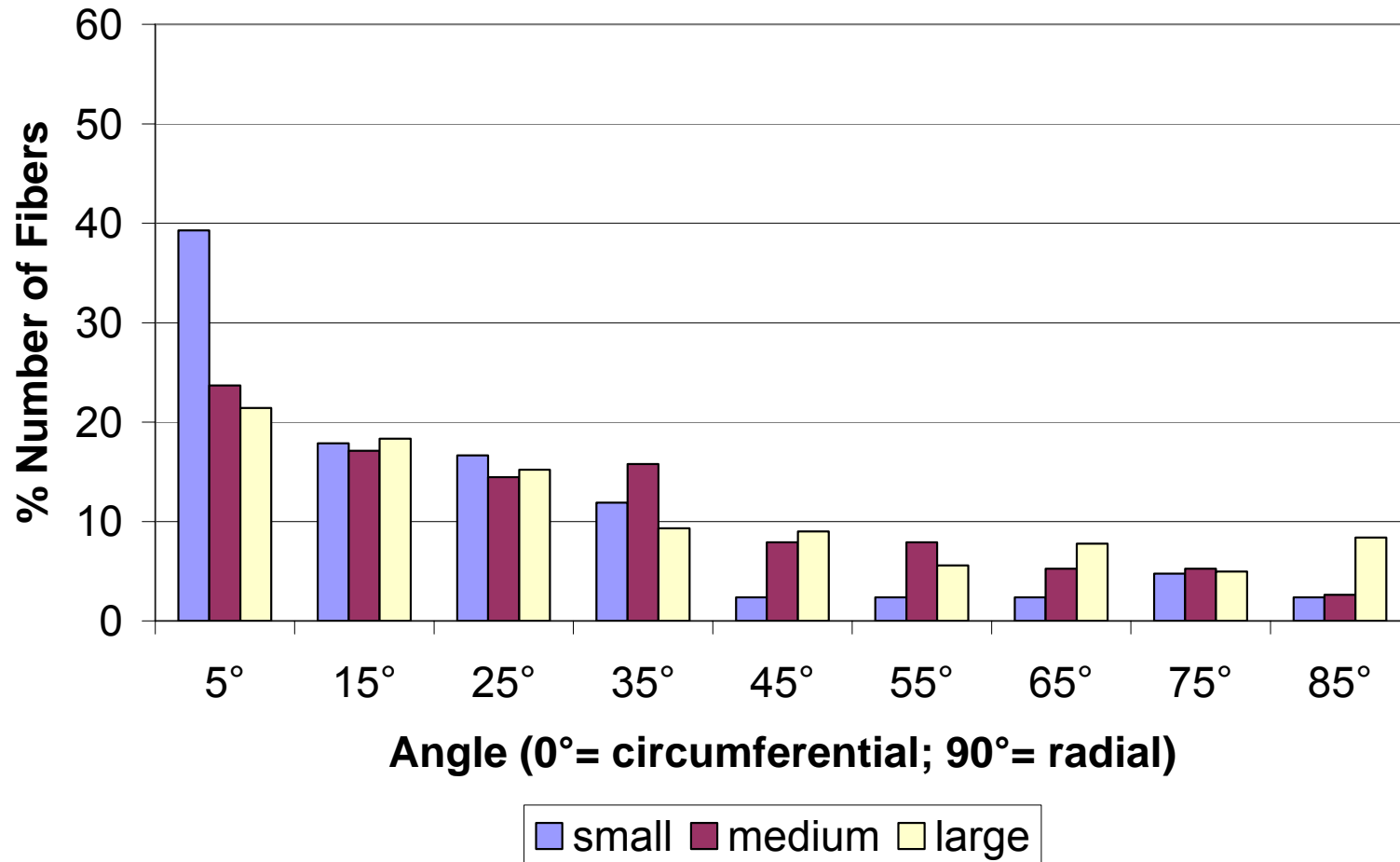


Figure 65: Fiber distribution histogram depending on the fiber lay-down rod diameter at 30cm electrode distance / 50kV electrostatic potential / 50rpm disc speed

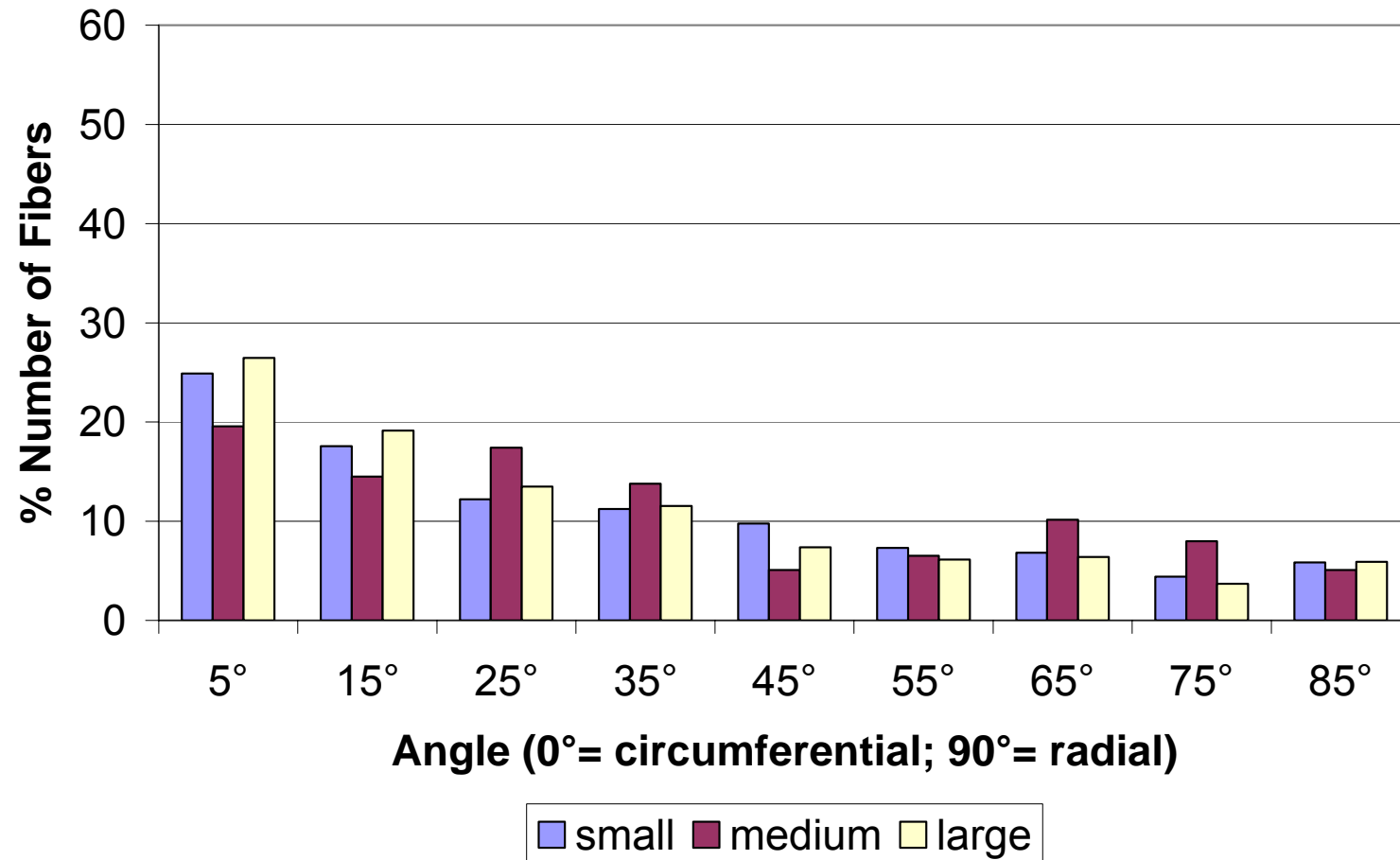


Figure 66: Fiber distribution histogram depending on the fiber lay-down rod diameter at 10cm electrode distance / 50kV electrostatic potential / 50rpm disc speed

## **6.5 Interaction between Parameters**

The ANOVA results (see Table 7) revealed that there is significant first order interaction between electrode distance and disc rotational speed as well as between potential and disc rotational speed on fiber circumferential orientation at 95% confidence level. Other first order interactions and second order interactions did not show significant influence on the percent number of fibers at 5°.

The findings from the p-value examination can be substantiated by graphs showing the impact of the two first order interactions that are significant. Figure 178 – Figure 181 in the Appendix III: First Order Interaction Graphs show the graphs of the first order interactions which have insignificant effect on the percent number of fibers at 5°. With the exception of one value in Figure 179, Figure 180 and Figure 181 the shape of the relationship between a parameter and the percent number of fibers at 5° does not change by the other parameters.

Figure 67 shows the nature of the effect of the first order interaction of the independent parameters electrode distance and disc rotational speed on percent number of fibers at 5° in the circumferential direction. At the lowest level of disc rotational speed, the electrode distance seems to have little or no effect on the percent number of fibers at 5°. At highest disc rotational speed level, however, the impact of distance between the electrodes on the percent number of fibers at 5° is significant. This indicates that high values of percent number of fibers at 5° can be obtained using highest values of disc rotational speed and electrode distance.

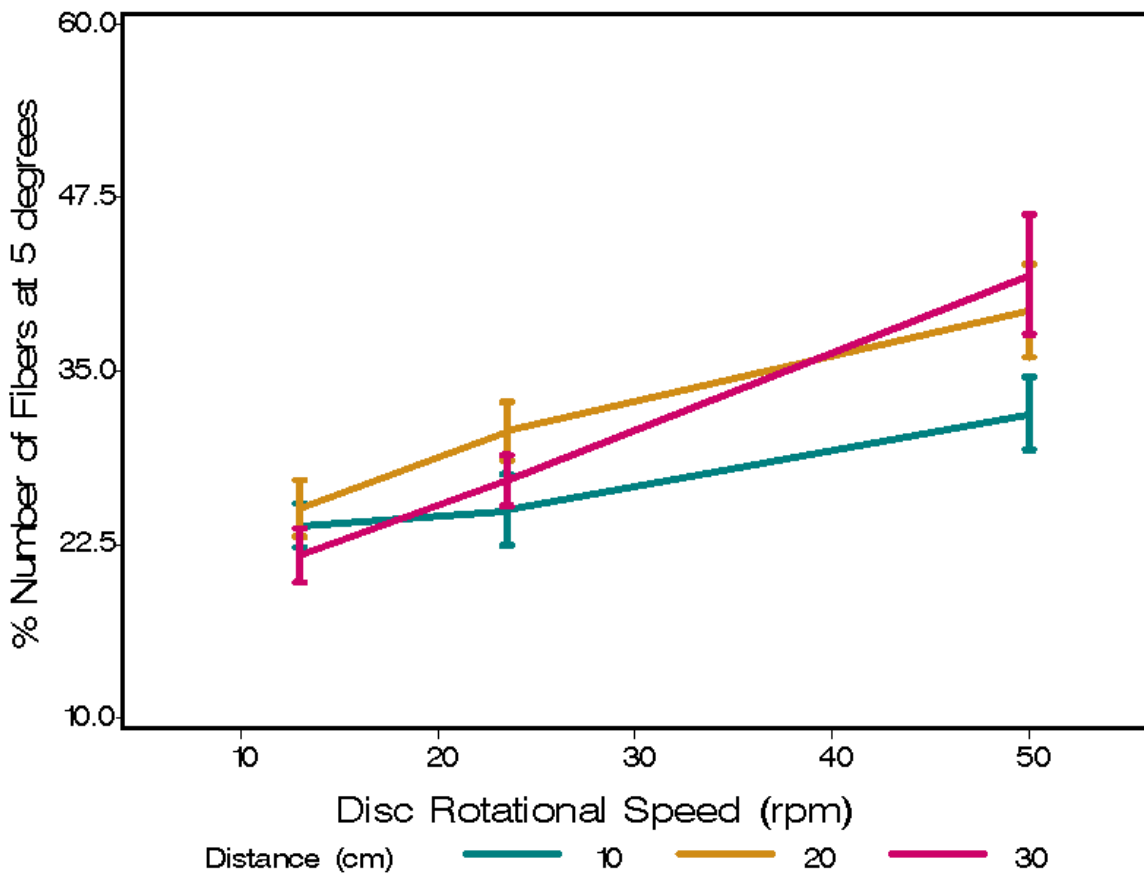


**Figure 67: Percent number of fibers at 5° corresponding to the interaction of disc rotational speed and distance**

The effect of the first order interaction between disc rotational speed and potential on the percent number of fibers at 5° is shown in Figure 68. The significance of potential on the percent number of fibers at 5° increases with disc rotational speed. At low speeds the potential has only slight influences. However, at high disc rotational speeds clearly a low potential leads to high percent number of fibers at 5°, which indicates that high disc rotational speeds and low potentials allow circumferential fiber orientation to dramatically increase.

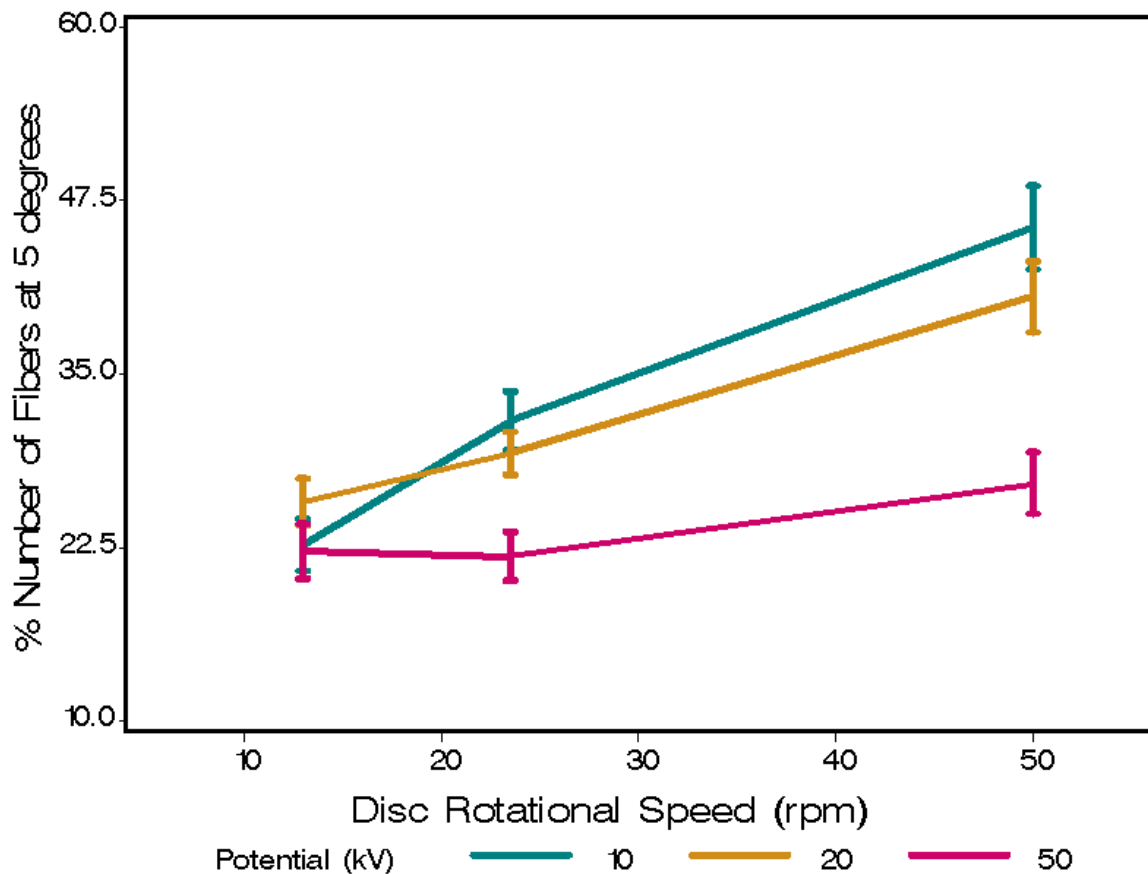


Figure 68: Percent number of fibers at 5° corresponding to the interaction of distance and potential

## 6.6 Summary

Table 8 is generated to show the rank of the percent number of fibers at 5° in descending order. It can be seen from the table that the highest percent number of fibers oriented circumferentially (57.64% of all fibers at 5°) is obtained by utilizing lowest potential ( $V_1=10\text{kV}$ ), highest disc rotational speed ( $v_3=50\text{rpm}$ ), highest electrode distance ( $h_3=30\text{cm}$ ) and highest rod diameter ( $d_3=20\text{mm}$ ).

**Table 8: Sample numbers and their corresponding parameters sorted from the highest to lowest “percent number of fibers at 5°”**

Field Strength [kV/cm]	Rod Diameter [mm]	Distance [cm]	Potential [kV]	Disc Rotational Speed [rpm]	Sample Number	% Number of Fibers at 5°
0.33	20.00	30	10	50	23	57.64
0.33	9.40	30	10	50	70	54.84
0.50	20.00	20	10	50	12	53.85
0.67	20.00	30	20	50	24	52.87
0.50	4.76	20	10	50	55	52.00
0.67	9.40	30	20	50	77	46.96
2.00	9.40	10	20	50	97	44.44
1.00	9.40	20	20	50	79	42.72
0.67	4.76	30	20	50	62	42.67
0.50	9.40	20	10	50	83	42.27
1.00	20.00	20	20	50	13	41.43
0.50	20.00	20	10	23.50	3	40.63
1.00	9.40	10	10	50	90	39.34
1.67	4.76	30	50	50	58	39.29
1.00	4.76	10	10	50	45	38.60
0.33	4.76	30	10	50	60	38.28
0.33	9.40	30	10	23.50	73	37.84
1.00	9.40	10	10	23.50	93	37.59
2.50	4.76	20	50	13	50	36.51
0.50	9.40	20	10	23.50	80	35.96
2.50	4.76	20	50	50	53	35.85
1.00	9.40	20	20	23.50	82	35.58
1.00	20.00	20	20	23.50	1	33.33
1.00	20.00	10	10	50	10	33.04
2.00	9.40	10	20	13	92	32.99
1.00	4.76	20	20	50	51	32.79
0.67	9.40	30	20	23.50	71	32.47
0.33	9.40	30	10	13	76	31.09
0.67	9.40	30	20	13	74	30.86
2.00	20.00	10	20	50	6	30.81
2.00	20.00	10	20	23.50	5	30.69
2.00	4.76	10	20	50	47	30.37
1.00	4.76	10	10	23.50	48	30.00
2.50	20.00	20	50	50	32	29.92
2.50	9.40	20	50	23.50	84	29.67
0.50	20.00	20	10	13	11	29.57
1.00	4.76	20	20	23.50	54	29.49
0.67	4.76	30	20	23.50	59	29.46
1.00	9.40	10	10	13	96	28.57
0.67	20.00	30	20	23.50	21	27.96
2.00	20.00	10	20	13	7	27.64
1.00	9.40	20	20	13	86	27.35
1.00	4.76	20	20	13	57	27.27
0.50	4.76	20	10	23.50	49	26.87
1.00	20.00	10	10	23.50	9	26.60
5.00	20.00	10	50	50	33	26.47
5.00	9.40	10	50	23.50	95	26.28
1.00	20.00	20	20	13	14	25.97
0.33	20.00	30	10	23.50	29	25.00
1.67	9.40	30	50	23.50	75	25.00
5.00	4.76	10	50	50	41	24.88
0.33	4.76	30	10	23.50	66	24.14
1.67	9.40	30	50	13	78	24.14
1.67	9.40	30	50	50	72	23.68

Table 8: continued

Field Strength [kV/cm]	Rod Diameter [mm]	Distance [cm]	Potential [kV]	Disc Rotational Speed [rpm]	Sample Number	% Number of Fibers at 5°
2.50	9.40	20	50	13	81	23.53
2.00	9.40	10	20	23.50	89	23.42
2.50	9.40	20	50	50	87	23.15
2.00	4.76	10	20	13	43	22.58
1.00	20.00	10	10	13	8	22.52
2.50	4.76	20	50	23.50	56	22.33
2.50	20.00	20	50	23.50	30	22.16
1.67	20.00	30	50	23.50	25	22.06
1.67	20.00	30	50	50	28	21.43
2.00	4.76	10	20	23.50	40	21.08
1.00	4.76	10	10	13	42	20.62
0.67	4.76	30	20	13	65	20.59
5.00	9.40	10	50	13	88	20.51
1.67	20.00	30	50	13	22	20.32
2.50	20.00	20	50	13	31	20.15
1.67	4.76	30	50	23.50	64	20.00
5.00	4.76	10	50	13	46	19.73
5.00	20.00	10	50	13	34	19.59
5.00	9.40	10	50	50	91	19.57
0.33	20.00	30	10	13	26	19.08
0.50	4.76	20	10	13	52	18.85
5.00	20.00	10	50	23.50	35	18.16
0.33	4.76	30	10	13	63	17.09
0.50	9.40	20	10	13	85	16.67
0.67	20.00	30	20	13	27	16.67
1.67	4.76	30	50	13	61	15.56
5.00	4.76	10	50	23.50	44	11.17

## 7. Carbon Fiber Brake Disc – A Introductory Market Study

As mentioned earlier, carbon fiber brake discs are seen as a potential application for the described technology. When looking at the product development process described by Cooper [8], a market analysis needs to be undertaken before extensive research and consequently tremendous amount of resources are spent on new technologies. A market analysis serves to determine if the innovation can be successfully placed in the market.

Cooper's Stage-Gate-Model guides technicians and managers through the product development process, which is divided into several stages. After each stage, the gate to the next stage needs to be passed. In order to pass through the gate, certain criteria need to be fulfilled, which are specified at the beginning of the product development process by the product development team. The whole product development process is designed to incrementally increase the financial and economical risk at each stage. Therefore it is critical to fulfill the criteria of each gate to minimize the overall risk.

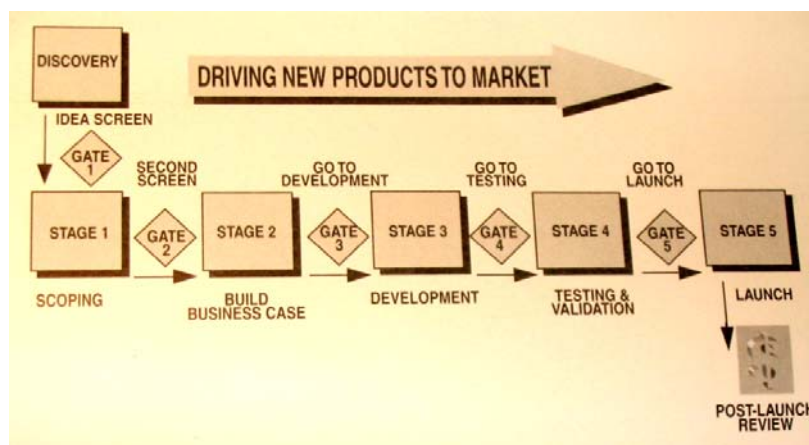


Figure 69: Stage-Gate-Model according to Robert Cooper [8]

After a preliminary technical feasibility assessment (stage 1), a market study needs to be done in order to evaluate the economical value of the technical idea

and to develop a business plan (stage 2), before intensive research is done to optimize the innovation (stage 3).

The technology presented in this paper can be considered a preliminary technical feasibility assessment. Consequently a market study needs to follow in order to evaluate if this innovation could be successfully introduced into the market.

In this chapter an introductory market study is presented for the use of the newly developed technology for carbon fiber brake discs and could therefore “open the gate” to undertake more research in the innovation, if the market study shows positive results.

### ***7.1 Why Market Study on Carbon Fiber Brake Discs?***

Two possible applications of the presented technology were mentioned in chapter 1, page 1: carbon fiber brake discs and grinding, cutting and sanding pads. The field of carbon fiber brake discs is seen as highly innovative with diverse market segments, some of which probably allow introducing highly priced products. The opportunity to operate in a higher price range is seen as a clear advantage for the technology, especially when the innovation is still developing at the beginning of the market introduction. These advantages are currently not seen in the field of grinding, cutting and sanding pads, since these markets are extremely price competitive. It is furthermore not clear if the use of circumferential fiber oriented reinforcing structures for such pads is really advantageous for such applications. On the other hand it is already shown that carbon fiber reinforced brake discs have advantages since they are used in some established markets (see section 2.4, page 14).

## **7.2 Competitive Analysis**

The competitive analysis of conventional brake systems is undertaken to provide a basis for a detailed cost analysis, which is necessary to evaluate the innovation's competitiveness.

Three different suppliers for brake disc were chosen from an internet search. The links to the suppliers websites are:

- [www.aaawebcarparts.com](http://www.aaawebcarparts.com)
- [www.mr-auto-parts.com](http://www.mr-auto-parts.com)
- [www.autopartwarehouse.com](http://www.autopartwarehouse.com).

Six different vehicles were compared:

- Porsche Carrera 4 (996)
- Ford Focus
- Nissan Maxima 3.5 SL
- Lincoln Navigator
- Mercedes Benz E320
- Honda Civic 1.7.

During the investigation the following manufacturers of brake discs could be identified:

- Otto Zimmermann GmbH, Germany
- Beck/Arnley Worldparts Corp., TN
- Powerstop, LLC, IL
- Brembo, Italy
- Winhere Auto Part Manufacturing Co., LTD, China
- FMP Group, Australia
- EBC Brakes Direct Ltd., England

- Brake Parts Inc., IL
- SP Performance Intl, Inc., NY

**Table 9: Selection of different brake disc prizes**

Car model	Price for one brake disc in USD (min – max)		
	aaawebcarparts.com	mr-auto-parts.com	autopartwarehouse.com
Porsche Carrera 4 (996)	130.70 – 137.07	125.22 – 131.31	124.90 – 187.73
Ford Focus	31.40	26.63	59.23 – 232.20
Nissan Maxima 3.5 SL	49.46	47.69	48.11 – 232.20
Lincoln Navigator	44.38 – 47.09	38.87 – 58.69	56.14 – 268.20
Mercedes Benz E320	46.55 – 137.34	37.61 – 127.97	38.60 – 178.20
Honda Civic 1.7	18.76 – 232.26	21.30 – 230.51	36.42 – 194.60

Generally it could be observed that:

- Brake discs with high prices are always high performance brake discs and of better quality, since they show shorter breaking distances and higher reliability in their function (according to the manufacturers).
- There are high and low price brake discs available independent of the car's value. When designing and manufacturing a brake disc for a specific car it is generally not complicated to transfer the disc to other models, since the technological principle stays the same.
- Higher priced products range between \$200 and almost \$300, which should be the main target when introducing new carbon fiber brake discs.

To successfully introduce a new carbon fiber brake disc into the passenger car market, the retail price needs to be competitive with conventional brake discs. The existing carbon fiber composite brake disc from SGL Carbon Group and Porsche is much too expensive to find a wide range of application (see section 2.4, page 14).

At this stage of research it is not fully clear if and how much more the consumer would be willing to pay for a high performance carbon fiber composite brake disc.

To pass gate 3 in Coopers Stage-Gate-Model (see Figure 69), which leads to the stage of the actual development of the technology, the business case needs to be successfully addressed. Prior to development it must be clear that the product can be sold in an appropriate number and at a competitive price level.

### **7.3 Market Potential**

As shown in section 7.1 the opportunities to provide added value appear to lie in the brake disc market. In order to determine the value of this market it is necessary to analyze the size of the market. Since it is not realistic to manufacture carbon fiber brake discs at the same price level as traditional grey cast iron brake discs, this review on market potential will not address the total number of passenger cars sold in the U.S. per year. In fact specific niche markets should be targeted instead.

According to the National Transportation Statistics 2005 [40] the total number of registered vehicles in the U.S. in 2004 was 243 million, of which 136 million were passenger cars. This number steadily increased annually since 1960. Also, the average cost of owning a car has increased (see Table 10).

Additionally it can be observed that the increase in the costs of owning and operating a car are higher than the increase in median household income. In fact the expenditures of average households on cars have more than doubled compared to 20 years ago.

**Table 10: Overview on the development of the number of passenger cars and the associated costs from 1985 to 2004 [40] (Fixed costs include: insurance, license, registration, taxes, depreciation, and finance charges; passenger cars do not include other 2-axle 4-tire vehicles like Pick-Ups, SUVs and Minivans) combined with population and income data [38, 39]**

	1985	2004
U.S. Population	238,466,283	293,027,571
Increase in % of U.S. Population	22.88%	
Number of all registered highway vehicles	177,133,282	243,023,486
Increase in % of total number of vehicles from 1985-2004	37.20%	
Number of vehicles per U.S. Population	0.743	0.829
Number of passenger cars	127,885,193	136,430,651
Increase in % of passenger cars form 1985-2004	6.68%	
Number of passenger cars per U.S. Population	0.536	0.466
Average total cost per 15,000 miles (current \$)	3,484	8,431
Increase in % of average total cost form 1985-2004	141.99%	
Variable cost	1,113	1,890
Increase in % of variable cost form 1985-2004	69.81%	
Fixed cost	2,371	6.541
Increase in % of fixed cost form 1985-2004	175.88%	
Real median Household Income (current \$)	39,545	44,389
Increase in % in Household Income	10.97%	
Average total vehicle cost per household income	0.088	0.190
Consumer Price Index (CPI)	164.3	275.1
Increase in % in CPI from 1985 to 2004	67.44%	

It is obvious that the increase in cost of cars in the U.S. did not lead to fewer cars. It seems that people “want to spend the money” instead of restraining from the use of cars. Interestingly the variable costs did not rise as much as fixed costs. In fact the percentage of gas cost to the total costs went down: 24.0% in 1985 to 11.6% in 2004 [40]. Table 11 provides an overview on the transportation costs.

**Table 11: Personal Consumption Expenditures on Transportation by Subcategory in current \$ millions (Repair and Rental includes greasing, washing, parking, storage, and leasing) [40]**

	1985	2004
<b>1. User-operated transportation, total</b>	<b>349,900</b>	<b>920,400</b>
New cars and net purchases of used cars	110,700	150,600
New and used trucks and RVs	41,000	236,900
Tires, tubes, accessories, and parts	24,300	54,300
Repair and rental	60,500	189,000
Gasoline and oil	97,200	230,400
Tolls	1,500	5,700
Insurance premiums, less claims paid	14,700	53,400
<b>2. Purchased intercity transportation, total</b>	<b>21,000</b>	<b>44,600</b>
Railroad	400	600
Intercity bus	1,300	2,100
Airline	17,600	33,100
Other	1,700	8,800
<b>3. Purchased local transportation, total</b>	<b>6,800</b>	<b>14,100</b>
Mass transit system	4,200	10,300
Taxi	2,600	3,800
<b>TOTAL transportation</b>	<b>377,700</b>	<b>979,100</b>

The Consumer Price Index did not increase as dramatically as the costs of owning and operating a vehicle, which further substantiates the conclusion that people are more willing to spend money on cars than they were 20 years ago.

Therefore it can be assumed that people in principle are willing to spend more money on cars. This can be substantiated by statistics saying that in 2000 63% of the U.S. households have 2 or more vehicles. Only 6% have no vehicle [25].

Additionally, it can be observed that the population will still increase in the next decades. In the year 2025 the U.S. population will exceed 350 million [41] and in 2050 it will reach 420 million [38]. From 2015 on, the baby boomer generation will start to retire, meaning that the generation which invented the “technological era” and formed social life like no generation before, will need to redefine themselves

as soon as they retire. Everywhere in industry, companies prepare for the most dramatic change in society since the 1970s [25, 41].

Criteria like safety, reliability and especially technical finesse (baby boomers feel much more comfortable with technology as a whole than elderly people do today, because baby boomers “invented and defined” today’s technology) will be critical for purchasing decisions of the “aging baby boomers”. It also needs to be considered that baby boomers, as the largest fraction of the population, will demand consumer products like they did before, but there will be an even higher demand on luxury goods than presently, as some kind of “retiring reward”.

Therefore it is assumed that willingness to pay “a little more” for high quality and technological challenging products may increase over the next decades. A carbon fiber reinforced brake system definitely increases the overall safety of a vehicle, it is a technological challenging product, and due to the fact that it is a composite, it represents one of the achievements of the baby boomer generation: invent and design new materials to explore new worlds. Composite materials made aerospace an overwhelming success, which is the greatest baby boomer achievement, since aerospace changed world’s life in the last few decades more than everything else. The previous argument contains a very important psychological effect, which may be extremely important for future marketing campaigns.

A detailed number for the market potential cannot be given at this stage, but it can be concluded that:

- The number of vehicles including passenger cars will still increase in the next years,
- People are spending much more money on their cars than before and a contrary trend cannot be observed,
- The largest population fraction, the baby boomers, will start to retire soon, which will dramatically change society until 2050 and beyond and probably

broaden the market for luxury goods since the retirees want “to reward themselves for a long working life”.

To specifically target niche markets, further investigations are necessary. Looking at Robert Coppers Stage-Gate-Model the next task would be to create a financial analysis of the product. The next section will provide the basis for a detailed cost analysis, since it will target the price range, which the final product needs to meet.

### 7.3.1 Market Estimation

Assuming that the majority of such brakes will be sold with new cars, the statistics of new car sales and motor vehicle production are important [40].

**Table 12: Passenger car sales and U.S. as well as world motor vehicle production (Note: passenger cars do not include Pick-Ups, SUVs and Minivans) [40]**

	1981	1985	2004
Retail New Passenger Car Sales in U.S.		10,979,187	7,505,932
World Motor Vehicle Production in Passenger Cars	27,407,000		42,831,904
U.S. Motor Vehicle Production in Passenger Cars	6,253,000		4,229,625
World Motor Vehicle Production in Commercial Vehicles	9,729,000		21,131,364
U.S. Motor Vehicle Production in Commercial Vehicles	1,690,000		7,730,729

The drop in U.S. car sales is not considered to be a critical issue for this study, since the world production in passenger and commercial vehicles indicates a still growing market.

Table 13: Annual sales and market shares of light trucks and automobiles in 2003 [40]

	Number of sales 2003 (in 1000 units)	Market Share 2003 (%)
<b>New Domestic and Imported Light Trucks</b>		
<b>TOTAL units</b>	<b>8,617</b>	
Small pickups	744	8,6
Large pickups	2,077	24,1
Small vans	1,066	12,4
Large vans	322	3,7
Small SUV	853	9,9
Medium SUV	2,692	31,2
Large SUV	864	10,0
<b>New Domestic and Imported Automobiles</b>		
<b>TOTAL units</b>	<b>7,698</b>	
Minicompact	80	1,0
Subcompact	459	6,0
Compact	3,018	39,2
Midsize	2,624	34,1
Large	1,351	17,5
Two-seater	165	2,1

Table 13 shows market share data in order to identify niche markets. The following vehicles can be targeted for the use of carbon fiber brake discs (sales in 2003):

- Large pickups: 2.08 million cars
- Large vans: 0.32 million cars
- Large SUVs: 0.86 million cars
- Large automobiles: 1.35 million cars
- Total niche market size: 4.61 million cars sold in 2003

These car types were chosen, because it is assumed that larger vehicles are more highly priced and that consumers of such cars are more willing to buy expensive carbon fiber brake discs. On the other hand it is much more reasonable to install carbon fiber brake discs in large, heavy and typically more powerful vehicles than

in smaller cars, because these vehicles require high performance brake systems due to their high inertia.

If it is possible to gain a market share of only 1% after 5 years in business with an average annual growth rate of 0.2%, which is a fairly conservative estimate, 184,400 brake discs for 46,100 cars can be sold, which makes a total business of \$73million if one brake disc retails at an average price of \$400. The business at the manufacturing level could reach \$36.5 million, assuming a 50% margin of the retailer.

### 7.3.2 Target Costing

Assuming a maximum average retail price of \$400, the maximum manufacturing costs should not exceed \$200 (assuming 50% margin at retail).

**Table 14: Cost estimate**

	Item	USD	
25%	Material		50.00
	85% of the material costs are raw material	42.50	
	15% of the material costs are material overhead	7.50	
7.5%	Labor		15.00
27.5%	Machinery		55.00
	90% of machinery costs are investment	49.50	
	10% of machinery costs are ongoing costs	5.50	
22.5%	Research and development (R&D)		45.00
	95% of R&D costs are investment	42.75	
	5% of R&D costs are ongoing costs	2.25	
10%	Profit		20.00
7.5%	Miscellaneous (other corporate overhead)		15.00
100%	TOTAL Manufacturing Costs		200.00

Total investments prior to product launch can be assumed as follows:

- \$10million for R&D
- \$10million for machinery
- \$20million total investment

The original investment of \$20million can be recovered via an allocated cost for machinery investment and R&D investment ( $\$49.50 + \$42.75 = \$92.25$ ), leading to a break even volume of 216,802 brake discs. This represents 1.18% market share of the annual new car sales in the targeted market niche.

## 8. Conclusion

In this chapter a summary of the technical part of this work and the carbon fiber brake disc market analysis are given. The technical summary includes an evaluation of the machinery itself and the experiments carried out.

### 8.1 *Technical Feasibility*

Looking back to the objectives, it can be summarized that all objectives could be met. The designed and tested equipment can be used for the production of disc shaped fiberwebs with circumferential fiber orientation.

The z-directional samples showed that it is even possible to manufacture fiberwebs with customized fiber orientation in circumferential direction as well as in the z-direction, which is seen as highly advantageous, since it will broaden the field of applications.

From the parameter studied it can be summarized:

- low electrostatic field strength,
  - especially a low potential ( $V_1=10\text{kV}$ ),
  - but also a high field distance ( $d_2=20\text{cm}$  or  $d_3=30\text{cm}$ ) and
- a high speed of the collecting disc ( $v_3=50\text{rpm}$ )

lead to high fiber orientation in circumferential direction.

Even though it was not possible to operate with carbon fibers, which would be interesting for the industrial field of brake discs, it can be concluded that the developed equipment should work with carbon fibers if the fiber separation problem can be solved. Since carbon fiber separation was not an objective of this work, this subject is being left for future research.

However the equipment still needs to be optimized. Chapter 9, page 111 will address this issue.

## **8.2 Market**

It could be explained that there is an increasing demand for automobiles in the U.S. in the next few decades. Generally it is also assumed that the need for luxury goods could increase, meaning that people are willing to spend more money for some extra features. In this context it could probably be possible to successfully introduce carbon fiber brake discs on the market, assumed that manufacturing costs can be limited on a competitive basis.

A detailed financial analysis of the technology for the production of carbon fiber webs with circumferential fiber orientation, which are suitable for the use as brake discs after finishing to a composite material, is crucial in order to evaluate the value of the presented technology in this paper. An introductory cost estimate and niche market analysis was given, but more extensive research is necessary to confirm the presented numbers.

A detailed cost or financial analysis is highly suggested before extensive further technical research is undertaken. Furthermore a detailed “customer wants and needs study” should be done to clarify the market need for carbon fiber high performance brake discs in specific niche markets. Cooperation with current brake disc manufacturers is inevitable in order to get correct and in-depth insight into the market.

The estimated numbers for targeted market segments and manufacturing costs appear optimistic. Therefore it is suggested to further investigate markets for carbon fiber brake discs.

## 9. Future Work

Some problems and areas for future work were already mentioned in previous chapters. The following list summarizes all topics for future research:

- The parametric study revealed that the optimal collecting disc speed is probably above 50rpm. The change of the ratio of the timing belt transmission is a very easy way to increase the collecting disc speed.
- Furthermore the parametric study indicated that low field strengths support a good fiber orientation. Unfortunately the fibers are subject to be blown away especially when operating with low field strengths. The enclosure of the electrostatic field, for example with a plastic sheet, could be a way to prevent fiber loss due to air movement. When the effect of fiber loss is eliminated, lower field strength could be implemented to check whether such low levels achieve better circumferential fiber orientation.
- Research on carbon fiber preparation to allow processability is needed. The issue of fiber separation may be handled by researching fiber parameters and fiber dispensing system design.
- To dispense an equal amount of fibers on the collecting disc, the fiber dispensing setup need to be redesigned to use conical brushes.
- The fiber lay-down method needs to be optimized, since “thick” fiberwebs, meaning webs with multiple layer of fibers, cannot be produced using the current lay-down rod. Extensive research is required to overcome the problem of contaminating the lay-down rod with resin (a fully developed setup assumed), when the rod is touching the disc surface.

## 10. Bibliography

- [1] M. Acar, B. Pourdeyhimi, D. Shiffler, R. Holmes and N. Vaidya, "The manufacturing of wet-lay hydroentangled glass fiber composites for industrial applications," in NCRC Annual Program Review, may 29, 2002, 2002,
- [2] K. H. G. Ashbee, *Fundamental Principles of Fiber Reinforced Composites*. Lancaster: Technomic Pub. Co., 1989, pp. 372.
- [3] R. Bansal, *Handbook of Engineering Electromagnetics*. New York: Marcel Dekker, 2004, pp. 706.
- [4] S. K. Batra, "Web formation: Carding technology," in NCRC Workshop Nonwovens Principles & Practice from Jan 15-18 2002, 2002,
- [5] D. Brokmeier, *Considerations on Improving Flock Production; from the 8th International Flock Symposium: Darmstadt, November 22th-23th, 1984*. Darmstadt: Fachhochschule Darmstadt, FB Kunststofftechnik, 1984,
- [6] J. Chang, A. J. Kelly and J. M. Crowley, *Handbook of Electrostatic Processes*. New York: M. Dekker, 1995, pp. 763.
- [7] D. D. L. Chung, *Carbon Fiber Composites*. Boston: Butterworth-Heinemann, 1994, pp. 215.
- [8] R. G. Cooper, *Winning at New Products : Accelerating the Process from Idea to Launch*. ,3rd ed. Reading, Mass.: Perseus, 2001, pp. 425.
- [9] figures confirmed by consulting company,
- [10] E. R. Frederick, G. W. Penney, 10 United States. Environmental Protection Agency. Office of Research and Development and 20 Carnegie-Mellon University, *Electrostatic Effects in Fabric Filtration*. Washington; Springfield, Va.: Environmental Protection Agency, Office of Research and Development; for sale by the National Technical Information Service, 1978,
- [11] K. Gabler, *Investigation of Flight Characterisitcs of Flock, by Means of High-Speed Photographic Camera; from the 6th International Flock Symposium: Aachen, 8.-10. Sept., 1980*. Aachen: Institut für Kunststoffverarbeitung an der RWTH Aachen, 1986, pp. 249.
- [12] R. M. Gill, *Carbon Fibres in Composite Materials*. London: Iliffe Books for the Plastics Institute, 1972, pp. [7], 207.

[13] D. J. Griffiths, Introduction to Electrodynamics. ,3rd ed.Upper Saddle River, NJ: Prentice Hall, 1999, pp. 576.

[14] U. Gruber, M. Heine and Kienzle, Andreas (SGL Carbon Group AG), "Method for producing brake discs consisting of ceramic parts with metal hubs and a brake disc obtainable by the method," EP 1117943B1, June 25, 2001,

[15] H. A. Haus and J. R. Melcher, Electromagnetic Fields and Energy. Englewood Cliffs, N.J.: Prentice Hall, 1989, pp. 742.

[16] D. M. Howell and J. D. Sanders, The Technology, Formulation and Application of Powder Coatings. , vol. 1, Chichester ; New York: Wiley in association with SITA Technology, 2000, pp. 361.

[17] [http://en.wikipedia.org/wiki/Disc\\_brake](http://en.wikipedia.org/wiki/Disc_brake) (retrieved on March 5, 2006),

[18] <http://www.autospecialty.com/index.html> (retrieved on February 28, 2006),

[19] <http://www.ebcbrakes.com/> (retrieved on March 11, 2006),

[20] <http://www.efiltd.co.uk/> (retrieved on March 11, 2006),

[21] <http://www.porsche.com/> (retrieved on March 1, 2006),

[22] [http://www.sglcarbon.de/sgl\\_t/brakedisc/index.html](http://www.sglcarbon.de/sgl_t/brakedisc/index.html) (retrieved on March 4, 2006),

[23] F. Kassack, F. Reich, A. Schmitz and Farbenfabriken Bayer Aktiengesellschaft, Flocking : Surface Styling of Textiles by Flocking. , vol. 2, Leverkusen; Union, N.J.: Farbenfabriken Bayer AG; Verona Dyestuffs distributor, 1967, pp. 40.

[24] P. A. Keller, The Cathode-Ray Tube : Technology, History, and Applications. New York: Palisades Press, 1991, pp. 314.

[25] P. Kotler and K. L. Keller, Marketing Management. ,Twelfth ed.Upper Saddle River, NJ: Pearson Prentice Hall, 2006, pp. 733 [45].

[26] M. Menghe, H. E. Glassey and M. Rastogi, "An Experimental Study of the Needled Nonwoven Process, Part III: Fiber Damage Due to Needling," Textile Research Journal, vol. 74, pp. 485-490, 2004.

[27] A. Mohan, "Formation and characterization of electrospun nonwoven webs," Thesis (M. S. ) North Carolina State University, 2002.

- [28] Morris, Edward L., Jr., J. A. Hasler, H. Lange and (The B.F. Goodrich Company, Akron, Ohio, USA), "Curved braid apparatus," Patent US 5417138, Nov.10, 1993.
- [29] D. A. Nethercot, Composite Construction. London ; New York: Spon Press, 2003, pp. 236.
- [30] W. Oxenham, A. M. Seyam and N. B. Doguc, "Carding dynamics: Improvement of the three-dimensional uniformity of carded and crosslapped fiberwebs," in NCRC Annual Program Review, may 29, 2002, 2002,
- [31] K. R. Parker and Institution of Electrical Engineers, Electrical Operation of Electrostatic Precipitators. , vol. 41, London: Institution of Electrical Engineers, 2003, pp. 270.
- [32] personal conversation with SGL Carbon Group representatives at JEC Paris 2002,
- [33] R. Resnick, D. Halliday and K. S. Krane, Physics. ,5th ed.New York: Wiley, 2002,
- [34] A. M. Seyam, B. P. Wendisch and Y. K. Kim, "New Devices for Forming Nonwoven Webs using Electrostatic Field," Proceedings of the 3rd International Conference of Textile Research Division, National Research Centre, Cairo, Egypt, April 2006,
- [35] P. W. Sheehan, R. Sze-Heng Liew and (The B.F. Goodrich Company, Akron, Ohio, USA), "Brake disc having a functional gradient z-fiber distribution," Patent EP 0767264B1, Oct.2, 1996.
- [36] D. Shiffler, "Air-lay nonwoven technology," in NCRC Workshop Nonwovens Principles & Practice, 2002,
- [37] Tanasescu, F. T., Dr.Ing, C. Antohi Dr.Ing and E. Stere Dipl.-Ing., Influence of the Flocking Process in the Electrostatic Field by Conditioning the Flock in Warm and Humid Air; from the 7th International Flock Symposium: Darmstadt, September 27th-29th, 1982. Darmstadt: Fachhochschule Darmstadt, FB Kunststofftechnik, 1982, pp. 254.
- [38] U.S. Census Bureau, Current Population Survey, 1968 to 2005 Annual Social and Economic Supplements available at [www.census.gov](http://www.census.gov),
- [39] U.S. Census Bureau, International Data Base, available at [www.census.gov](http://www.census.gov),
- [40] U.S. Department of Transportation, Research and Innovative Technology Administration, Bureau of Transportation Statistics, "National Transportation

Statistics 2005, Washington , DC, summer 2005, available at [http://www.bts.gov/publications/national\\_transportation\\_statistics/2005](http://www.bts.gov/publications/national_transportation_statistics/2005),"

[41] A. S. Wellner, "THE NEXT 25 YEARS. (cover story)," American Demographics, vol. 25, pp. 24-4, 2003.

[42] Zarembka, Robert L. (Goodyear Aerospace Corporation, Akron, Ohio, USA), "Ribbon-wrapped carbon brake disc," Patent US 4187932, Feb.1, 1978,

## Appendices

## Appendix I: Fiber Distribution Data Tables

Table 15: Fiber distribution data table for sample number 1

Sample Number:	1				
Angle	Radius [mm]			Number of Fibers	% Number of Fibers
	~72	~122	~172		
0° ... ≤ ±10°	15	8	6	29	33.33
< ±10° ... ≤ ±20°	4	6	8	18	20.69
< ±20° ... ≤ ±30°	6	4	3	13	14.94
< ±30° ... ≤ ±40°	8	0	2	10	11.49
< ±40° ... ≤ ±50°	2	5	1	8	9.20
< ±50° ... ≤ ±60°	0	1	1	2	2.30
< ±60° ... ≤ ±70°	2	1	0	3	3.45
< ±70° ... ≤ ±80°	1	1	0	2	2.30
< ±80° ... ≤ 90°	1	1	0	2	2.30
<b>Total</b>	<b>39</b>	<b>27</b>	<b>21</b>	<b>87</b>	<b>100.00</b>

Table 16: Fiber distribution data table for sample number 3

Sample Number:	3				
Angle	Radius [mm]			Number of Fibers	% Number of Fibers
	~72	~122	~172		
0° ... ≤ ±10°	20	12	7	39	40.63
< ±10° ... ≤ ±20°	11	8	4	23	23.96
< ±20° ... ≤ ±30°	7	4	2	13	13.54
< ±30° ... ≤ ±40°	7	3	2	12	12.50
< ±40° ... ≤ ±50°	2	1	1	4	4.17
< ±50° ... ≤ ±60°	3	0	0	3	3.13
< ±60° ... ≤ ±70°	0	0	0	0	0.00
< ±70° ... ≤ ±80°	1	0	1	2	2.08
< ±80° ... ≤ 90°	0	0	0	0	0.00
<b>Total</b>	<b>51</b>	<b>28</b>	<b>17</b>	<b>96</b>	<b>100.00</b>

Table 17: Fiber distribution data table for sample number 5

Sample Number:	5			Number of Fibers	% Number of Fibers
	Angle	Radius [mm]			
	~72	~122	~172		
$0^\circ \dots \leq \pm 10^\circ$	13	13	5	31	30.69
$< \pm 10^\circ \dots \leq \pm 20^\circ$	10	9	1	20	19.80
$< \pm 20^\circ \dots \leq \pm 30^\circ$	2	9	3	14	13.86
$< \pm 30^\circ \dots \leq \pm 40^\circ$	5	2	1	8	7.92
$< \pm 40^\circ \dots \leq \pm 50^\circ$	6	2	0	8	7.92
$< \pm 50^\circ \dots \leq \pm 60^\circ$	2	3	2	7	6.93
$< \pm 60^\circ \dots \leq \pm 70^\circ$	0	2	1	3	2.97
$< \pm 70^\circ \dots \leq \pm 80^\circ$	4	1	1	6	5.94
$< \pm 80^\circ \dots \leq 90^\circ$	3	0	1	4	3.96
<b>Total</b>	<b>45</b>	<b>41</b>	<b>15</b>	<b>101</b>	<b>100.00</b>

Table 18: Fiber distribution data table for sample number 6

Sample Number:	6			Number of Fibers	% Number of Fibers
	Angle	Radius [mm]			
	~72	~122	~172		
$0^\circ \dots \leq \pm 10^\circ$	16	27	10	53	30.81
$< \pm 10^\circ \dots \leq \pm 20^\circ$	16	13	7	36	20.93
$< \pm 20^\circ \dots \leq \pm 30^\circ$	12	15	7	34	19.77
$< \pm 30^\circ \dots \leq \pm 40^\circ$	5	9	1	15	8.72
$< \pm 40^\circ \dots \leq \pm 50^\circ$	3	7	1	11	6.40
$< \pm 50^\circ \dots \leq \pm 60^\circ$	7	2	0	9	5.23
$< \pm 60^\circ \dots \leq \pm 70^\circ$	2	3	2	7	4.07
$< \pm 70^\circ \dots \leq \pm 80^\circ$	0	3	0	3	1.74
$< \pm 80^\circ \dots \leq 90^\circ$	2	2	0	4	2.33
<b>Total</b>	<b>63</b>	<b>81</b>	<b>28</b>	<b>172</b>	<b>100.00</b>

Table 19: Fiber distribution data table for sample number 7

Sample Number:	7			Number of Fibers	% Number of Fibers
	Angle	Radius [mm]			
	~72	~122	~172		
$0^\circ \dots \leq \pm 10^\circ$	12	12	10	34	27.64
$< \pm 10^\circ \dots \leq \pm 20^\circ$	11	11	2	24	19.51
$< \pm 20^\circ \dots \leq \pm 30^\circ$	4	4	9	17	13.82
$< \pm 30^\circ \dots \leq \pm 40^\circ$	6	5	2	13	10.57
$< \pm 40^\circ \dots \leq \pm 50^\circ$	6	1	2	9	7.32
$< \pm 50^\circ \dots \leq \pm 60^\circ$	2	3	2	7	5.69
$< \pm 60^\circ \dots \leq \pm 70^\circ$	4	2	0	6	4.88
$< \pm 70^\circ \dots \leq \pm 80^\circ$	4	2	2	8	6.50
$< \pm 80^\circ \dots \leq 90^\circ$	2	2	1	5	4.07
<b>Total</b>	<b>51</b>	<b>42</b>	<b>30</b>	<b>123</b>	<b>100.00</b>

Table 20: Fiber distribution data table for sample number 8

Sample Number:	8				
Angle	Radius [mm]			Number of Fibers	% Number of Fibers
	~72	~122	~172		
$0^\circ \dots \leq \pm 10^\circ$	12	5	8	25	22.52
$< \pm 10^\circ \dots \leq \pm 20^\circ$	11	7	9	27	24.32
$< \pm 20^\circ \dots \leq \pm 30^\circ$	5	9	4	18	16.22
$< \pm 30^\circ \dots \leq \pm 40^\circ$	3	2	4	9	8.11
$< \pm 40^\circ \dots \leq \pm 50^\circ$	5	1	4	10	9.01
$< \pm 50^\circ \dots \leq \pm 60^\circ$	4	3	0	7	6.31
$< \pm 60^\circ \dots \leq \pm 70^\circ$	2	0	3	5	4.50
$< \pm 70^\circ \dots \leq \pm 80^\circ$	2	0	1	3	2.70
$< \pm 80^\circ \dots \leq 90^\circ$	4	0	3	7	6.31
<b>Total</b>	<b>48</b>	<b>27</b>	<b>36</b>	<b>111</b>	<b>100.00</b>

Table 21: Fiber distribution data table for sample number 9

Sample Number:	9				
Angle	Radius [mm]			Number of Fibers	% Number of Fibers
	~72	~122	~172		
$0^\circ \dots \leq \pm 10^\circ$	10	10	5	25	26.60
$< \pm 10^\circ \dots \leq \pm 20^\circ$	14	8	5	27	28.72
$< \pm 20^\circ \dots \leq \pm 30^\circ$	7	6	4	17	18.09
$< \pm 30^\circ \dots \leq \pm 40^\circ$	6	2	3	11	11.70
$< \pm 40^\circ \dots \leq \pm 50^\circ$	5	1	0	6	6.38
$< \pm 50^\circ \dots \leq \pm 60^\circ$	2	0	1	3	3.19
$< \pm 60^\circ \dots \leq \pm 70^\circ$	1	1	0	2	2.13
$< \pm 70^\circ \dots \leq \pm 80^\circ$	0	0	0	0	0.00
$< \pm 80^\circ \dots \leq 90^\circ$	3	0	0	3	3.19
<b>Total</b>	<b>48</b>	<b>28</b>	<b>18</b>	<b>94</b>	<b>100.00</b>

Table 22: Fiber distribution data table for sample number 10

Sample Number:	10				
Angle	Radius [mm]			Number of Fibers	% Number of Fibers
	~72	~122	~172		
$0^\circ \dots \leq \pm 10^\circ$	17	16	5	38	33.04
$< \pm 10^\circ \dots \leq \pm 20^\circ$	20	6	3	29	25.22
$< \pm 20^\circ \dots \leq \pm 30^\circ$	12	3	2	17	14.78
$< \pm 30^\circ \dots \leq \pm 40^\circ$	10	2	1	13	11.30
$< \pm 40^\circ \dots \leq \pm 50^\circ$	5	1	0	6	5.22
$< \pm 50^\circ \dots \leq \pm 60^\circ$	1	1	1	3	2.61
$< \pm 60^\circ \dots \leq \pm 70^\circ$	3	1	0	4	3.48
$< \pm 70^\circ \dots \leq \pm 80^\circ$	1	1	1	3	2.61
$< \pm 80^\circ \dots \leq 90^\circ$	0	0	2	2	1.74
<b>Total</b>	<b>69</b>	<b>31</b>	<b>15</b>	<b>115</b>	<b>100.00</b>

Table 23: Fiber distribution data table for sample number 11

Sample Number:	11				
Angle	Radius [mm]			Number of Fibers	% Number of Fibers
	~72	~122	~172		
$0^\circ \dots \leq \pm 10^\circ$	21	9	4	34	29.57
$< \pm 10^\circ \dots \leq \pm 20^\circ$	18	9	5	32	27.83
$< \pm 20^\circ \dots \leq \pm 30^\circ$	10	2	2	14	12.17
$< \pm 30^\circ \dots \leq \pm 40^\circ$	5	4	6	15	13.04
$< \pm 40^\circ \dots \leq \pm 50^\circ$	6	2	0	8	6.96
$< \pm 50^\circ \dots \leq \pm 60^\circ$	4	3	0	7	6.09
$< \pm 60^\circ \dots \leq \pm 70^\circ$	0	0	1	1	0.87
$< \pm 70^\circ \dots \leq \pm 80^\circ$	1	0	0	1	0.87
$< \pm 80^\circ \dots \leq 90^\circ$	1	2	0	3	2.61
<b>Total</b>	<b>66</b>	<b>31</b>	<b>18</b>	<b>115</b>	<b>100.00</b>

Table 24: Fiber distribution data table for sample number 12

Sample Number:	12				
Angle	Radius [mm]			Number of Fibers	% Number of Fibers
	~72	~122	~172		
$0^\circ \dots \leq \pm 10^\circ$	26	20	10	56	53.85
$< \pm 10^\circ \dots \leq \pm 20^\circ$	11	4	5	20	19.23
$< \pm 20^\circ \dots \leq \pm 30^\circ$	5	4	1	10	9.62
$< \pm 30^\circ \dots \leq \pm 40^\circ$	5	2	1	8	7.69
$< \pm 40^\circ \dots \leq \pm 50^\circ$	1	1	1	3	2.88
$< \pm 50^\circ \dots \leq \pm 60^\circ$	3	0	0	3	2.88
$< \pm 60^\circ \dots \leq \pm 70^\circ$	1	0	1	2	1.92
$< \pm 70^\circ \dots \leq \pm 80^\circ$	0	0	0	0	0.00
$< \pm 80^\circ \dots \leq 90^\circ$	2	0	0	2	1.92
<b>Total</b>	<b>54</b>	<b>31</b>	<b>19</b>	<b>104</b>	<b>100.00</b>

Table 25: Fiber distribution data table for sample number 13

Sample Number:	13				
Angle	Radius [mm]			Number of Fibers	% Number of Fibers
	~72	~122	~172		
$0^\circ \dots \leq \pm 10^\circ$	22	17	19	58	41.43
$< \pm 10^\circ \dots \leq \pm 20^\circ$	24	13	7	44	31.43
$< \pm 20^\circ \dots \leq \pm 30^\circ$	16	5	4	25	17.86
$< \pm 30^\circ \dots \leq \pm 40^\circ$	3	1	1	5	3.57
$< \pm 40^\circ \dots \leq \pm 50^\circ$	1	0	1	2	1.43
$< \pm 50^\circ \dots \leq \pm 60^\circ$	2	1	1	4	2.86
$< \pm 60^\circ \dots \leq \pm 70^\circ$	0	0	0	0	0.00
$< \pm 70^\circ \dots \leq \pm 80^\circ$	0	0	0	0	0.00
$< \pm 80^\circ \dots \leq 90^\circ$	2	0	0	2	1.43
<b>Total</b>	<b>70</b>	<b>37</b>	<b>33</b>	<b>140</b>	<b>100.00</b>

Table 26: Fiber distribution data table for sample number 14

Sample Number:	14				
Angle	Radius [mm]			Number of Fibers	% Number of Fibers
	~72	~122	~172		
0° ... ≤ ±10°	9	9	2	20	25.97
< ±10° ... ≤ ±20°	10	4	5	19	24.68
< ±20° ... ≤ ±30°	10	2	2	14	18.18
< ±30° ... ≤ ±40°	4	3	1	8	10.39
< ±40° ... ≤ ±50°	5	2	1	8	10.39
< ±50° ... ≤ ±60°	3	0	0	3	3.90
< ±60° ... ≤ ±70°	1	0	0	1	1.30
< ±70° ... ≤ ±80°	3	0	0	3	3.90
< ±80° ... ≤ 90°	1	0	0	1	1.30
<b>Total</b>	<b>46</b>	<b>20</b>	<b>11</b>	<b>77</b>	<b>100.00</b>

Table 27: Fiber distribution data table for sample number 21

Sample Number:	21				
Angle	Radius [mm]			Number of Fibers	% Number of Fibers
	~72	~122	~172		
0° ... ≤ ±10°	19	23	10	52	27.96
< ±10° ... ≤ ±20°	14	11	7	32	17.20
< ±20° ... ≤ ±30°	9	9	3	21	11.29
< ±30° ... ≤ ±40°	9	5	2	16	8.60
< ±40° ... ≤ ±50°	9	4	2	15	8.06
< ±50° ... ≤ ±60°	15	1	2	18	9.68
< ±60° ... ≤ ±70°	9	1	0	10	5.38
< ±70° ... ≤ ±80°	8	2	2	12	6.45
< ±80° ... ≤ 90°	6	2	2	10	5.38
<b>Total</b>	<b>98</b>	<b>58</b>	<b>30</b>	<b>186</b>	<b>100.00</b>

Table 28: Fiber distribution data table for sample number 22

Sample Number:	22				
Angle	Radius [mm]			Number of Fibers	% Number of Fibers
	~72	~122	~172		
0° ... ≤ ±10°	25	20	18	63	20.32
< ±10° ... ≤ ±20°	19	17	10	46	14.84
< ±20° ... ≤ ±30°	9	11	8	28	9.03
< ±30° ... ≤ ±40°	19	16	12	47	15.16
< ±40° ... ≤ ±50°	12	10	5	27	8.71
< ±50° ... ≤ ±60°	7	8	5	20	6.45
< ±60° ... ≤ ±70°	12	13	10	35	11.29
< ±70° ... ≤ ±80°	6	6	4	16	5.16
< ±80° ... ≤ 90°	13	6	9	28	9.03
<b>Total</b>	<b>122</b>	<b>107</b>	<b>81</b>	<b>310</b>	<b>100.00</b>

Table 29: Fiber distribution data table for sample number 23

Sample Number:	23				
Angle	Radius [mm]			Number of Fibers	% Number of Fibers
	~72	~122	~172		
0° ... ≤ ±10°	23	30	30	83	57.64
< ±10° ... ≤ ±20°	15	4	3	22	15.28
< ±20° ... ≤ ±30°	10	5	3	18	12.50
< ±30° ... ≤ ±40°	2	4	3	9	6.25
< ±40° ... ≤ ±50°	2	3	1	6	4.17
< ±50° ... ≤ ±60°	0	0	0	0	0.00
< ±60° ... ≤ ±70°	0	0	1	1	0.69
< ±70° ... ≤ ±80°	0	2	1	3	2.08
< ±80° ... ≤ 90°	1	0	1	2	1.39
<b>Total</b>	<b>53</b>	<b>48</b>	<b>43</b>	<b>144</b>	<b>100.00</b>

Table 30: Fiber distribution data table for sample number 24

Sample Number:	24				
Angle	Radius [mm]			Number of Fibers	% Number of Fibers
	~72	~122	~172		
0° ... ≤ ±10°	24	31	28	83	52.87
< ±10° ... ≤ ±20°	13	14	6	33	21.02
< ±20° ... ≤ ±30°	12	6	3	21	13.38
< ±30° ... ≤ ±40°	4	4	0	8	5.10
< ±40° ... ≤ ±50°	3	1	1	5	3.18
< ±50° ... ≤ ±60°	2	1	0	3	1.91
< ±60° ... ≤ ±70°	0	0	1	1	0.64
< ±70° ... ≤ ±80°	1	0	0	1	0.64
< ±80° ... ≤ 90°	2	0	0	2	1.27
<b>Total</b>	<b>61</b>	<b>57</b>	<b>39</b>	<b>157</b>	<b>100.00</b>

Table 31: Fiber distribution data table for sample number 25

Sample Number:	25				
Angle	Radius [mm]			Number of Fibers	% Number of Fibers
	~72	~122	~172		
0° ... ≤ ±10°	33	21	21	75	22.06
< ±10° ... ≤ ±20°	37	11	11	59	17.35
< ±20° ... ≤ ±30°	22	10	16	48	14.12
< ±30° ... ≤ ±40°	19	8	9	36	10.59
< ±40° ... ≤ ±50°	13	6	13	32	9.41
< ±50° ... ≤ ±60°	15	4	7	26	7.65
< ±60° ... ≤ ±70°	17	4	7	28	8.24
< ±70° ... ≤ ±80°	4	5	6	15	4.41
< ±80° ... ≤ 90°	8	6	7	21	6.18
<b>Total</b>	<b>168</b>	<b>75</b>	<b>97</b>	<b>340</b>	<b>100.00</b>

Table 32: Fiber distribution data table for sample number 26

Sample Number:	26				
Angle	Radius [mm]			Number of Fibers	% Number of Fibers
	~72	~122	~172		
$0^\circ \dots \leq \pm 10^\circ$	16	8	1	25	19.08
$< \pm 10^\circ \dots \leq \pm 20^\circ$	13	4	6	23	17.56
$< \pm 20^\circ \dots \leq \pm 30^\circ$	10	10	3	23	17.56
$< \pm 30^\circ \dots \leq \pm 40^\circ$	14	5	4	23	17.56
$< \pm 40^\circ \dots \leq \pm 50^\circ$	7	2	2	11	8.40
$< \pm 50^\circ \dots \leq \pm 60^\circ$	6	3	2	11	8.40
$< \pm 60^\circ \dots \leq \pm 70^\circ$	1	4	3	8	6.11
$< \pm 70^\circ \dots \leq \pm 80^\circ$	3	1	0	4	3.05
$< \pm 80^\circ \dots \leq 90^\circ$	1	0	2	3	2.29
<b>Total</b>	<b>71</b>	<b>37</b>	<b>23</b>	<b>131</b>	<b>100.00</b>

Table 33: Fiber distribution data table for sample number 27

Sample Number:	27				
Angle	Radius [mm]			Number of Fibers	% Number of Fibers
	~72	~122	~172		
$0^\circ \dots \leq \pm 10^\circ$	11	9	5	25	16.67
$< \pm 10^\circ \dots \leq \pm 20^\circ$	12	11	3	26	17.33
$< \pm 20^\circ \dots \leq \pm 30^\circ$	14	6	1	21	14.00
$< \pm 30^\circ \dots \leq \pm 40^\circ$	11	7	7	25	16.67
$< \pm 40^\circ \dots \leq \pm 50^\circ$	4	2	3	9	6.00
$< \pm 50^\circ \dots \leq \pm 60^\circ$	11	3	2	16	10.67
$< \pm 60^\circ \dots \leq \pm 70^\circ$	7	5	4	16	10.67
$< \pm 70^\circ \dots \leq \pm 80^\circ$	1	2	0	3	2.00
$< \pm 80^\circ \dots \leq 90^\circ$	3	6	0	9	6.00
<b>Total</b>	<b>74</b>	<b>51</b>	<b>25</b>	<b>150</b>	<b>100.00</b>

Table 34: Fiber distribution data table for sample number 28

Sample Number:	28				
Angle	Radius [mm]			Number of Fibers	% Number of Fibers
	~72	~122	~172		
$0^\circ \dots \leq \pm 10^\circ$	25	32	12	69	21.43
$< \pm 10^\circ \dots \leq \pm 20^\circ$	15	28	16	59	18.32
$< \pm 20^\circ \dots \leq \pm 30^\circ$	20	18	11	49	15.22
$< \pm 30^\circ \dots \leq \pm 40^\circ$	12	5	13	30	9.32
$< \pm 40^\circ \dots \leq \pm 50^\circ$	14	8	7	29	9.01
$< \pm 50^\circ \dots \leq \pm 60^\circ$	8	6	4	18	5.59
$< \pm 60^\circ \dots \leq \pm 70^\circ$	14	4	7	25	7.76
$< \pm 70^\circ \dots \leq \pm 80^\circ$	10	2	4	16	4.97
$< \pm 80^\circ \dots \leq 90^\circ$	13	7	7	27	8.39
<b>Total</b>	<b>131</b>	<b>110</b>	<b>81</b>	<b>322</b>	<b>100.00</b>

Table 35: Fiber distribution data table for sample number 29

Sample Number:	29				
Angle	Radius [mm]			Number of Fibers	% Number of Fibers
	~72	~122	~172		
0° ... ≤ ±10°	15	13	12	40	25.00
< ±10° ... ≤ ±20°	12	14	8	34	21.25
< ±20° ... ≤ ±30°	12	8	4	24	15.00
< ±30° ... ≤ ±40°	6	7	5	18	11.25
< ±40° ... ≤ ±50°	7	4	1	12	7.50
< ±50° ... ≤ ±60°	7	2	3	12	7.50
< ±60° ... ≤ ±70°	3	2	2	7	4.38
< ±70° ... ≤ ±80°	5	3	1	9	5.63
< ±80° ... ≤ 90°	3	0	1	4	2.50
<b>Total</b>	<b>70</b>	<b>53</b>	<b>37</b>	<b>160</b>	<b>100.00</b>

Table 36: Fiber distribution data table for sample number 30

Sample Number:	30				
Angle	Radius [mm]			Number of Fibers	% Number of Fibers
	~72	~122	~172		
0° ... ≤ ±10°	41	30	13	84	22.16
< ±10° ... ≤ ±20°	21	26	19	66	17.41
< ±20° ... ≤ ±30°	13	26	14	53	13.98
< ±30° ... ≤ ±40°	15	5	11	31	8.18
< ±40° ... ≤ ±50°	12	11	12	35	9.23
< ±50° ... ≤ ±60°	13	11	4	28	7.39
< ±60° ... ≤ ±70°	7	7	8	22	5.80
< ±70° ... ≤ ±80°	11	9	14	34	8.97
< ±80° ... ≤ 90°	11	5	10	26	6.86
<b>Total</b>	<b>144</b>	<b>130</b>	<b>105</b>	<b>379</b>	<b>100.00</b>

Table 37: Fiber distribution data table for sample number 31

Sample Number:	31				
Angle	Radius [mm]			Number of Fibers	% Number of Fibers
	~72	~122	~172		
0° ... ≤ ±10°	21	12	21	54	20.15
< ±10° ... ≤ ±20°	20	21	12	53	19.78
< ±20° ... ≤ ±30°	6	6	11	23	8.58
< ±30° ... ≤ ±40°	10	9	5	24	8.96
< ±40° ... ≤ ±50°	10	10	4	24	8.96
< ±50° ... ≤ ±60°	10	10	8	28	10.45
< ±60° ... ≤ ±70°	4	10	5	19	7.09
< ±70° ... ≤ ±80°	10	7	6	23	8.58
< ±80° ... ≤ 90°	11	4	5	20	7.46
<b>Total</b>	<b>102</b>	<b>89</b>	<b>77</b>	<b>268</b>	<b>100.00</b>

Table 38: Fiber distribution data table for sample number 32

Sample Number:	32				
Angle	Radius [mm]			Number of Fibers	% Number of Fibers
	~72	~122	~172		
$0^\circ \dots \leq \pm 10^\circ$	50	33	31	114	29.92
$< \pm 10^\circ \dots \leq \pm 20^\circ$	28	23	18	69	18.11
$< \pm 20^\circ \dots \leq \pm 30^\circ$	17	15	20	52	13.65
$< \pm 30^\circ \dots \leq \pm 40^\circ$	11	11	8	30	7.87
$< \pm 40^\circ \dots \leq \pm 50^\circ$	11	5	2	18	4.72
$< \pm 50^\circ \dots \leq \pm 60^\circ$	7	5	5	17	4.46
$< \pm 60^\circ \dots \leq \pm 70^\circ$	9	8	4	21	5.51
$< \pm 70^\circ \dots \leq \pm 80^\circ$	7	11	10	28	7.35
$< \pm 80^\circ \dots \leq 90^\circ$	12	15	5	32	8.40
<b>Total</b>	<b>152</b>	<b>126</b>	<b>103</b>	<b>381</b>	<b>100.00</b>

Table 39: Fiber distribution data table for sample number 33

Sample Number:	33				
Angle	Radius [mm]			Number of Fibers	% Number of Fibers
	~72	~122	~172		
$0^\circ \dots \leq \pm 10^\circ$	43	49	16	108	26.47
$< \pm 10^\circ \dots \leq \pm 20^\circ$	34	26	18	78	19.12
$< \pm 20^\circ \dots \leq \pm 30^\circ$	17	26	12	55	13.48
$< \pm 30^\circ \dots \leq \pm 40^\circ$	20	12	15	47	11.52
$< \pm 40^\circ \dots \leq \pm 50^\circ$	11	8	11	30	7.35
$< \pm 50^\circ \dots \leq \pm 60^\circ$	9	9	7	25	6.13
$< \pm 60^\circ \dots \leq \pm 70^\circ$	15	3	8	26	6.37
$< \pm 70^\circ \dots \leq \pm 80^\circ$	6	6	3	15	3.68
$< \pm 80^\circ \dots \leq 90^\circ$	8	11	5	24	5.88
<b>Total</b>	<b>163</b>	<b>150</b>	<b>95</b>	<b>408</b>	<b>100.00</b>

Table 40: Fiber distribution data table for sample number 34

Sample Number:	34				
Angle	Radius [mm]			Number of Fibers	% Number of Fibers
	~72	~122	~172		
$0^\circ \dots \leq \pm 10^\circ$	24	34	9	67	19.59
$< \pm 10^\circ \dots \leq \pm 20^\circ$	21	22	12	55	16.08
$< \pm 20^\circ \dots \leq \pm 30^\circ$	20	16	10	46	13.45
$< \pm 30^\circ \dots \leq \pm 40^\circ$	15	12	6	33	9.65
$< \pm 40^\circ \dots \leq \pm 50^\circ$	21	10	4	35	10.23
$< \pm 50^\circ \dots \leq \pm 60^\circ$	7	8	9	24	7.02
$< \pm 60^\circ \dots \leq \pm 70^\circ$	8	11	4	23	6.73
$< \pm 70^\circ \dots \leq \pm 80^\circ$	13	6	12	31	9.06
$< \pm 80^\circ \dots \leq 90^\circ$	10	9	9	28	8.19
<b>Total</b>	<b>139</b>	<b>128</b>	<b>75</b>	<b>342</b>	<b>100.00</b>

Table 41: Fiber distribution data table for sample number 35

Sample Number:	35				
Angle	Radius [mm]			Number of Fibers	% Number of Fibers
	~72	~122	~172		
0° ... ≤ ±10°	24	40	13	77	18.16
< ±10° ... ≤ ±20°	26	35	16	77	18.16
< ±20° ... ≤ ±30°	30	32	10	72	16.98
< ±30° ... ≤ ±40°	23	7	13	43	10.14
< ±40° ... ≤ ±50°	13	11	6	30	7.08
< ±50° ... ≤ ±60°	12	8	8	28	6.60
< ±60° ... ≤ ±70°	15	20	10	45	10.61
< ±70° ... ≤ ±80°	17	7	3	27	6.37
< ±80° ... ≤ 90°	11	7	7	25	5.90
<b>Total</b>	<b>171</b>	<b>167</b>	<b>86</b>	<b>424</b>	<b>100.00</b>

Table 42: Fiber distribution data table for sample number 40

Sample Number:	40				
Angle	Radius [mm]			Number of Fibers	% Number of Fibers
	~72	~122	~172		
0° ... ≤ ±10°	18	11	10	39	21.08
< ±10° ... ≤ ±20°	12	12	11	35	18.92
< ±20° ... ≤ ±30°	10	10	8	28	15.14
< ±30° ... ≤ ±40°	13	3	6	22	11.89
< ±40° ... ≤ ±50°	10	5	4	19	10.27
< ±50° ... ≤ ±60°	11	3	4	18	9.73
< ±60° ... ≤ ±70°	9	1	4	14	7.57
< ±70° ... ≤ ±80°	3	1	3	7	3.78
< ±80° ... ≤ 90°	1	1	1	3	1.62
<b>Total</b>	<b>87</b>	<b>47</b>	<b>51</b>	<b>185</b>	<b>100.00</b>

Table 43: Fiber distribution data table for sample number 41

Sample Number:	41				
Angle	Radius [mm]			Number of Fibers	% Number of Fibers
	~72	~122	~172		
0° ... ≤ ±10°	25	17	9	51	24.88
< ±10° ... ≤ ±20°	23	10	3	36	17.56
< ±20° ... ≤ ±30°	12	12	1	25	12.20
< ±30° ... ≤ ±40°	10	8	5	23	11.22
< ±40° ... ≤ ±50°	8	8	4	20	9.76
< ±50° ... ≤ ±60°	6	7	2	15	7.32
< ±60° ... ≤ ±70°	4	8	2	14	6.83
< ±70° ... ≤ ±80°	5	3	1	9	4.39
< ±80° ... ≤ 90°	3	8	1	12	5.85
<b>Total</b>	<b>96</b>	<b>81</b>	<b>28</b>	<b>205</b>	<b>100.00</b>

Table 44: Fiber distribution data table for sample number 42

Sample Number:	42				
Angle	Radius [mm]			Number of Fibers	% Number of Fibers
	~72	~122	~172		
0° ... ≤ ±10°	15	13	12	40	20.62
< ±10° ... ≤ ±20°	17	11	8	36	18.56
< ±20° ... ≤ ±30°	9	11	6	26	13.40
< ±30° ... ≤ ±40°	8	11	4	23	11.86
< ±40° ... ≤ ±50°	13	9	1	23	11.86
< ±50° ... ≤ ±60°	9	4	1	14	7.22
< ±60° ... ≤ ±70°	4	6	0	10	5.15
< ±70° ... ≤ ±80°	7	0	1	8	4.12
< ±80° ... ≤ 90°	9	5	0	14	7.22
<b>Total</b>	<b>91</b>	<b>70</b>	<b>33</b>	<b>194</b>	<b>100.00</b>

Table 45: Fiber distribution data table for sample number 43

Sample Number:	43				
Angle	Radius [mm]			Number of Fibers	% Number of Fibers
	~72	~122	~172		
0° ... ≤ ±10°	29	16	11	56	22.58
< ±10° ... ≤ ±20°	25	8	7	40	16.13
< ±20° ... ≤ ±30°	17	15	4	36	14.52
< ±30° ... ≤ ±40°	6	16	6	28	11.29
< ±40° ... ≤ ±50°	6	11	5	22	8.87
< ±50° ... ≤ ±60°	8	6	3	17	6.85
< ±60° ... ≤ ±70°	6	11	2	19	7.66
< ±70° ... ≤ ±80°	8	5	5	18	7.26
< ±80° ... ≤ 90°	6	6	0	12	4.84
<b>Total</b>	<b>111</b>	<b>94</b>	<b>43</b>	<b>248</b>	<b>100.00</b>

Table 46: Fiber distribution data table for sample number 44

Sample Number:	44				
Angle	Radius [mm]			Number of Fibers	% Number of Fibers
	~72	~122	~172		
0° ... ≤ ±10°	11	5	5	21	11.17
< ±10° ... ≤ ±20°	18	9	7	34	18.09
< ±20° ... ≤ ±30°	14	5	3	22	11.70
< ±30° ... ≤ ±40°	15	3	3	21	11.17
< ±40° ... ≤ ±50°	9	11	2	22	11.70
< ±50° ... ≤ ±60°	7	6	2	15	7.98
< ±60° ... ≤ ±70°	8	5	2	15	7.98
< ±70° ... ≤ ±80°	5	7	5	17	9.04
< ±80° ... ≤ 90°	9	11	1	21	11.17
<b>Total</b>	<b>96</b>	<b>62</b>	<b>30</b>	<b>188</b>	<b>100.00</b>

Table 47: Fiber distribution data table for sample number 45

Sample Number:	45				
Angle	Radius [mm]			Number of Fibers	% Number of Fibers
	~72	~122	~172		
0° ... ≤ ±10°	26	25	15	66	38.60
< ±10° ... ≤ ±20°	25	8	6	39	22.81
< ±20° ... ≤ ±30°	6	9	6	21	12.28
< ±30° ... ≤ ±40°	5	6	2	13	7.60
< ±40° ... ≤ ±50°	7	5	1	13	7.60
< ±50° ... ≤ ±60°	4	1	1	6	3.51
< ±60° ... ≤ ±70°	5	0	1	6	3.51
< ±70° ... ≤ ±80°	2	2	0	4	2.34
< ±80° ... ≤ 90°	2	0	1	3	1.75
<b>Total</b>	<b>82</b>	<b>56</b>	<b>33</b>	<b>171</b>	<b>100.00</b>

Table 48: Fiber distribution data table for sample number 46

Sample Number:	46				
Angle	Radius [mm]			Number of Fibers	% Number of Fibers
	~72	~122	~172		
0° ... ≤ ±10°	21	17	6	44	19.73
< ±10° ... ≤ ±20°	22	5	4	31	13.90
< ±20° ... ≤ ±30°	22	8	6	36	16.14
< ±30° ... ≤ ±40°	10	9	2	21	9.42
< ±40° ... ≤ ±50°	9	10	4	23	10.31
< ±50° ... ≤ ±60°	8	7	4	19	8.52
< ±60° ... ≤ ±70°	10	4	2	16	7.17
< ±70° ... ≤ ±80°	13	2	3	18	8.07
< ±80° ... ≤ 90°	6	3	6	15	6.73
<b>Total</b>	<b>121</b>	<b>65</b>	<b>37</b>	<b>223</b>	<b>100.00</b>

Table 49: Fiber distribution data table for sample number 47

Sample Number:	47				
Angle	Radius [mm]			Number of Fibers	% Number of Fibers
	~72	~122	~172		
0° ... ≤ ±10°	30	20	15	65	30.37
< ±10° ... ≤ ±20°	20	14	12	46	21.50
< ±20° ... ≤ ±30°	19	12	4	35	16.36
< ±30° ... ≤ ±40°	9	10	4	23	10.75
< ±40° ... ≤ ±50°	12	4	2	18	8.41
< ±50° ... ≤ ±60°	2	2	0	4	1.87
< ±60° ... ≤ ±70°	6	1	2	9	4.21
< ±70° ... ≤ ±80°	3	2	1	6	2.80
< ±80° ... ≤ 90°	3	4	1	8	3.74
<b>Total</b>	<b>104</b>	<b>69</b>	<b>41</b>	<b>214</b>	<b>100.00</b>

Table 50: Fiber distribution data table for sample number 48

Sample Number:	48				
Angle	Radius [mm]			Number of Fibers	% Number of Fibers
	~72	~122	~172		
0° ... ≤ ±10°	22	20	24	66	30.00
< ±10° ... ≤ ±20°	14	19	15	48	21.82
< ±20° ... ≤ ±30°	13	10	8	31	14.09
< ±30° ... ≤ ±40°	6	8	4	18	8.18
< ±40° ... ≤ ±50°	6	5	1	12	5.45
< ±50° ... ≤ ±60°	8	4	2	14	6.36
< ±60° ... ≤ ±70°	6	4	2	12	5.45
< ±70° ... ≤ ±80°	8	3	0	11	5.00
< ±80° ... ≤ 90°	5	1	2	8	3.64
<b>Total</b>	<b>88</b>	<b>74</b>	<b>58</b>	<b>220</b>	<b>100.00</b>

Table 51: Fiber distribution data table for sample number 49

Sample Number:	49				
Angle	Radius [mm]			Number of Fibers	% Number of Fibers
	~72	~122	~172		
0° ... ≤ ±10°	8	9	1	18	26.87
< ±10° ... ≤ ±20°	13	2	2	17	25.37
< ±20° ... ≤ ±30°	4	2	3	9	13.43
< ±30° ... ≤ ±40°	5	0	5	10	14.93
< ±40° ... ≤ ±50°	0	3	4	7	10.45
< ±50° ... ≤ ±60°	0	0	2	2	2.99
< ±60° ... ≤ ±70°	0	0	2	2	2.99
< ±70° ... ≤ ±80°	0	1	1	2	2.99
< ±80° ... ≤ 90°	0	0	0	0	0.00
<b>Total</b>	<b>30</b>	<b>17</b>	<b>20</b>	<b>67</b>	<b>100.00</b>

Table 52: Fiber distribution data table for sample number 50

Sample Number:	50				
Angle	Radius [mm]			Number of Fibers	% Number of Fibers
	~72	~122	~172		
0° ... ≤ ±10°	9	6	8	23	36.51
< ±10° ... ≤ ±20°	7	6	2	15	23.81
< ±20° ... ≤ ±30°	1	2	0	3	4.76
< ±30° ... ≤ ±40°	3	1	0	4	6.35
< ±40° ... ≤ ±50°	3	1	1	5	7.94
< ±50° ... ≤ ±60°	2	0	1	3	4.76
< ±60° ... ≤ ±70°	0	0	0	0	0.00
< ±70° ... ≤ ±80°	7	1	0	8	12.70
< ±80° ... ≤ 90°	1	1	0	2	3.17
<b>Total</b>	<b>33</b>	<b>18</b>	<b>12</b>	<b>63</b>	<b>100.00</b>

Table 53: Fiber distribution data table for sample number 51

Sample Number:	51				
Angle	Radius [mm]			Number of Fibers	% Number of Fibers
	~72	~122	~172		
0° ... ≤ ±10°	12	9	19	40	32.79
< ±10° ... ≤ ±20°	9	13	8	30	24.59
< ±20° ... ≤ ±30°	8	1	2	11	9.02
< ±30° ... ≤ ±40°	6	8	1	15	12.30
< ±40° ... ≤ ±50°	6	2	1	9	7.38
< ±50° ... ≤ ±60°	2	1	0	3	2.46
< ±60° ... ≤ ±70°	3	1	0	4	3.28
< ±70° ... ≤ ±80°	3	1	2	6	4.92
< ±80° ... ≤ 90°	3	1	0	4	3.28
<b>Total</b>	<b>52</b>	<b>37</b>	<b>33</b>	<b>122</b>	<b>100.00</b>

Table 54: Fiber distribution data table for sample number 52

Sample Number:	52				
Angle	Radius [mm]			Number of Fibers	% Number of Fibers
	~72	~122	~172		
0° ... ≤ ±10°	9	9	5	23	18.85
< ±10° ... ≤ ±20°	9	11	3	23	18.85
< ±20° ... ≤ ±30°	11	5	6	22	18.03
< ±30° ... ≤ ±40°	4	3	5	12	9.84
< ±40° ... ≤ ±50°	4	5	1	10	8.20
< ±50° ... ≤ ±60°	5	6	0	11	9.02
< ±60° ... ≤ ±70°	2	3	2	7	5.74
< ±70° ... ≤ ±80°	3	2	1	6	4.92
< ±80° ... ≤ 90°	4	0	4	8	6.56
<b>Total</b>	<b>51</b>	<b>44</b>	<b>27</b>	<b>122</b>	<b>100.00</b>

Table 55: Fiber distribution data table for sample number 53

Sample Number:	53				
Angle	Radius [mm]			Number of Fibers	% Number of Fibers
	~72	~122	~172		
0° ... ≤ ±10°	8	7	4	19	35.85
< ±10° ... ≤ ±20°	6	1	2	9	16.98
< ±20° ... ≤ ±30°	6	2	0	8	15.09
< ±30° ... ≤ ±40°	5	1	0	6	11.32
< ±40° ... ≤ ±50°	0	1	0	1	1.89
< ±50° ... ≤ ±60°	2	0	0	2	3.77
< ±60° ... ≤ ±70°	0	0	0	0	0.00
< ±70° ... ≤ ±80°	1	1	0	2	3.77
< ±80° ... ≤ 90°	4	2	0	6	11.32
<b>Total</b>	<b>32</b>	<b>15</b>	<b>6</b>	<b>53</b>	<b>100.00</b>

Table 56: Fiber distribution data table for sample number 54

Sample Number:	54				
Angle	Radius [mm]			Number of Fibers	% Number of Fibers
	~72	~122	~172		
$0^\circ \dots \leq \pm 10^\circ$	9	11	3	23	29.49
$< \pm 10^\circ \dots \leq \pm 20^\circ$	7	3	3	13	16.67
$< \pm 20^\circ \dots \leq \pm 30^\circ$	7	6	2	15	19.23
$< \pm 30^\circ \dots \leq \pm 40^\circ$	4	1	5	10	12.82
$< \pm 40^\circ \dots \leq \pm 50^\circ$	5	0	1	6	7.69
$< \pm 50^\circ \dots \leq \pm 60^\circ$	3	0	1	4	5.13
$< \pm 60^\circ \dots \leq \pm 70^\circ$	1	1	0	2	2.56
$< \pm 70^\circ \dots \leq \pm 80^\circ$	0	0	0	0	0.00
$< \pm 80^\circ \dots \leq 90^\circ$	2	2	1	5	6.41
<b>Total</b>	<b>38</b>	<b>24</b>	<b>16</b>	<b>78</b>	<b>100.00</b>

Table 57: Fiber distribution data table for sample number 55

Sample Number:	55				
Angle	Radius [mm]			Number of Fibers	% Number of Fibers
	~72	~122	~172		
$0^\circ \dots \leq \pm 10^\circ$	24	16	12	52	52.00
$< \pm 10^\circ \dots \leq \pm 20^\circ$	8	9	10	27	27.00
$< \pm 20^\circ \dots \leq \pm 30^\circ$	4	5	1	10	10.00
$< \pm 30^\circ \dots \leq \pm 40^\circ$	1	3	2	6	6.00
$< \pm 40^\circ \dots \leq \pm 50^\circ$	0	0	0	0	0.00
$< \pm 50^\circ \dots \leq \pm 60^\circ$	0	0	1	1	1.00
$< \pm 60^\circ \dots \leq \pm 70^\circ$	0	1	0	1	1.00
$< \pm 70^\circ \dots \leq \pm 80^\circ$	1	1	0	2	2.00
$< \pm 80^\circ \dots \leq 90^\circ$	0	0	1	1	1.00
<b>Total</b>	<b>38</b>	<b>35</b>	<b>27</b>	<b>100</b>	<b>100.00</b>

Table 58: Fiber distribution data table for sample number 56

Sample Number:	56				
Angle	Radius [mm]			Number of Fibers	% Number of Fibers
	~72	~122	~172		
$0^\circ \dots \leq \pm 10^\circ$	9	9	5	23	22.33
$< \pm 10^\circ \dots \leq \pm 20^\circ$	11	7	6	24	23.30
$< \pm 20^\circ \dots \leq \pm 30^\circ$	8	2	2	12	11.65
$< \pm 30^\circ \dots \leq \pm 40^\circ$	6	1	2	9	8.74
$< \pm 40^\circ \dots \leq \pm 50^\circ$	6	0	0	6	5.83
$< \pm 50^\circ \dots \leq \pm 60^\circ$	3	1	2	6	5.83
$< \pm 60^\circ \dots \leq \pm 70^\circ$	10	1	0	11	10.68
$< \pm 70^\circ \dots \leq \pm 80^\circ$	4	1	0	5	4.85
$< \pm 80^\circ \dots \leq 90^\circ$	7	0	0	7	6.80
<b>Total</b>	<b>64</b>	<b>22</b>	<b>17</b>	<b>103</b>	<b>100.00</b>

Table 59: Fiber distribution data table for sample number 57

Sample Number:	57				
Angle	Radius [mm]			Number of Fibers	% Number of Fibers
	~72	~122	~172		
0° ... ≤ ±10°	9	4	5	18	27.27
< ±10° ... ≤ ±20°	7	3	4	14	21.21
< ±20° ... ≤ ±30°	3	3	2	8	12.12
< ±30° ... ≤ ±40°	3	1	0	4	6.06
< ±40° ... ≤ ±50°	3	1	2	6	9.09
< ±50° ... ≤ ±60°	1	1	1	3	4.55
< ±60° ... ≤ ±70°	1	1	2	4	6.06
< ±70° ... ≤ ±80°	1	3	1	5	7.58
< ±80° ... ≤ 90°	2	2	0	4	6.06
<b>Total</b>	<b>30</b>	<b>19</b>	<b>17</b>	<b>66</b>	<b>100.00</b>

Table 60: Fiber distribution data table for sample number 58

Sample Number:	58				
Angle	Radius [mm]			Number of Fibers	% Number of Fibers
	~72	~122	~172		
0° ... ≤ ±10°	12	15	6	33	39.29
< ±10° ... ≤ ±20°	6	3	6	15	17.86
< ±20° ... ≤ ±30°	9	4	1	14	16.67
< ±30° ... ≤ ±40°	8	1	1	10	11.90
< ±40° ... ≤ ±50°	1	1	0	2	2.38
< ±50° ... ≤ ±60°	1	1	0	2	2.38
< ±60° ... ≤ ±70°	1	0	1	2	2.38
< ±70° ... ≤ ±80°	1	3	0	4	4.76
< ±80° ... ≤ 90°	1	1	0	2	2.38
<b>Total</b>	<b>40</b>	<b>29</b>	<b>15</b>	<b>84</b>	<b>100.00</b>

Table 61: Fiber distribution data table for sample number 59

Sample Number:	59				
Angle	Radius [mm]			Number of Fibers	% Number of Fibers
	~72	~122	~172		
0° ... ≤ ±10°	17	13	8	38	29.46
< ±10° ... ≤ ±20°	13	11	8	32	24.81
< ±20° ... ≤ ±30°	9	9	2	20	15.50
< ±30° ... ≤ ±40°	6	5	2	13	10.08
< ±40° ... ≤ ±50°	5	2	1	8	6.20
< ±50° ... ≤ ±60°	6	0	0	6	4.65
< ±60° ... ≤ ±70°	4	0	1	5	3.88
< ±70° ... ≤ ±80°	3	0	0	3	2.33
< ±80° ... ≤ 90°	2	1	1	4	3.10
<b>Total</b>	<b>65</b>	<b>41</b>	<b>23</b>	<b>129</b>	<b>100.00</b>

Table 62: Fiber distribution data table for sample number 60

Sample Number:	60				
Angle	Radius [mm]			Number of Fibers	% Number of Fibers
	~72	~122	~172		
0° ... ≤ ±10°	20	22	7	49	38.28
< ±10° ... ≤ ±20°	21	11	8	40	31.25
< ±20° ... ≤ ±30°	3	3	4	10	7.81
< ±30° ... ≤ ±40°	4	7	6	17	13.28
< ±40° ... ≤ ±50°	2	0	1	3	2.34
< ±50° ... ≤ ±60°	1	2	0	3	2.34
< ±60° ... ≤ ±70°	1	0	1	2	1.56
< ±70° ... ≤ ±80°	1	0	1	2	1.56
< ±80° ... ≤ 90°	0	1	1	2	1.56
<b>Total</b>	<b>53</b>	<b>46</b>	<b>29</b>	<b>128</b>	<b>100.00</b>

Table 63: Fiber distribution data table for sample number 61

Sample Number:	61				
Angle	Radius [mm]			Number of Fibers	% Number of Fibers
	~72	~122	~172		
0° ... ≤ ±10°	5	6	3	14	15.56
< ±10° ... ≤ ±20°	6	6	8	20	22.22
< ±20° ... ≤ ±30°	1	6	6	13	14.44
< ±30° ... ≤ ±40°	4	2	1	7	7.78
< ±40° ... ≤ ±50°	4	1	3	8	8.89
< ±50° ... ≤ ±60°	4	2	1	7	7.78
< ±60° ... ≤ ±70°	4	2	0	6	6.67
< ±70° ... ≤ ±80°	6	1	1	8	8.89
< ±80° ... ≤ 90°	4	0	3	7	7.78
<b>Total</b>	<b>38</b>	<b>26</b>	<b>26</b>	<b>90</b>	<b>100.00</b>

Table 64: Fiber distribution data table for sample number 62

Sample Number:	62				
Angle	Radius [mm]			Number of Fibers	% Number of Fibers
	~72	~122	~172		
0° ... ≤ ±10°	14	12	6	32	42.67
< ±10° ... ≤ ±20°	9	4	2	15	20.00
< ±20° ... ≤ ±30°	2	1	6	9	12.00
< ±30° ... ≤ ±40°	1	1	4	6	8.00
< ±40° ... ≤ ±50°	4	1	0	5	6.67
< ±50° ... ≤ ±60°	0	0	1	1	1.33
< ±60° ... ≤ ±70°	0	1	1	2	2.67
< ±70° ... ≤ ±80°	1	0	0	1	1.33
< ±80° ... ≤ 90°	3	0	1	4	5.33
<b>Total</b>	<b>34</b>	<b>20</b>	<b>21</b>	<b>75</b>	<b>100.00</b>

Table 65: Fiber distribution data table for sample number 63

Sample Number:	63				
Angle	Radius [mm]			Number of Fibers	% Number of Fibers
	~72	~122	~172		
0° ... ≤ ±10°	8	9	3	20	17.09
< ±10° ... ≤ ±20°	15	5	3	23	19.66
< ±20° ... ≤ ±30°	16	11	2	29	24.79
< ±30° ... ≤ ±40°	5	3	1	9	7.69
< ±40° ... ≤ ±50°	7	2	0	9	7.69
< ±50° ... ≤ ±60°	8	2	0	10	8.55
< ±60° ... ≤ ±70°	5	2	1	8	6.84
< ±70° ... ≤ ±80°	1	2	0	3	2.56
< ±80° ... ≤ 90°	3	3	0	6	5.13
<b>Total</b>	<b>68</b>	<b>39</b>	<b>10</b>	<b>117</b>	<b>100.00</b>

Table 66: Fiber distribution data table for sample number 64

Sample Number:	64				
Angle	Radius [mm]			Number of Fibers	% Number of Fibers
	~72	~122	~172		
0° ... ≤ ±10°	8	4	1	13	20.00
< ±10° ... ≤ ±20°	7	4	3	14	21.54
< ±20° ... ≤ ±30°	3	4	2	9	13.85
< ±30° ... ≤ ±40°	4	0	0	4	6.15
< ±40° ... ≤ ±50°	2	1	2	5	7.69
< ±50° ... ≤ ±60°	3	1	1	5	7.69
< ±60° ... ≤ ±70°	0	4	3	7	10.77
< ±70° ... ≤ ±80°	1	3	1	5	7.69
< ±80° ... ≤ 90°	2	1	0	3	4.62
<b>Total</b>	<b>30</b>	<b>22</b>	<b>13</b>	<b>65</b>	<b>100.00</b>

Table 67: Fiber distribution data table for sample number 65

Sample Number:	65				
Angle	Radius [mm]			Number of Fibers	% Number of Fibers
	~72	~122	~172		
0° ... ≤ ±10°	4	10	7	21	20.59
< ±10° ... ≤ ±20°	10	7	4	21	20.59
< ±20° ... ≤ ±30°	7	3	7	17	16.67
< ±30° ... ≤ ±40°	2	4	3	9	8.82
< ±40° ... ≤ ±50°	3	5	3	11	10.78
< ±50° ... ≤ ±60°	3	2	2	7	6.86
< ±60° ... ≤ ±70°	4	1	1	6	5.88
< ±70° ... ≤ ±80°	3	5	1	9	8.82
< ±80° ... ≤ 90°	0	1	0	1	0.98
<b>Total</b>	<b>36</b>	<b>38</b>	<b>28</b>	<b>102</b>	<b>100.00</b>

Table 68: Fiber distribution data table for sample number 66

Sample Number:	66				
Angle	Radius [mm]			Number of Fibers	% Number of Fibers
	~72	~122	~172		
0° ... ≤ ±10°	6	7	22	35	24.14
< ±10° ... ≤ ±20°	12	12	13	37	25.52
< ±20° ... ≤ ±30°	11	8	3	22	15.17
< ±30° ... ≤ ±40°	7	7	1	15	10.34
< ±40° ... ≤ ±50°	9	9	1	19	13.10
< ±50° ... ≤ ±60°	3	3	0	6	4.14
< ±60° ... ≤ ±70°	3	2	0	5	3.45
< ±70° ... ≤ ±80°	2	2	0	4	2.76
< ±80° ... ≤ 90°	2	0	0	2	1.38
<b>Total</b>	<b>55</b>	<b>50</b>	<b>40</b>	<b>145</b>	<b>100.00</b>

Table 69: Fiber distribution data table for sample number 70

Sample Number:	70				
Angle	Radius [mm]			Number of Fibers	% Number of Fibers
	~72	~122	~172		
0° ... ≤ ±10°	7	17	10	34	54.84
< ±10° ... ≤ ±20°	6	2	5	13	20.97
< ±20° ... ≤ ±30°	8	1	1	10	16.13
< ±30° ... ≤ ±40°	1	1	1	3	4.84
< ±40° ... ≤ ±50°	0	0	0	0	0.00
< ±50° ... ≤ ±60°	0	0	0	0	0.00
< ±60° ... ≤ ±70°	1	1	0	2	3.23
< ±70° ... ≤ ±80°	0	0	0	0	0.00
< ±80° ... ≤ 90°	0	0	0	0	0.00
<b>Total</b>	<b>23</b>	<b>22</b>	<b>17</b>	<b>62</b>	<b>100.00</b>

Table 70: Fiber distribution data table for sample number 71

Sample Number:	71				
Angle	Radius [mm]			Number of Fibers	% Number of Fibers
	~72	~122	~172		
0° ... ≤ ±10°	2	17	6	25	32.47
< ±10° ... ≤ ±20°	5	6	2	13	16.88
< ±20° ... ≤ ±30°	10	6	1	17	22.08
< ±30° ... ≤ ±40°	4	1	1	6	7.79
< ±40° ... ≤ ±50°	2	2	2	6	7.79
< ±50° ... ≤ ±60°	1	0	0	1	1.30
< ±60° ... ≤ ±70°	2	0	1	3	3.90
< ±70° ... ≤ ±80°	3	0	0	3	3.90
< ±80° ... ≤ 90°	3	0	0	3	3.90
<b>Total</b>	<b>32</b>	<b>32</b>	<b>13</b>	<b>77</b>	<b>100.00</b>

Table 71: Fiber distribution data table for sample number 72

Sample Number:	72				
Angle	Radius [mm]			Number of Fibers	% Number of Fibers
	~72	~122	~172		
0° ... ≤ ±10°	10	3	5	18	23.68
< ±10° ... ≤ ±20°	7	3	3	13	17.11
< ±20° ... ≤ ±30°	6	2	3	11	14.47
< ±30° ... ≤ ±40°	4	4	4	12	15.79
< ±40° ... ≤ ±50°	3	2	1	6	7.89
< ±50° ... ≤ ±60°	4	2	0	6	7.89
< ±60° ... ≤ ±70°	2	1	1	4	5.26
< ±70° ... ≤ ±80°	4	0	0	4	5.26
< ±80° ... ≤ 90°	1	0	1	2	2.63
<b>Total</b>	<b>41</b>	<b>17</b>	<b>18</b>	<b>76</b>	<b>100.00</b>

Table 72: Fiber distribution data table for sample number 73

Sample Number:	73				
Angle	Radius [mm]			Number of Fibers	% Number of Fibers
	~72	~122	~172		
0° ... ≤ ±10°	12	20	10	42	37.84
< ±10° ... ≤ ±20°	10	9	6	25	22.52
< ±20° ... ≤ ±30°	9	5	1	15	13.51
< ±30° ... ≤ ±40°	8	0	2	10	9.01
< ±40° ... ≤ ±50°	2	0	0	2	1.80
< ±50° ... ≤ ±60°	4	1	2	7	6.31
< ±60° ... ≤ ±70°	3	0	0	3	2.70
< ±70° ... ≤ ±80°	3	1	0	4	3.60
< ±80° ... ≤ 90°	2	1	0	3	2.70
<b>Total</b>	<b>53</b>	<b>37</b>	<b>21</b>	<b>111</b>	<b>100.00</b>

Table 73: Fiber distribution data table for sample number 74

Sample Number:	74				
Angle	Radius [mm]			Number of Fibers	% Number of Fibers
	~72	~122	~172		
0° ... ≤ ±10°	7	11	7	25	30.86
< ±10° ... ≤ ±20°	9	8	2	19	23.46
< ±20° ... ≤ ±30°	4	5	1	10	12.35
< ±30° ... ≤ ±40°	4	6	2	12	14.81
< ±40° ... ≤ ±50°	4	3	2	9	11.11
< ±50° ... ≤ ±60°	0	0	1	1	1.23
< ±60° ... ≤ ±70°	1	2	0	3	3.70
< ±70° ... ≤ ±80°	0	0	0	0	0.00
< ±80° ... ≤ 90°	2	0	0	2	2.47
<b>Total</b>	<b>31</b>	<b>35</b>	<b>15</b>	<b>81</b>	<b>100.00</b>

Table 74: Fiber distribution data table for sample number 75

Sample Number:	75				
Angle	Radius [mm]			Number of Fibers	% Number of Fibers
	~72	~122	~172		
0° ... ≤ ±10°	5	11	7	23	25.00
< ±10° ... ≤ ±20°	13	5	9	27	29.35
< ±20° ... ≤ ±30°	9	4	2	15	16.30
< ±30° ... ≤ ±40°	4	3	0	7	7.61
< ±40° ... ≤ ±50°	7	0	3	10	10.87
< ±50° ... ≤ ±60°	3	0	0	3	3.26
< ±60° ... ≤ ±70°	2	0	3	5	5.43
< ±70° ... ≤ ±80°	1	0	1	2	2.17
< ±80° ... ≤ 90°	0	0	0	0	0.00
<b>Total</b>	<b>44</b>	<b>23</b>	<b>25</b>	<b>92</b>	<b>100.00</b>

Table 75: Fiber distribution data table for sample number 76

Sample Number:	76				
Angle	Radius [mm]			Number of Fibers	% Number of Fibers
	~72	~122	~172		
0° ... ≤ ±10°	15	20	2	37	31.09
< ±10° ... ≤ ±20°	15	6	4	25	21.01
< ±20° ... ≤ ±30°	6	6	2	14	11.76
< ±30° ... ≤ ±40°	7	4	1	12	10.08
< ±40° ... ≤ ±50°	11	1	1	13	10.92
< ±50° ... ≤ ±60°	4	2	0	6	5.04
< ±60° ... ≤ ±70°	3	3	0	6	5.04
< ±70° ... ≤ ±80°	3	1	0	4	3.36
< ±80° ... ≤ 90°	2	0	0	2	1.68
<b>Total</b>	<b>66</b>	<b>43</b>	<b>10</b>	<b>119</b>	<b>100.00</b>

Table 76: Fiber distribution data table for sample number 77

Sample Number:	77				
Angle	Radius [mm]			Number of Fibers	% Number of Fibers
	~72	~122	~172		
0° ... ≤ ±10°	23	21	10	54	46.96
< ±10° ... ≤ ±20°	15	5	4	24	20.87
< ±20° ... ≤ ±30°	15	3	5	23	20.00
< ±30° ... ≤ ±40°	6	1	0	7	6.09
< ±40° ... ≤ ±50°	0	0	0	0	0.00
< ±50° ... ≤ ±60°	3	1	0	4	3.48
< ±60° ... ≤ ±70°	1	0	1	2	1.74
< ±70° ... ≤ ±80°	0	0	1	1	0.87
< ±80° ... ≤ 90°	0	0	0	0	0.00
<b>Total</b>	<b>63</b>	<b>31</b>	<b>21</b>	<b>115</b>	<b>100.00</b>

Table 77: Fiber distribution data table for sample number 78

Sample Number:	78				
Angle	Radius [mm]			Number of Fibers	% Number of Fibers
	~72	~122	~172		
0° ... ≤ ±10°	7	8	6	21	24.14
< ±10° ... ≤ ±20°	5	5	4	14	16.09
< ±20° ... ≤ ±30°	9	6	6	21	24.14
< ±30° ... ≤ ±40°	5	1	0	6	6.90
< ±40° ... ≤ ±50°	4	2	1	7	8.05
< ±50° ... ≤ ±60°	1	1	2	4	4.60
< ±60° ... ≤ ±70°	3	2	1	6	6.90
< ±70° ... ≤ ±80°	1	1	0	2	2.30
< ±80° ... ≤ 90°	2	3	1	6	6.90
<b>Total</b>	<b>37</b>	<b>29</b>	<b>21</b>	<b>87</b>	<b>100.00</b>

Table 78: Fiber distribution data table for sample number 79

Sample Number:	79				
Angle	Radius [mm]			Number of Fibers	% Number of Fibers
	~72	~122	~172		
0° ... ≤ ±10°	17	15	12	44	42.72
< ±10° ... ≤ ±20°	13	15	5	33	32.04
< ±20° ... ≤ ±30°	3	3	2	8	7.77
< ±30° ... ≤ ±40°	2	2	2	6	5.83
< ±40° ... ≤ ±50°	4	0	0	4	3.88
< ±50° ... ≤ ±60°	3	1	0	4	3.88
< ±60° ... ≤ ±70°	0	2	0	2	1.94
< ±70° ... ≤ ±80°	0	0	1	1	0.97
< ±80° ... ≤ 90°	1	0	0	1	0.97
<b>Total</b>	<b>43</b>	<b>38</b>	<b>22</b>	<b>103</b>	<b>100.00</b>

Table 79: Fiber distribution data table for sample number 80

Sample Number:	80				
Angle	Radius [mm]			Number of Fibers	% Number of Fibers
	~72	~122	~172		
0° ... ≤ ±10°	20	10	11	41	35.96
< ±10° ... ≤ ±20°	13	8	12	33	28.95
< ±20° ... ≤ ±30°	8	5	2	15	13.16
< ±30° ... ≤ ±40°	4	2	1	7	6.14
< ±40° ... ≤ ±50°	1	1	2	4	3.51
< ±50° ... ≤ ±60°	3	0	0	3	2.63
< ±60° ... ≤ ±70°	0	2	1	3	2.63
< ±70° ... ≤ ±80°	2	2	2	6	5.26
< ±80° ... ≤ 90°	2	0	0	2	1.75
<b>Total</b>	<b>53</b>	<b>30</b>	<b>31</b>	<b>114</b>	<b>100.00</b>

Table 80: Fiber distribution data table for sample number 81

Sample Number:	81				
Angle	Radius [mm]			Number of Fibers	% Number of Fibers
	~72	~122	~172		
0° ... ≤ ±10°	12	9	3	24	23.53
< ±10° ... ≤ ±20°	6	2	5	13	12.75
< ±20° ... ≤ ±30°	9	1	5	15	14.71
< ±30° ... ≤ ±40°	5	2	2	9	8.82
< ±40° ... ≤ ±50°	4	2	5	11	10.78
< ±50° ... ≤ ±60°	2	1	2	5	4.90
< ±60° ... ≤ ±70°	2	4	3	9	8.82
< ±70° ... ≤ ±80°	5	1	3	9	8.82
< ±80° ... ≤ 90°	4	2	1	7	6.86
<b>Total</b>	<b>49</b>	<b>24</b>	<b>29</b>	<b>102</b>	<b>100.00</b>

Table 81: Fiber distribution data table for sample number 82

Sample Number:	82				
Angle	Radius [mm]			Number of Fibers	% Number of Fibers
	~72	~122	~172		
0° ... ≤ ±10°	14	15	8	37	35.58
< ±10° ... ≤ ±20°	9	7	1	17	16.35
< ±20° ... ≤ ±30°	5	3	4	12	11.54
< ±30° ... ≤ ±40°	6	4	1	11	10.58
< ±40° ... ≤ ±50°	3	2	2	7	6.73
< ±50° ... ≤ ±60°	2	2	0	4	3.85
< ±60° ... ≤ ±70°	2	1	0	3	2.88
< ±70° ... ≤ ±80°	5	3	0	8	7.69
< ±80° ... ≤ 90°	1	4	0	5	4.81
<b>Total</b>	<b>47</b>	<b>41</b>	<b>16</b>	<b>104</b>	<b>100.00</b>

Table 82: Fiber distribution data table for sample number 83

Sample Number:	83				
Angle	Radius [mm]			Number of Fibers	% Number of Fibers
	~72	~122	~172		
0° ... ≤ ±10°	14	19	8	41	42.27
< ±10° ... ≤ ±20°	12	9	4	25	25.77
< ±20° ... ≤ ±30°	8	7	0	15	15.46
< ±30° ... ≤ ±40°	4	3	0	7	7.22
< ±40° ... ≤ ±50°	2	0	0	2	2.06
< ±50° ... ≤ ±60°	0	0	0	0	0.00
< ±60° ... ≤ ±70°	2	2	1	5	5.15
< ±70° ... ≤ ±80°	2	0	0	2	2.06
< ±80° ... ≤ 90°	0	0	0	0	0.00
<b>Total</b>	<b>44</b>	<b>40</b>	<b>13</b>	<b>97</b>	<b>100.00</b>

Table 83: Fiber distribution data table for sample number 84

Sample Number:	84				
Angle	Radius [mm]			Number of Fibers	% Number of Fibers
	~72	~122	~172		
0° ... ≤ ±10°	6	11	10	27	29.67
< ±10° ... ≤ ±20°	7	9	5	21	23.08
< ±20° ... ≤ ±30°	6	4	0	10	10.99
< ±30° ... ≤ ±40°	8	5	2	15	16.48
< ±40° ... ≤ ±50°	1	2	0	3	3.30
< ±50° ... ≤ ±60°	2	2	0	4	4.40
< ±60° ... ≤ ±70°	2	1	3	6	6.59
< ±70° ... ≤ ±80°	1	0	2	3	3.30
< ±80° ... ≤ 90°	2	0	0	2	2.20
<b>Total</b>	<b>35</b>	<b>34</b>	<b>22</b>	<b>91</b>	<b>100.00</b>

Table 84: Fiber distribution data table for sample number 85

Sample Number:	85				
Angle	Radius [mm]			Number of Fibers	% Number of Fibers
	~72	~122	~172		
0° ... ≤ ±10°	7	6	2	15	16.67
< ±10° ... ≤ ±20°	7	5	8	20	22.22
< ±20° ... ≤ ±30°	6	2	2	10	11.11
< ±30° ... ≤ ±40°	8	6	1	15	16.67
< ±40° ... ≤ ±50°	7	4	3	14	15.56
< ±50° ... ≤ ±60°	1	4	1	6	6.67
< ±60° ... ≤ ±70°	2	3	1	6	6.67
< ±70° ... ≤ ±80°	0	1	0	1	1.11
< ±80° ... ≤ 90°	2	1	0	3	3.33
<b>Total</b>	<b>40</b>	<b>32</b>	<b>18</b>	<b>90</b>	<b>100.00</b>

Table 85: Fiber distribution data table for sample number 86

Sample Number:	86				
Angle	Radius [mm]			Number of Fibers	% Number of Fibers
	~72	~122	~172		
0° ... ≤ ±10°	10	13	9	32	27.35
< ±10° ... ≤ ±20°	10	1	4	15	12.82
< ±20° ... ≤ ±30°	10	2	2	14	11.97
< ±30° ... ≤ ±40°	7	2	1	10	8.55
< ±40° ... ≤ ±50°	10	3	1	14	11.97
< ±50° ... ≤ ±60°	11	1	2	14	11.97
< ±60° ... ≤ ±70°	4	4	0	8	6.84
< ±70° ... ≤ ±80°	1	2	1	4	3.42
< ±80° ... ≤ 90°	3	2	1	6	5.13
<b>Total</b>	<b>66</b>	<b>30</b>	<b>21</b>	<b>117</b>	<b>100.00</b>

Table 86: Fiber distribution data table for sample number 87

Sample Number:	87				
Angle	Radius [mm]			Number of Fibers	% Number of Fibers
	~72	~122	~172		
0° ... ≤ ±10°	12	6	7	25	23.15
< ±10° ... ≤ ±20°	9	10	8	27	25.00
< ±20° ... ≤ ±30°	3	4	7	14	12.96
< ±30° ... ≤ ±40°	7	1	0	8	7.41
< ±40° ... ≤ ±50°	4	1	2	7	6.48
< ±50° ... ≤ ±60°	0	0	1	1	0.93
< ±60° ... ≤ ±70°	3	2	4	9	8.33
< ±70° ... ≤ ±80°	7	6	1	14	12.96
< ±80° ... ≤ 90°	1	2	0	3	2.78
<b>Total</b>	<b>46</b>	<b>32</b>	<b>30</b>	<b>108</b>	<b>100.00</b>

Table 87: Fiber distribution data table for sample number 88

Sample Number:	88				
Angle	Radius [mm]			Number of Fibers	% Number of Fibers
	~72	~122	~172		
0° ... ≤ ±10°	11	16	5	32	20.51
< ±10° ... ≤ ±20°	21	9	2	32	20.51
< ±20° ... ≤ ±30°	10	5	2	17	10.90
< ±30° ... ≤ ±40°	13	3	3	19	12.18
< ±40° ... ≤ ±50°	8	2	2	12	7.69
< ±50° ... ≤ ±60°	10	1	1	12	7.69
< ±60° ... ≤ ±70°	1	0	9	10	6.41
< ±70° ... ≤ ±80°	8	2	3	13	8.33
< ±80° ... ≤ 90°	5	2	2	9	5.77
<b>Total</b>	<b>87</b>	<b>40</b>	<b>29</b>	<b>156</b>	<b>100.00</b>

Table 88: Fiber distribution data table for sample number 89

Sample Number:	89				
Angle	Radius [mm]			Number of Fibers	% Number of Fibers
	~72	~122	~172		
0° ... ≤ ±10°	9	7	10	26	23.42
< ±10° ... ≤ ±20°	17	8	5	30	27.03
< ±20° ... ≤ ±30°	6	1	4	11	9.91
< ±30° ... ≤ ±40°	3	2	5	10	9.01
< ±40° ... ≤ ±50°	5	4	0	9	8.11
< ±50° ... ≤ ±60°	2	1	0	3	2.70
< ±60° ... ≤ ±70°	3	2	1	6	5.41
< ±70° ... ≤ ±80°	6	2	2	10	9.01
< ±80° ... ≤ 90°	3	1	2	6	5.41
<b>Total</b>	<b>54</b>	<b>28</b>	<b>29</b>	<b>111</b>	<b>100.00</b>

Table 89: Fiber distribution data table for sample number 90

Sample Number:	90				
Angle	Radius [mm]			Number of Fibers	% Number of Fibers
	~72	~122	~172		
0° ... ≤ ±10°	21	18	9	48	39.34
< ±10° ... ≤ ±20°	11	11	10	32	26.23
< ±20° ... ≤ ±30°	8	6	4	18	14.75
< ±30° ... ≤ ±40°	2	3	1	6	4.92
< ±40° ... ≤ ±50°	4	2	0	6	4.92
< ±50° ... ≤ ±60°	4	0	0	4	3.28
< ±60° ... ≤ ±70°	3	0	1	4	3.28
< ±70° ... ≤ ±80°	0	0	1	1	0.82
< ±80° ... ≤ 90°	2	0	1	3	2.46
<b>Total</b>	<b>55</b>	<b>40</b>	<b>27</b>	<b>122</b>	<b>100.00</b>

Table 90: Fiber distribution data table for sample number 91

Sample Number:	91				
Angle	Radius [mm]			Number of Fibers	% Number of Fibers
	~72	~122	~172		
0° ... ≤ ±10°	14	6	7	27	19.57
< ±10° ... ≤ ±20°	11	5	4	20	14.49
< ±20° ... ≤ ±30°	11	6	7	24	17.39
< ±30° ... ≤ ±40°	9	7	3	19	13.77
< ±40° ... ≤ ±50°	4	3	0	7	5.07
< ±50° ... ≤ ±60°	6	2	1	9	6.52
< ±60° ... ≤ ±70°	10	4	0	14	10.14
< ±70° ... ≤ ±80°	7	4	0	11	7.97
< ±80° ... ≤ 90°	6	0	1	7	5.07
<b>Total</b>	<b>78</b>	<b>37</b>	<b>23</b>	<b>138</b>	<b>100.00</b>

Table 91: Fiber distribution data table for sample number 92

Sample Number:	92				
Angle	Radius [mm]			Number of Fibers	% Number of Fibers
	~72	~122	~172		
0° ... ≤ ±10°	12	13	7	32	32.99
< ±10° ... ≤ ±20°	10	2	1	13	13.40
< ±20° ... ≤ ±30°	8	4	2	14	14.43
< ±30° ... ≤ ±40°	12	3	3	18	18.56
< ±40° ... ≤ ±50°	1	1	0	2	2.06
< ±50° ... ≤ ±60°	3	3	1	7	7.22
< ±60° ... ≤ ±70°	1	2	0	3	3.09
< ±70° ... ≤ ±80°	0	3	0	3	3.09
< ±80° ... ≤ 90°	3	1	1	5	5.15
<b>Total</b>	<b>50</b>	<b>32</b>	<b>15</b>	<b>97</b>	<b>100.00</b>

Table 92: Fiber distribution data table for sample number 93

Sample Number:	93				
Angle	Radius [mm]			Number of Fibers	% Number of Fibers
	~72	~122	~172		
0° ... ≤ ±10°	8	17	25	50	37.59
< ±10° ... ≤ ±20°	15	6	2	23	17.29
< ±20° ... ≤ ±30°	9	5	7	21	15.79
< ±30° ... ≤ ±40°	4	5	3	12	9.02
< ±40° ... ≤ ±50°	7	2	2	11	8.27
< ±50° ... ≤ ±60°	5	1	0	6	4.51
< ±60° ... ≤ ±70°	4	1	1	6	4.51
< ±70° ... ≤ ±80°	2	0	0	2	1.50
< ±80° ... ≤ 90°	1	1	0	2	1.50
<b>Total</b>	<b>55</b>	<b>38</b>	<b>40</b>	<b>133</b>	<b>100.00</b>

Table 93: Fiber distribution data table for sample number 95

Sample Number:	95				
Angle	Radius [mm]			Number of Fibers	% Number of Fibers
	~72	~122	~172		
0° ... ≤ ±10°	14	8	14	36	26.28
< ±10° ... ≤ ±20°	6	4	5	15	10.95
< ±20° ... ≤ ±30°	10	5	3	18	13.14
< ±30° ... ≤ ±40°	5	4	3	12	8.76
< ±40° ... ≤ ±50°	7	3	1	11	8.03
< ±50° ... ≤ ±60°	5	6	3	14	10.22
< ±60° ... ≤ ±70°	8	1	2	11	8.03
< ±70° ... ≤ ±80°	5	6	0	11	8.03
< ±80° ... ≤ 90°	2	6	1	9	6.57
<b>Total</b>	<b>62</b>	<b>43</b>	<b>32</b>	<b>137</b>	<b>100.00</b>

Table 94: Fiber distribution data table for sample number 96

Sample Number:	96				
Angle	Radius [mm]			Number of Fibers	% Number of Fibers
	~72	~122	~172		
0° ... ≤ ±10°	14	11	15	40	28.57
< ±10° ... ≤ ±20°	9	13	4	26	18.57
< ±20° ... ≤ ±30°	10	6	2	18	12.86
< ±30° ... ≤ ±40°	8	6	2	16	11.43
< ±40° ... ≤ ±50°	7	3	1	11	7.86
< ±50° ... ≤ ±60°	3	4	1	8	5.71
< ±60° ... ≤ ±70°	4	3	0	7	5.00
< ±70° ... ≤ ±80°	5	1	0	6	4.29
< ±80° ... ≤ 90°	4	2	2	8	5.71
<b>Total</b>	<b>64</b>	<b>49</b>	<b>27</b>	<b>140</b>	<b>100.00</b>

Table 95: Fiber distribution data table for sample number 97

<b>Sample Number:</b>	<b>97</b>				
<b>Angle</b>	<b>Radius [mm]</b>			<b>Number of Fibers</b>	<b>% Number of Fibers</b>
	<b>~72</b>	<b>~122</b>	<b>~172</b>		
0° ... ≤ ±10°	15	21	20	<b>56</b>	<b>44.44</b>
< ±10° ... ≤ ±20°	6	9	7	<b>22</b>	<b>17.46</b>
< ±20° ... ≤ ±30°	5	9	0	<b>14</b>	<b>11.11</b>
< ±30° ... ≤ ±40°	5	4	3	<b>12</b>	<b>9.52</b>
< ±40° ... ≤ ±50°	4	1	0	<b>5</b>	<b>3.97</b>
< ±50° ... ≤ ±60°	5	2	0	<b>7</b>	<b>5.56</b>
< ±60° ... ≤ ±70°	3	1	0	<b>4</b>	<b>3.17</b>
< ±70° ... ≤ ±80°	4	1	0	<b>5</b>	<b>3.97</b>
< ±80° ... ≤ 90°	1	0	0	<b>1</b>	<b>0.79</b>
<b>Total</b>	<b>48</b>	<b>48</b>	<b>30</b>	<b>126</b>	<b>100.00</b>

## Appendix II: Fiber Distribution Histograms

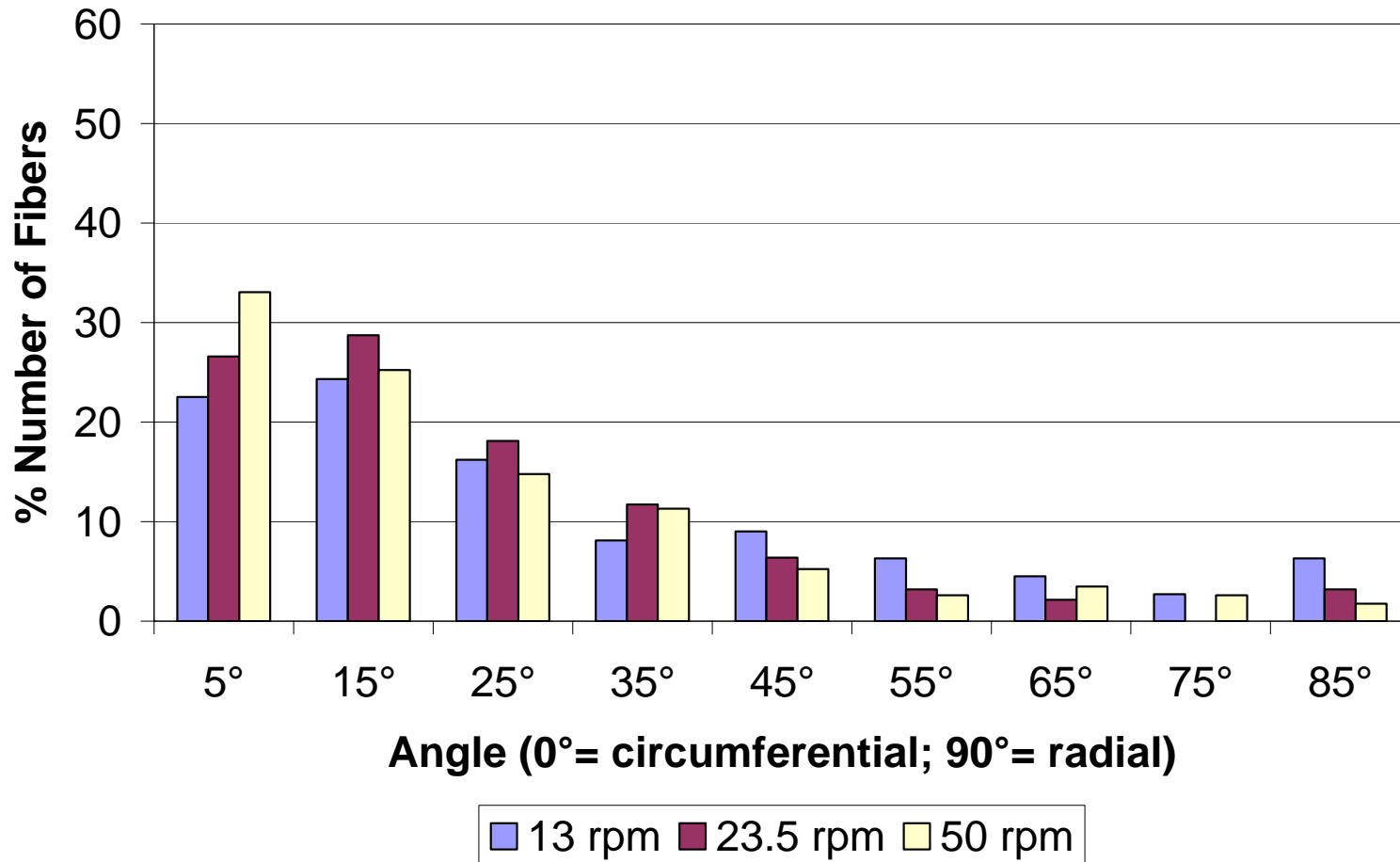


Figure 70: Distribution depending on disc AAspeed at 10cm electrode distance / 10kV electrostatic potential / 20mm lay-down rod

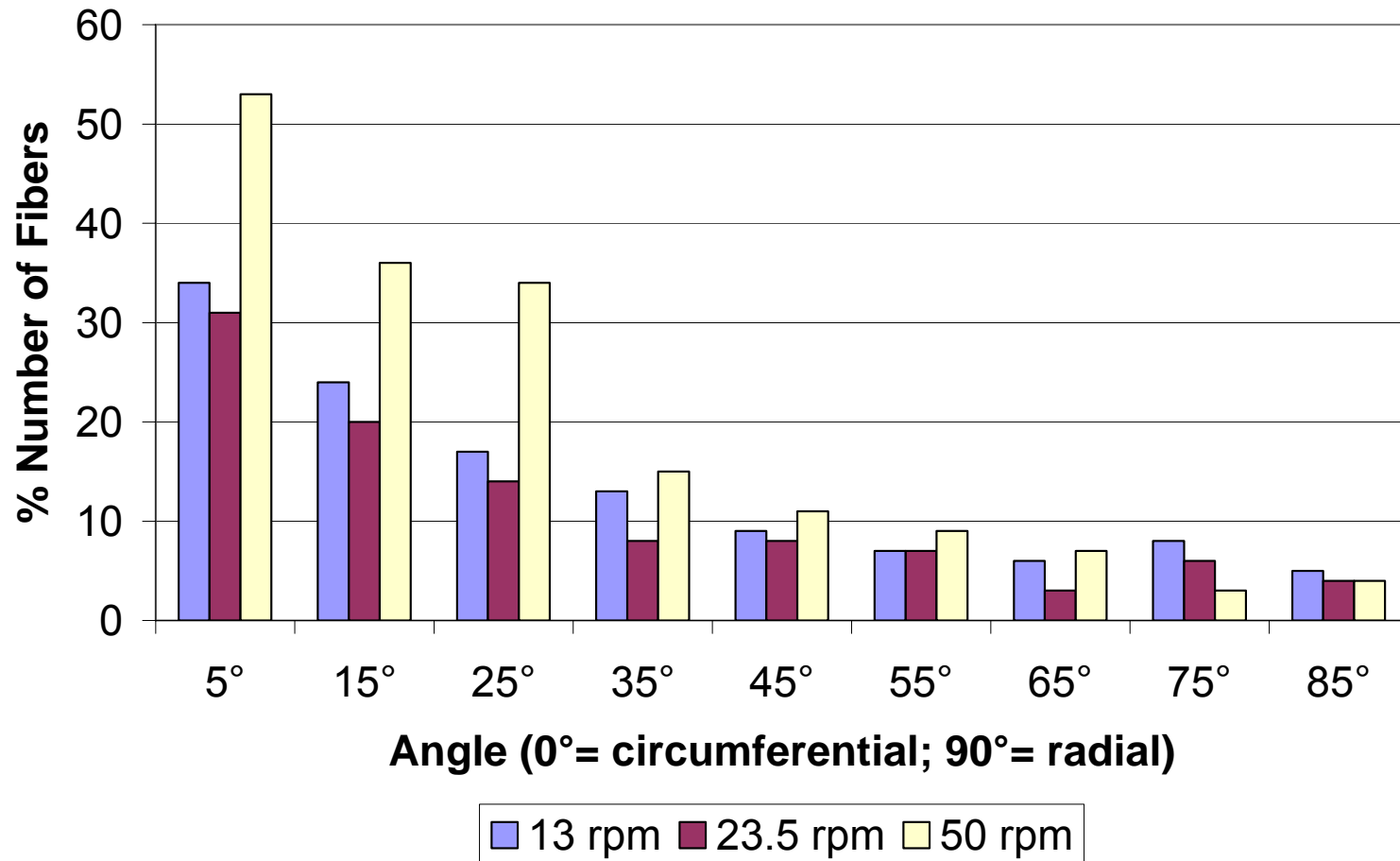


Figure 71: Distribution depending on disc speed at 10cm electrode distance / 20kV electrostatic potential / 20mm lay-down rod

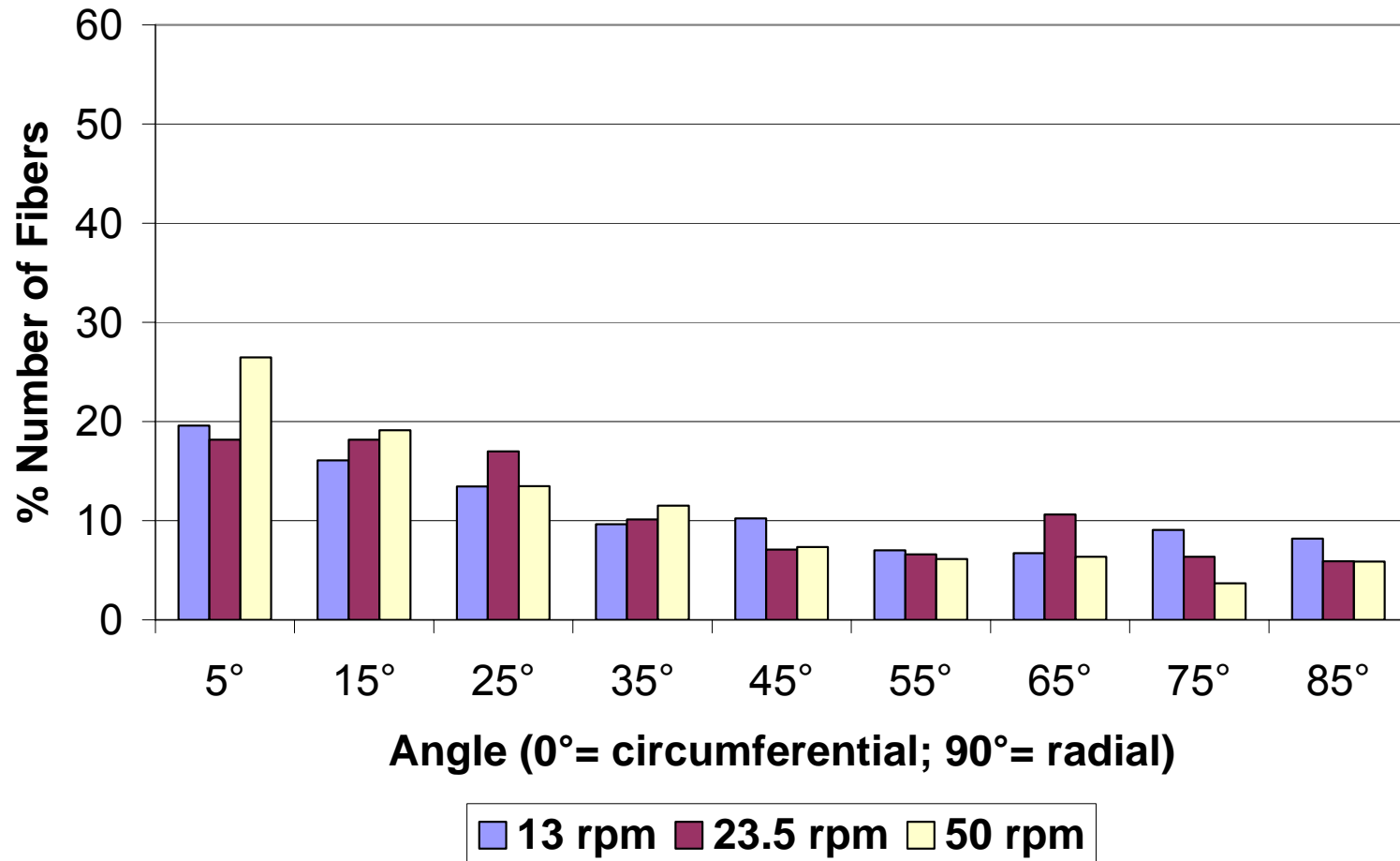


Figure 72: Distribution depending on disc speed at 10cm electrode distance / 50kV electrostatic potential / 20mm lay-down rod

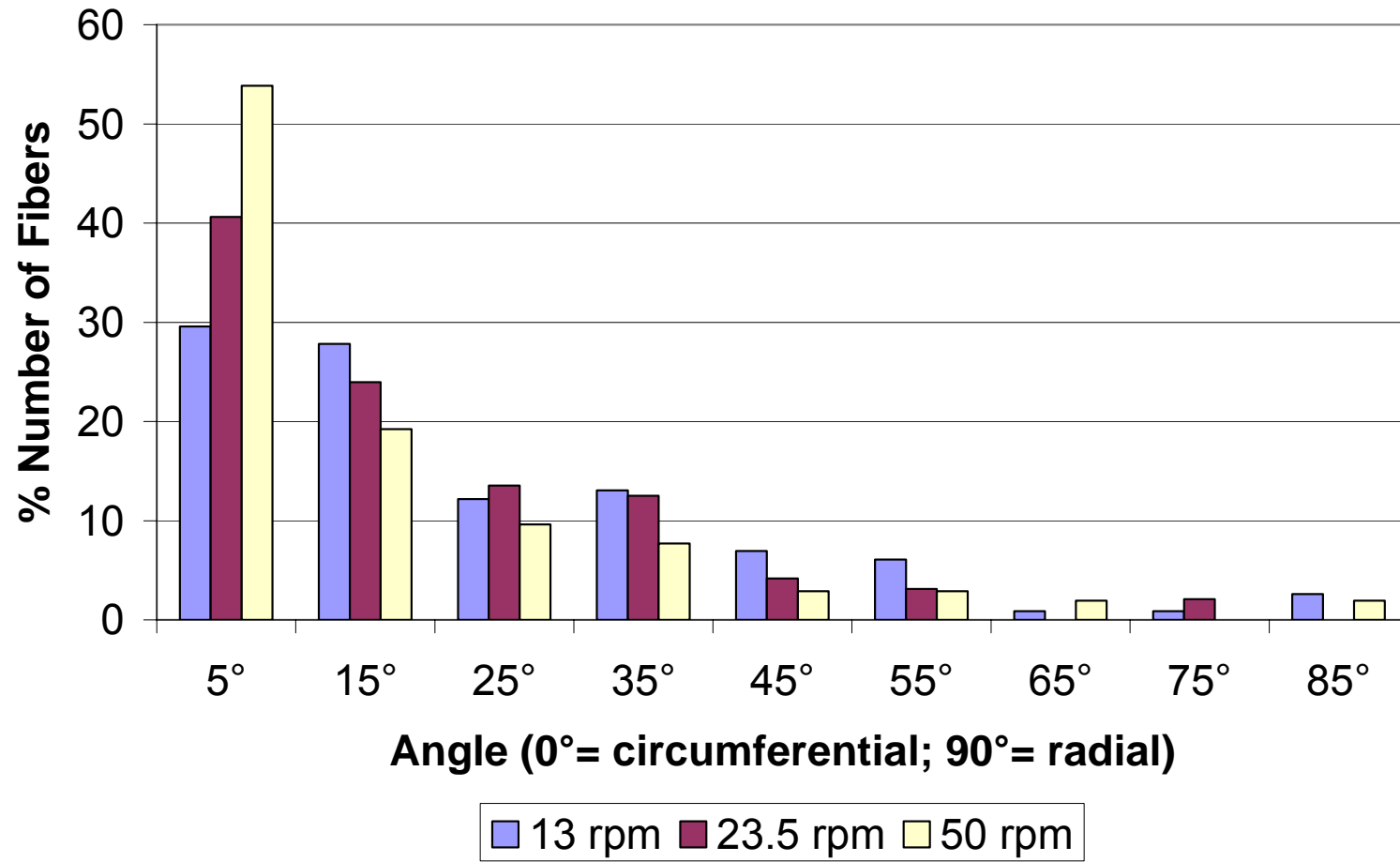


Figure 73: Distribution depending on disc speed at 20cm electrode distance / 10kV electrostatic potential / 20mm lay-down rod

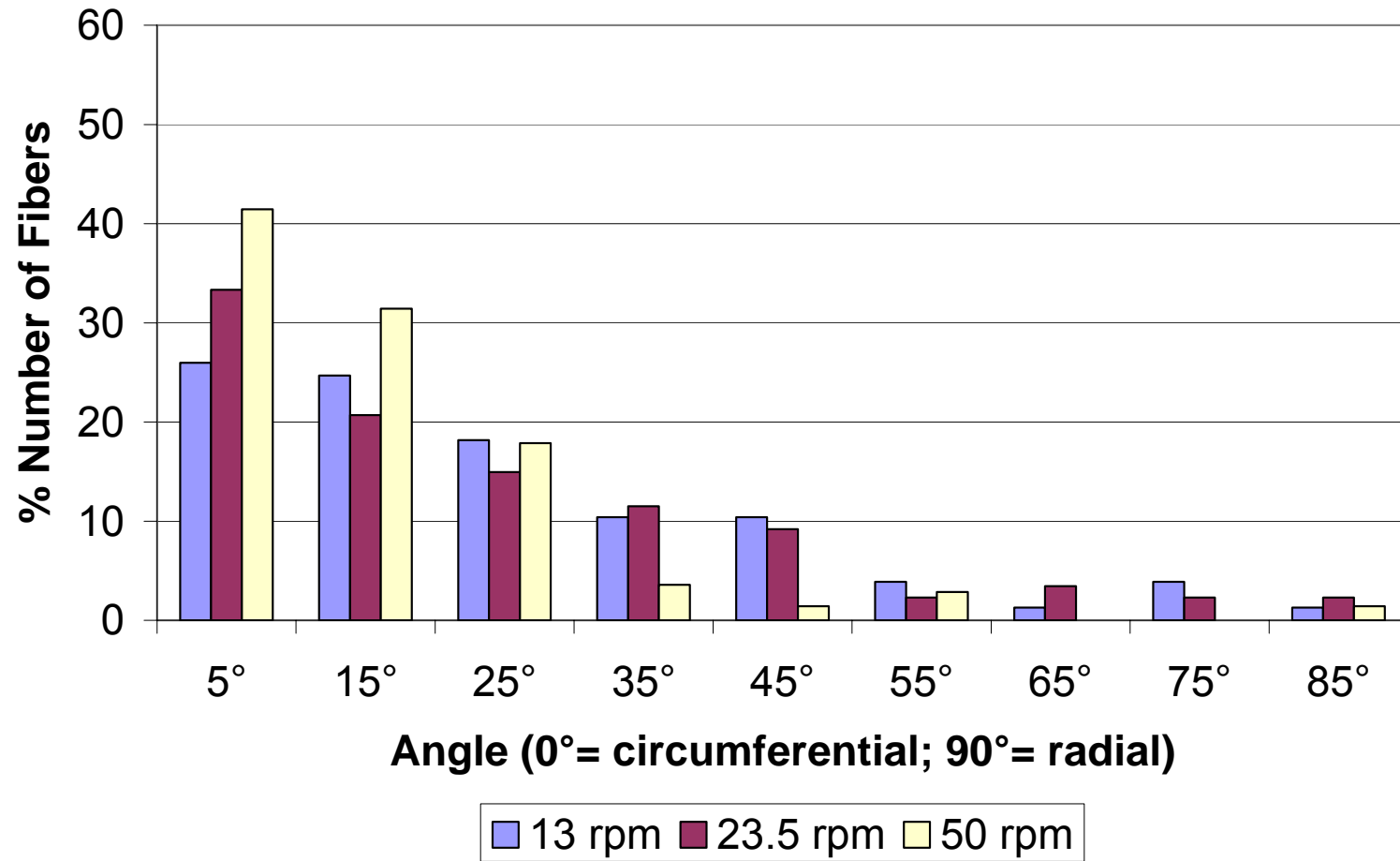


Figure 74: Distribution depending on disc speed at 20cm electrode distance / 20kV electrostatic potential / 20mm lay-down rod

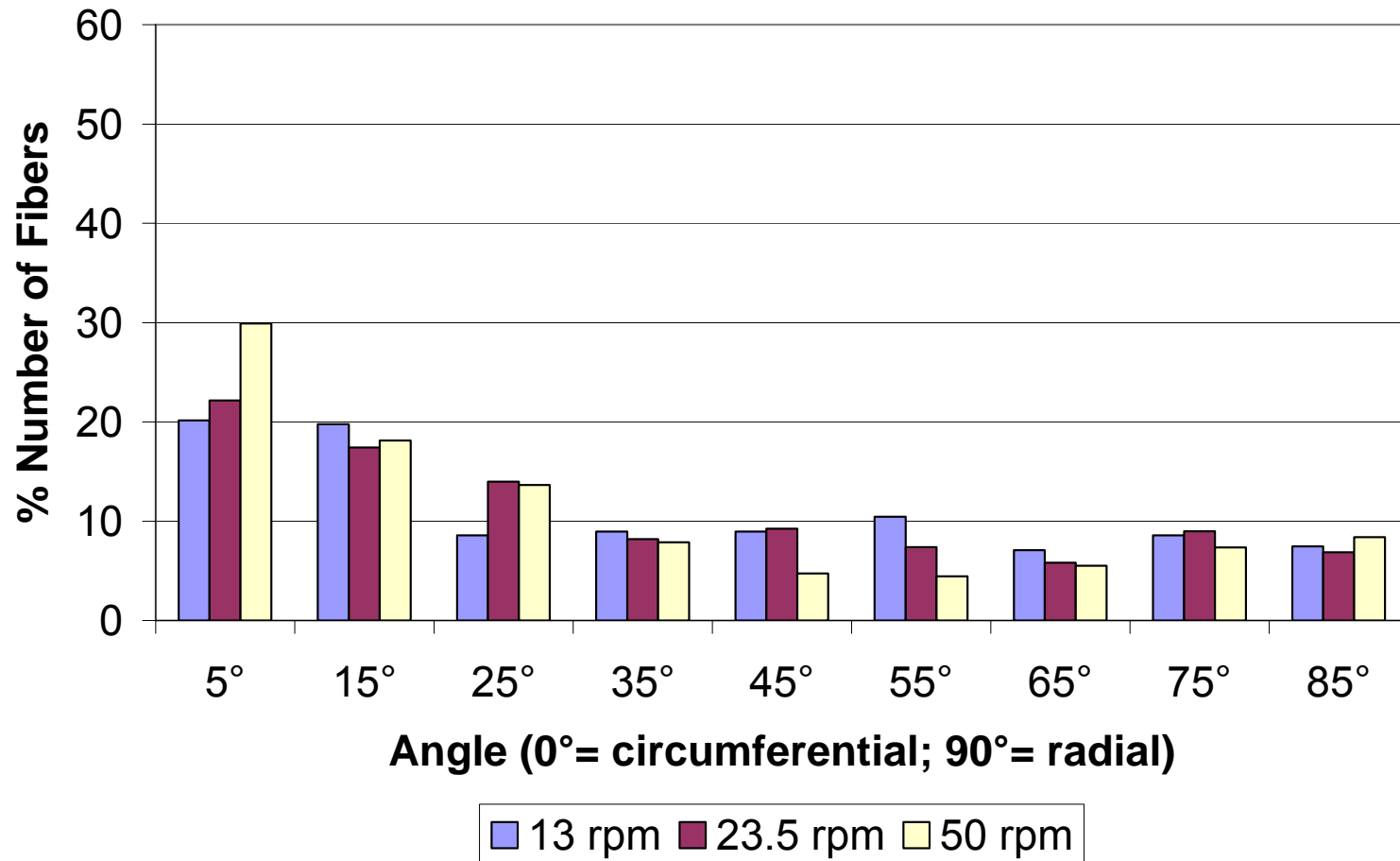


Figure 75: Distribution depending on disc speed at 20cm electrode distance / 50kV electrostatic potential / 20mm lay-down rod

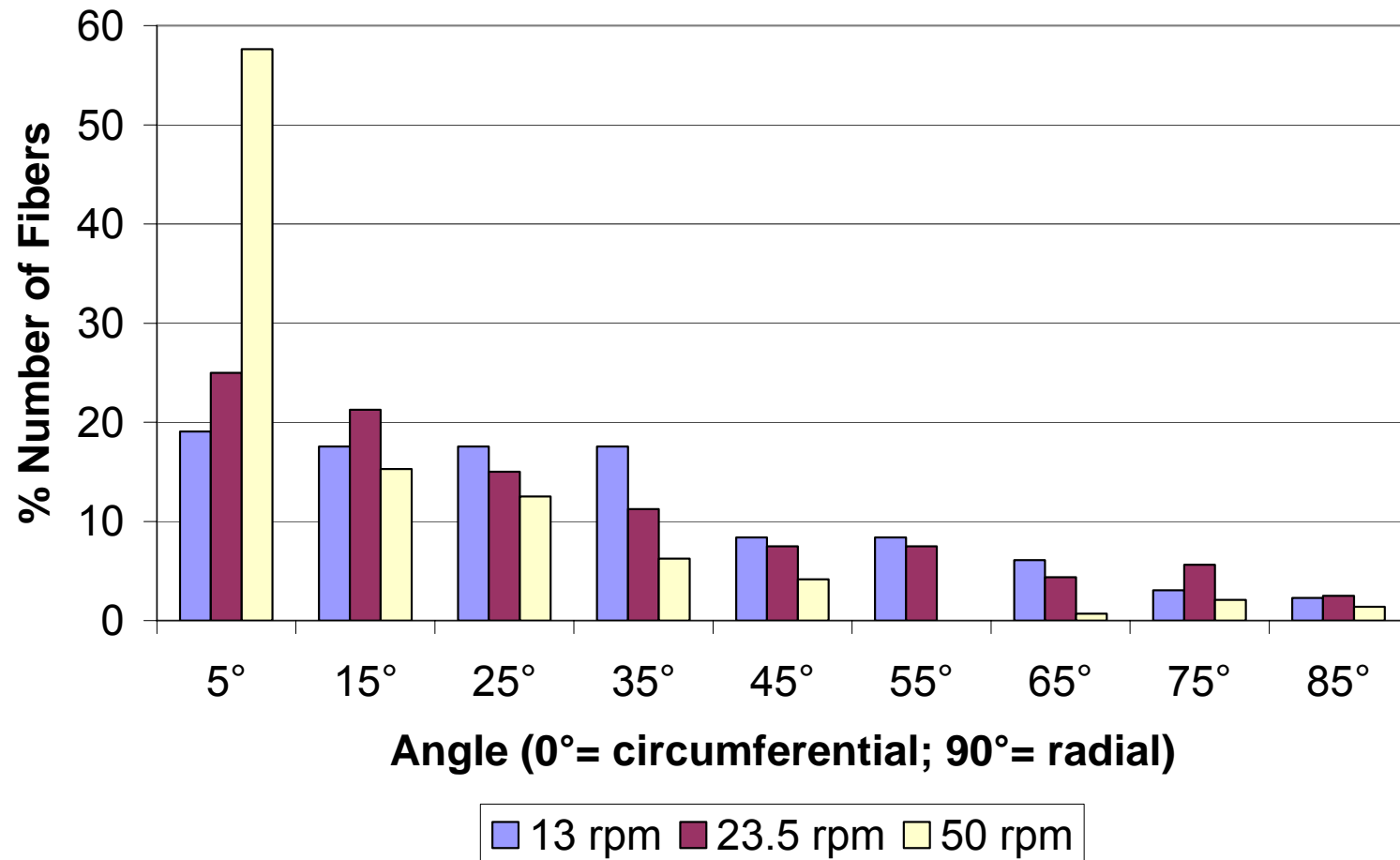


Figure 76: Distribution depending on disc speed at 30cm electrode distance / 10kV electrostatic potential / 20mm lay-down rod

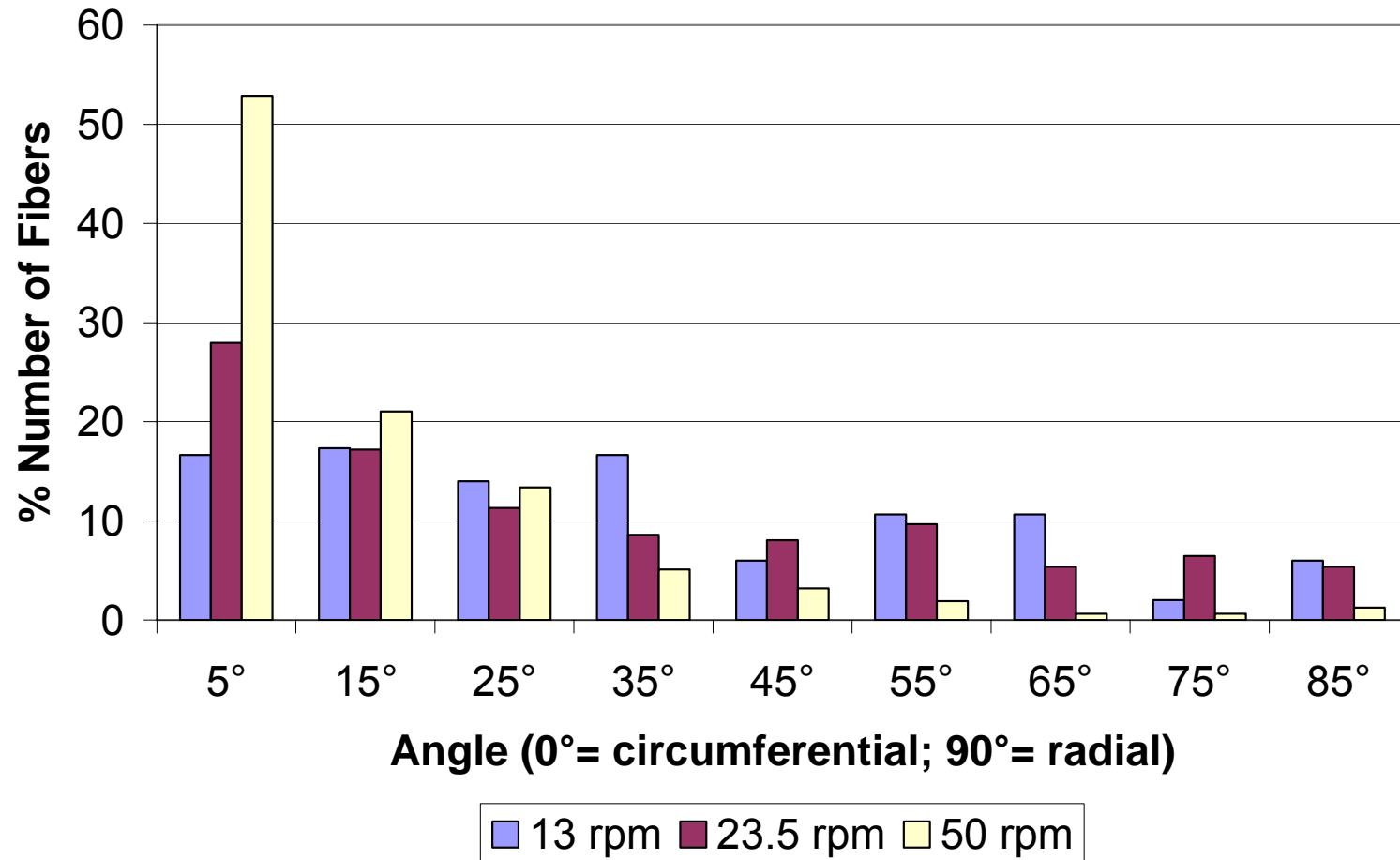


Figure 77: Distribution depending on disc speed at 30cm electrode distance / 20kV electrostatic potential / 20mm lay-down rod

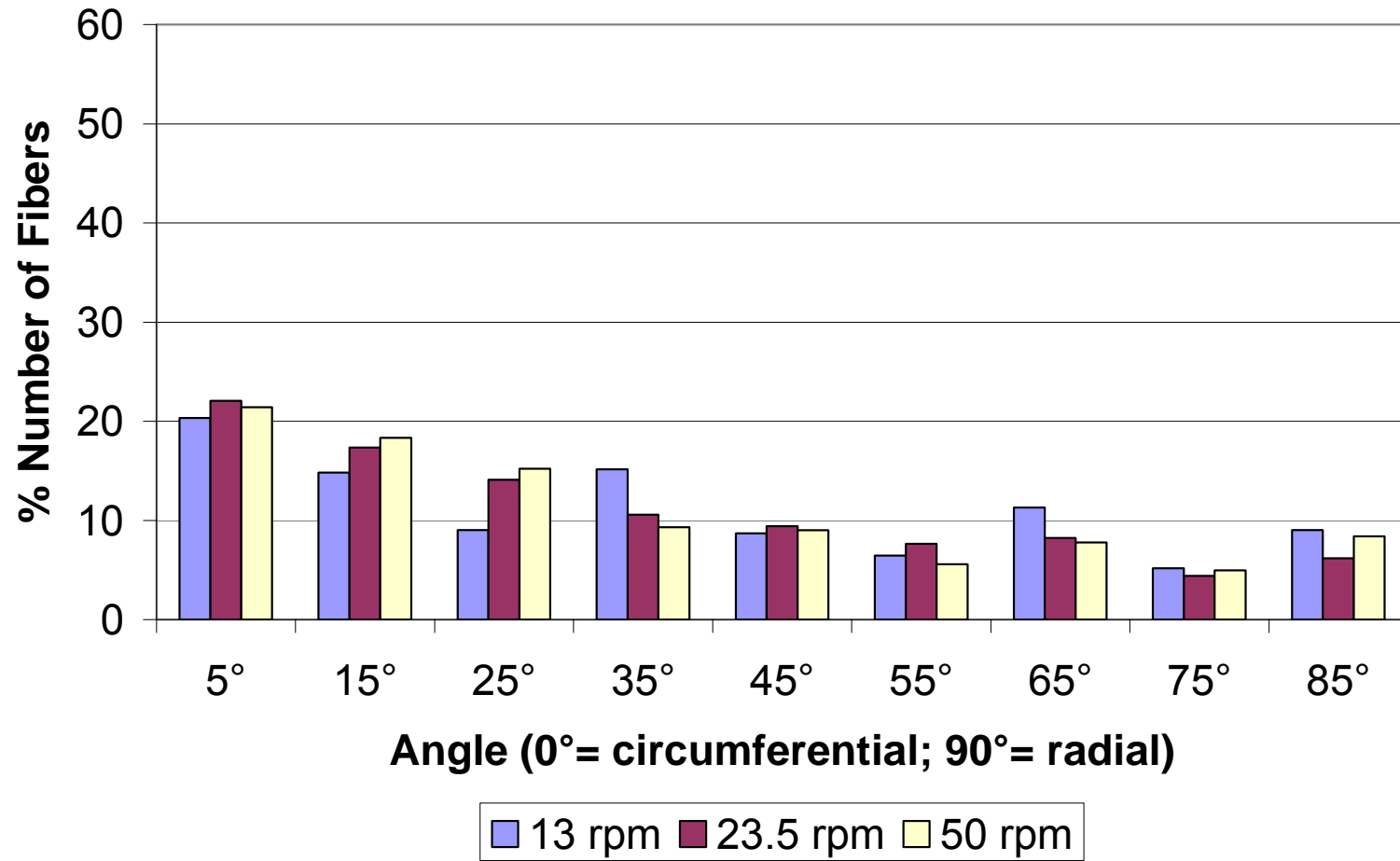


Figure 78: Distribution depending on disc speed at 30cm electrode distance / 50kV electrostatic potential / 20mm lay-down rod

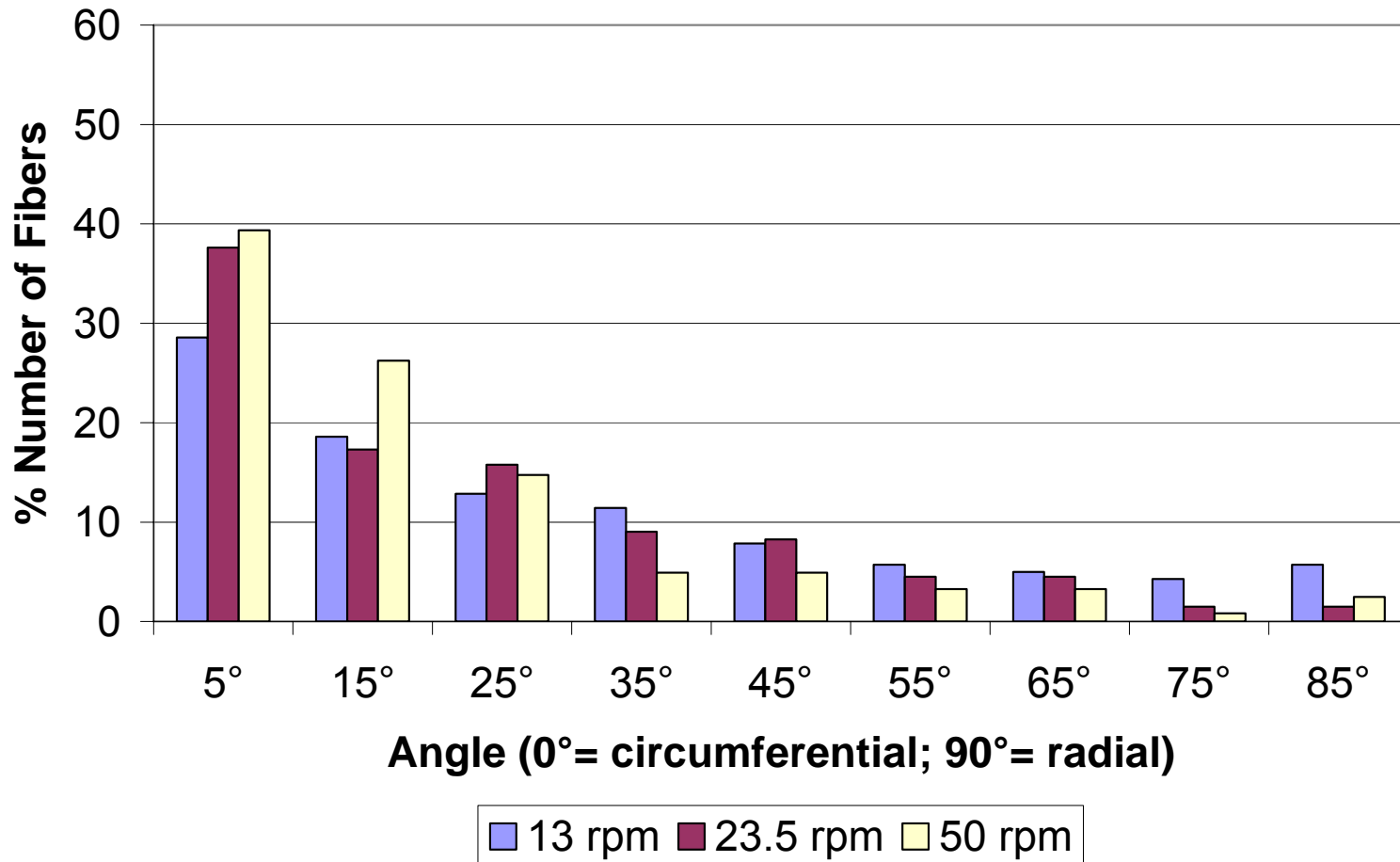


Figure 79: Distribution depending on disc speed at 10cm electrode distance / 10kV electrostatic potential / 9.4mm lay-down rod

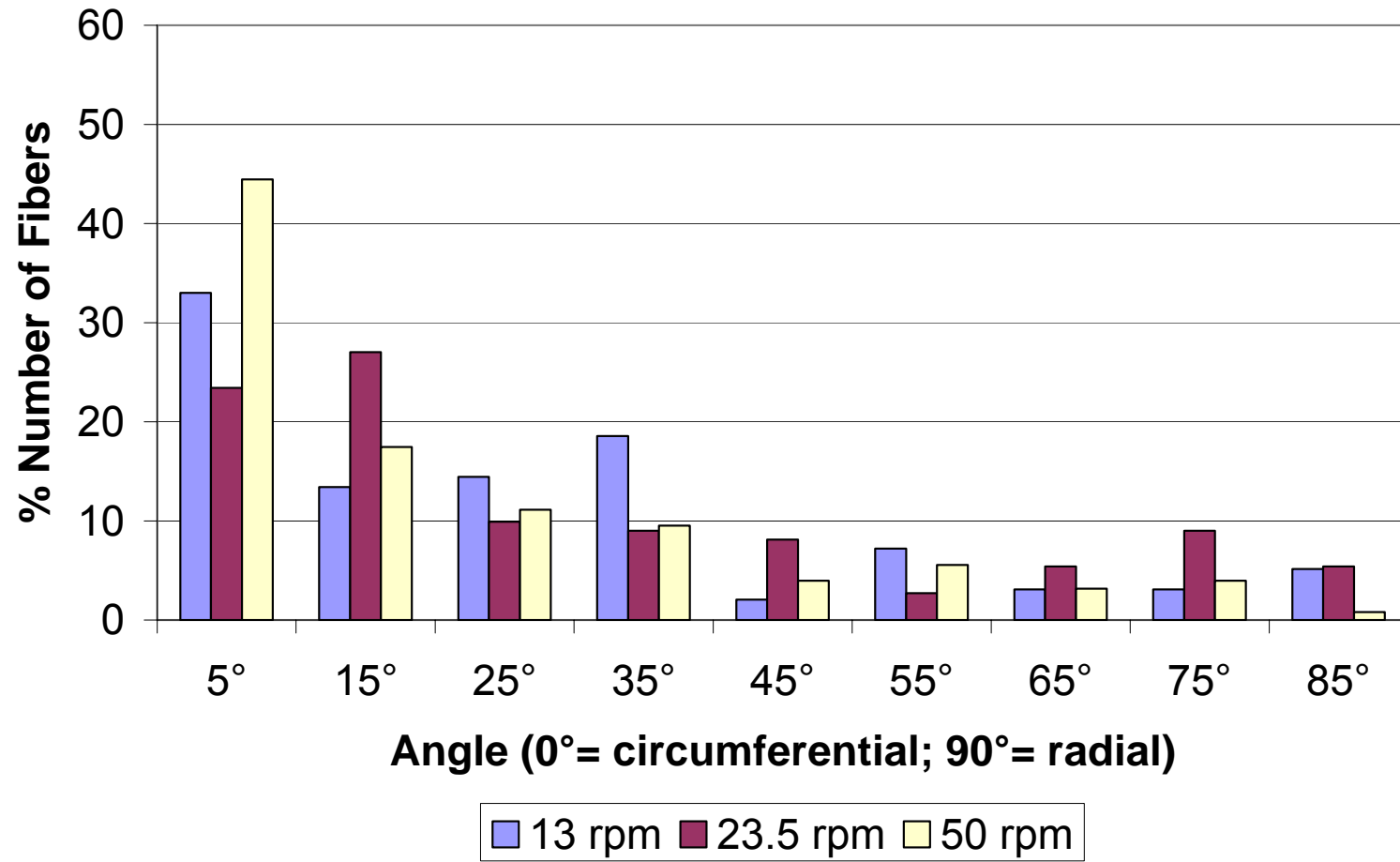


Figure 80: Distribution depending on disc speed at 10cm electrode distance / 20kV electrostatic potential / 9.4mm lay-down rod

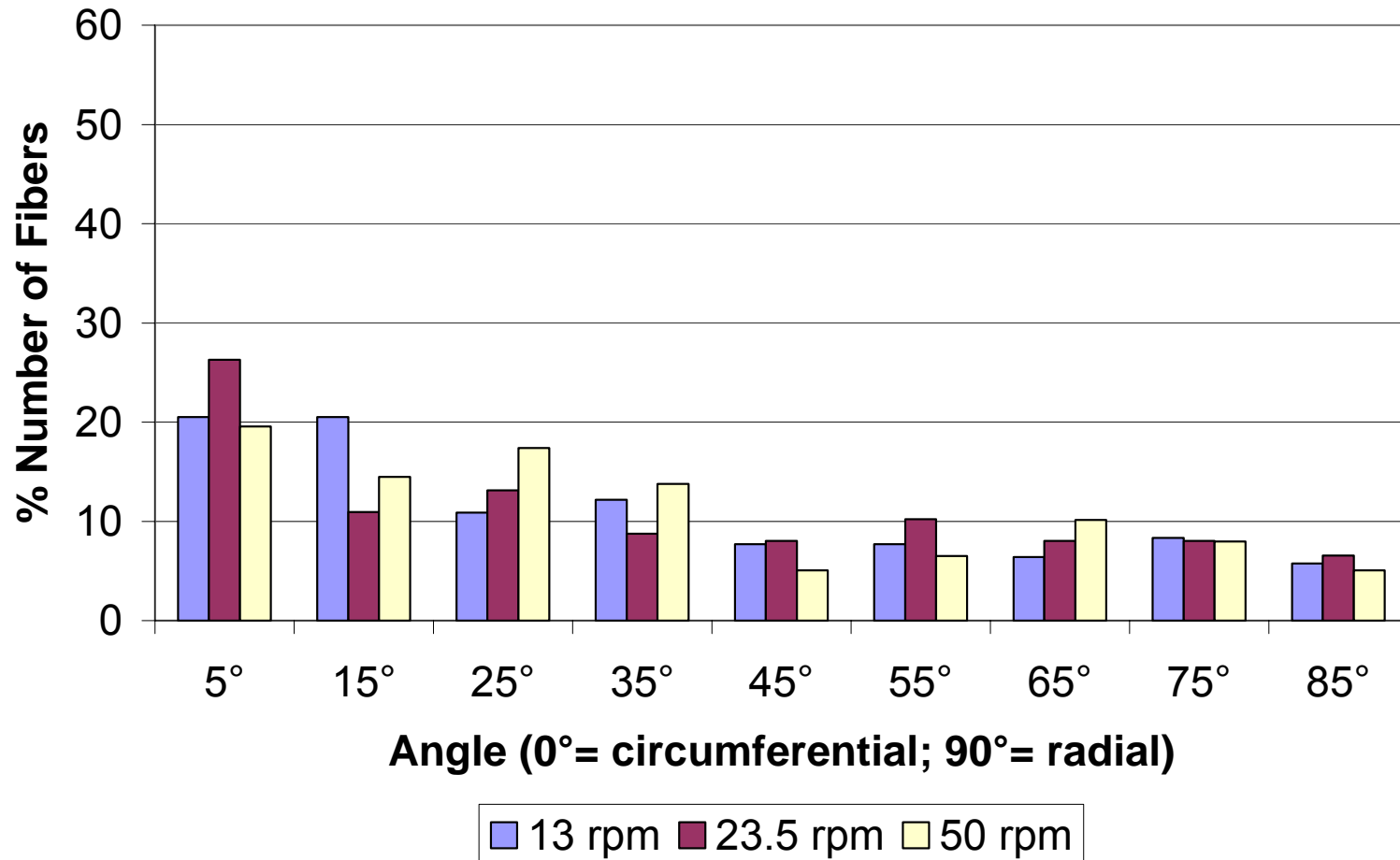


Figure 81: Distribution depending on disc speed at 10cm electrode distance / 50kV electrostatic potential / 9.4mm lay-down rod

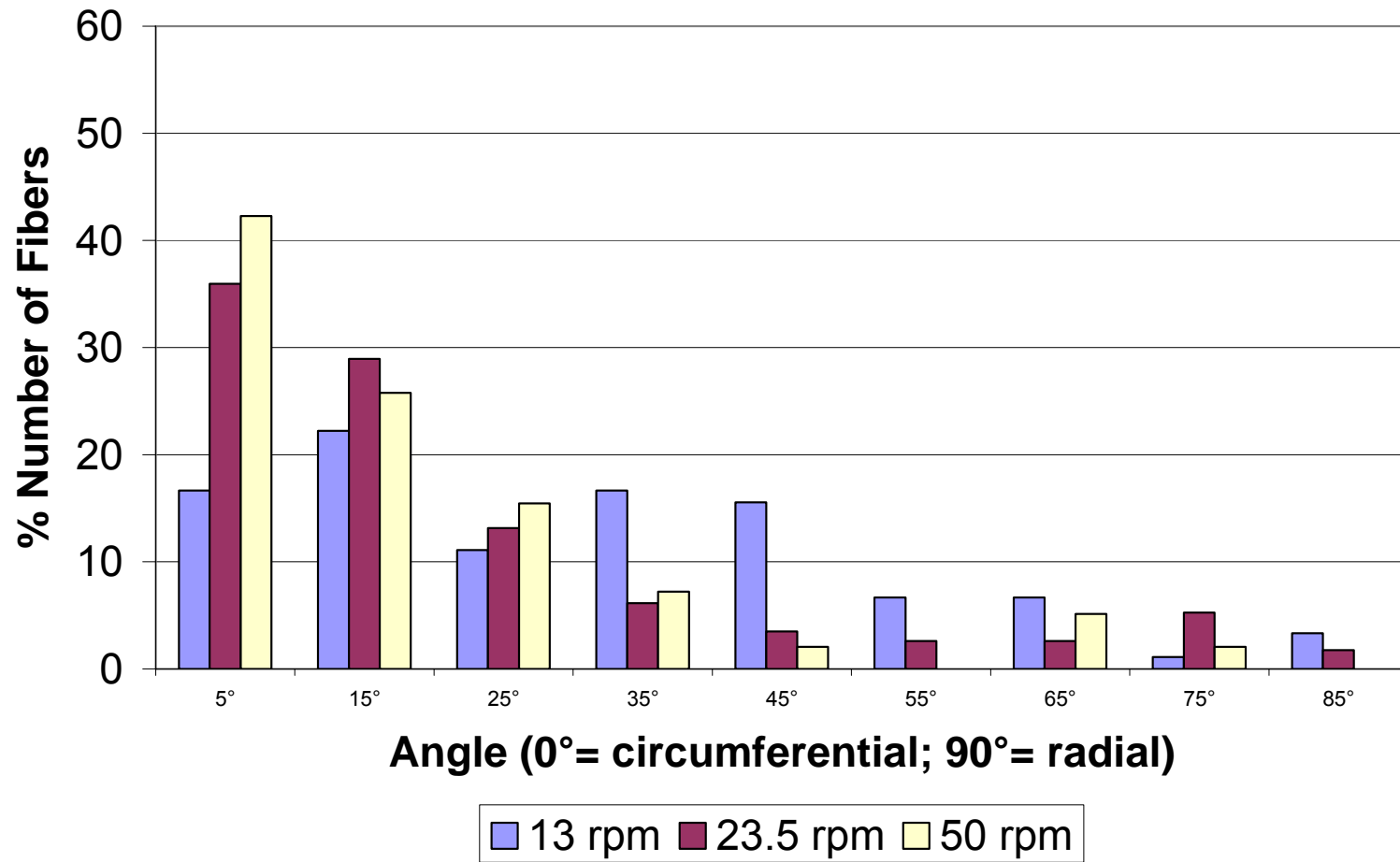


Figure 82: Distribution depending on disc speed at 20cm electrode distance / 10kV electrostatic potential / 9.4mm lay-down rod

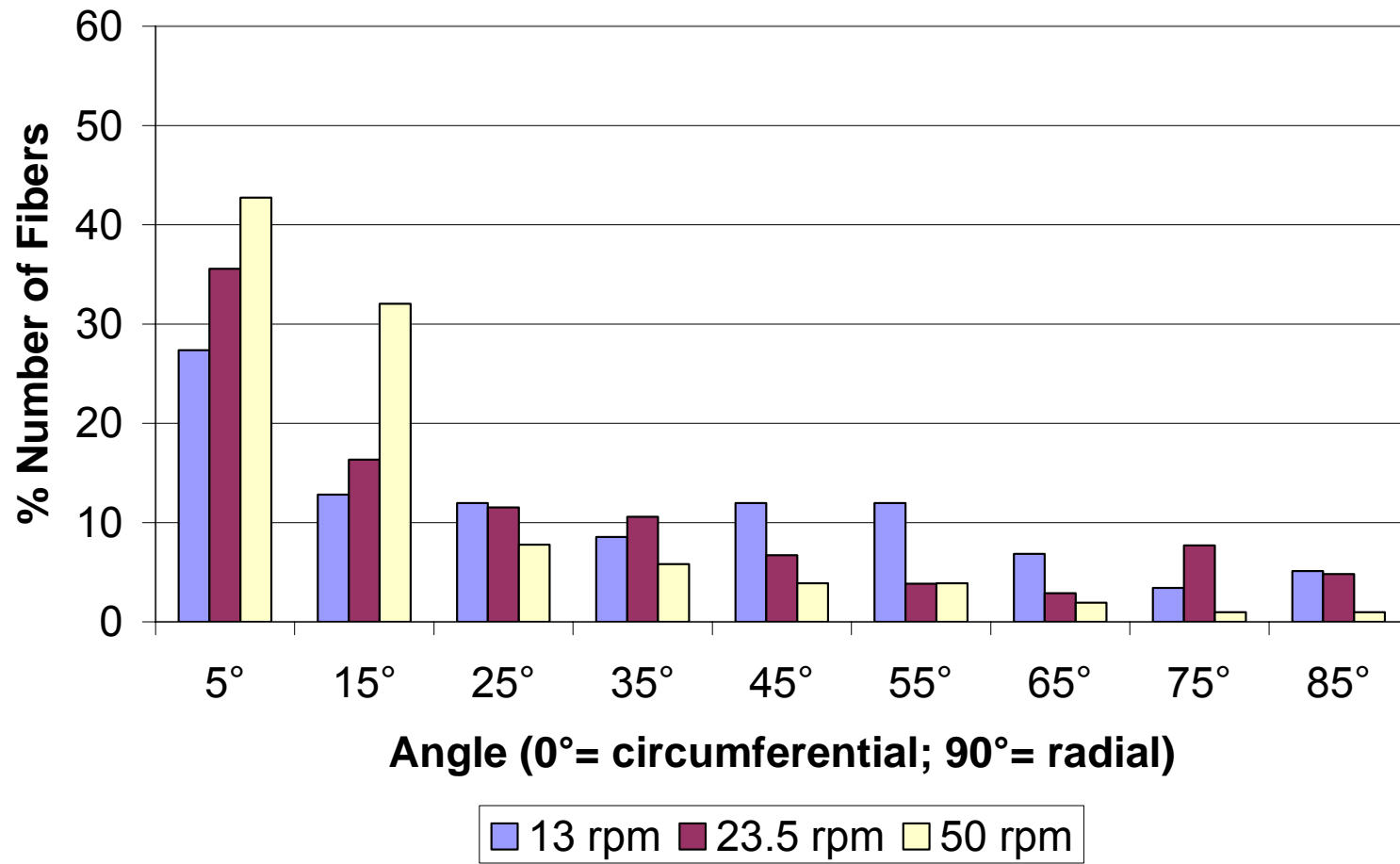


Figure 83: Distribution depending on disc speed at 20cm electrode distance / 20kV electrostatic potential / 9.4mm lay-down rod

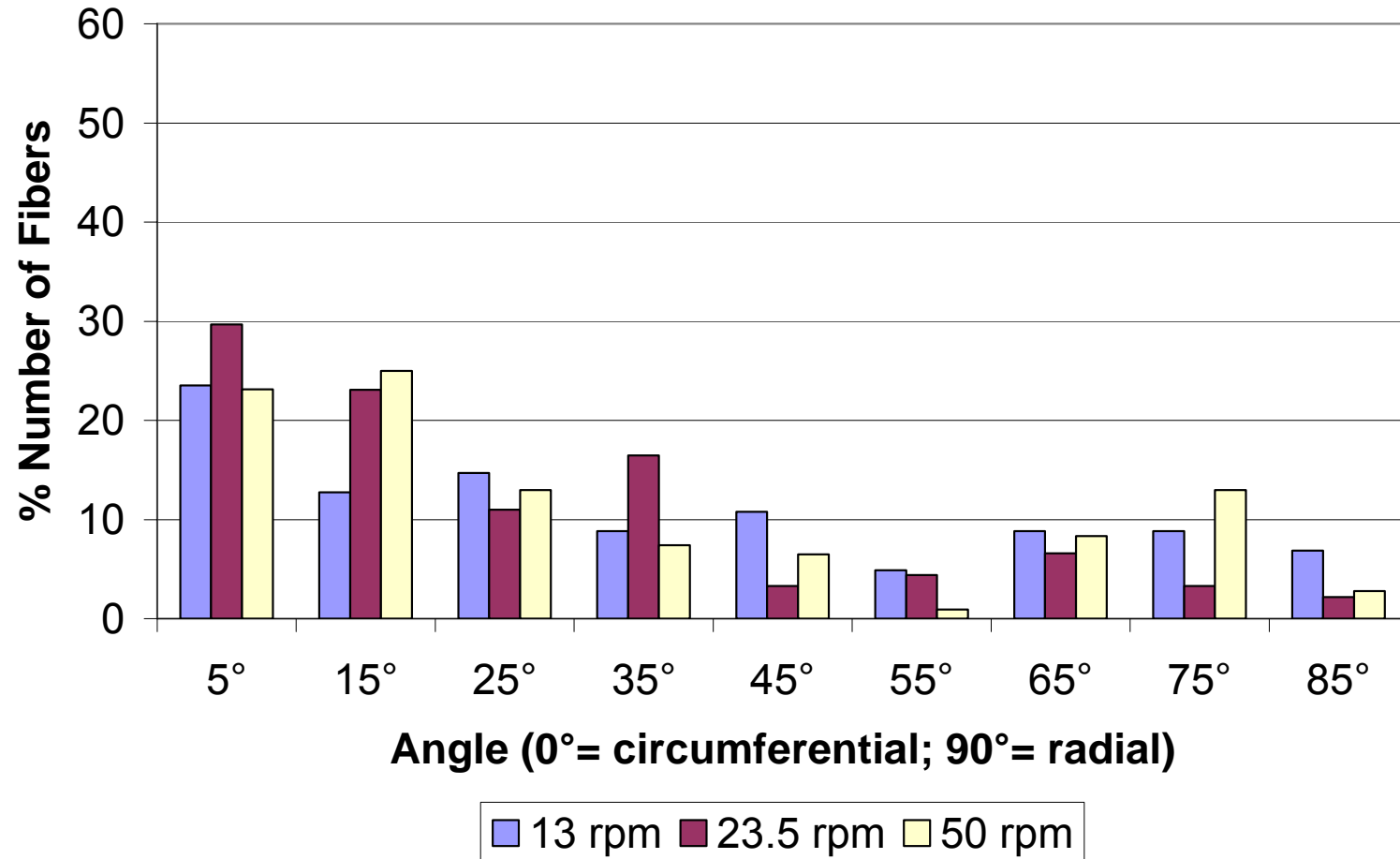


Figure 84: Distribution depending on disc speed at 20cm electrode distance / 50kV electrostatic potential / 9.4mm lay-down rod

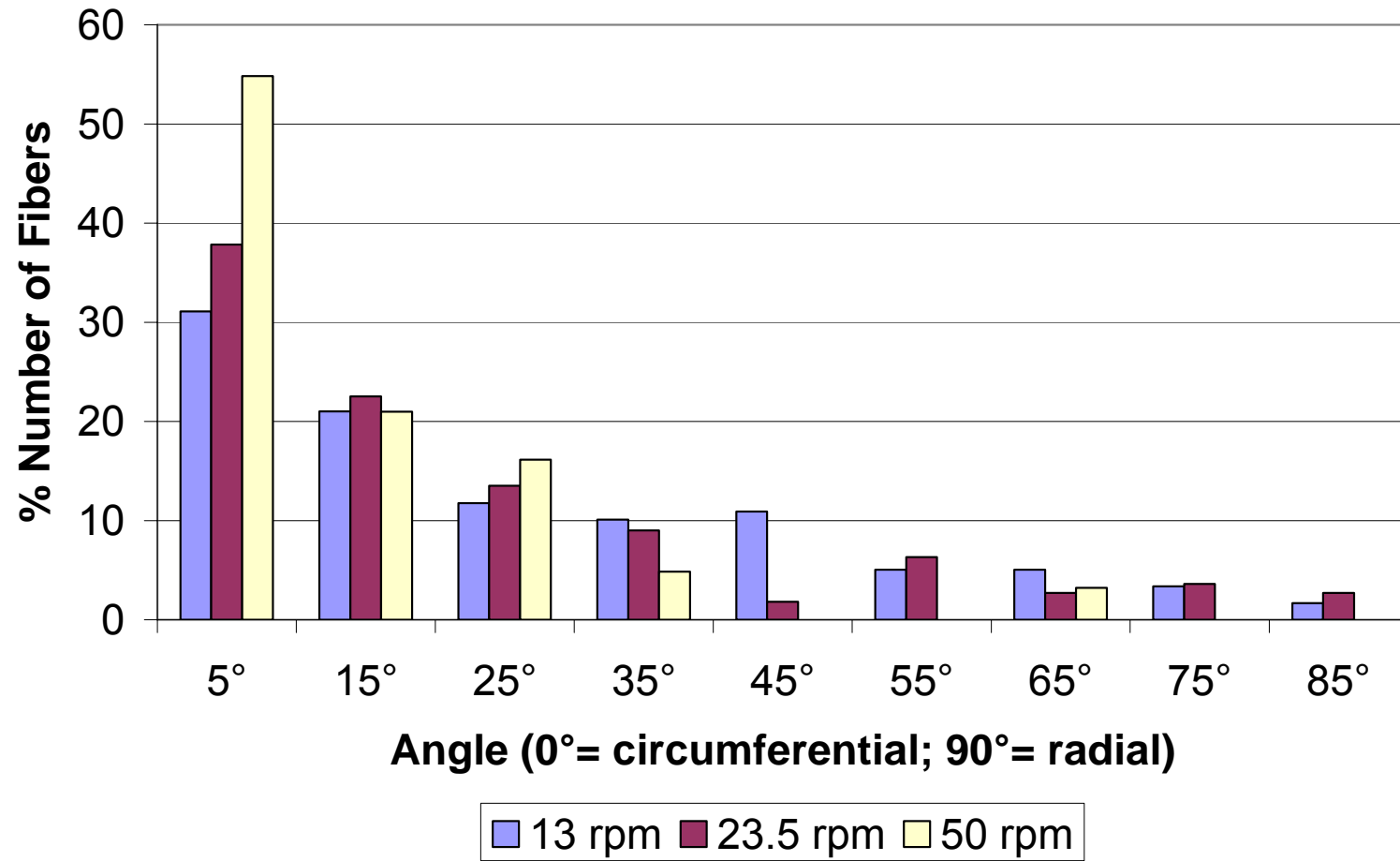


Figure 85: Distribution depending on disc speed at 30cm electrode distance / 10kV electrostatic potential / 9.4mm lay-down rod

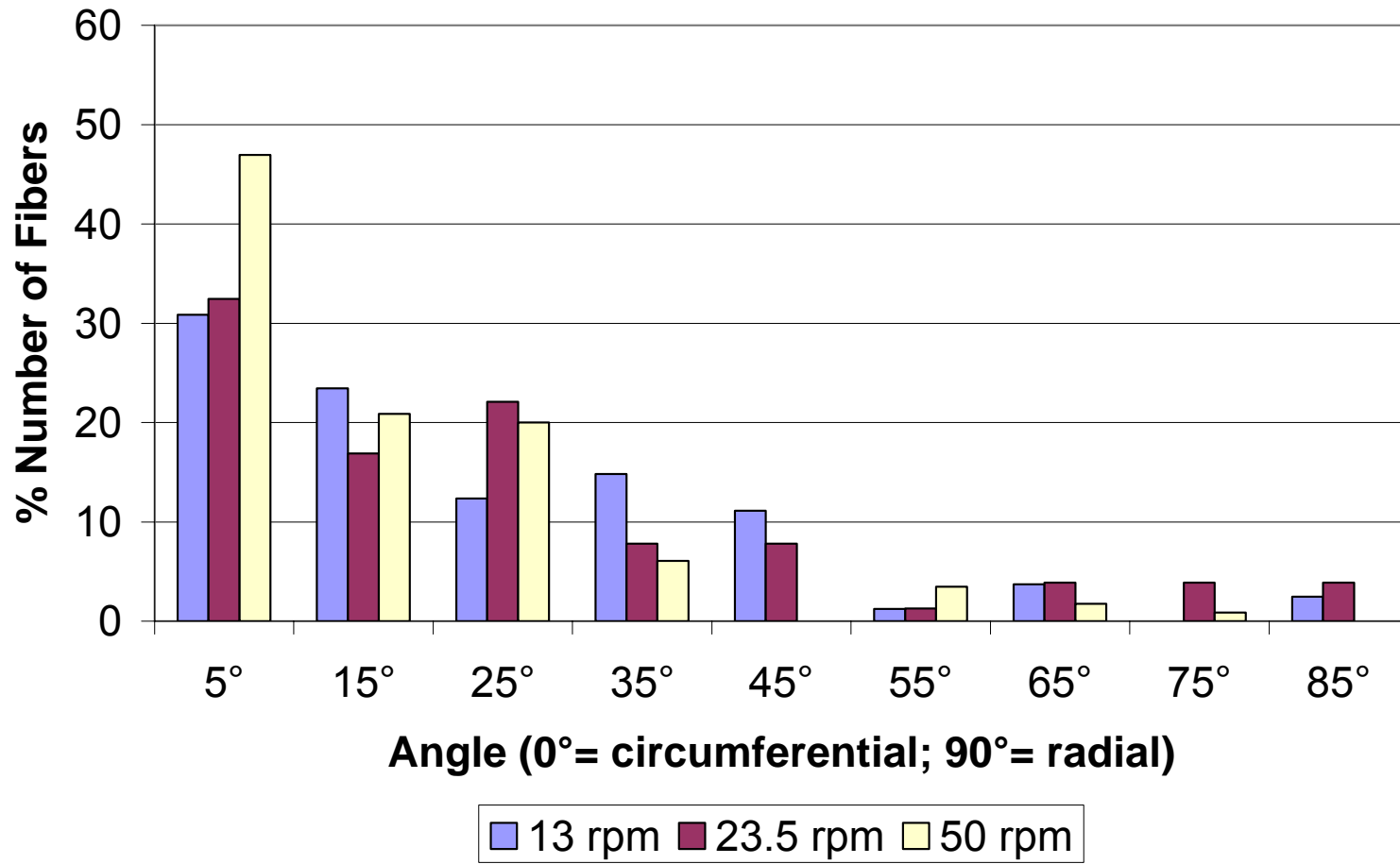


Figure 86: Distribution depending on disc speed at 30cm electrode distance / 20kV electrostatic potential / 9.4mm lay-down rod

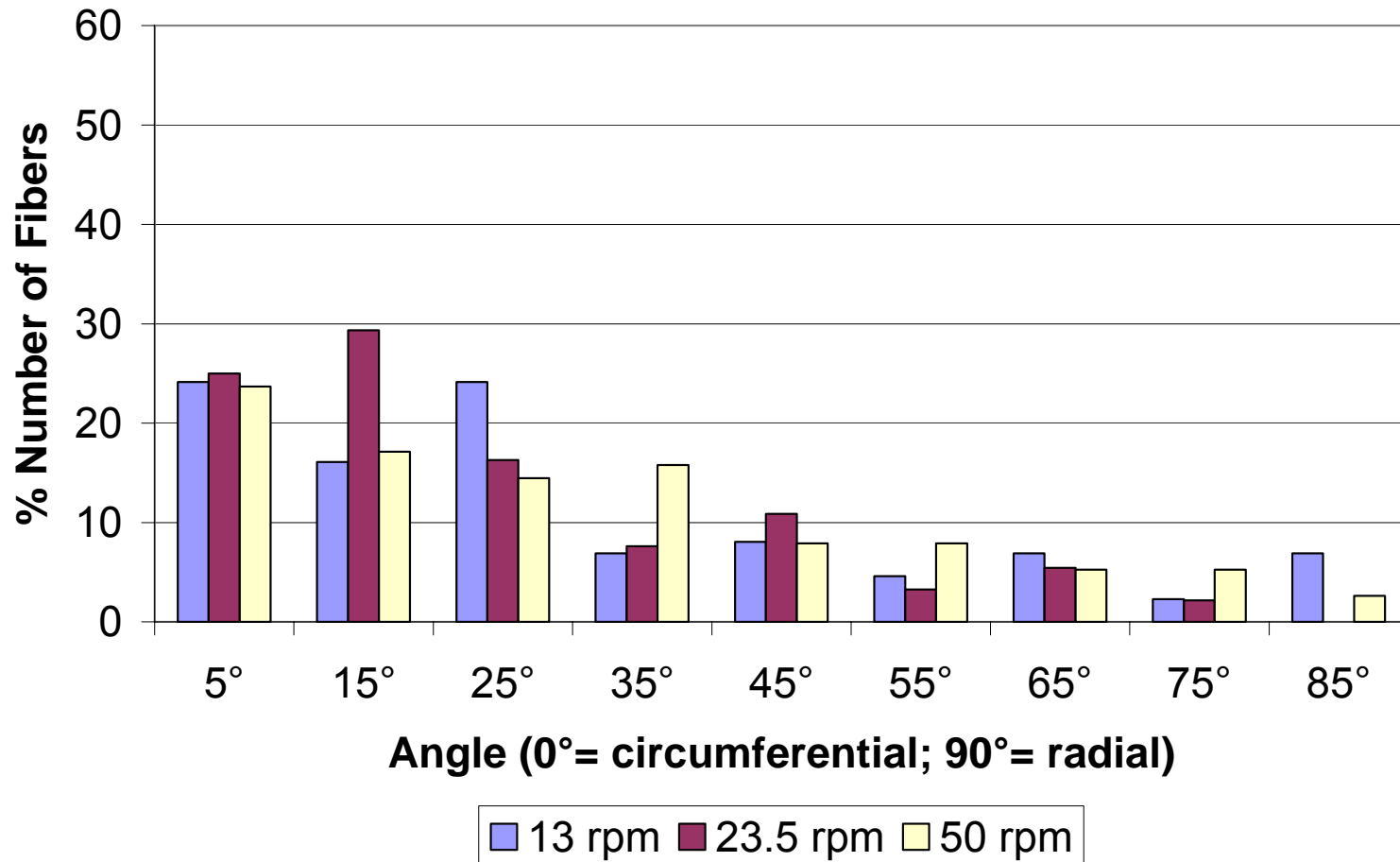


Figure 87: Distribution depending on disc speed at 30cm electrode distance / 50kV electrostatic potential / 9.4mm lay-down rod

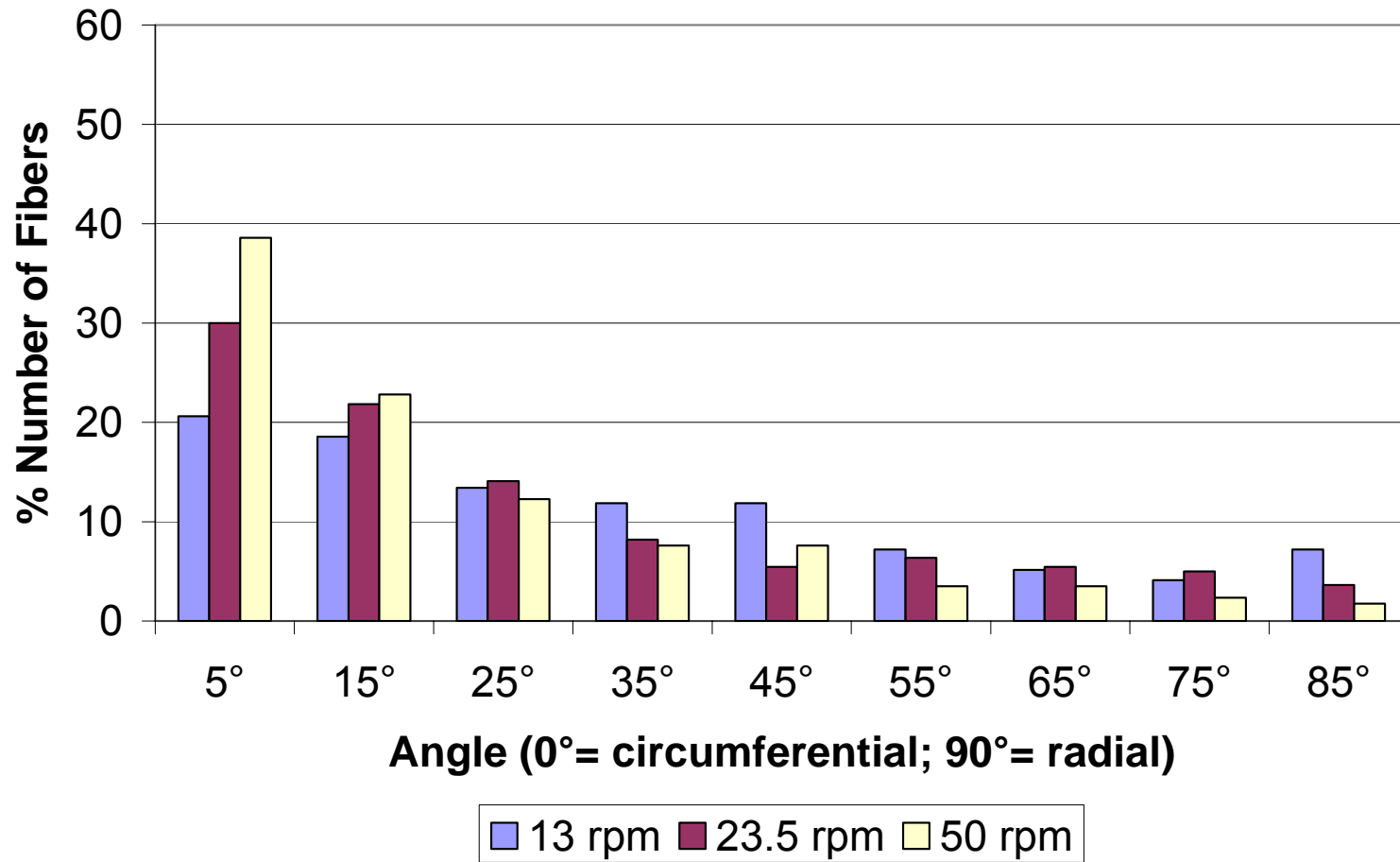


Figure 88: Distribution depending on disc speed at 10cm electrode distance / 10kV electrostatic potential / 4.76mm lay-down rod

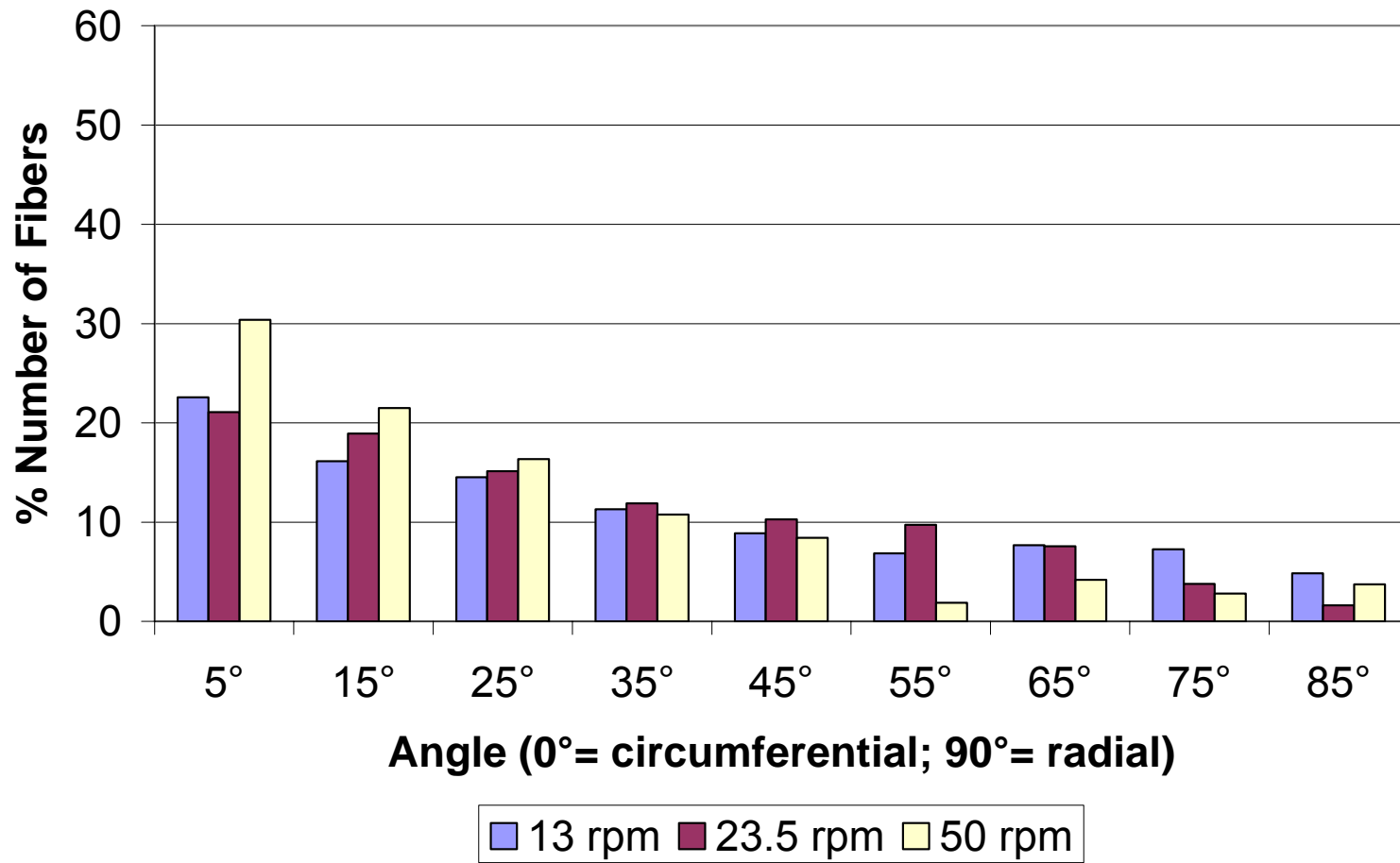


Figure 89: Distribution depending on disc speed at 10cm electrode distance / 20kV electrostatic potential / 4.76mm lay-down rod

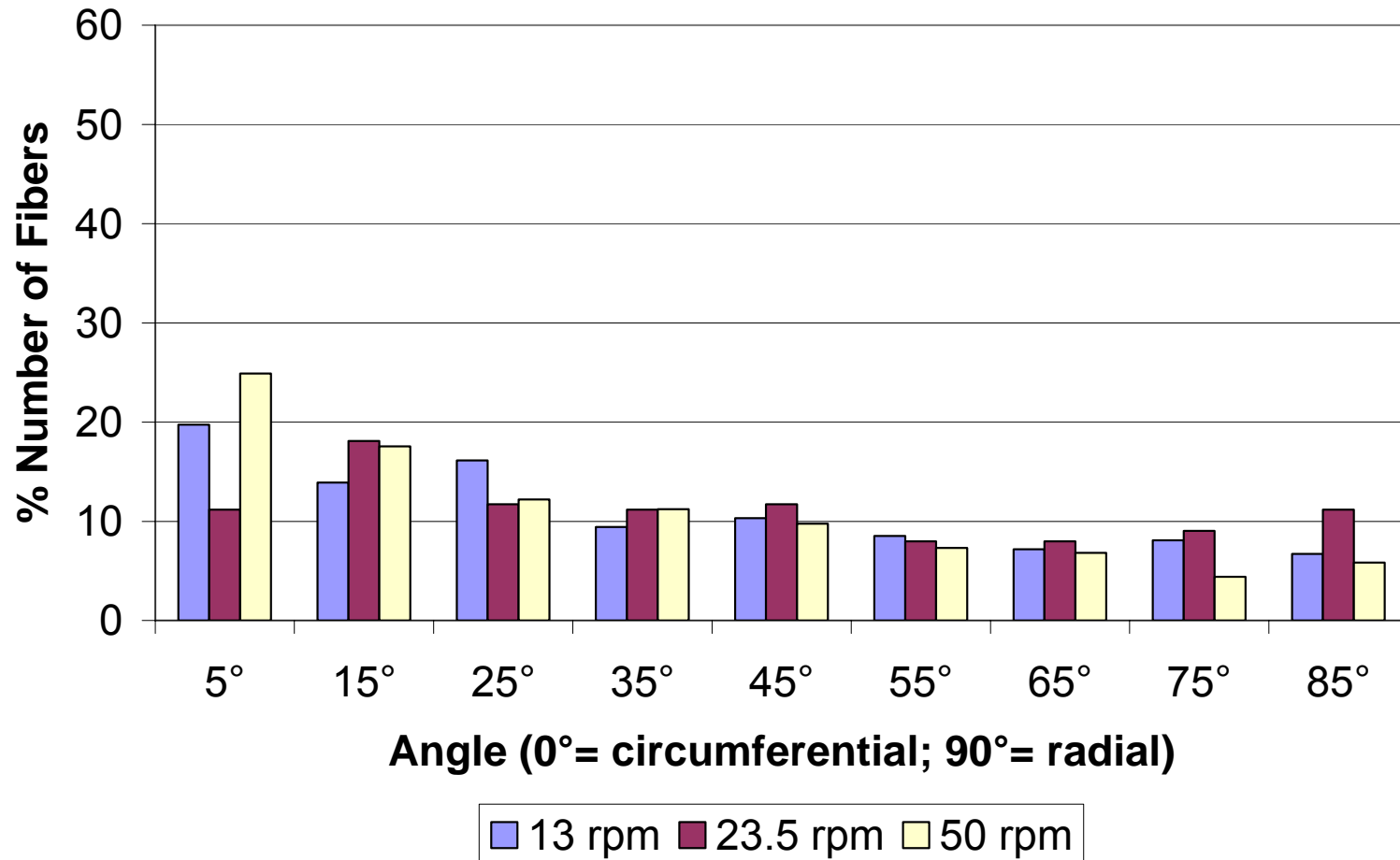


Figure 90: Distribution depending on disc speed at 10cm electrode distance / 50kV electrostatic potential / 4.76mm lay-down rod

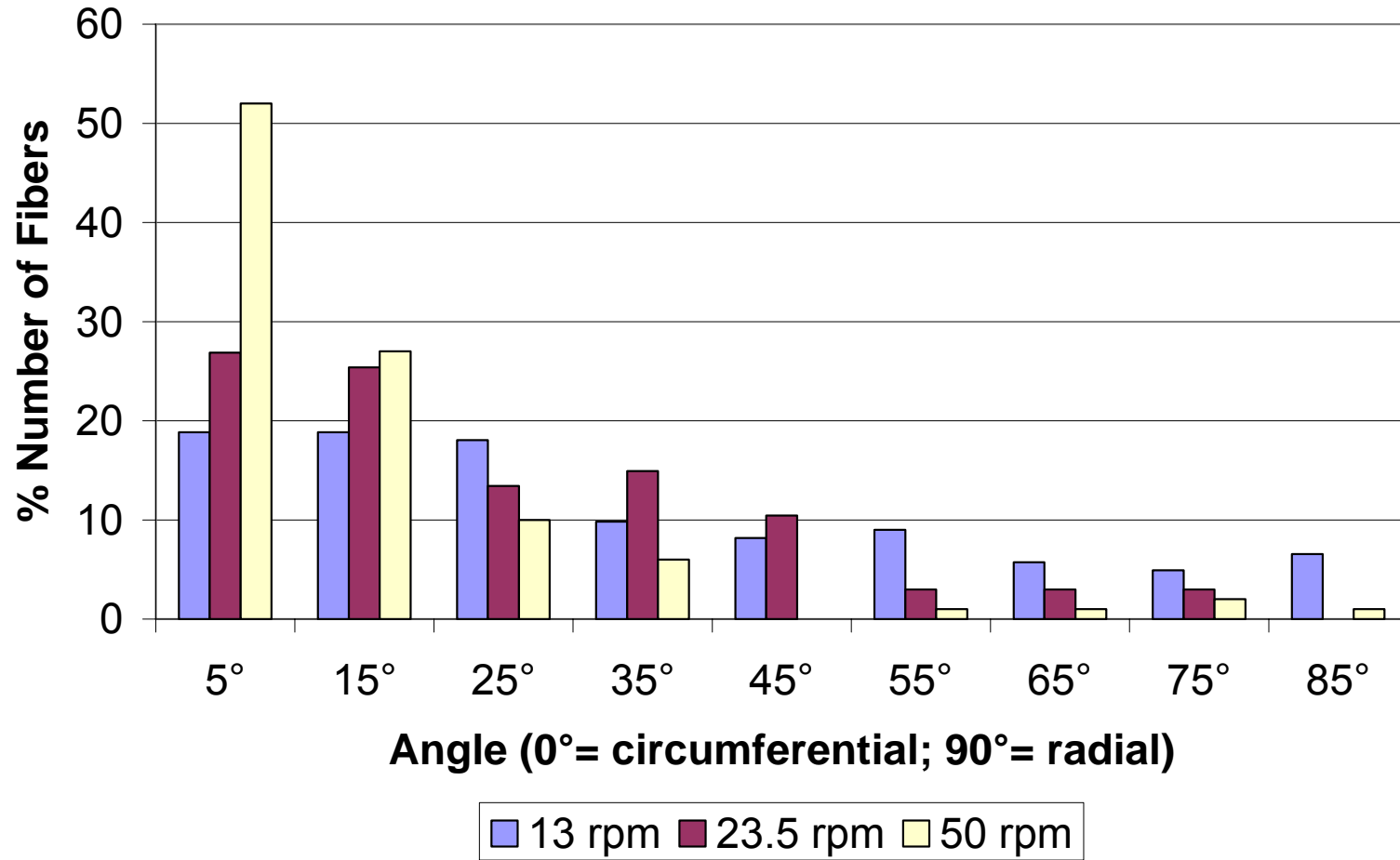


Figure 91: Distribution depending on disc speed at 20cm electrode distance / 10kV electrostatic potential / 4.76mm lay-down rod

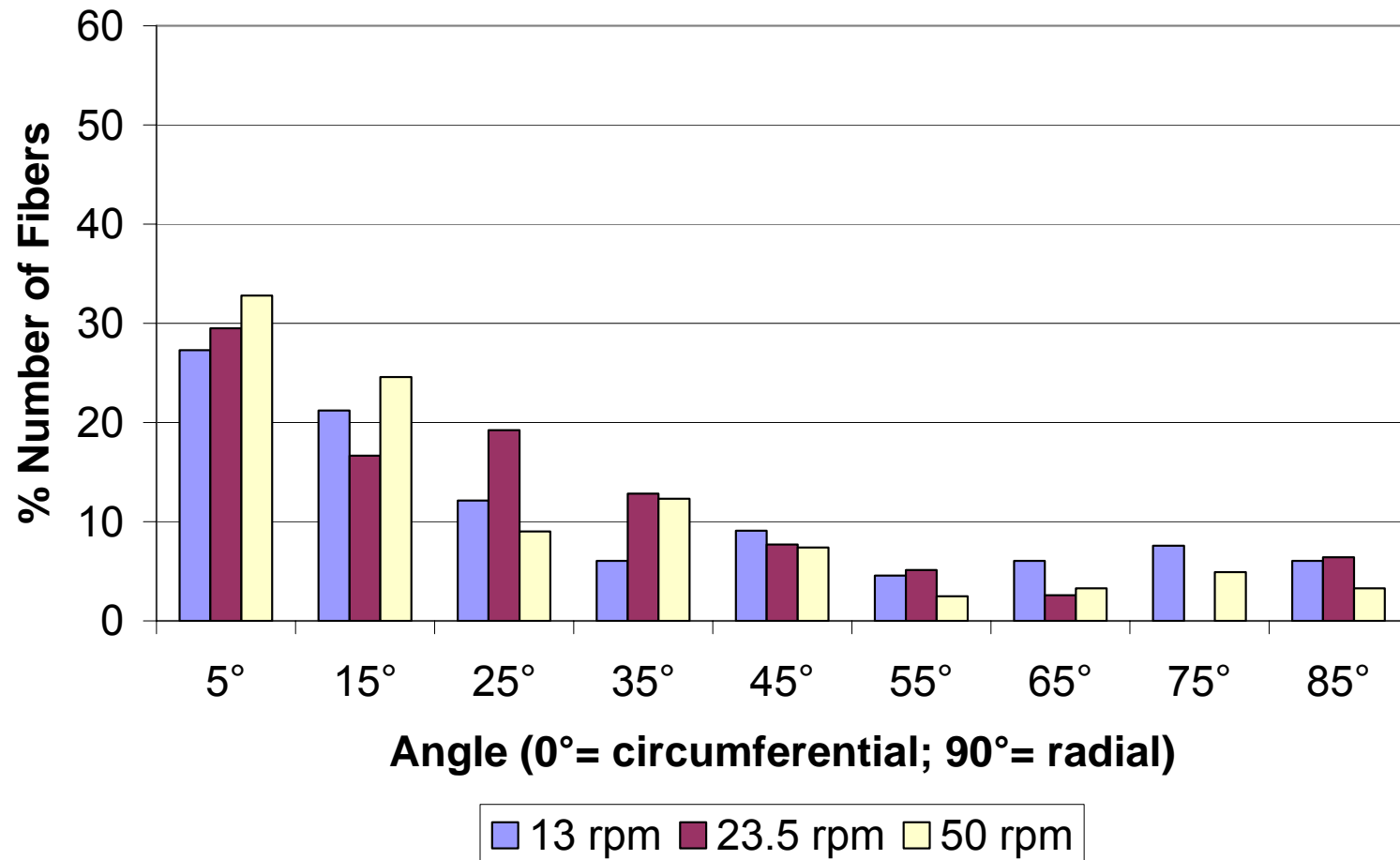


Figure 92: Distribution depending on disc speed at 20cm electrode distance / 20kV electrostatic potential / 4.76mm lay-down rod

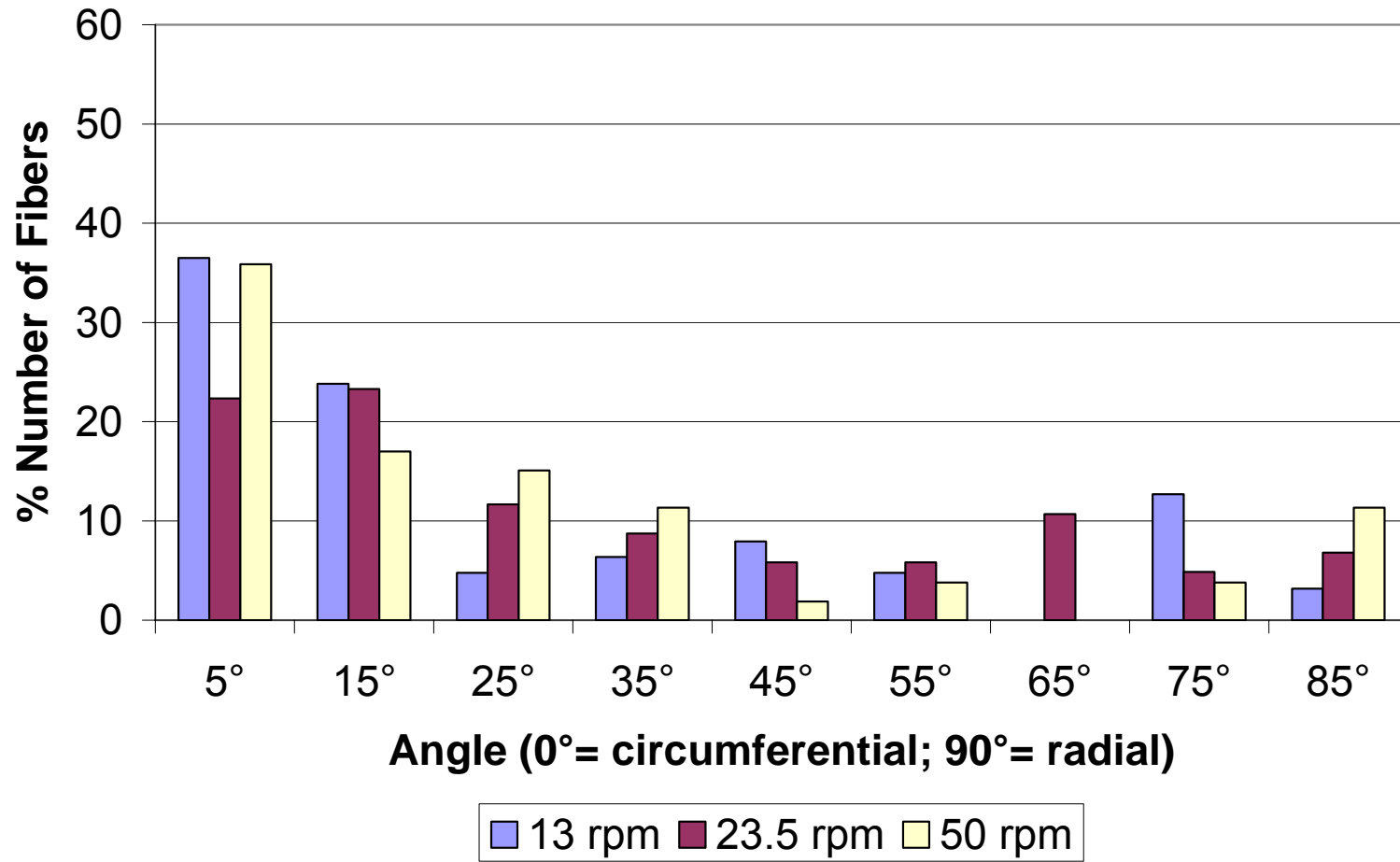


Figure 93: Distribution depending on disc speed at 20cm electrode distance / 50kV electrostatic potential / 4.76mm lay-down rod

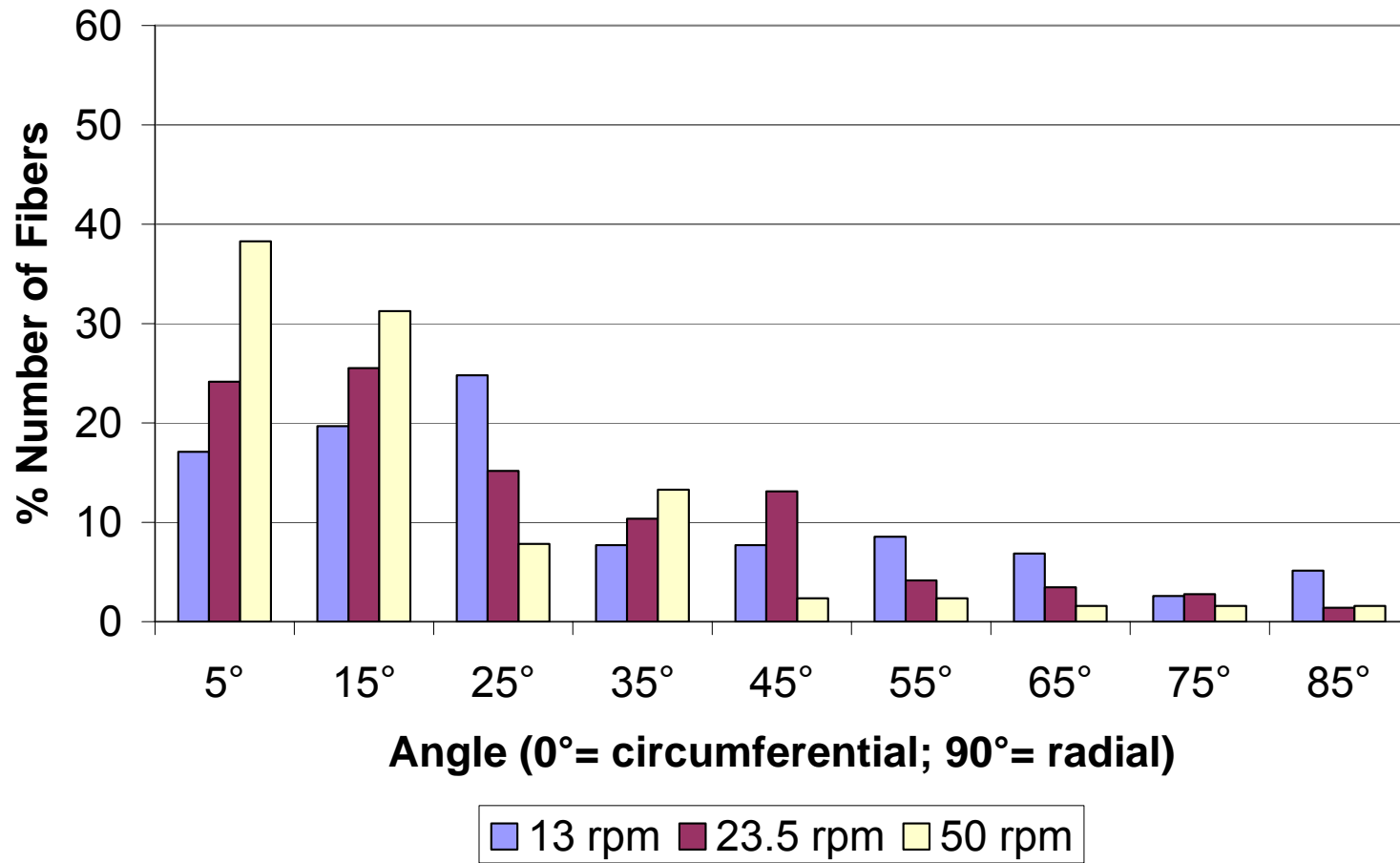


Figure 94: Distribution depending on disc speed at 30cm electrode distance / 10kV electrostatic potential / 4.76mm lay-down rod

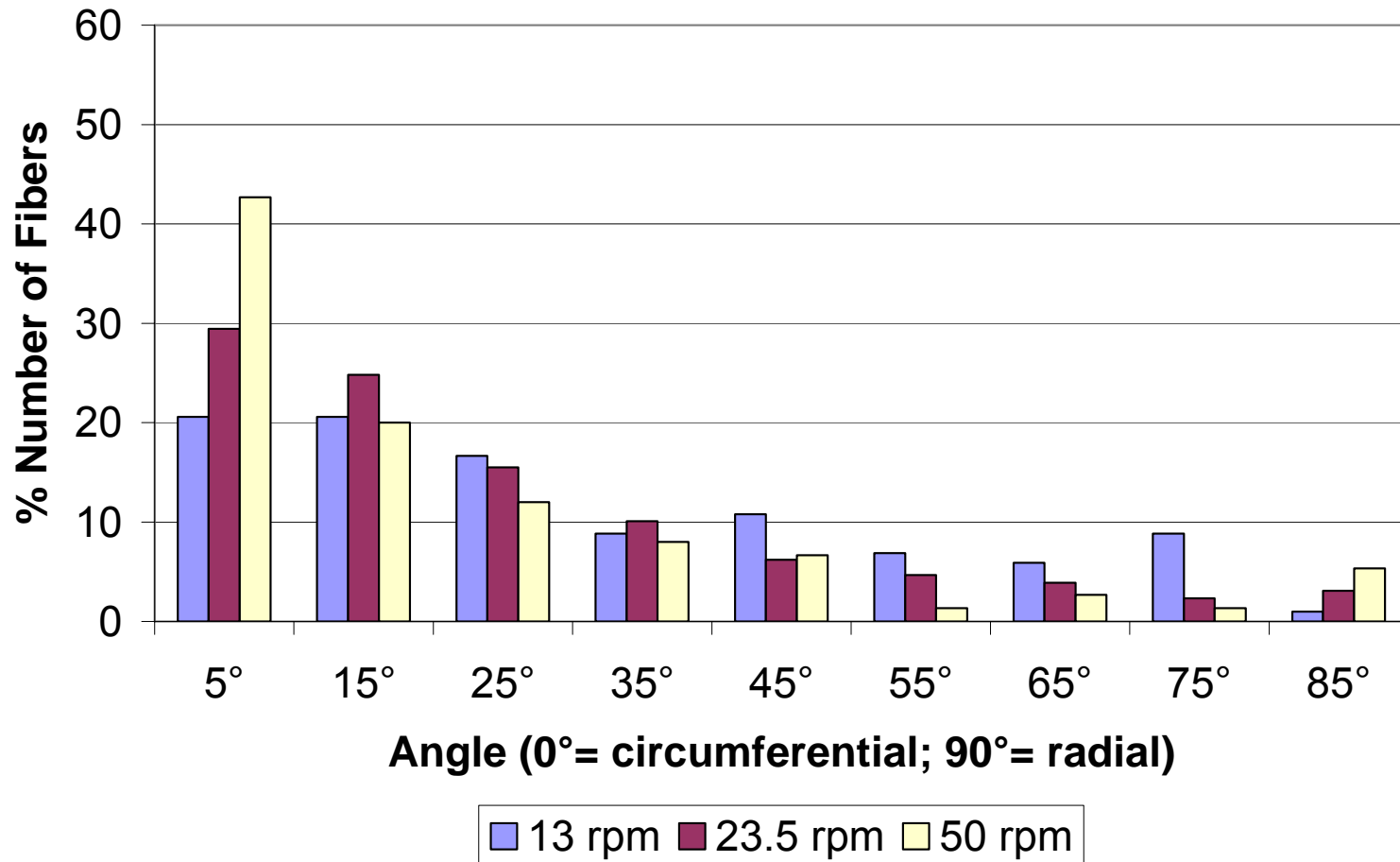


Figure 95: Distribution depending on disc speed at 30cm electrode distance / 20kV electrostatic potential / 4.76mm lay-down rod

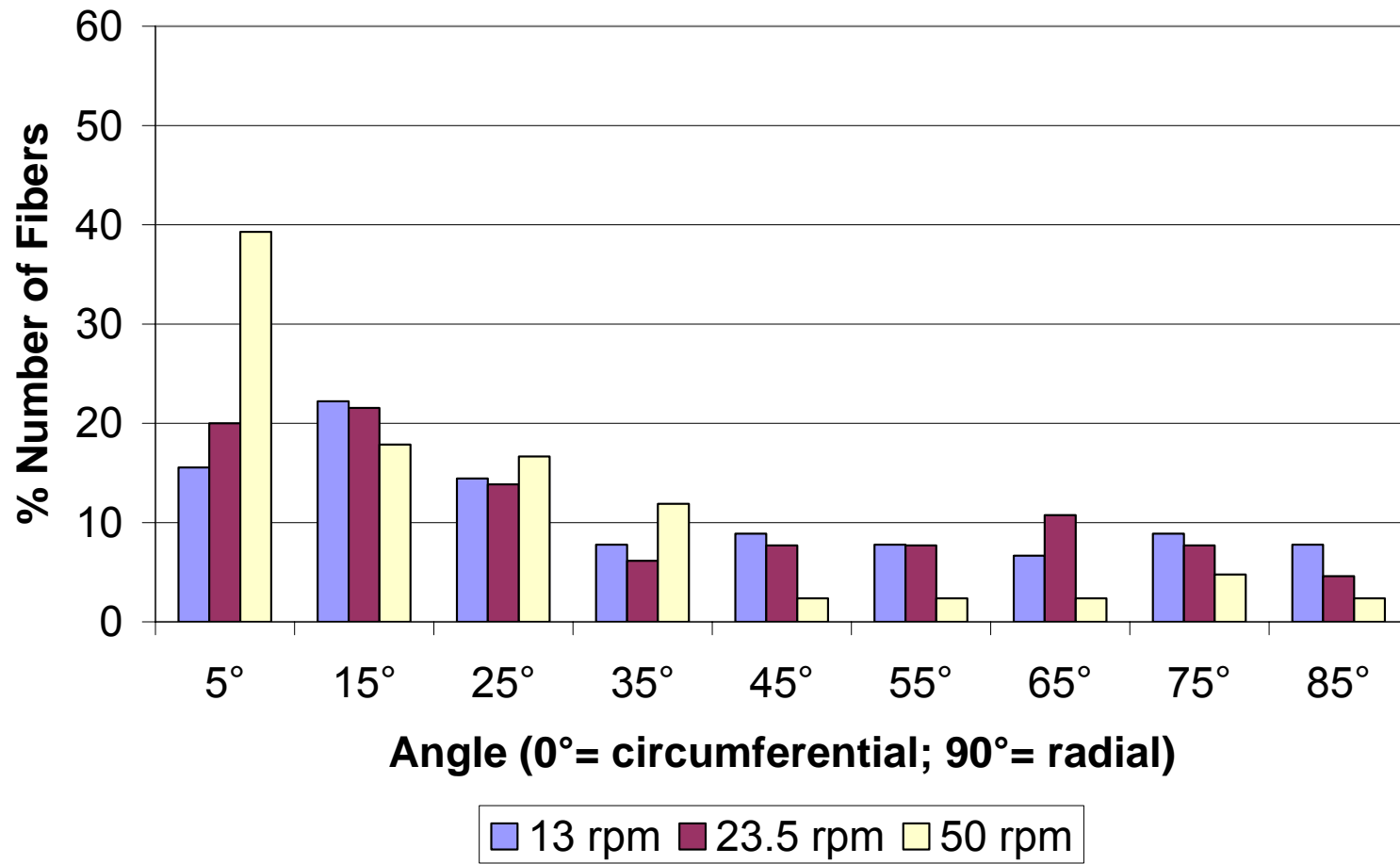


Figure 96: Distribution depending on disc speed at 30cm electrode distance / 50kV electrostatic potential / 4.76mm lay-down rod

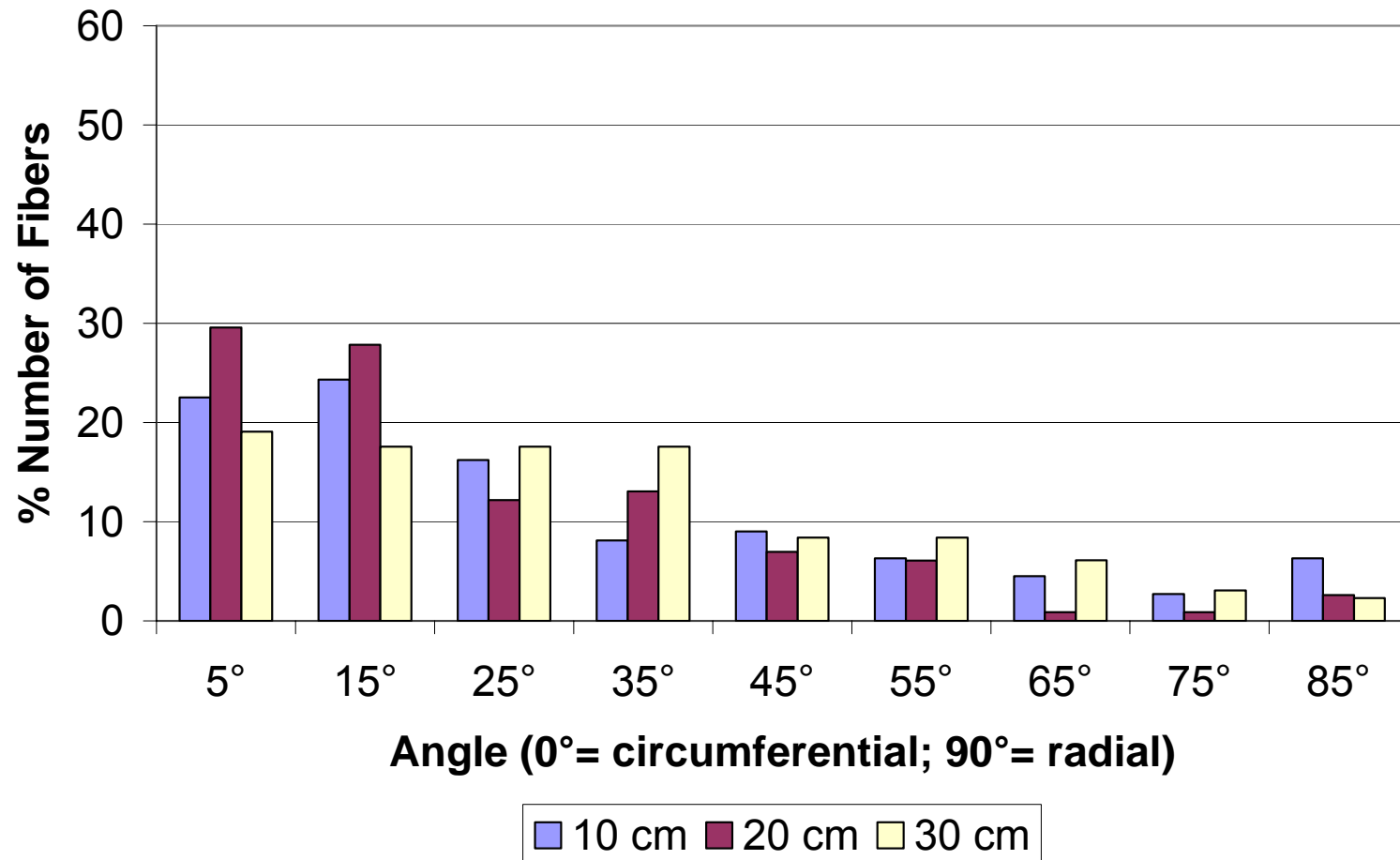


Figure 97: Distribution depending on distance at 13rpm disc speed / 10kV electrostatic potential / 20mm lay-down rod

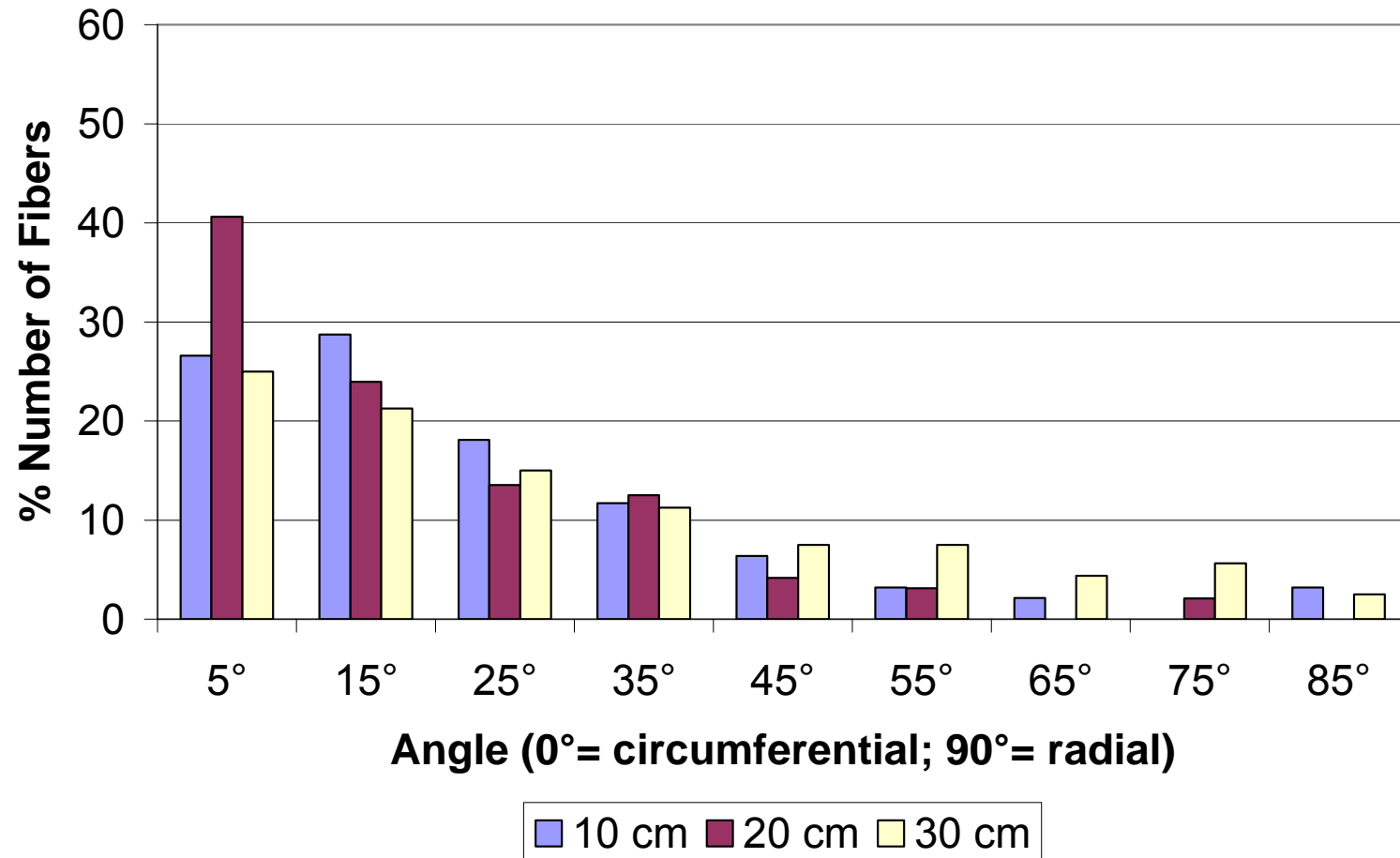


Figure 98: Distribution depending on distance at 23.5rpm disc speed / 10kV electrostatic potential / 20mm lay-down rod

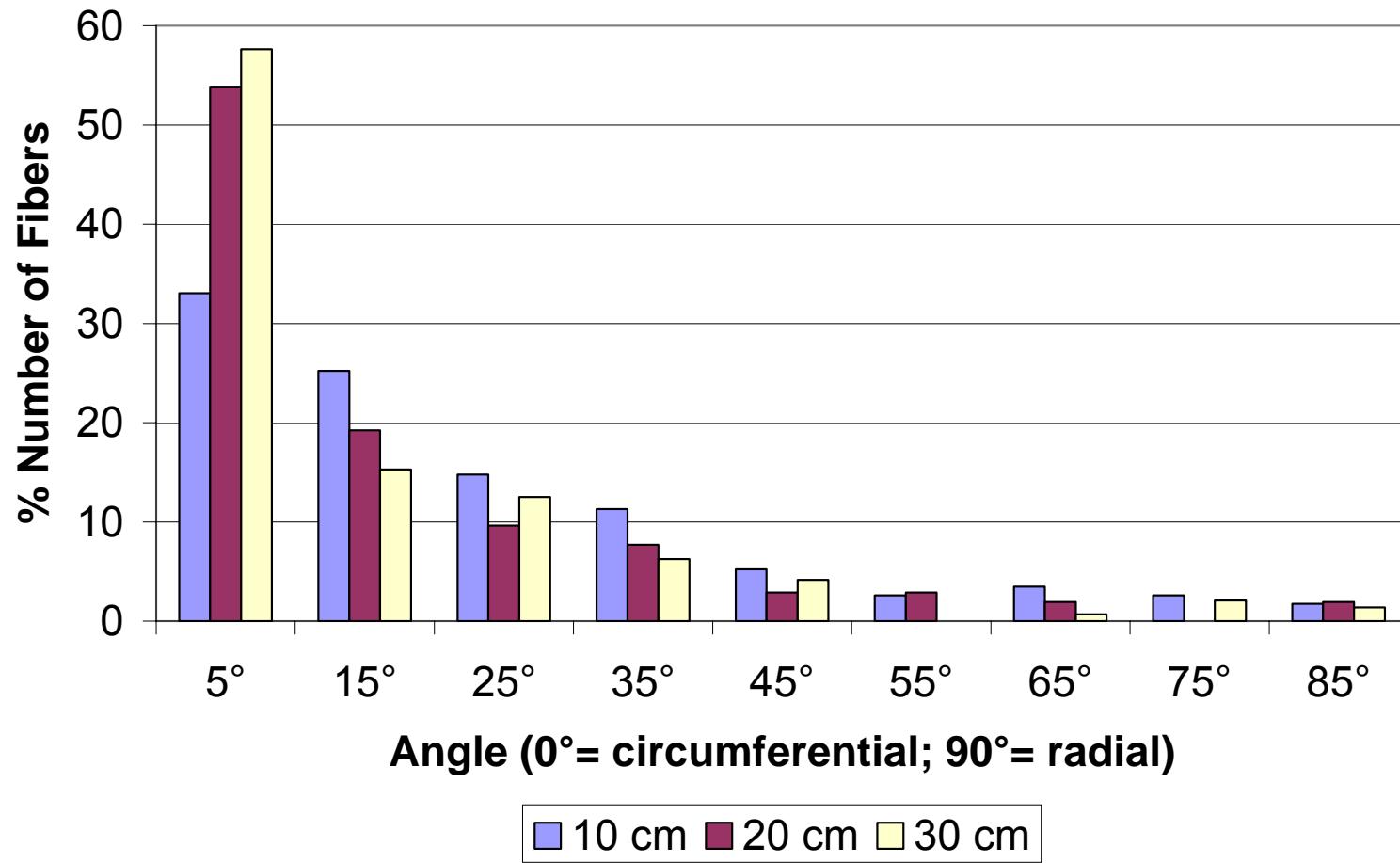


Figure 99: Distribution depending on distance at 50rpm disc speed / 10kV electrostatic potential / 20mm lay-down rod

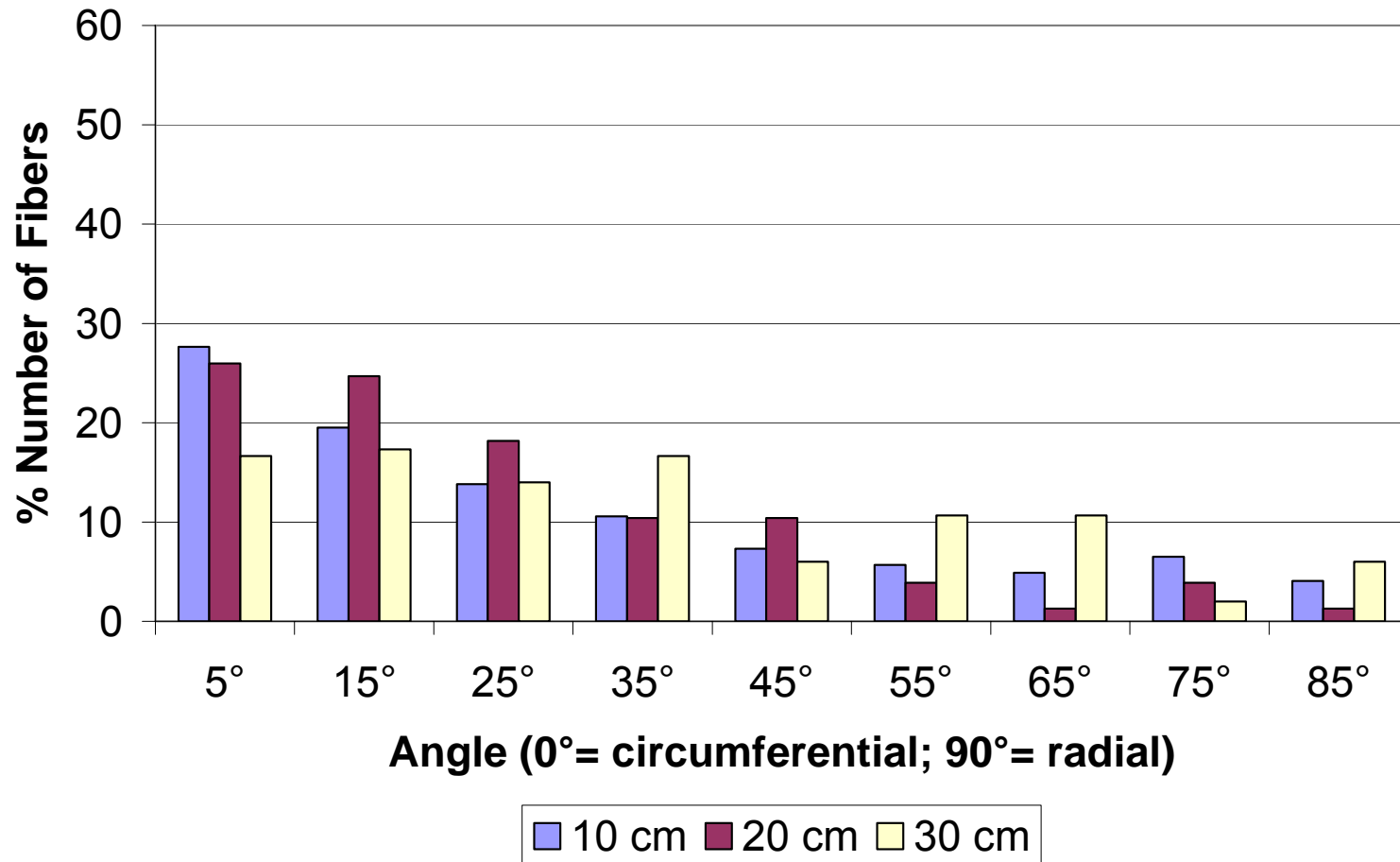


Figure 100: Distribution depending on distance at 13rpm disc speed / 20kV electrostatic potential / 20mm lay-down rod

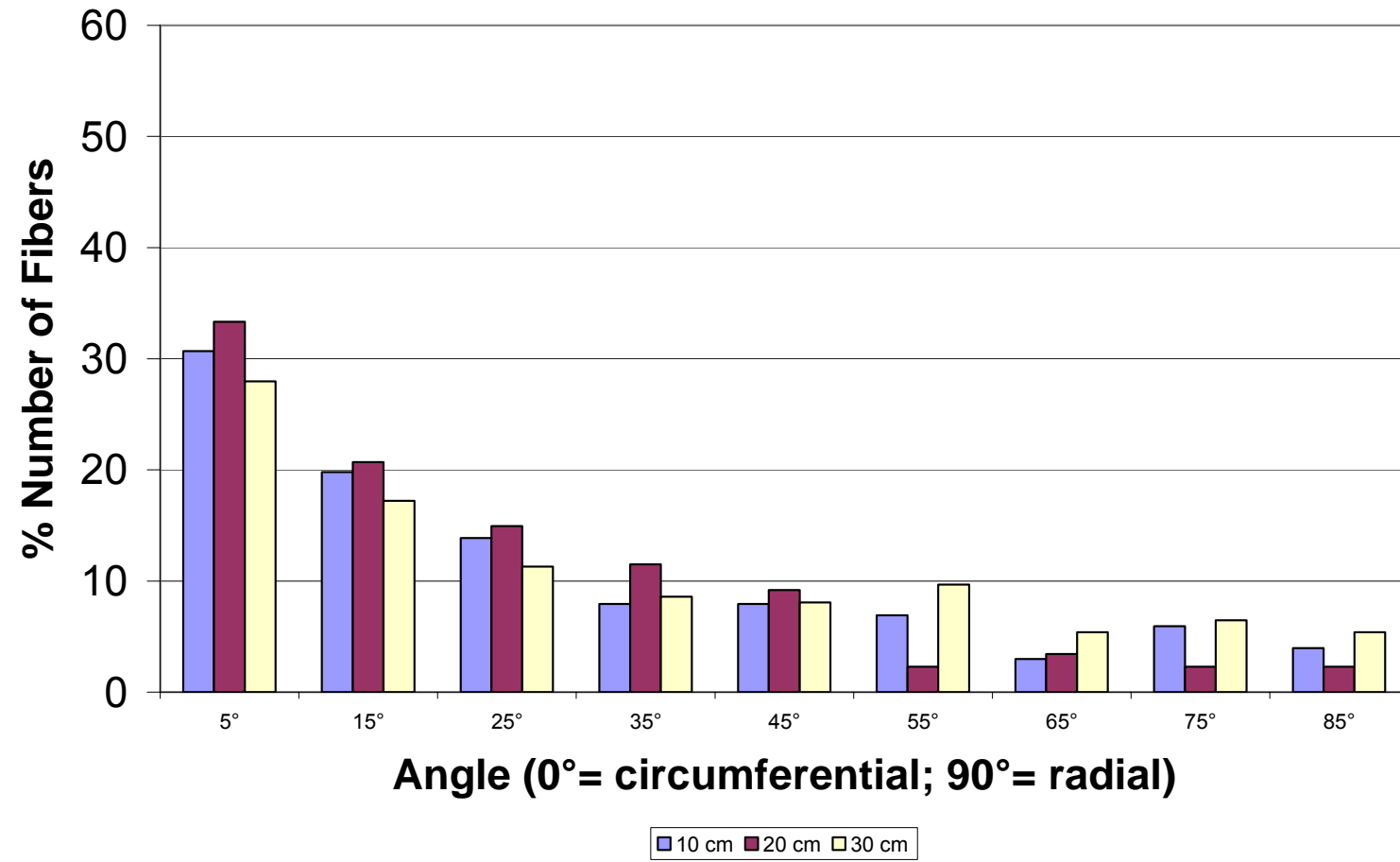


Figure 101: Distribution depending on distance at 23.5rpm disc speed / 20kV electrostatic potential / 20mm lay-down rod

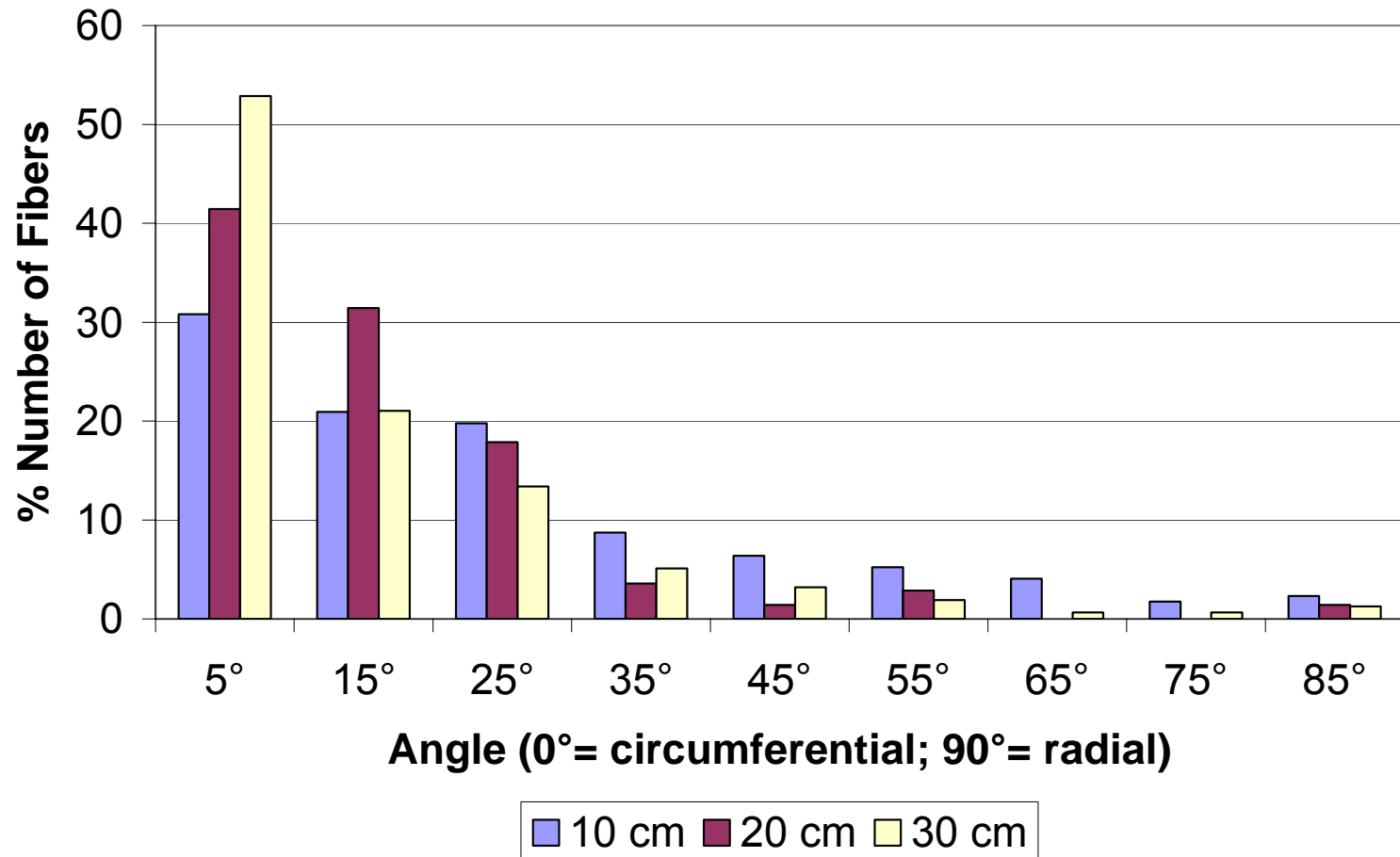


Figure 102: Distribution depending on distance at 50rpm disc speed / 20kV electrostatic potential / 20mm lay-down rod

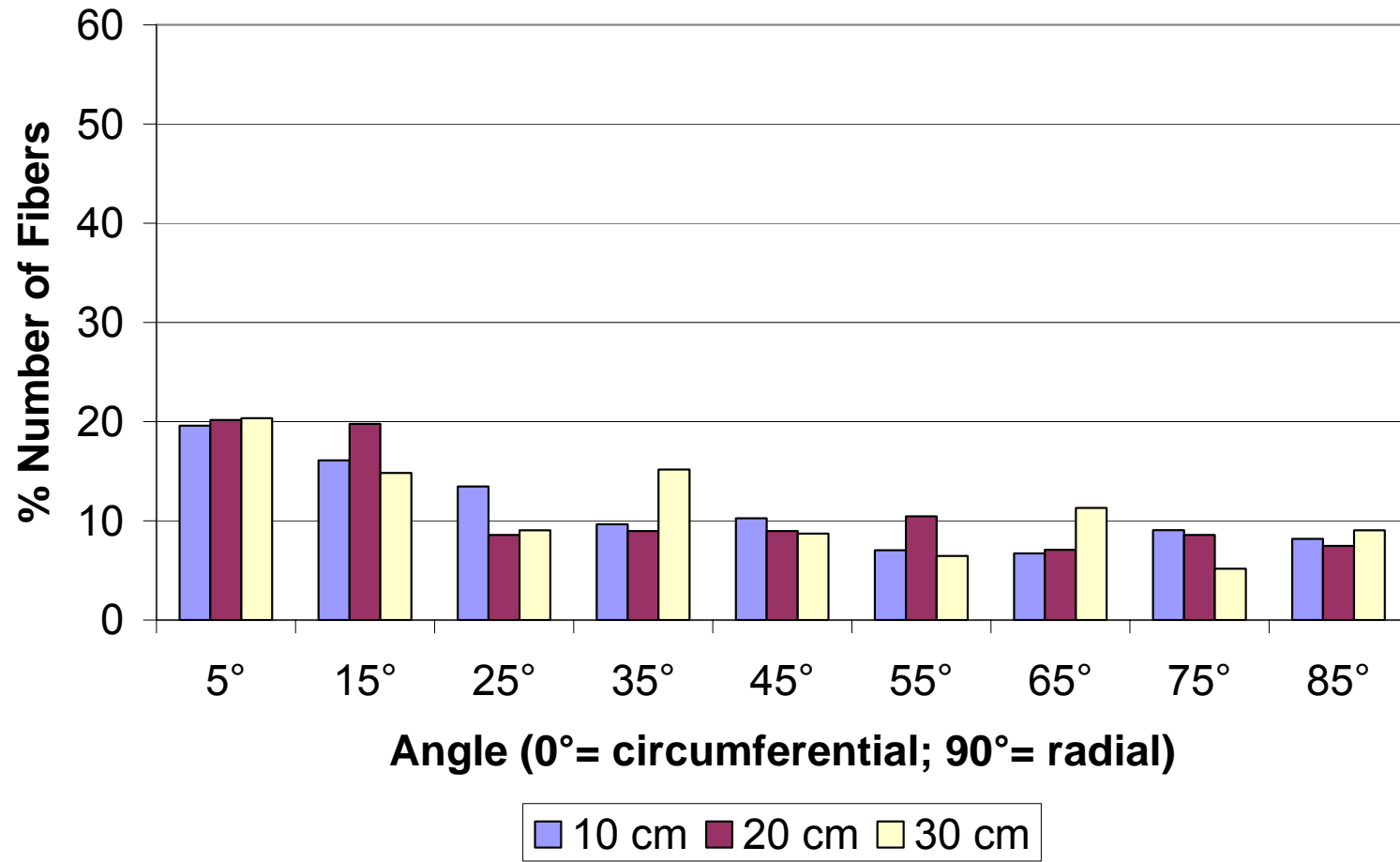


Figure 103: Distribution depending on distance at 13rpm disc speed / 50kV electrostatic potential / 20mm lay-down rod

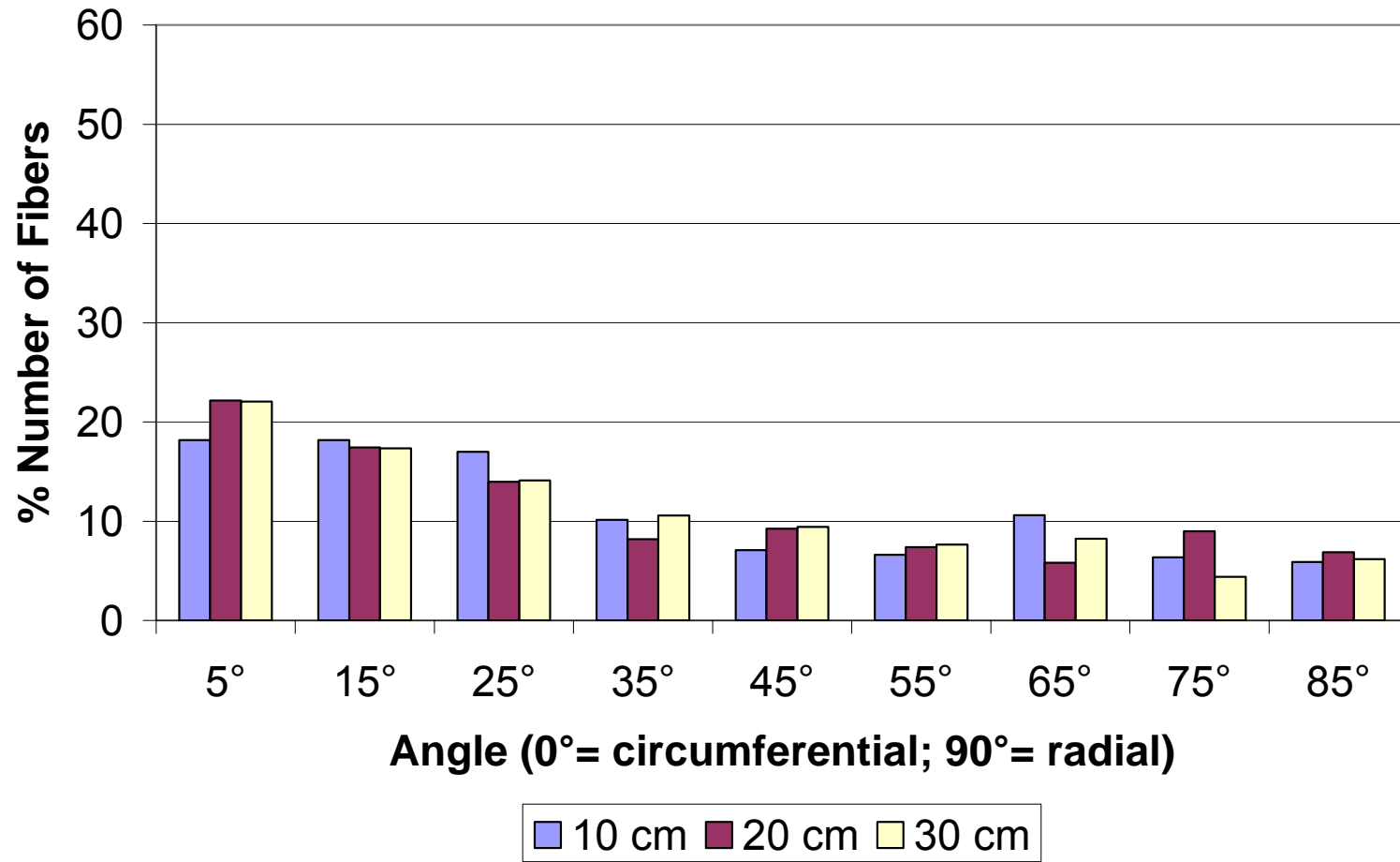


Figure 104: Distribution depending on distance at 23.5rpm disc speed / 50kV electrostatic potential / 20mm lay-down rod

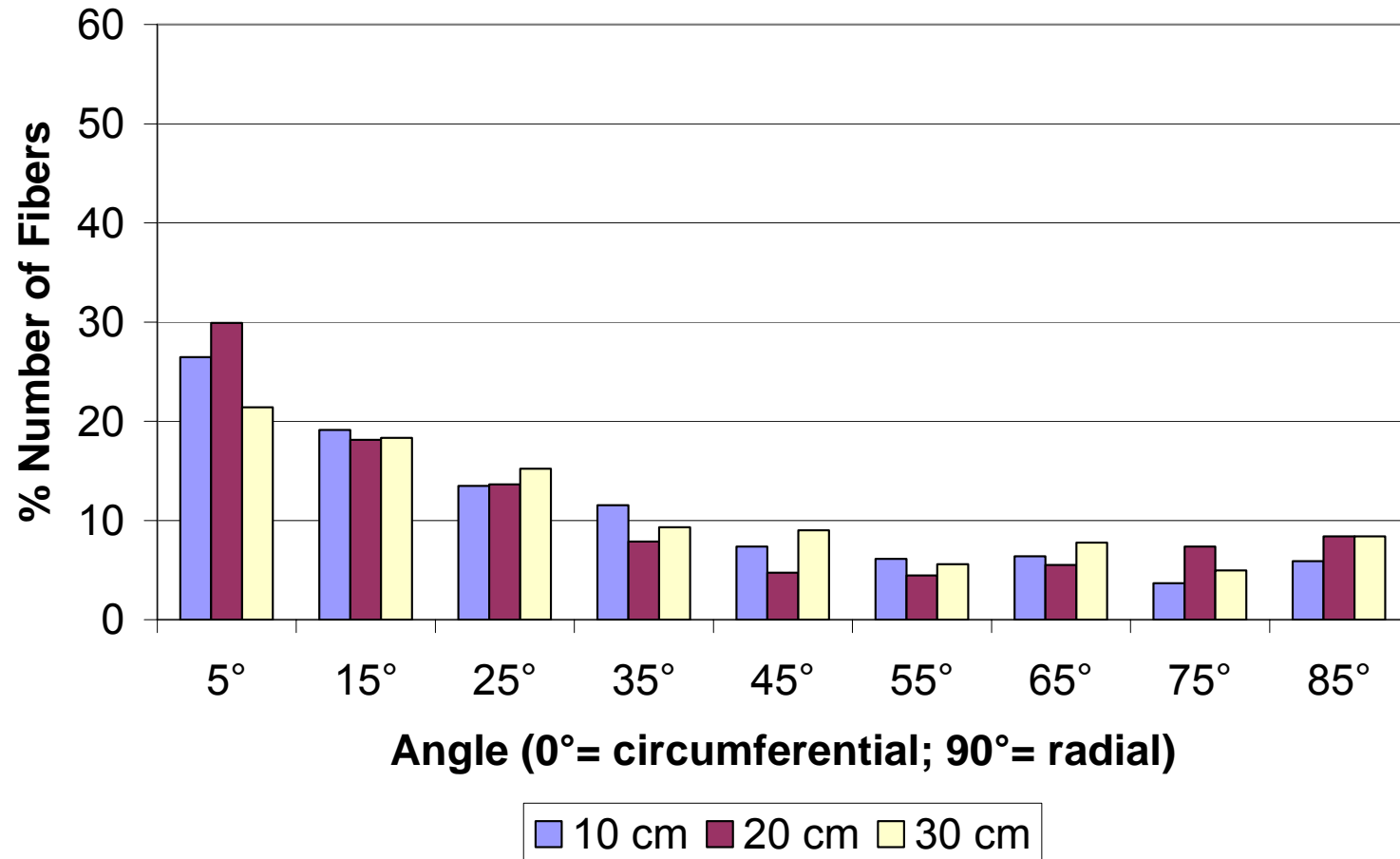


Figure 105: Distribution depending on distance at 50rpm disc speed / 50kV electrostatic potential / 20mm lay-down rod

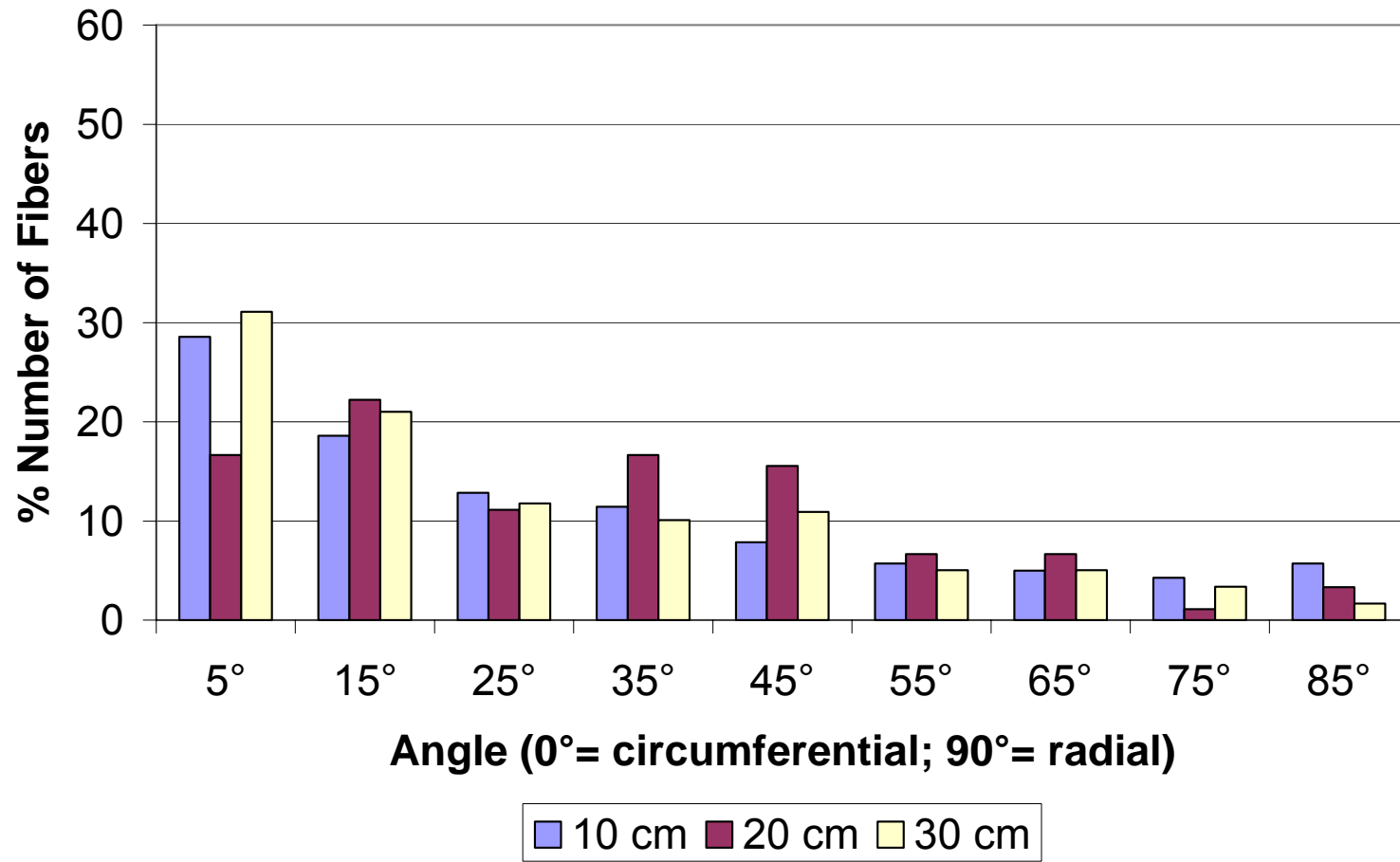


Figure 106: Distribution depending on distance at 13rpm disc speed / 10kV electrostatic potential / 9.4mm lay-down rod

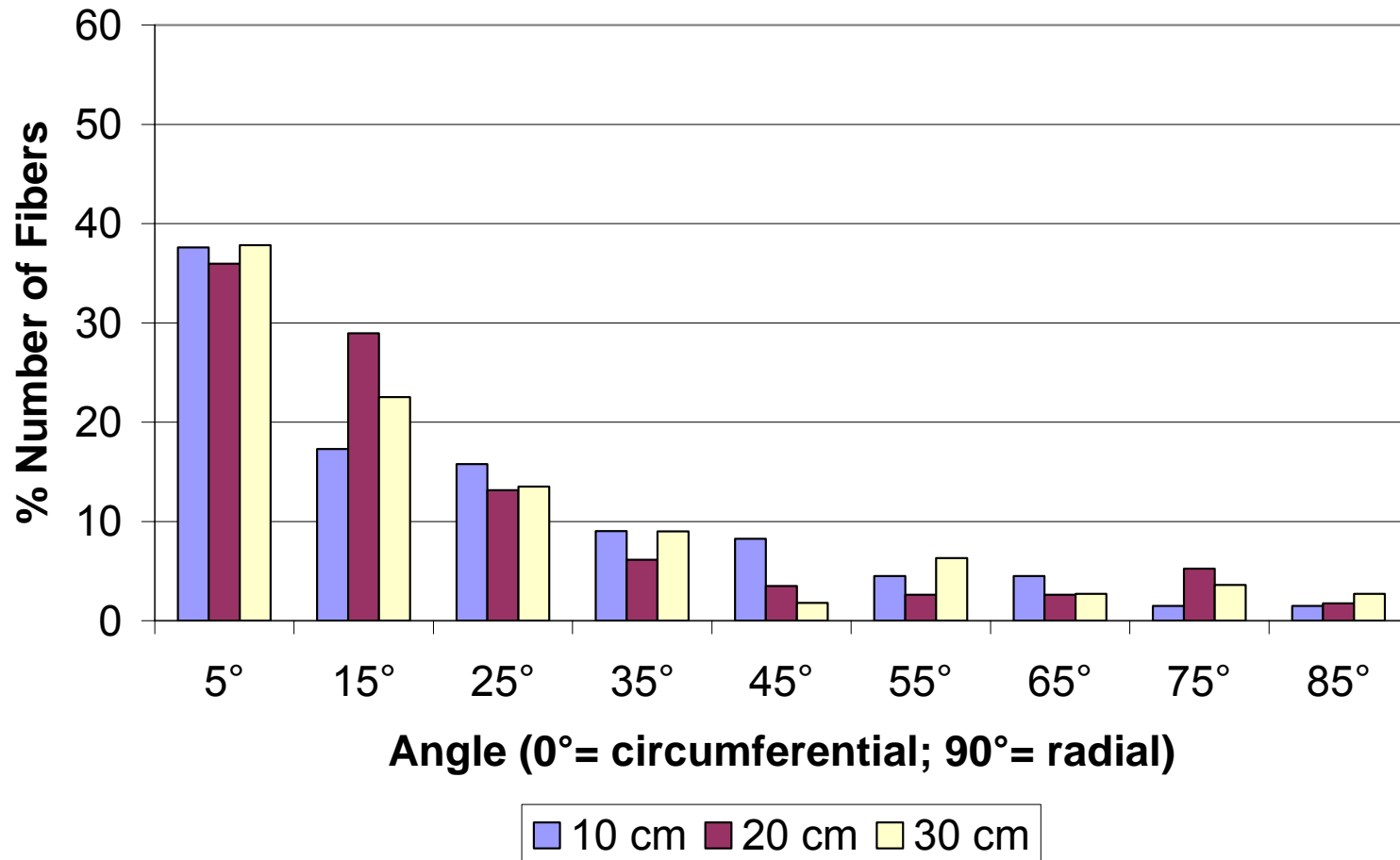


Figure 107: Distribution depending on distance at 23.5rpm disc speed / 10kV electrostatic potential / 9.4mm lay-down rod

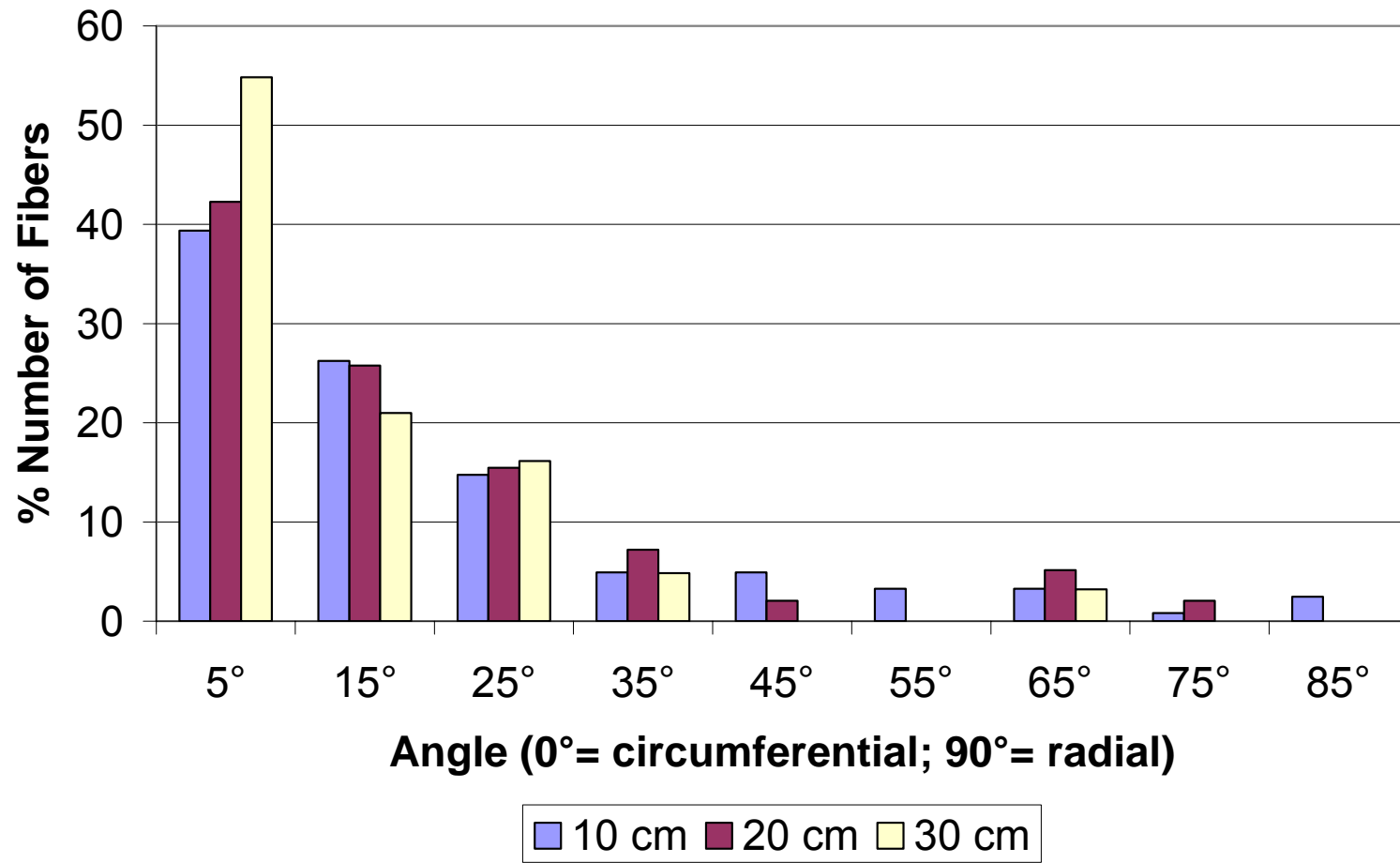


Figure 108: Distribution depending on distance at 50rpm disc speed / 10kV electrostatic potential / 9.4mm lay-down rod

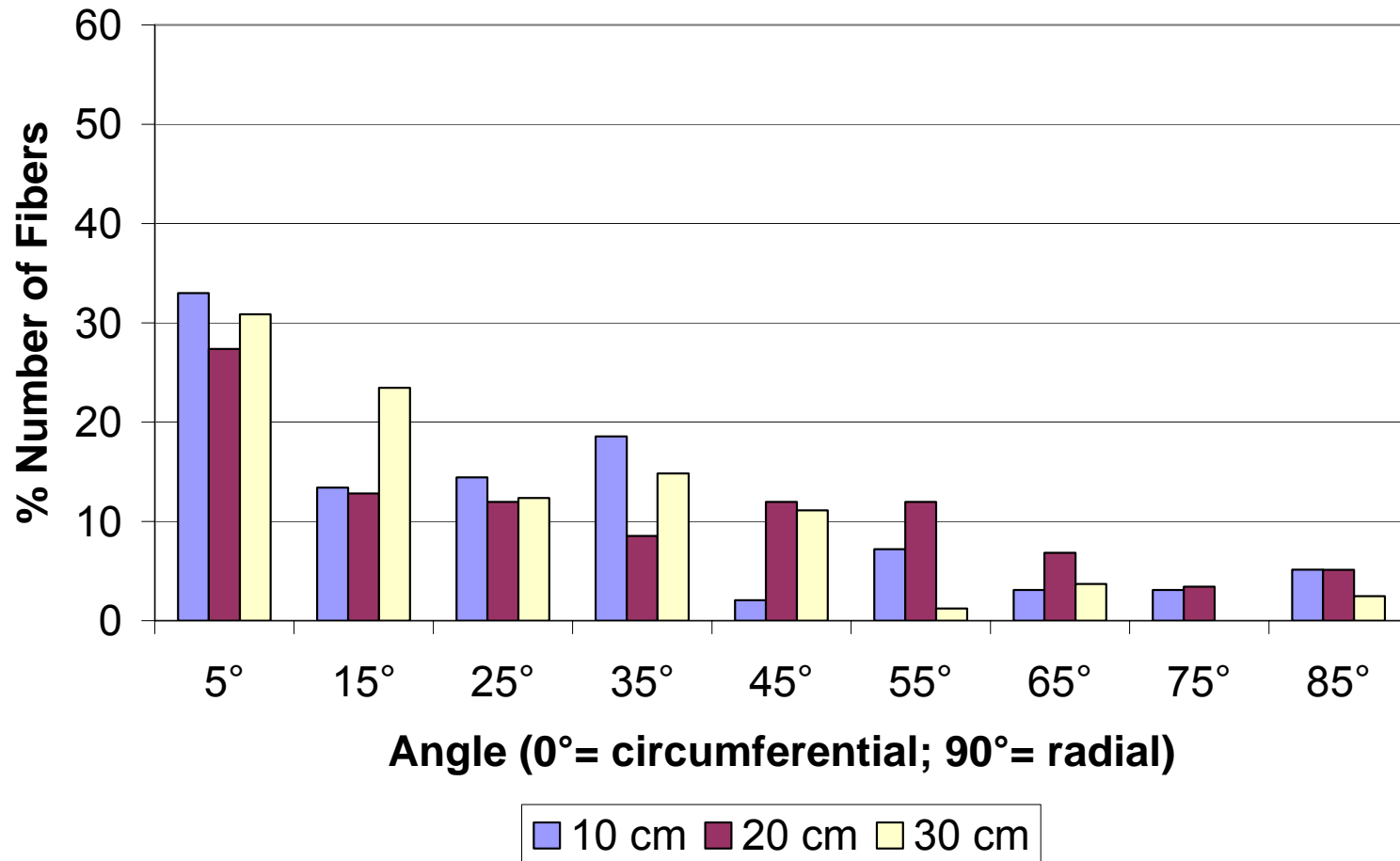


Figure 109: Distribution depending on distance at 13rpm disc speed / 20kV electrostatic potential / 9.4mm lay-down rod

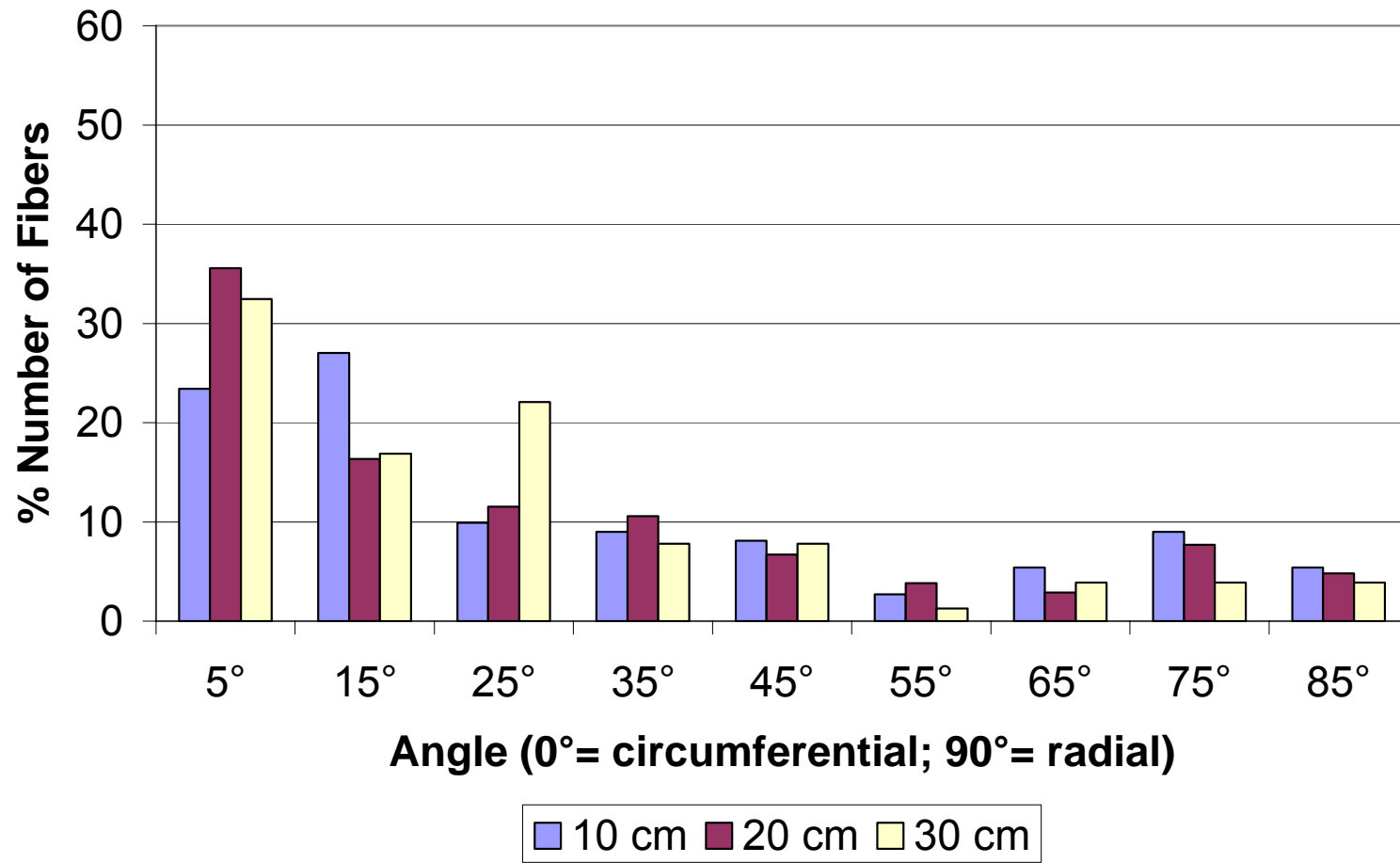


Figure 110: Distribution depending on distance at 23.5rpm disc speed / 20kV electrostatic potential / 9.4mm lay-down rod

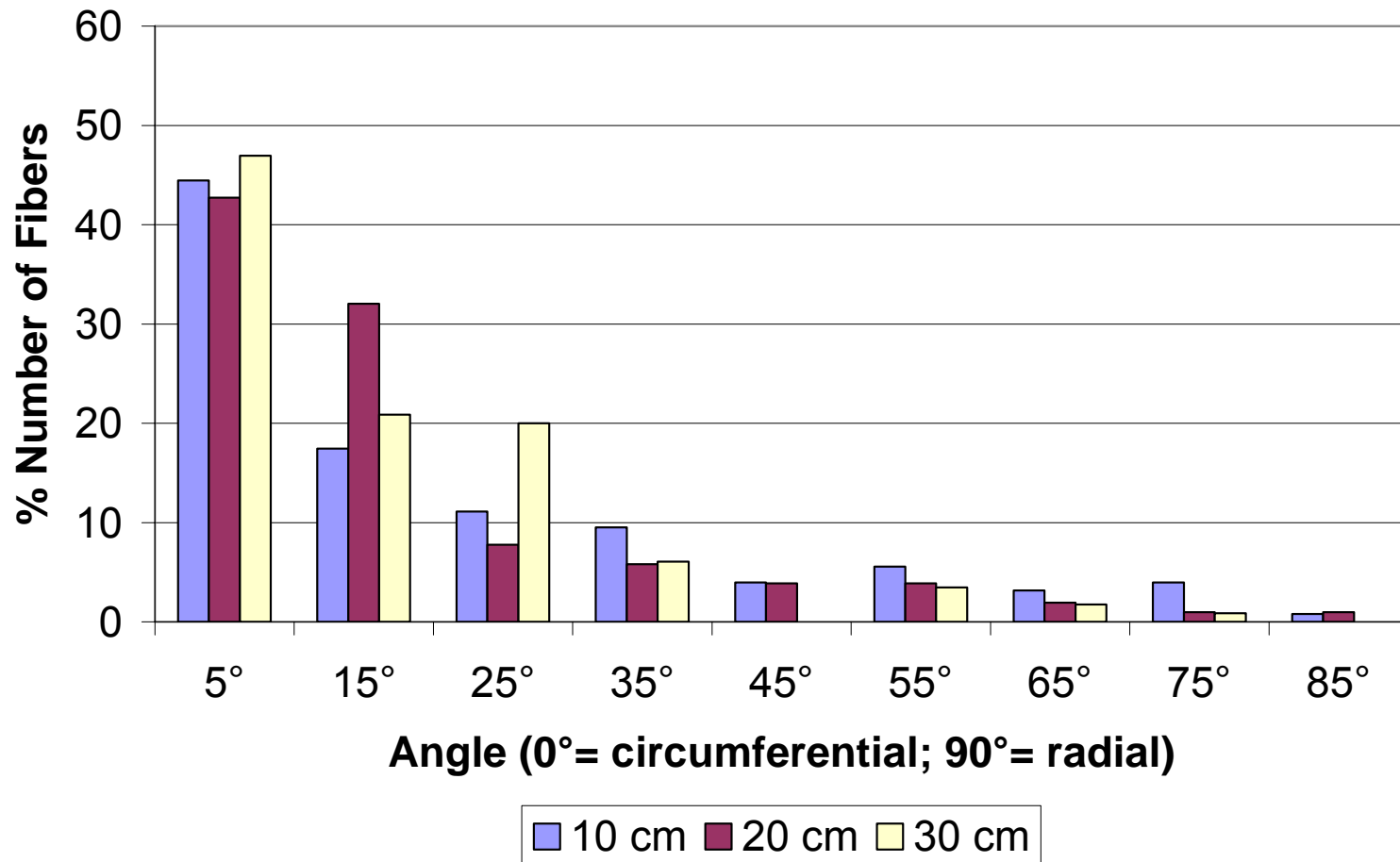


Figure 111: Distribution depending on distance at 50rpm disc speed / 20kV electrostatic potential / 9.4mm lay-down rod

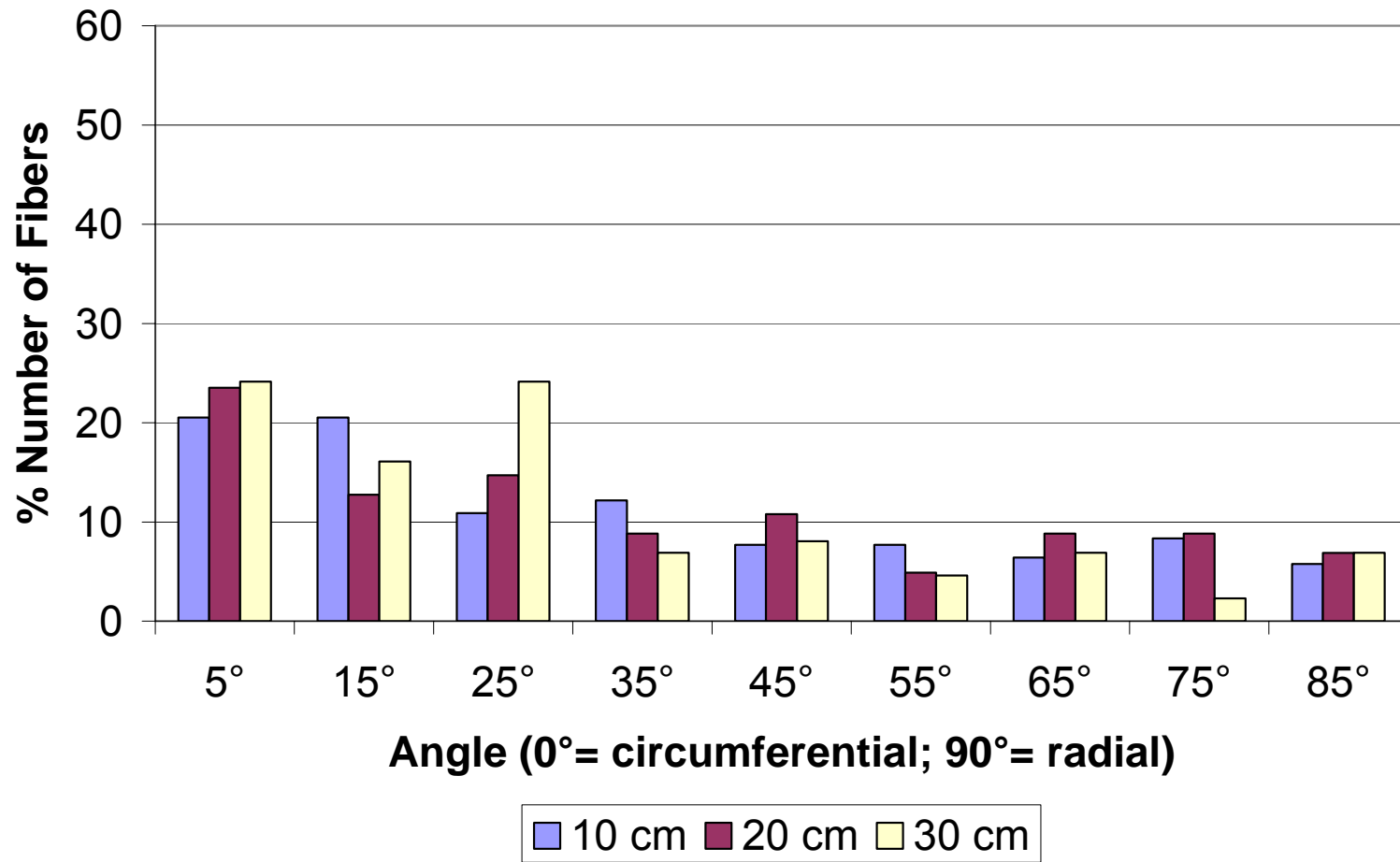


Figure 112: Distribution depending on distance at 13rpm disc speed / 50kV electrostatic potential / 9.4mm lay-down rod

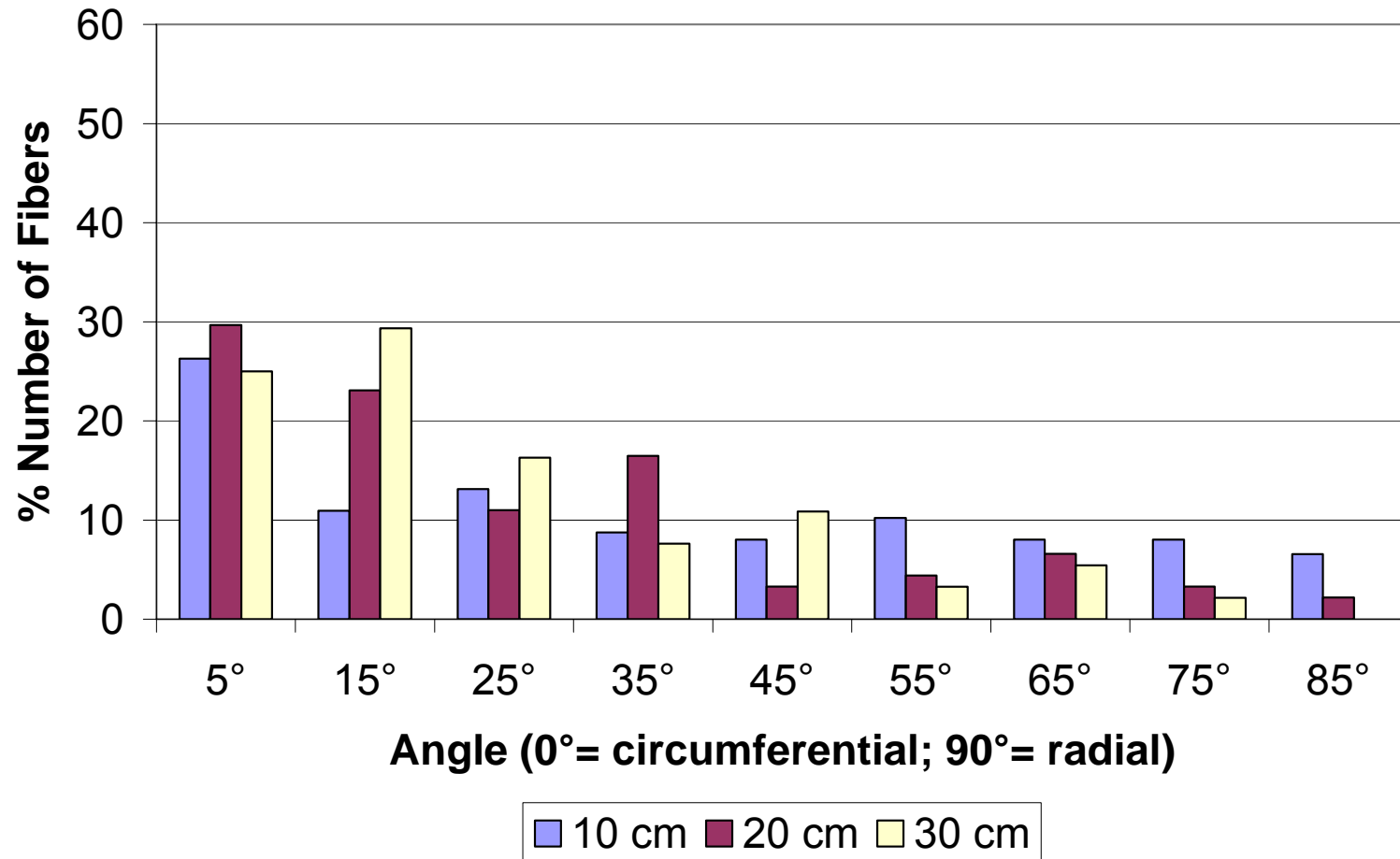


Figure 113: Distribution depending on distance at 23.5rpm disc speed / 50kV electrostatic potential / 9.4mm lay-down rod

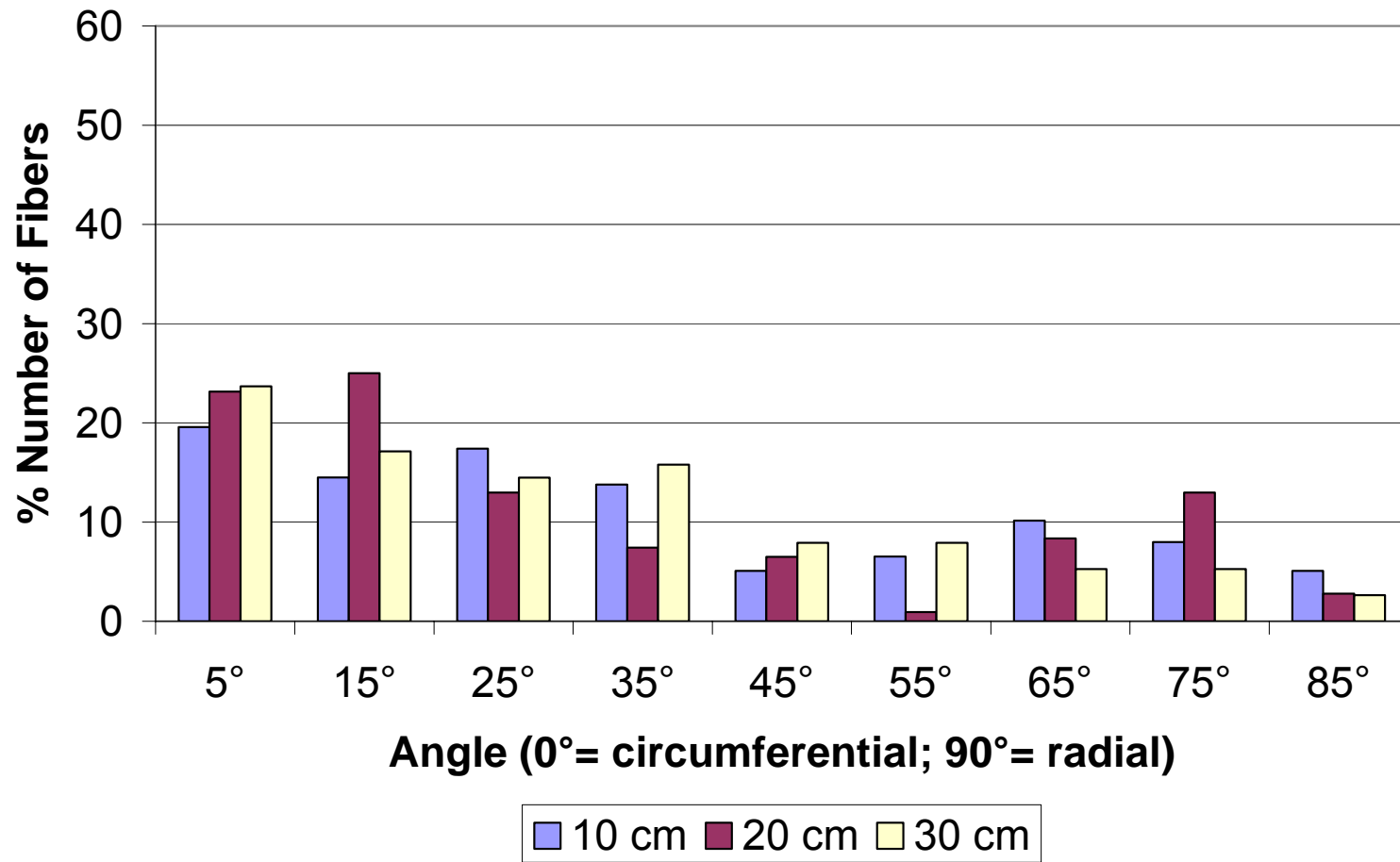


Figure 114: Distribution depending on distance at 50rpm disc speed / 50kV electrostatic potential / 9.4mm lay-down rod

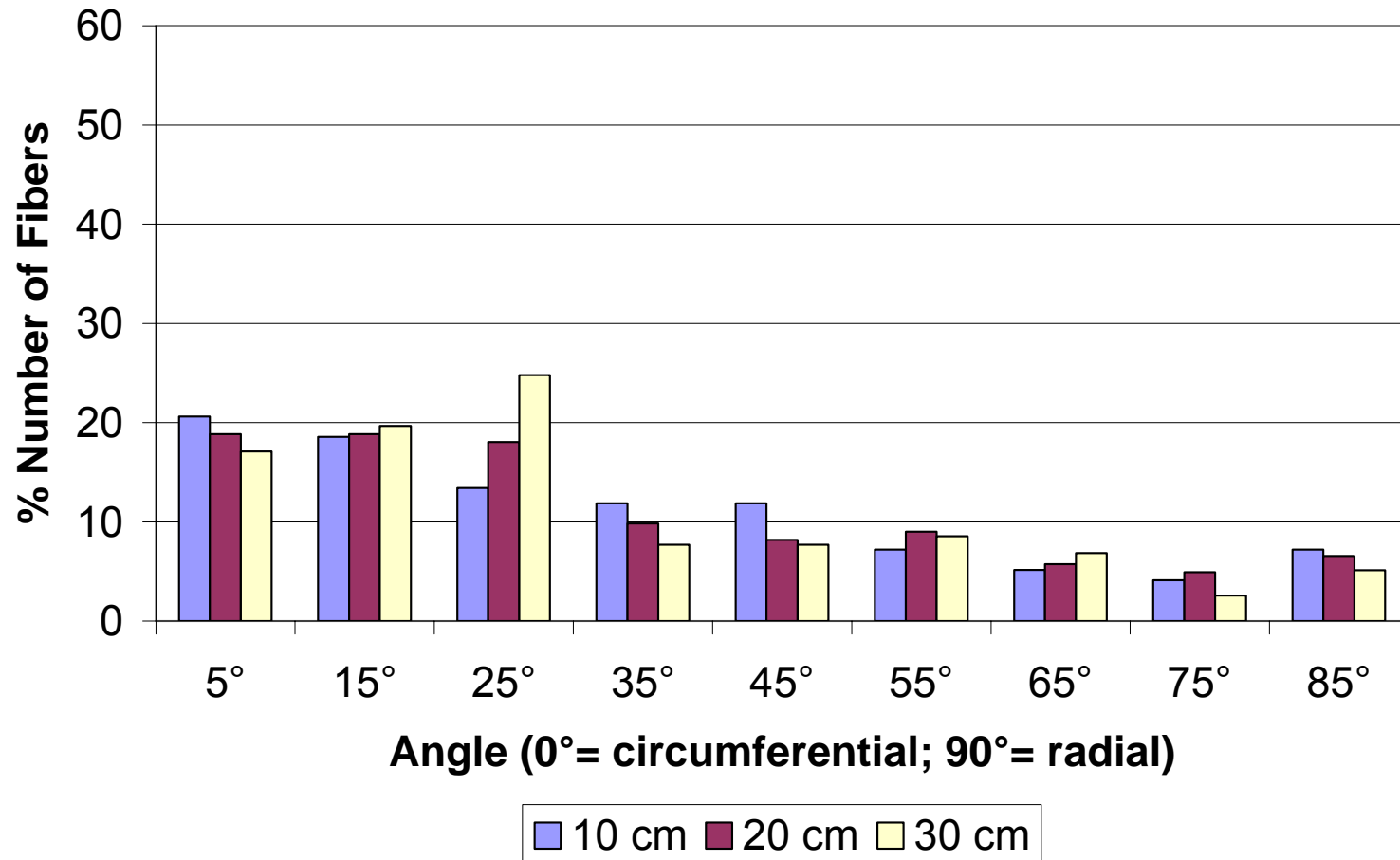


Figure 115: Distribution depending on distance at 13rpm disc speed / 10kV electrostatic potential / 4.76mm lay-down rod

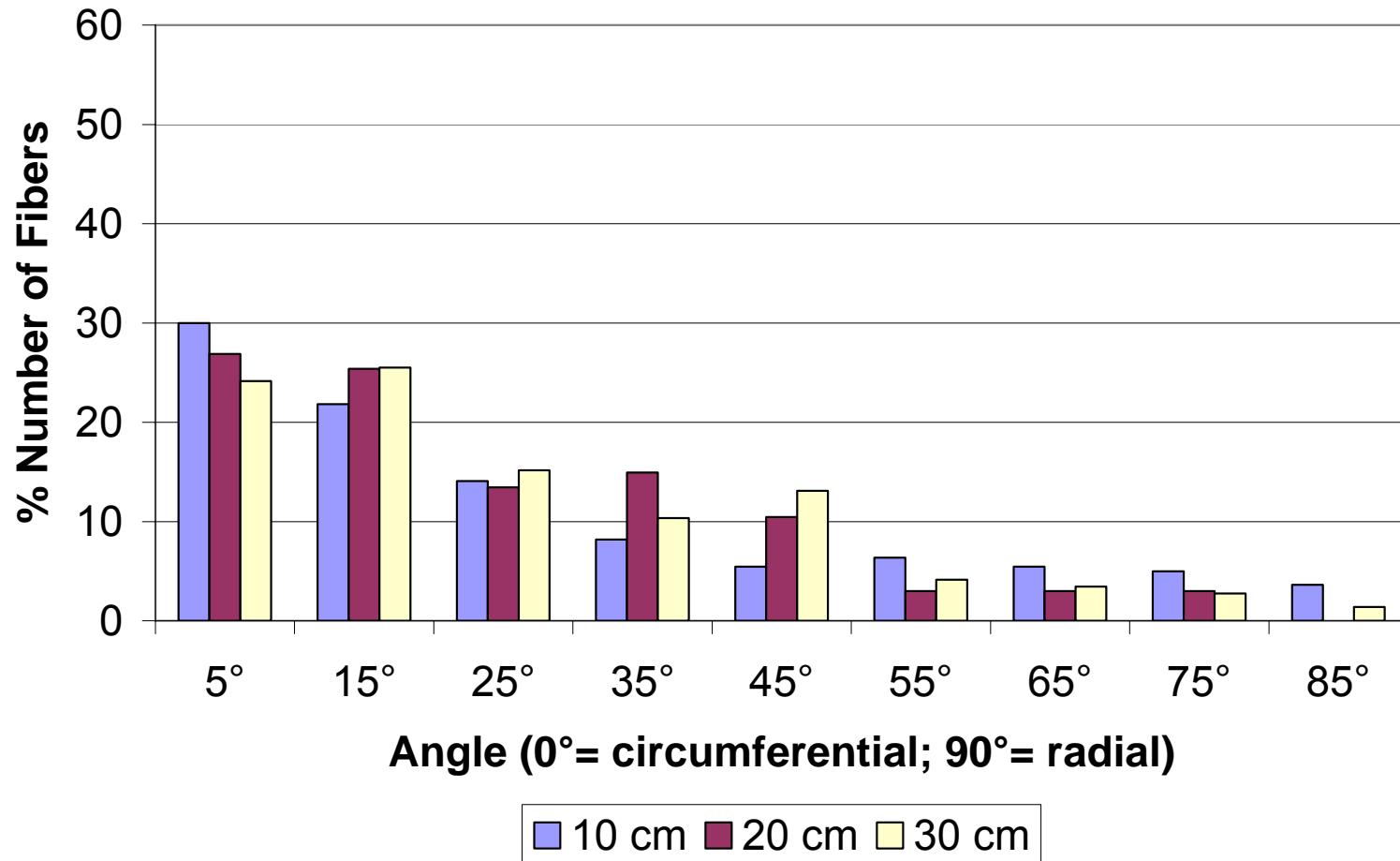


Figure 116: Distribution depending on distance at 23.5rpm disc speed / 10kV electrostatic potential / 4.76mm lay-down rod

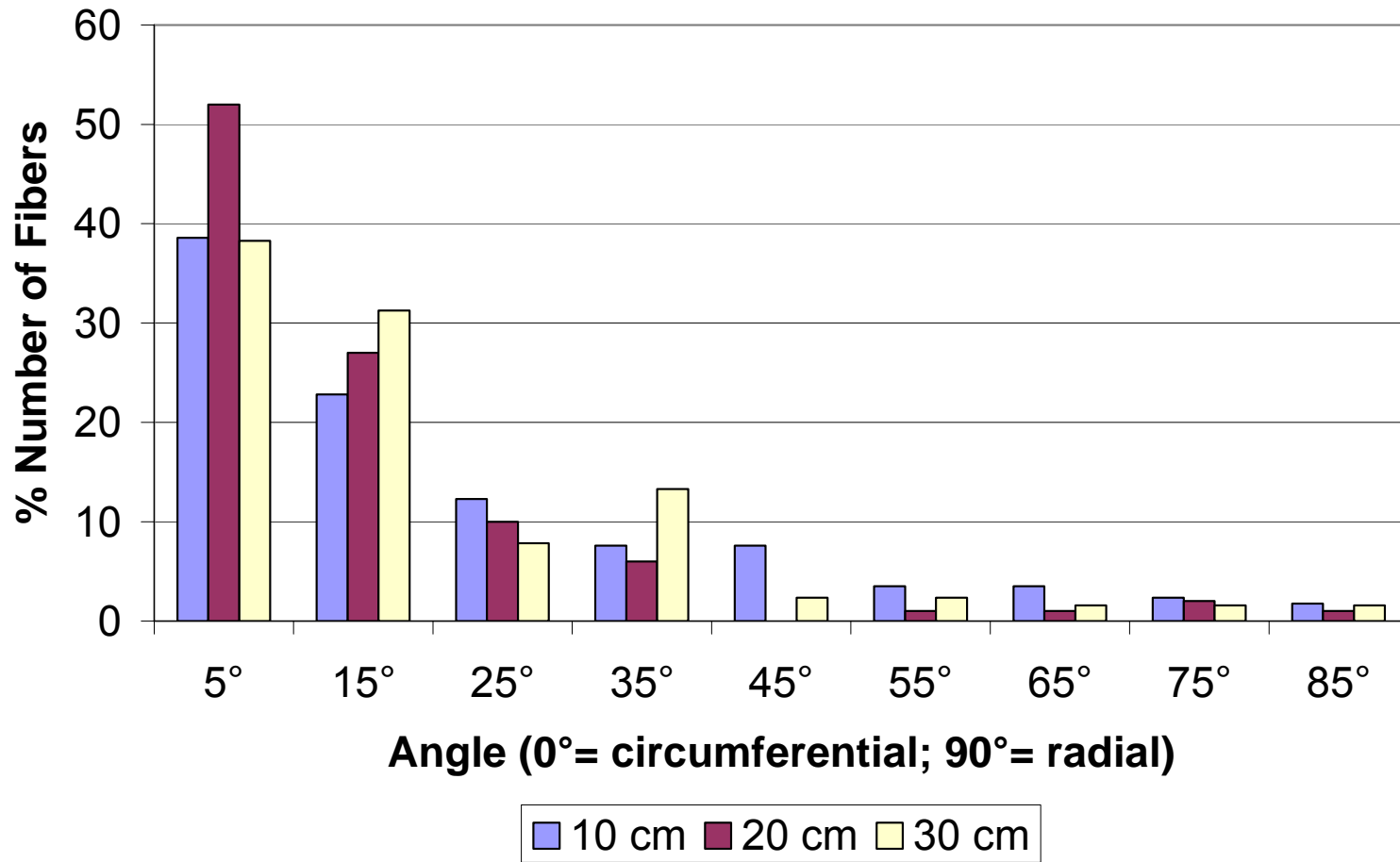


Figure 117: Distribution depending on distance at 50rpm disc speed / 10kV electrostatic potential / 4.76mm lay-down rod

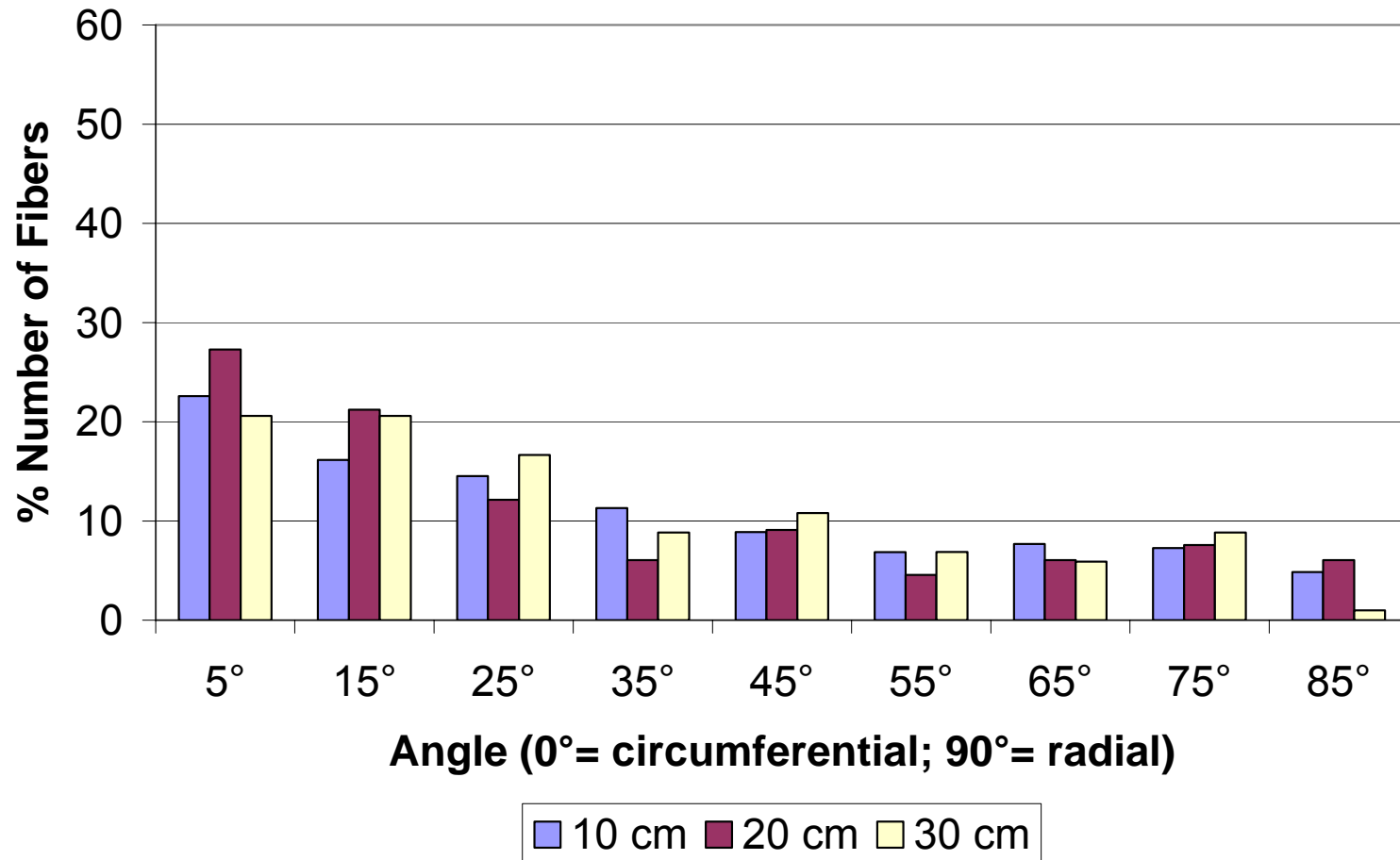


Figure 118: Distribution depending on distance at 13rpm disc speed / 20kV electrostatic potential / 4.76mm lay-down rod

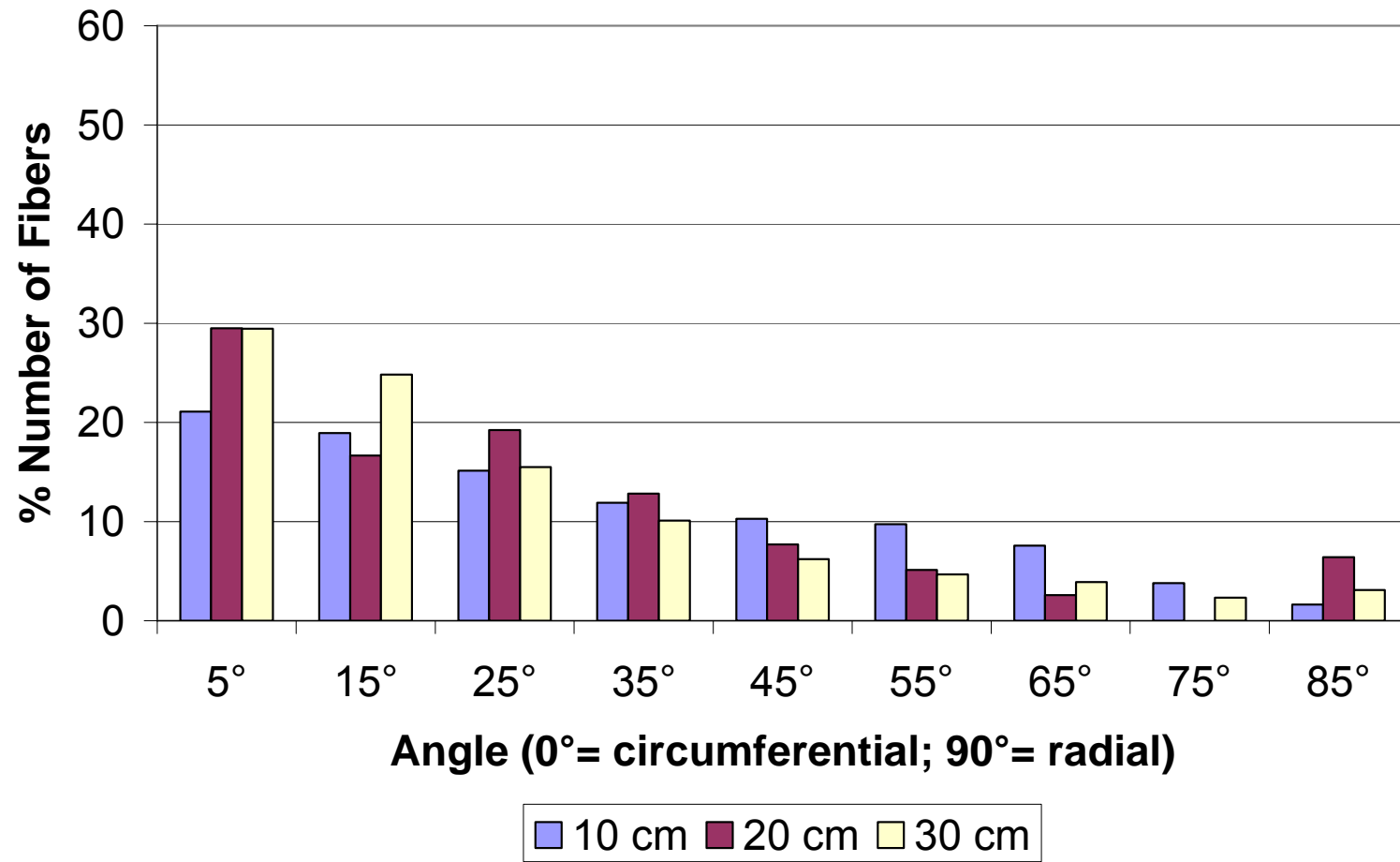


Figure 119: Distribution depending on distance at 23.5rpm disc speed / 20kV electrostatic potential / 4.76mm lay-down rod

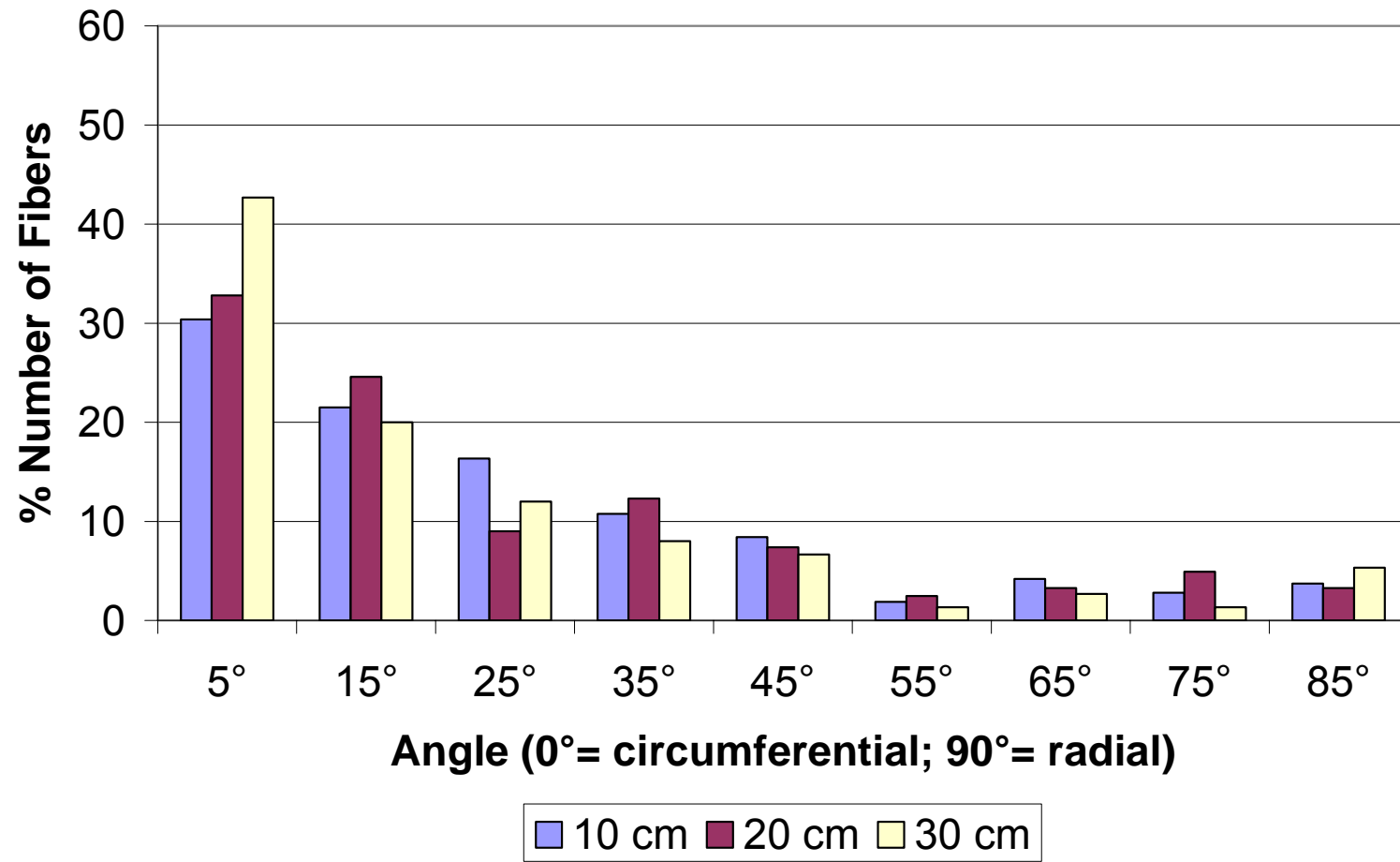


Figure 120: Distribution depending on distance at 50rpm disc speed / 20kV electrostatic potential / 4.76mm lay-down rod

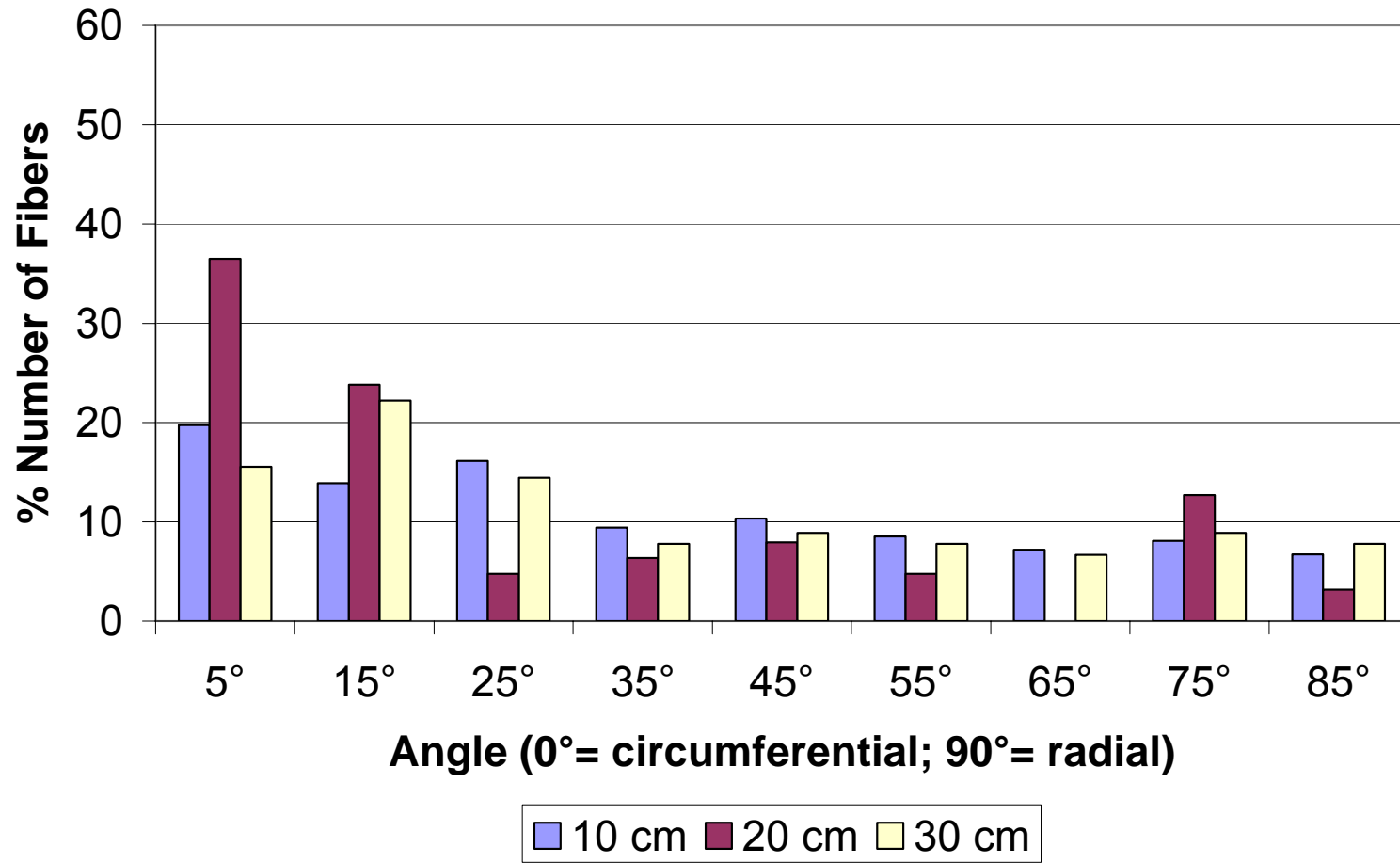


Figure 121: Distribution depending on distance at 13rpm disc speed / 50kV electrostatic potential / 4.76mm lay-down rod

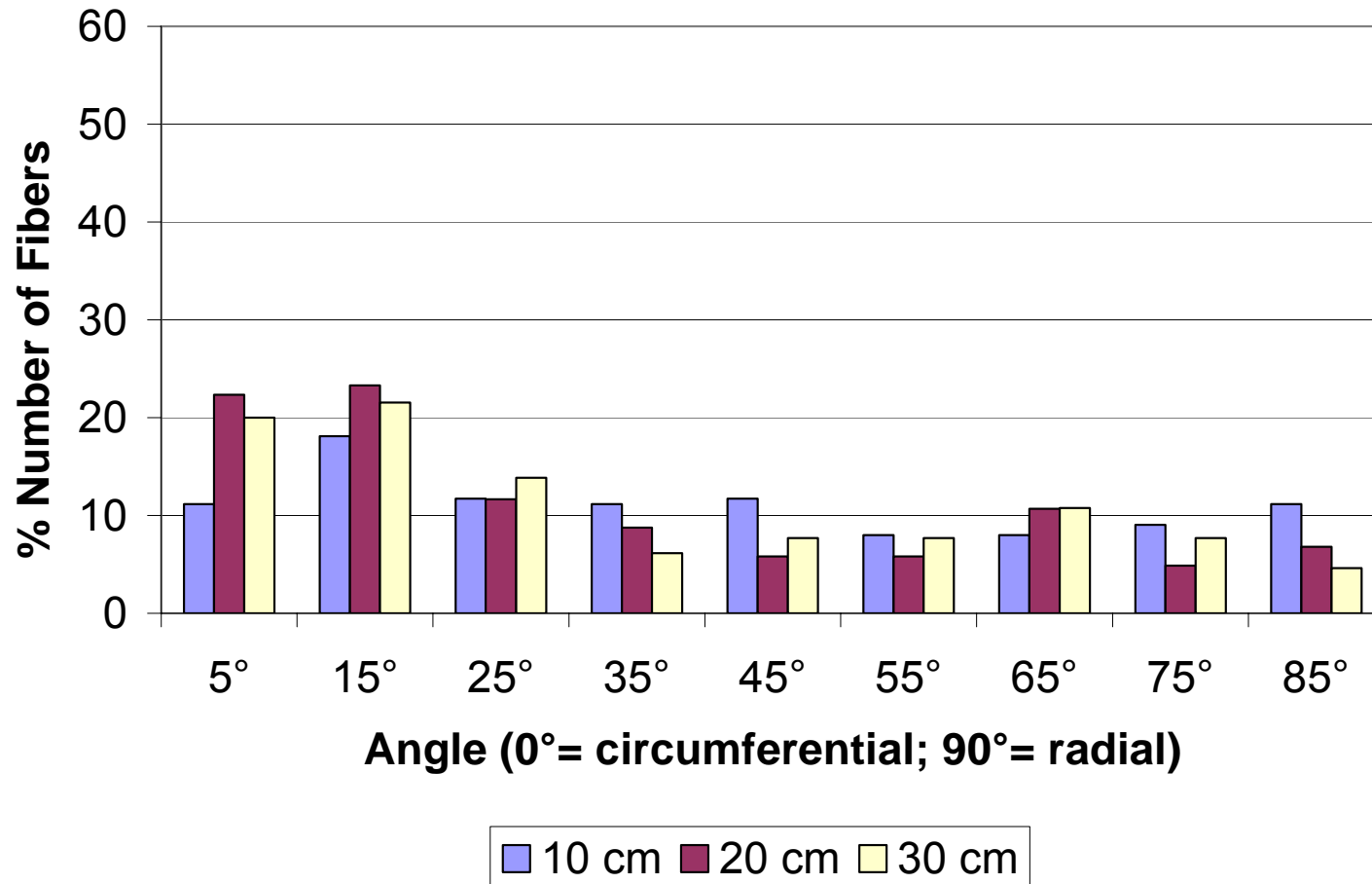


Figure 122: Distribution depending on distance at 23.5rpm disc speed / 50kV electrostatic potential / 4.76mm lay-down rod

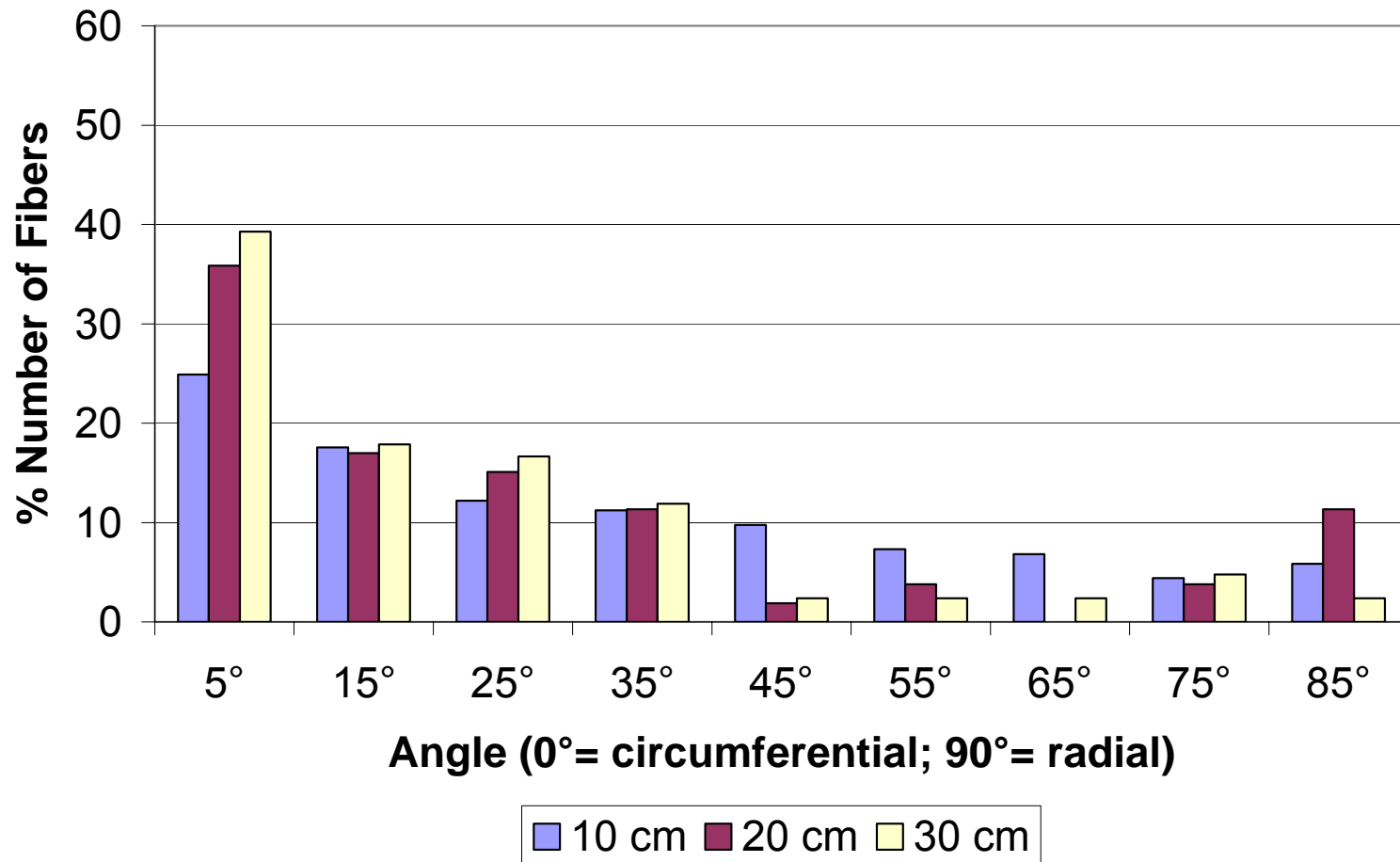


Figure 123: Distribution depending on distance at 50rpm disc speed / 50kV electrostatic potential / 4.76mm lay-down rod

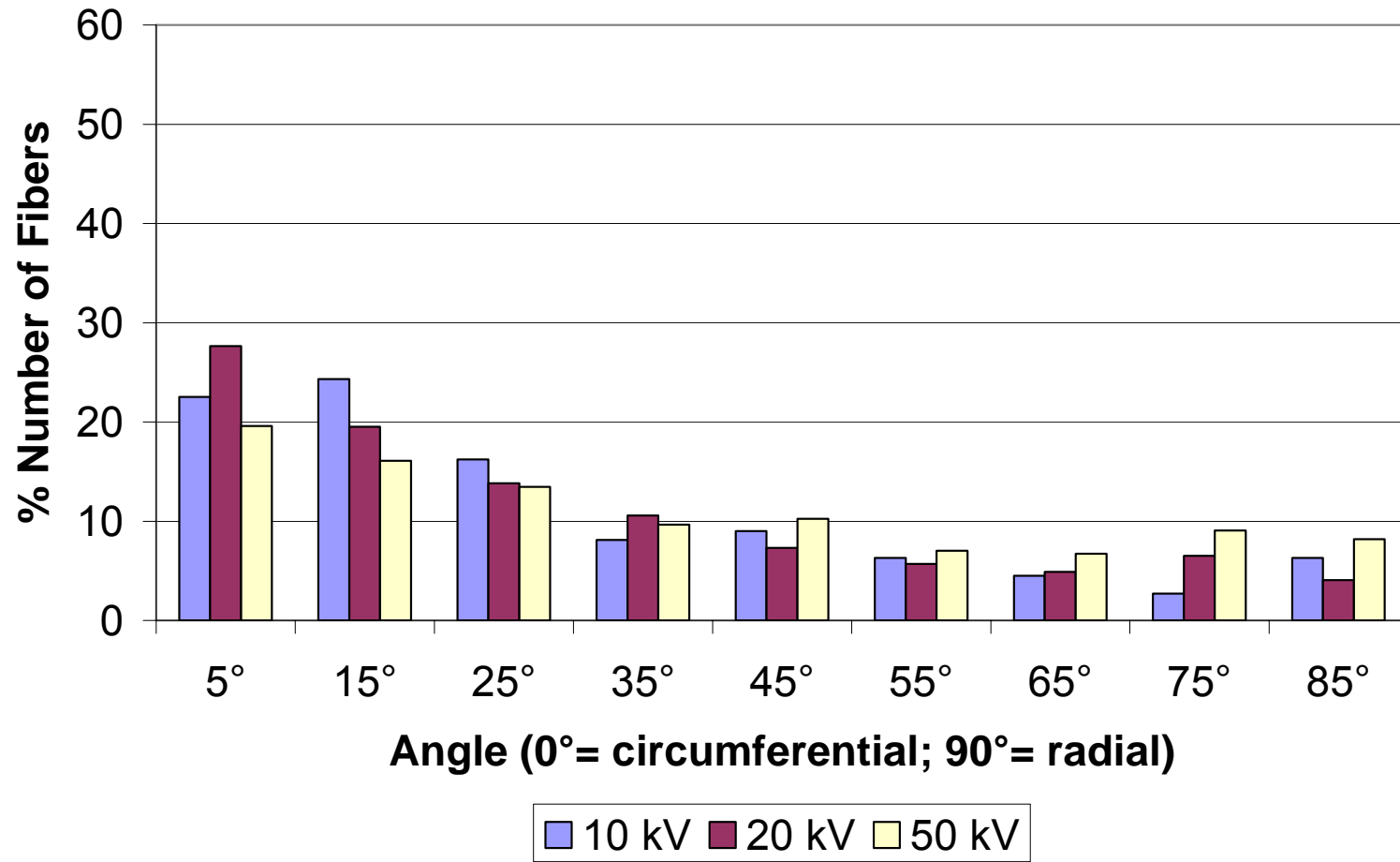


Figure 124: Distribution depending on potential at 13rpm disc speed / 10cm electrode distance / 20mm lay-down rod

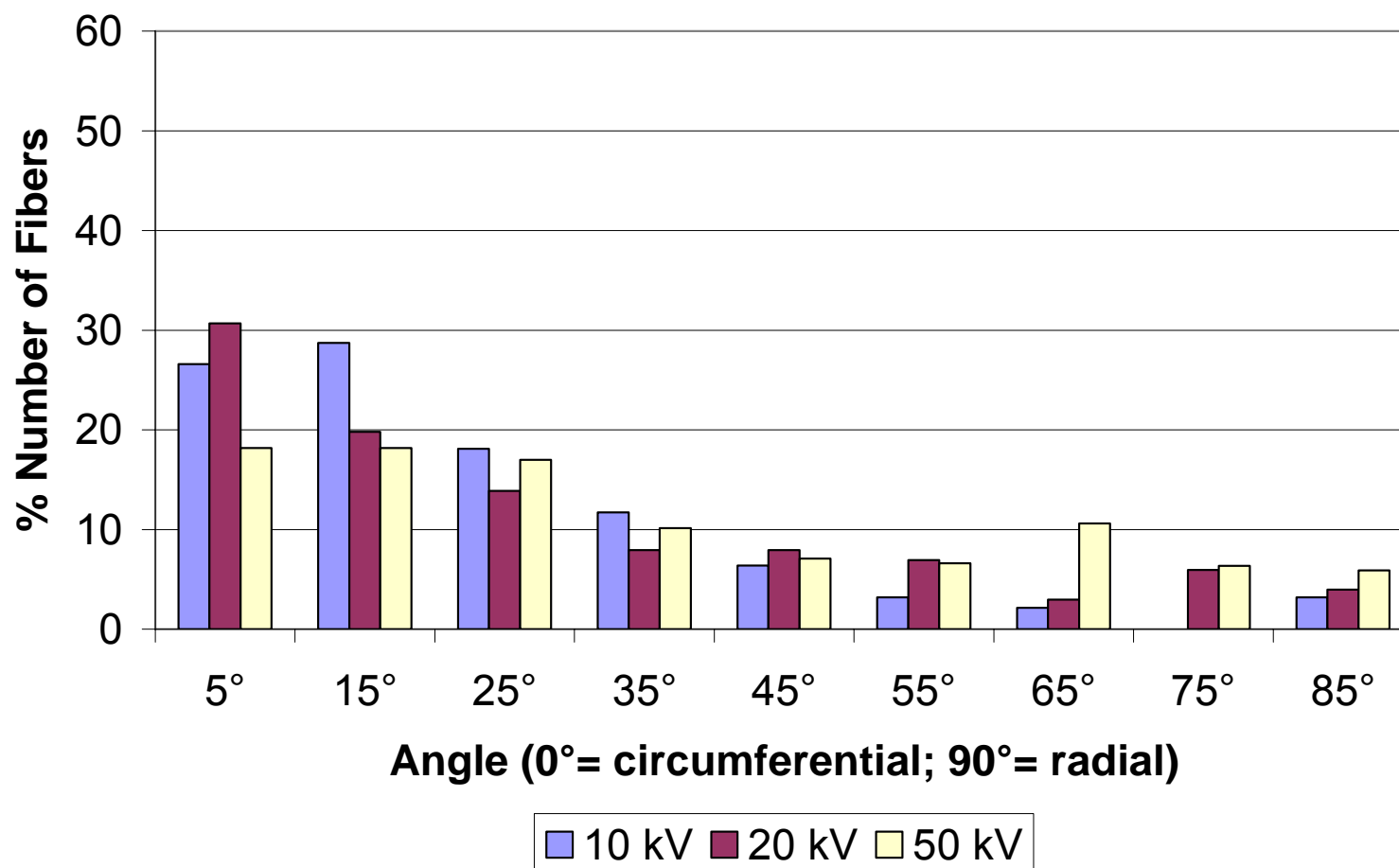


Figure 125: Distribution depending on potential at 23.5rpm disc speed / 10cm electrode distance / 20mm lay-down rod

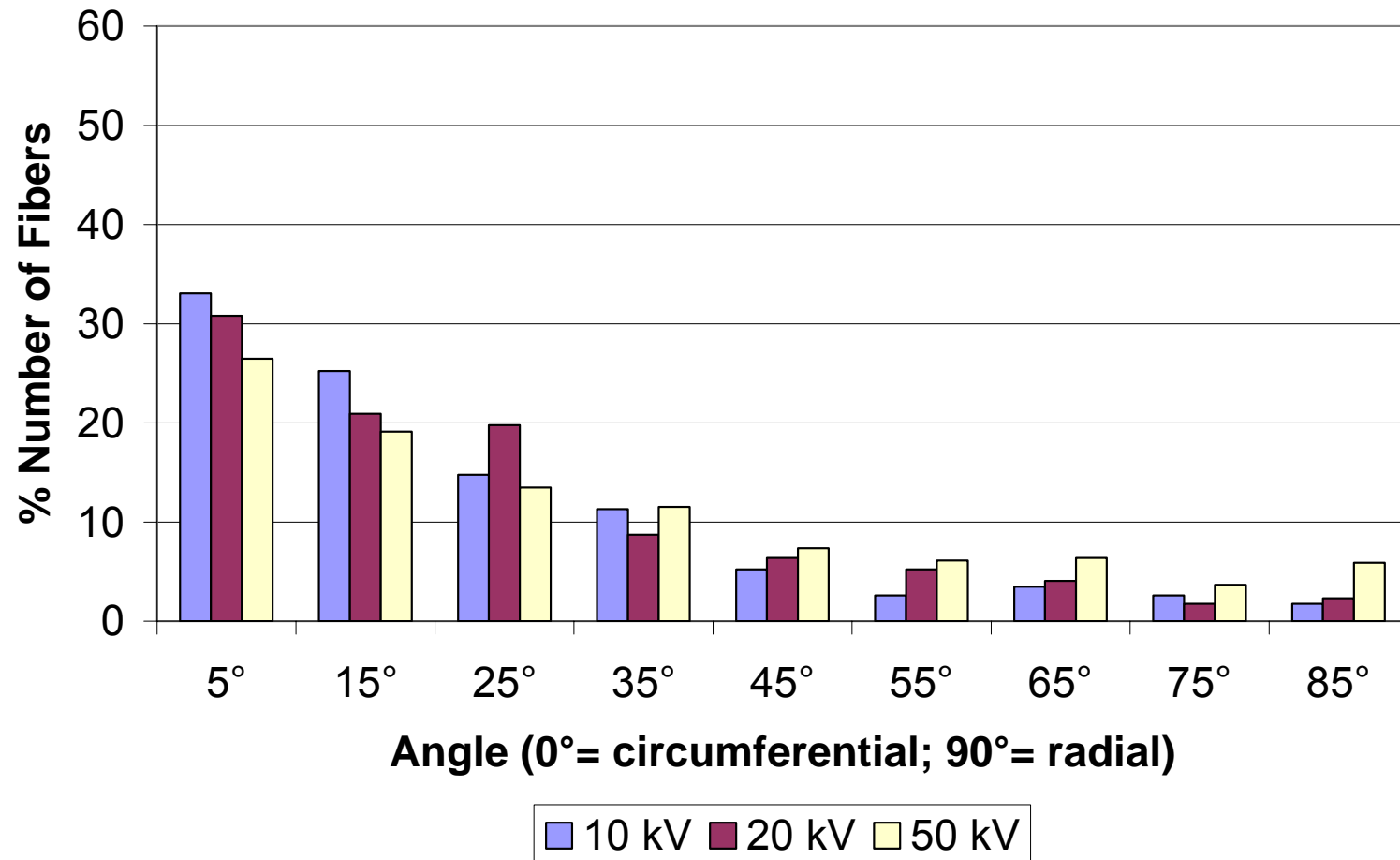


Figure 126: Distribution depending on potential at 50rpm disc speed / 10cm electrode distance / 20mm lay-down rod

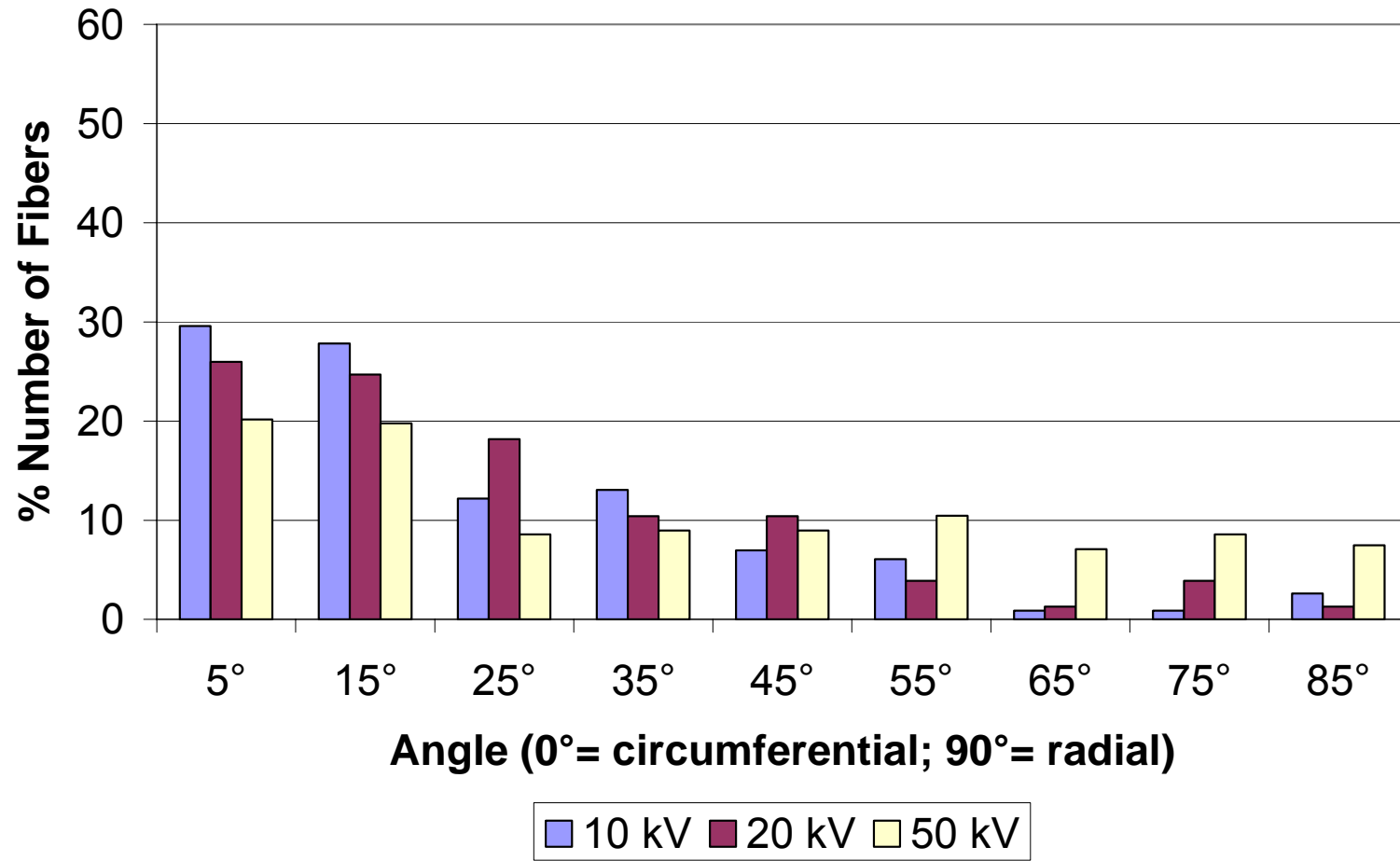


Figure 127: Distribution depending on potential at 13rpm disc speed / 20cm electrode distance / 20mm lay-down rod

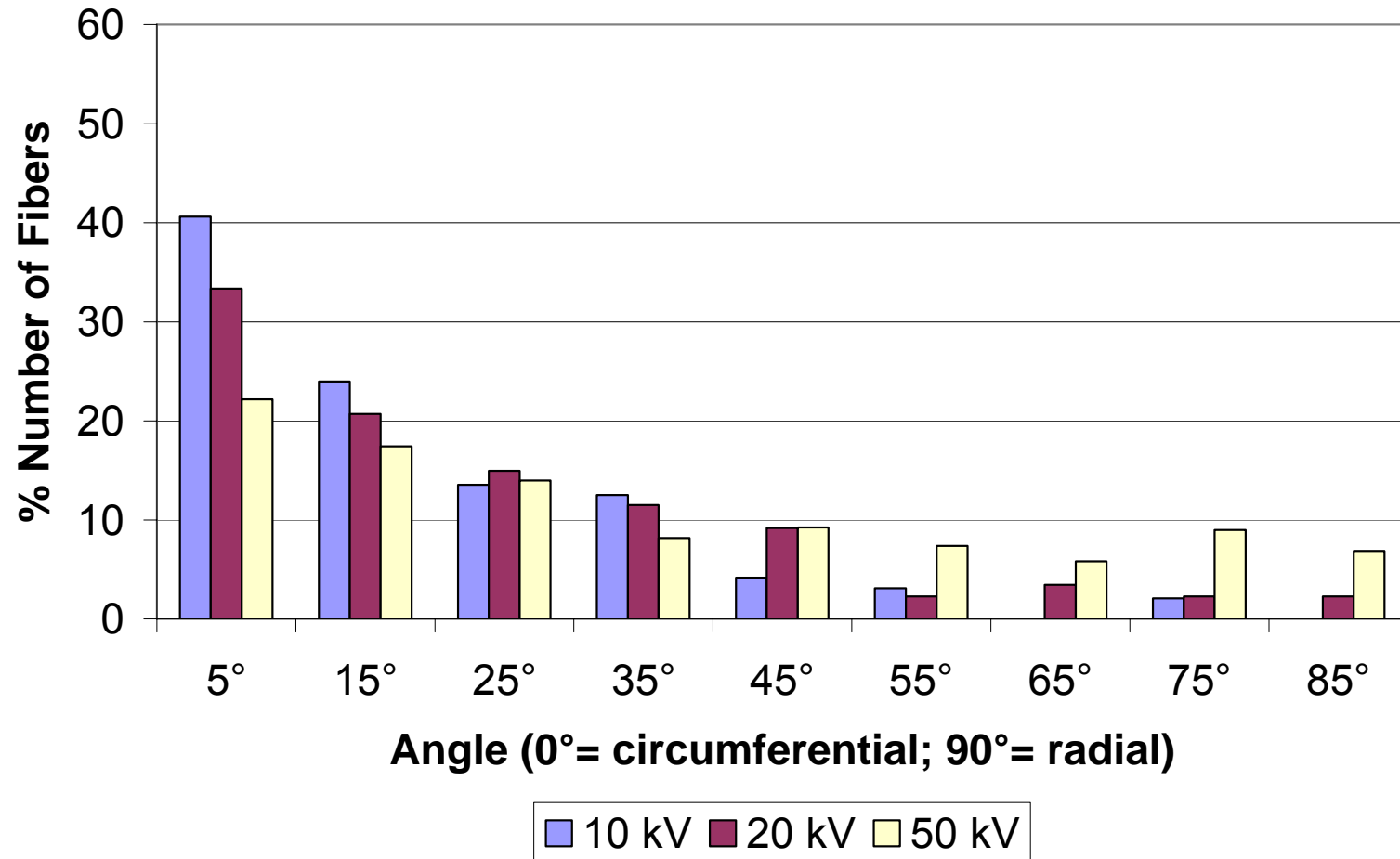


Figure 128: Distribution depending on potential at 23.5rpm disc speed / 20cm electrode distance / 20mm lay-down rod

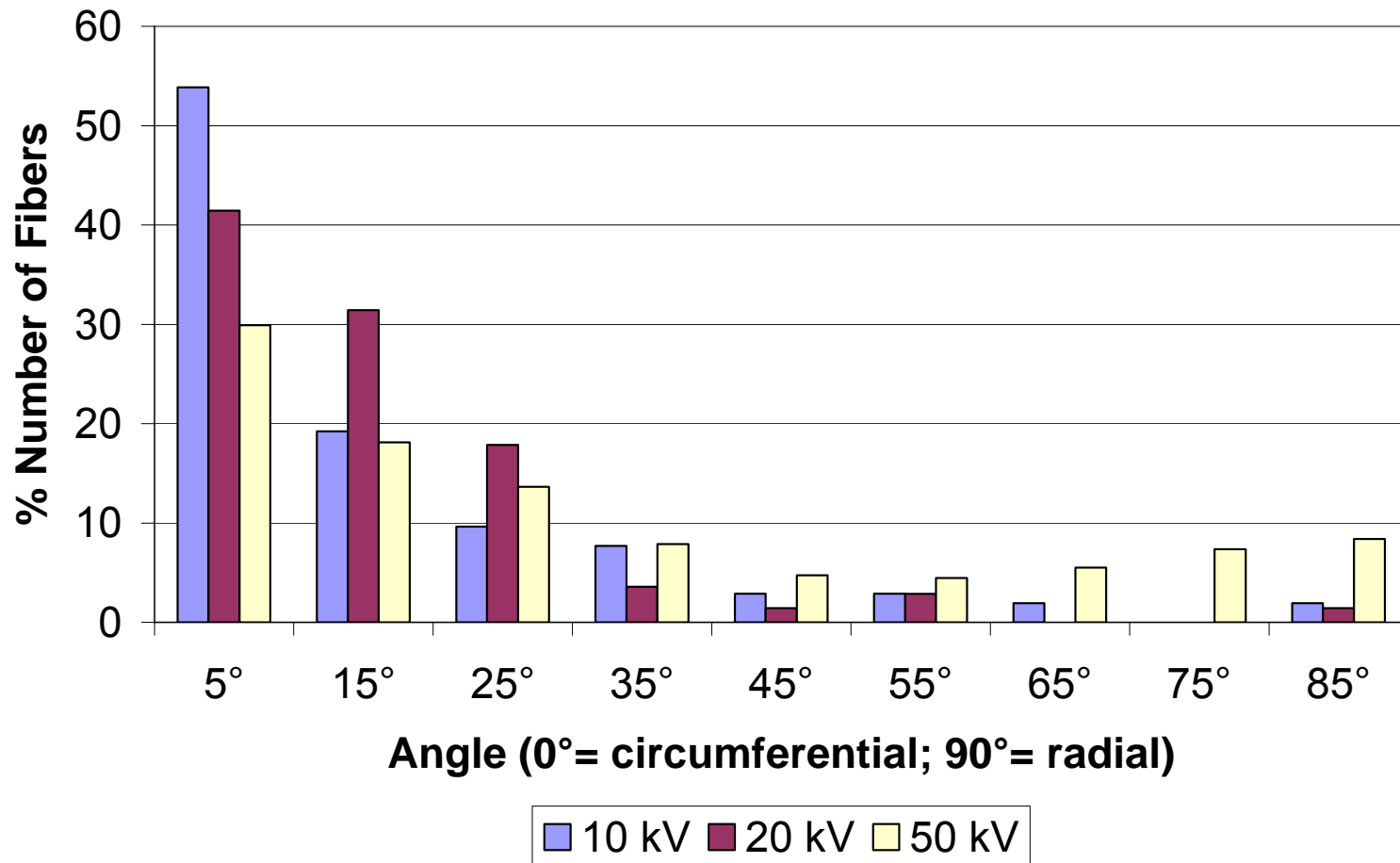


Figure 129: Distribution depending on potential at 50rpm disc speed / 20cm electrode distance / 20mm lay-down rod

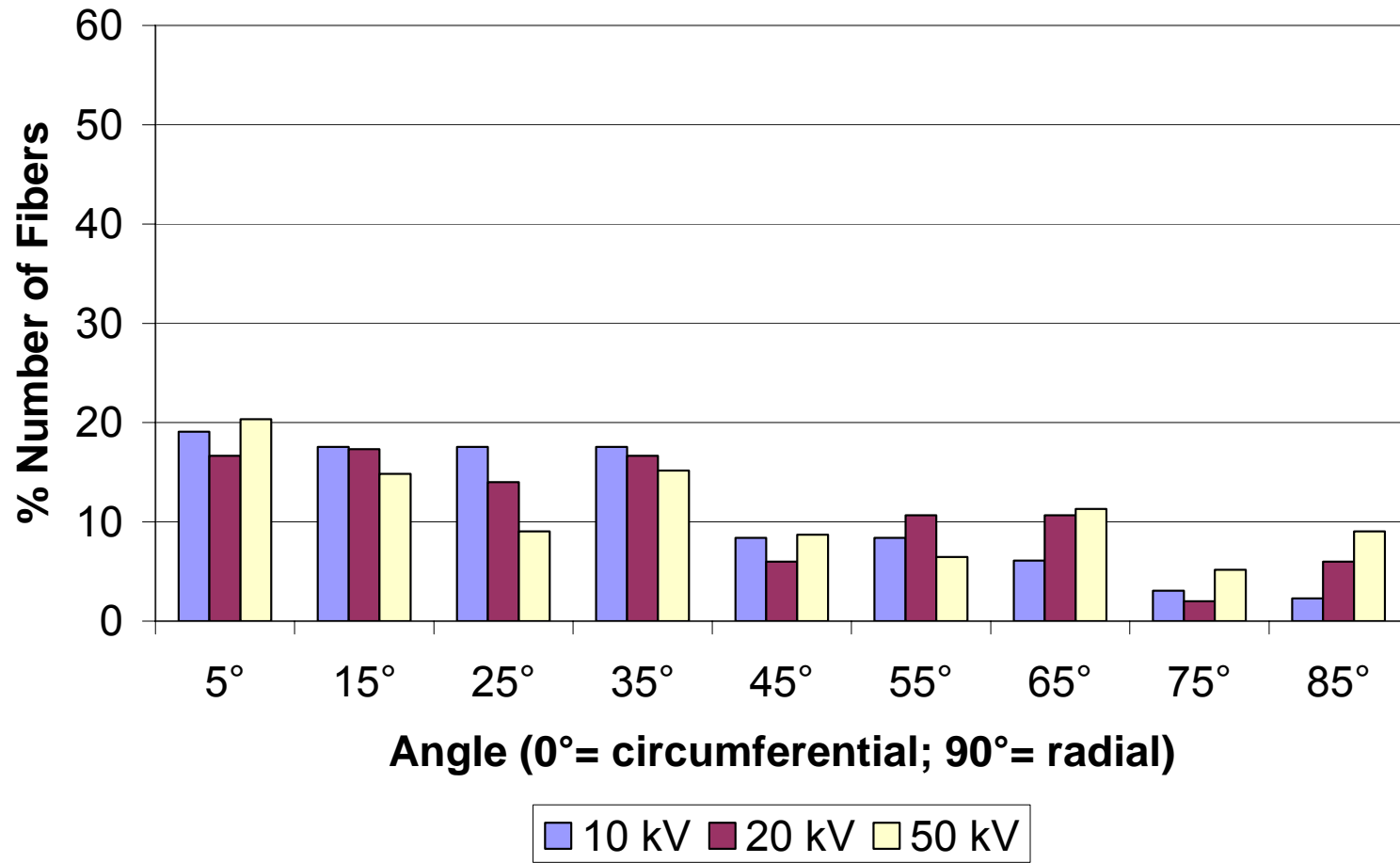


Figure 130: Distribution depending on potential at 13rpm disc speed / 30cm electrode distance / 20mm lay-down rod

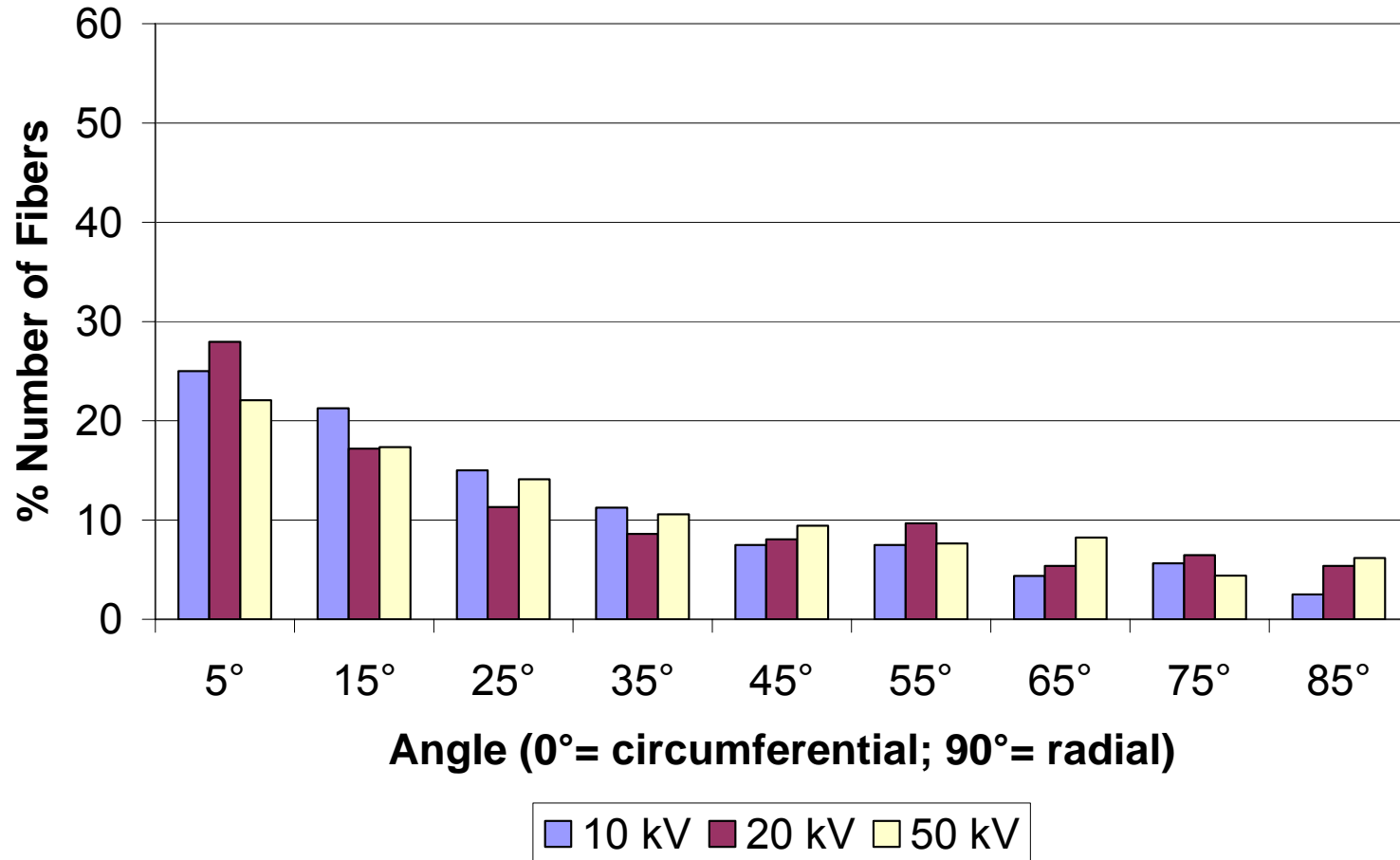


Figure 131: Distribution depending on potential at 23.5rpm disc speed / 30cm electrode distance / 20mm lay-down rod

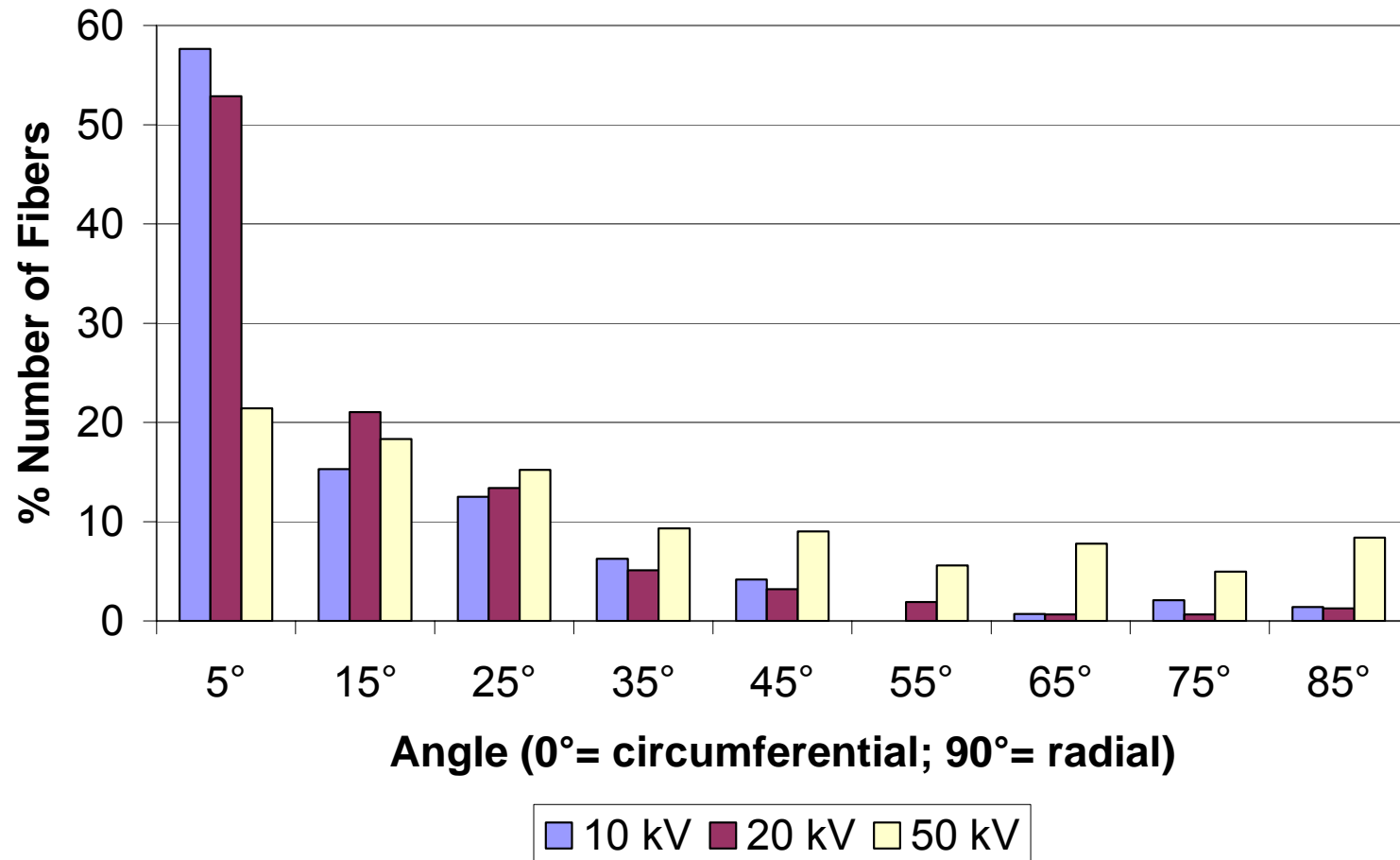


Figure 132: Distribution depending on potential at 50rpm disc speed / 30cm electrode distance / 20mm lay-down rod

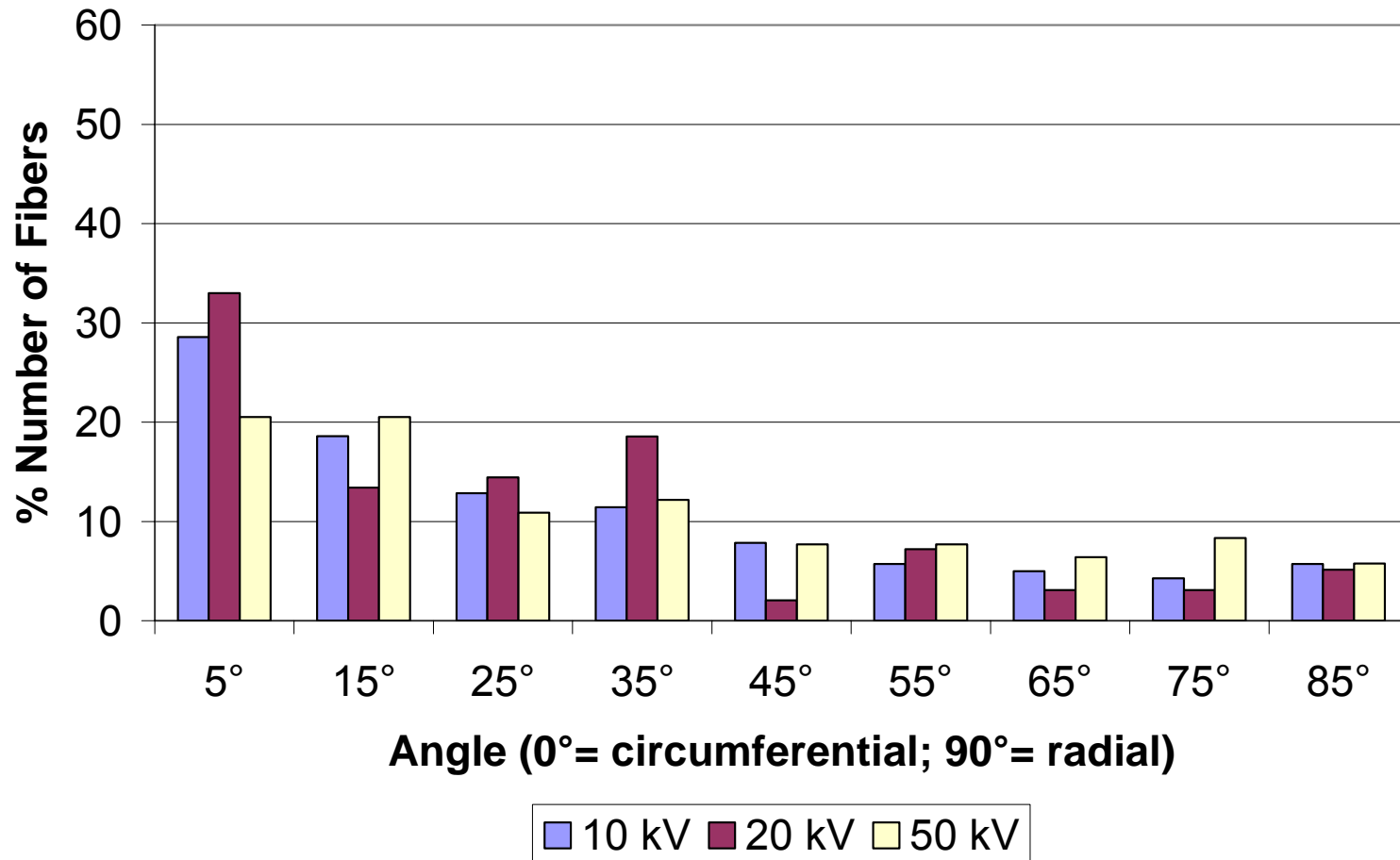


Figure 133: Distribution depending on potential at 13rpm disc speed / 10cm electrode distance / 9.4mm lay-down rod

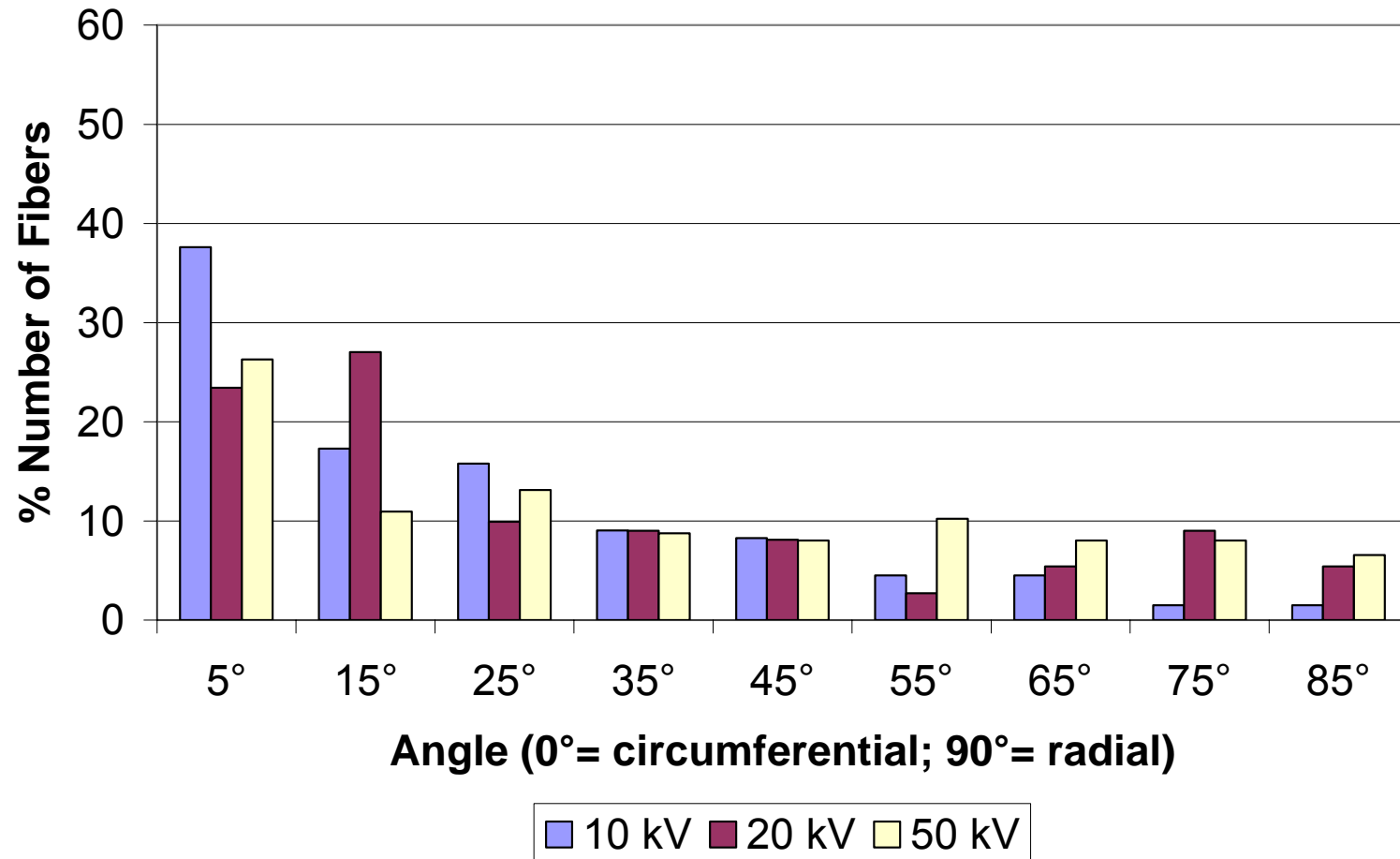


Figure 134: Distribution depending on potential at 23.5rpm disc speed / 10cm electrode distance / 9.4mm lay-down rod

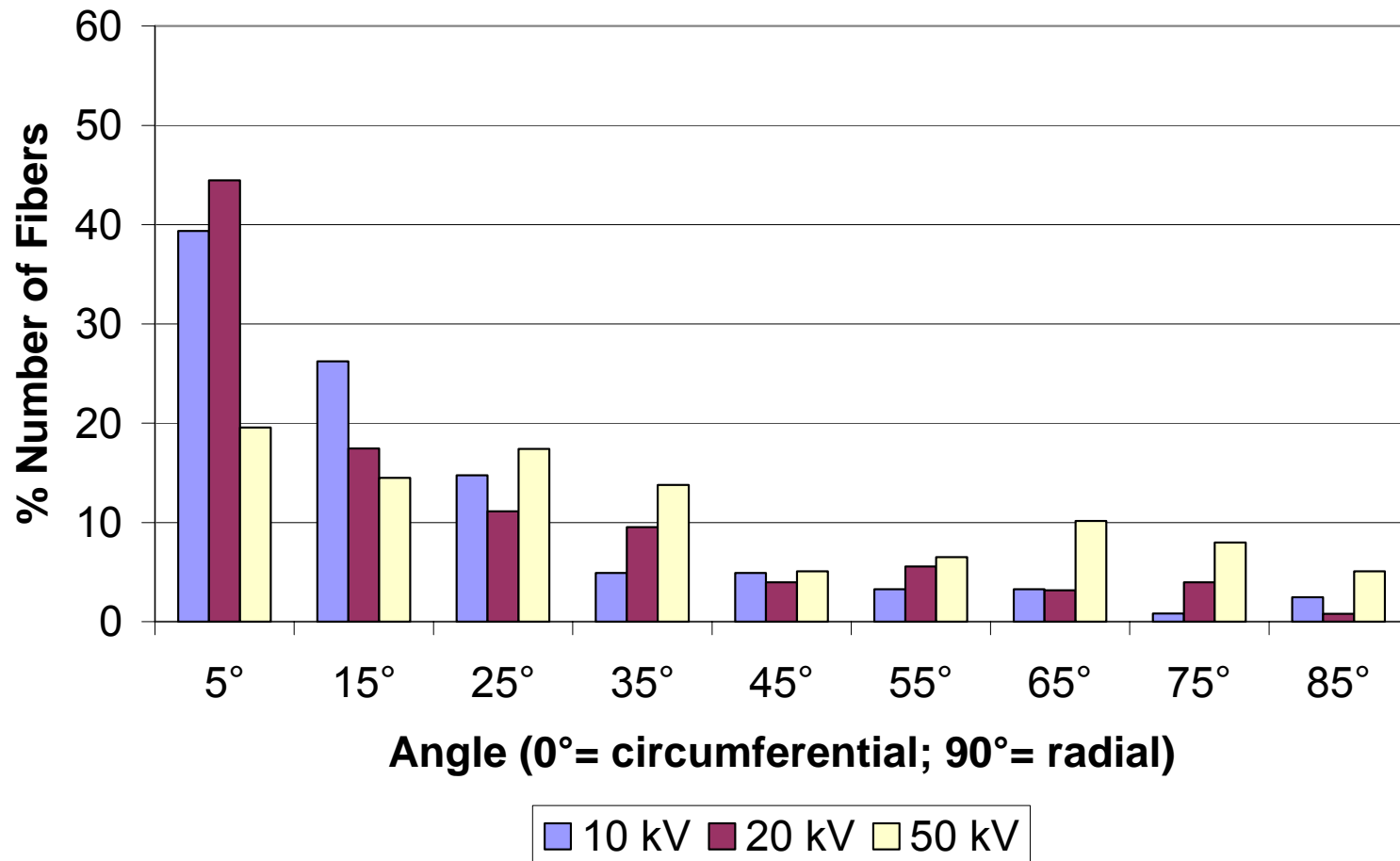


Figure 135: Distribution depending on potential at 50rpm disc speed / 10cm electrode distance / 9.4mm lay-down rod

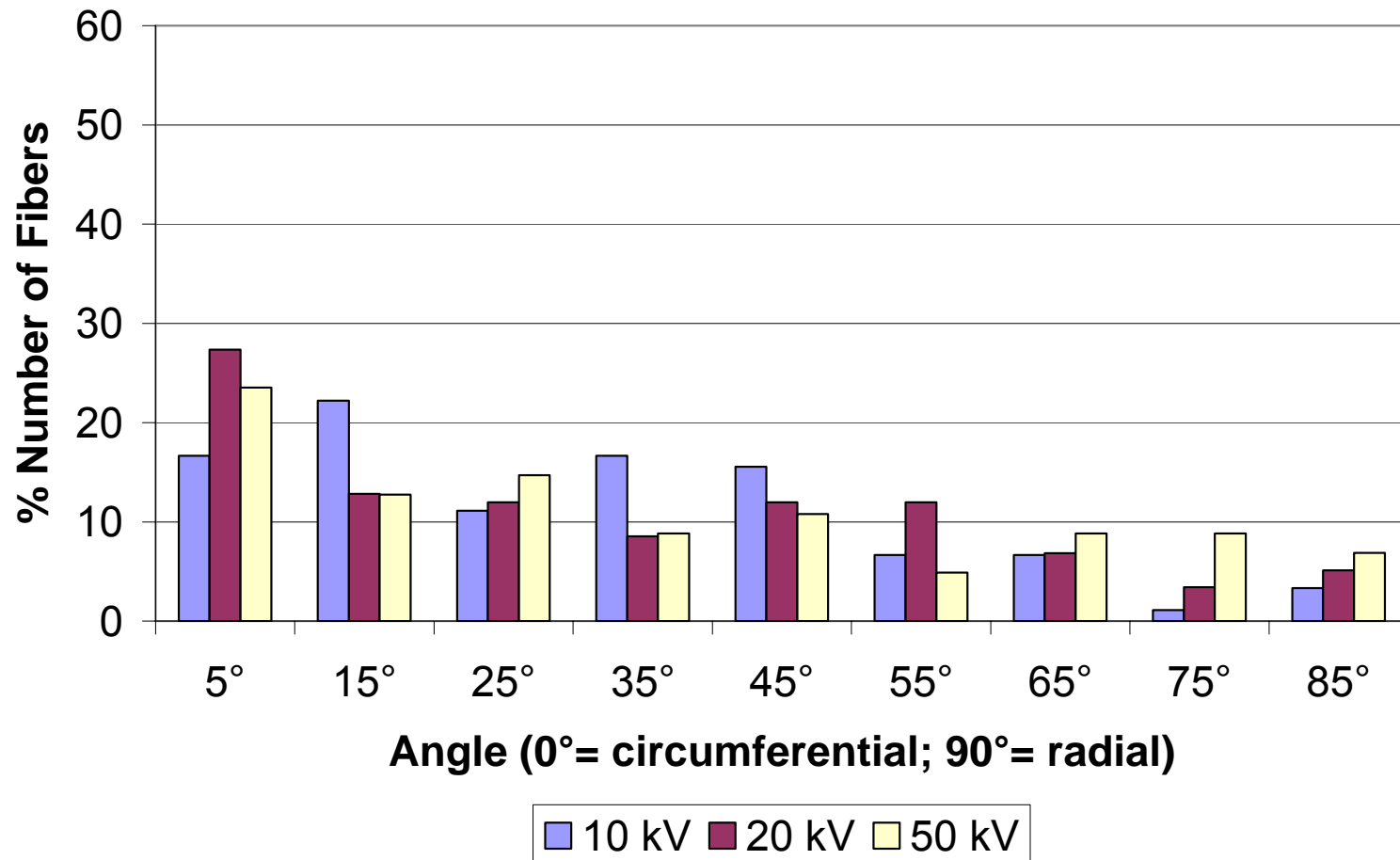


Figure 136: Distribution depending on potential at 13rpm disc speed / 20cm electrode distance / 9.4mm lay-down rod

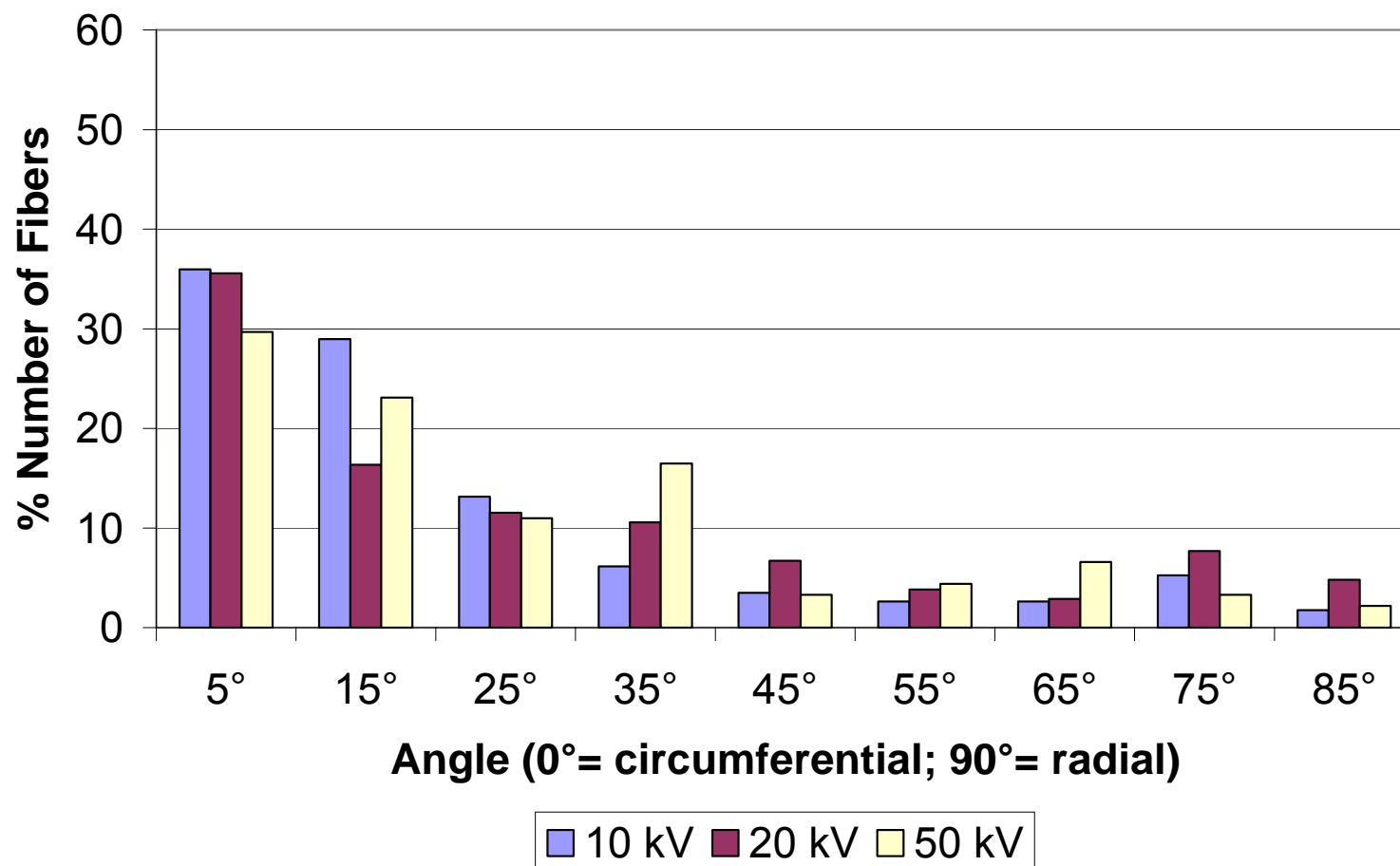


Figure 137: Distribution depending on potential at 23.5rpm disc speed / 20cm electrode distance / 9.4mm lay-down rod

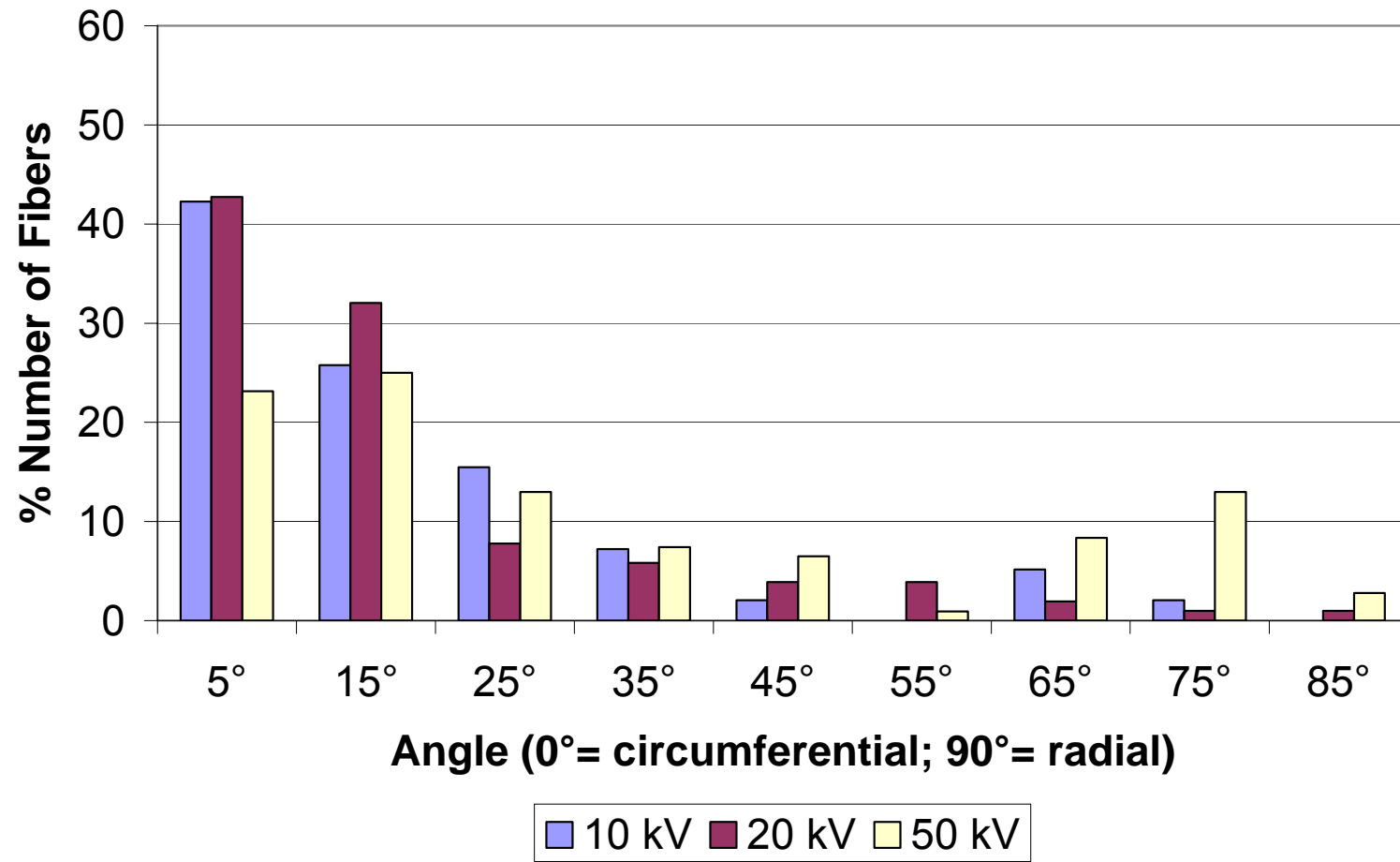


Figure 138: Distribution depending on potential at 50rpm disc speed / 20cm electrode distance / 9.4mm lay-down rod

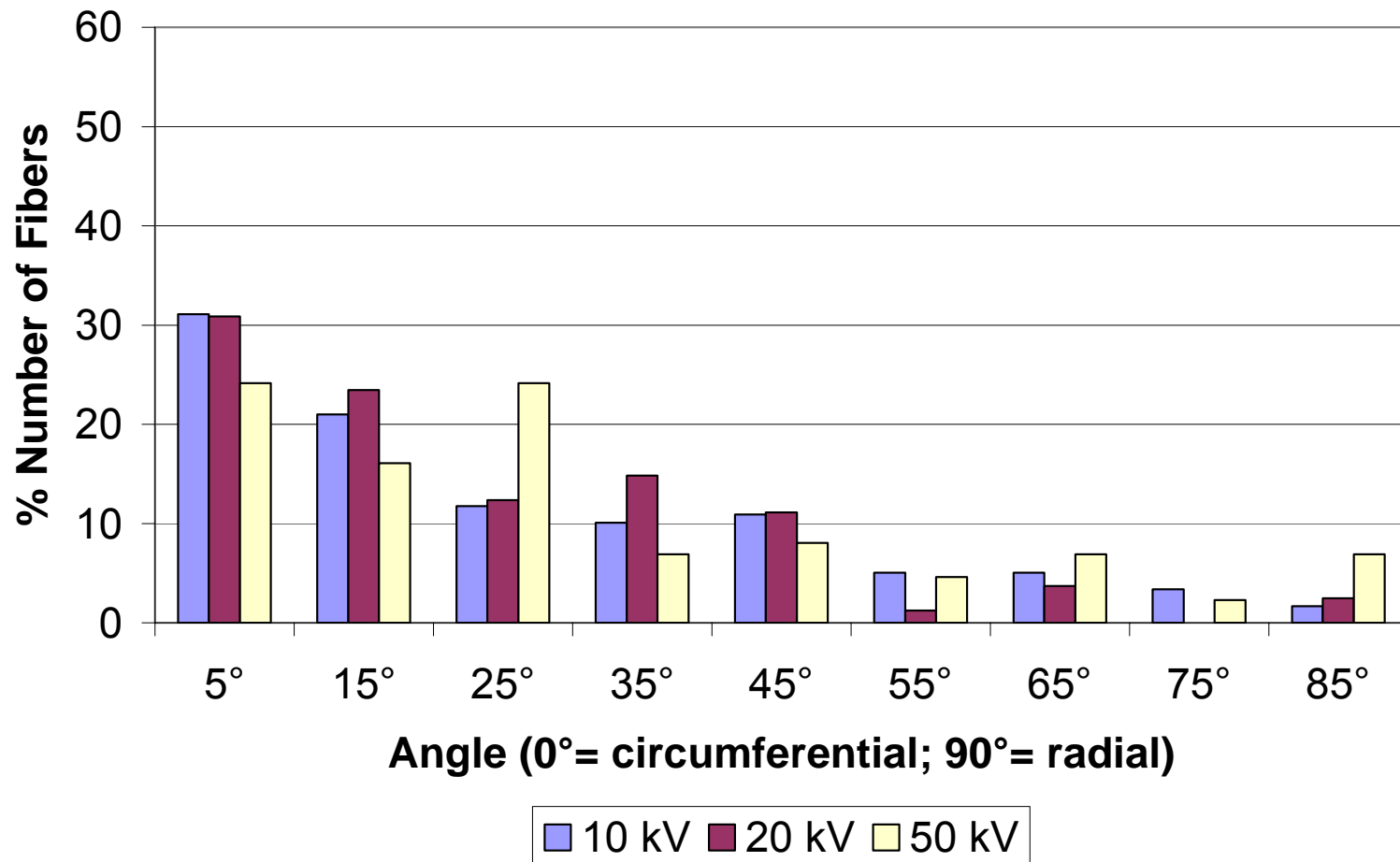


Figure 139: Distribution depending on potential at 13rpm disc speed / 30cm electrode distance / 9.4mm lay-down rod

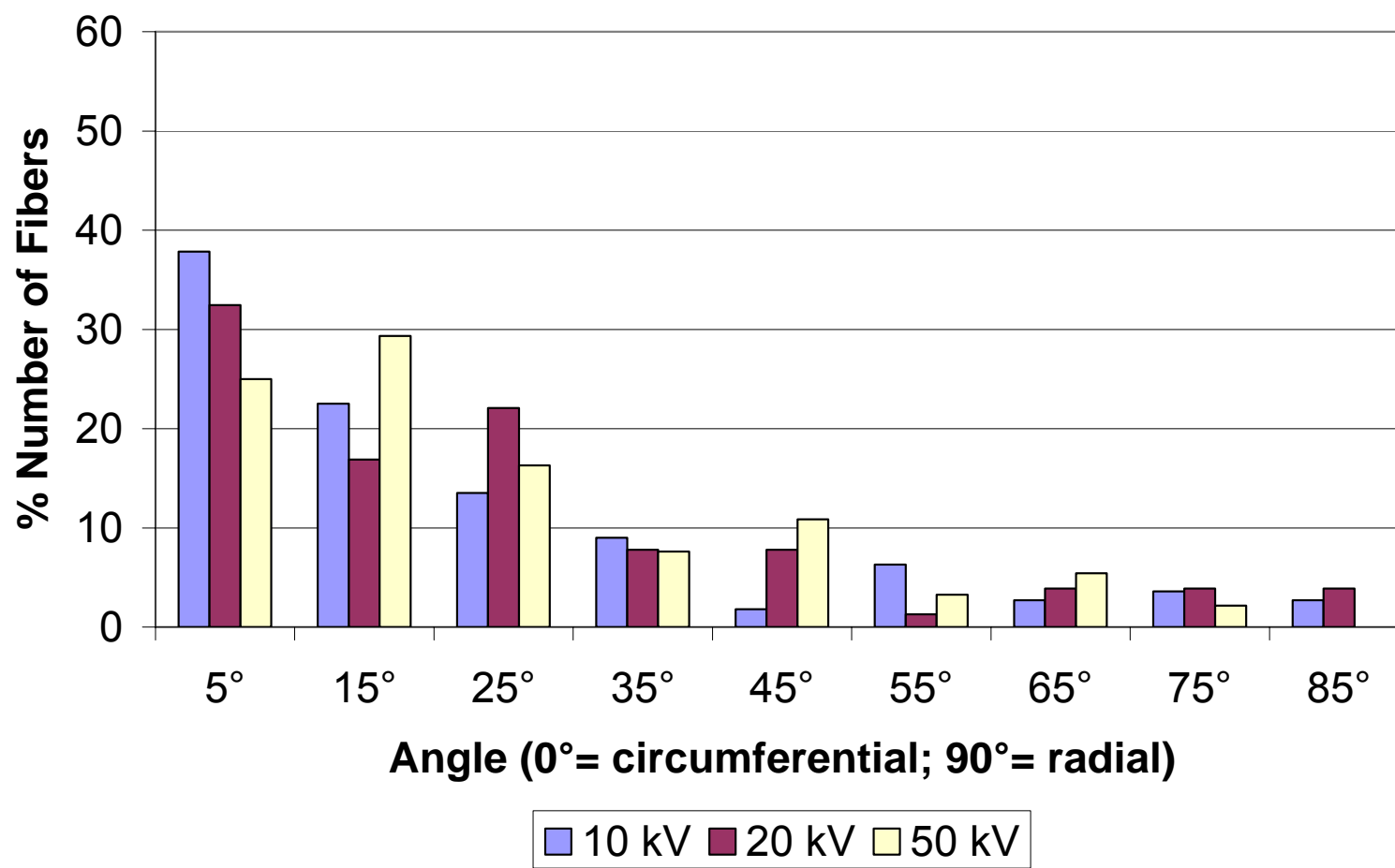


Figure 140: Distribution depending on potential at 23.5rpm disc speed / 30cm electrode distance / 9.4mm lay-down rod

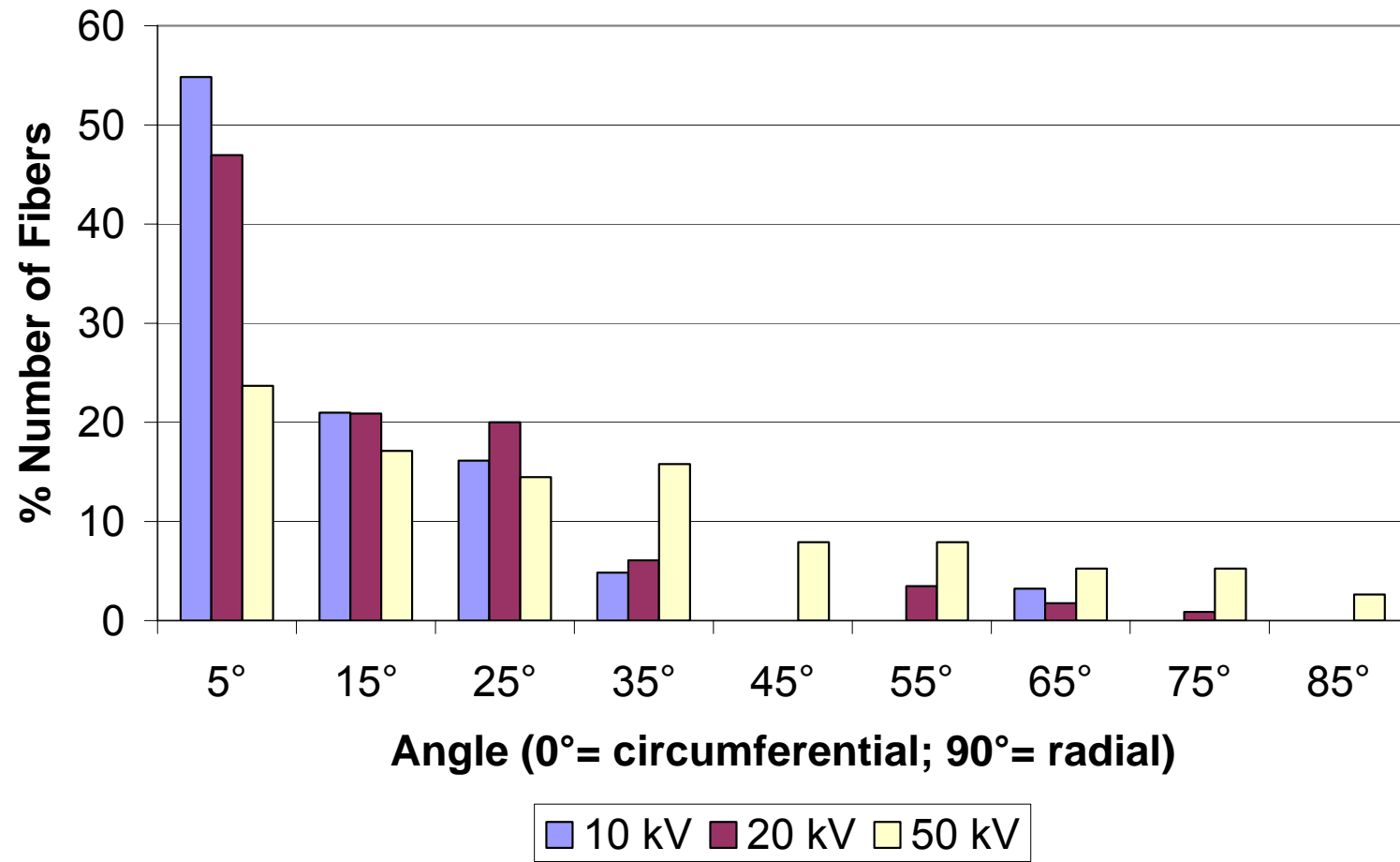


Figure 141: Distribution depending on potential at 50rpm disc speed / 30cm electrode distance / 9.4mm lay-down rod

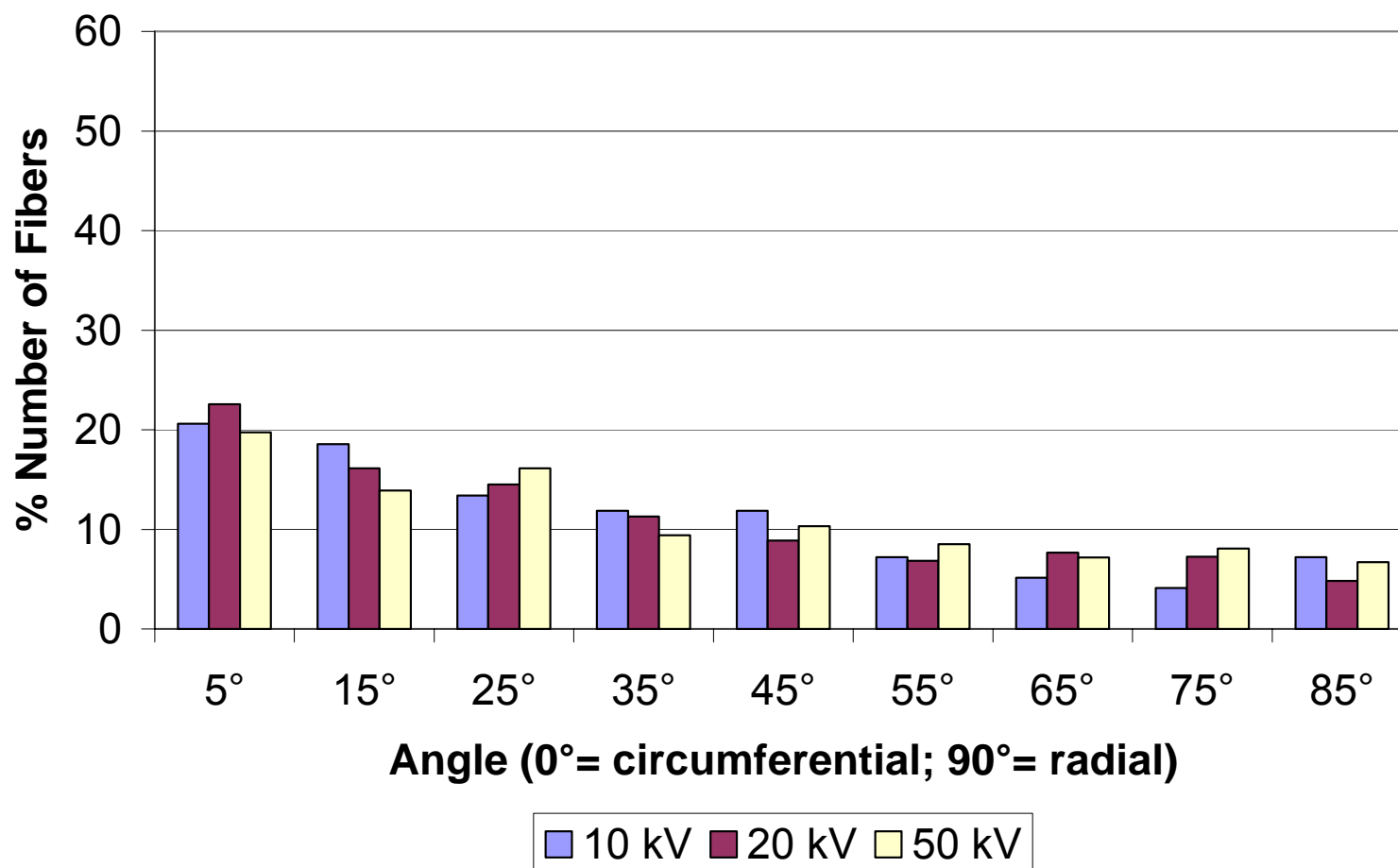


Figure 142: Distribution depending on potential at 13rpm disc speed / 10cm electrode distance / 4.76mm lay-down rod

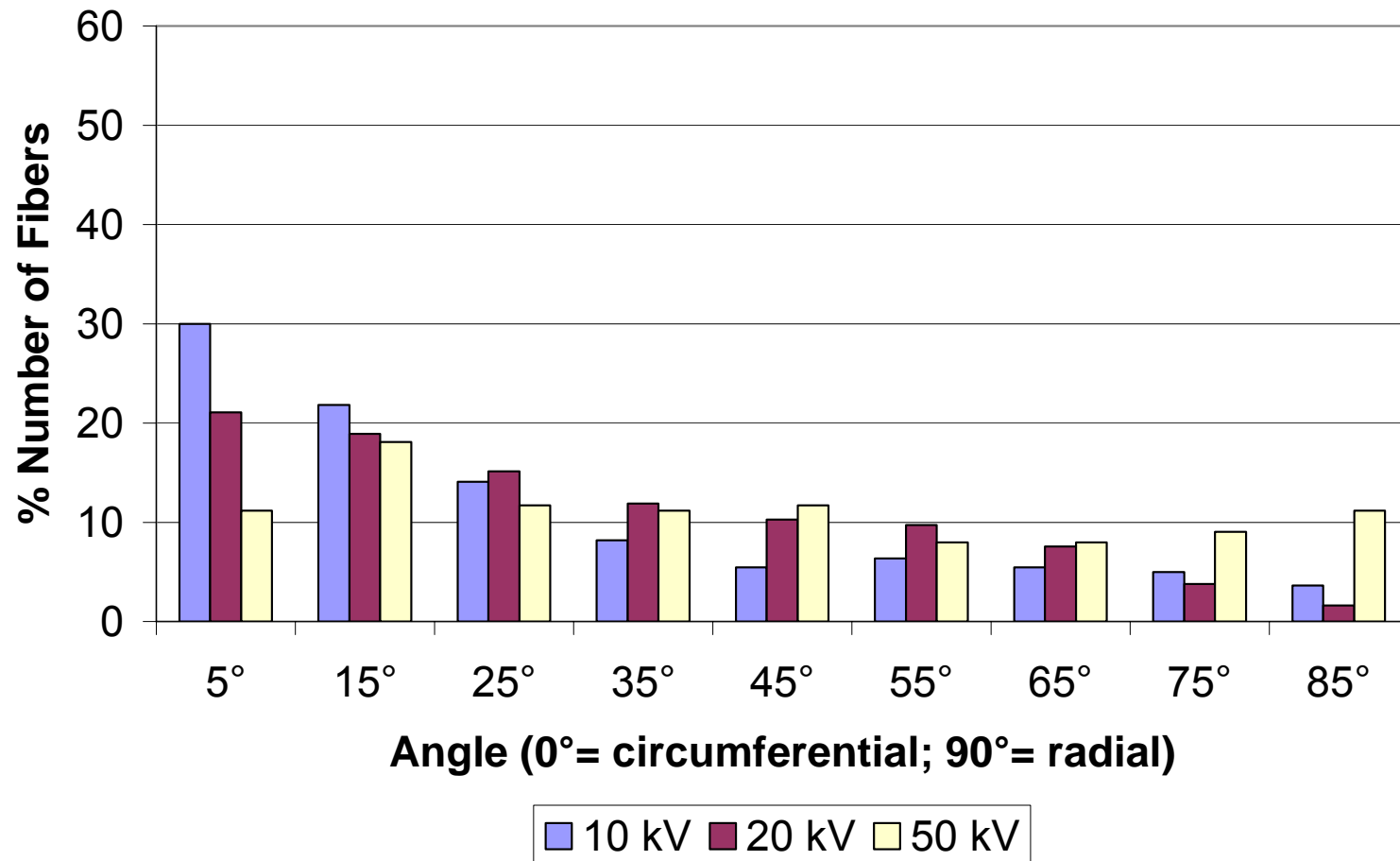


Figure 143: Distribution depending on potential at 23.5rpm disc speed / 10cm electrode distance / 4.76mm lay-down rod

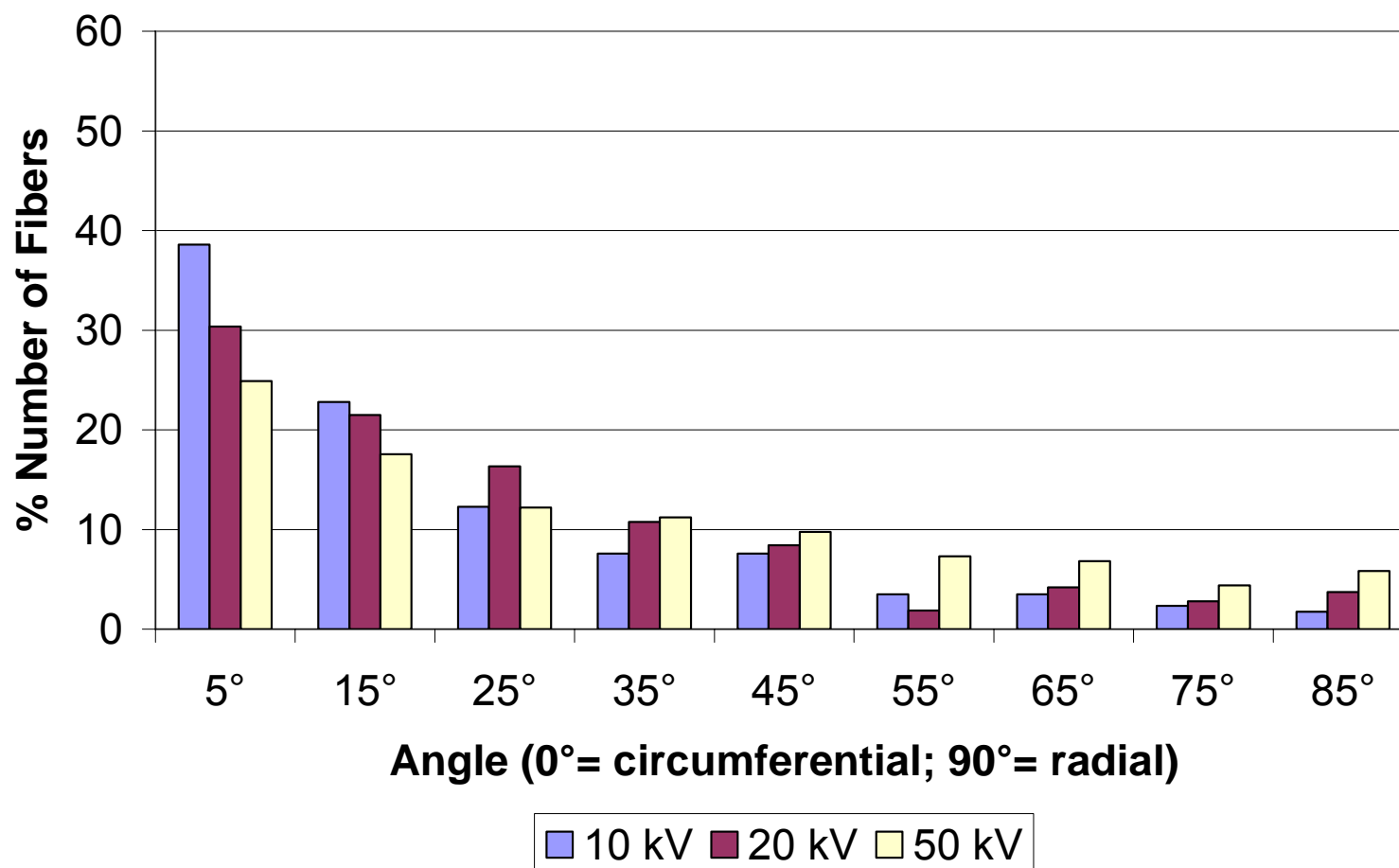


Figure 144: Distribution depending on potential at 50rpm disc speed / 10cm electrode distance / 4.76mm lay-down rod

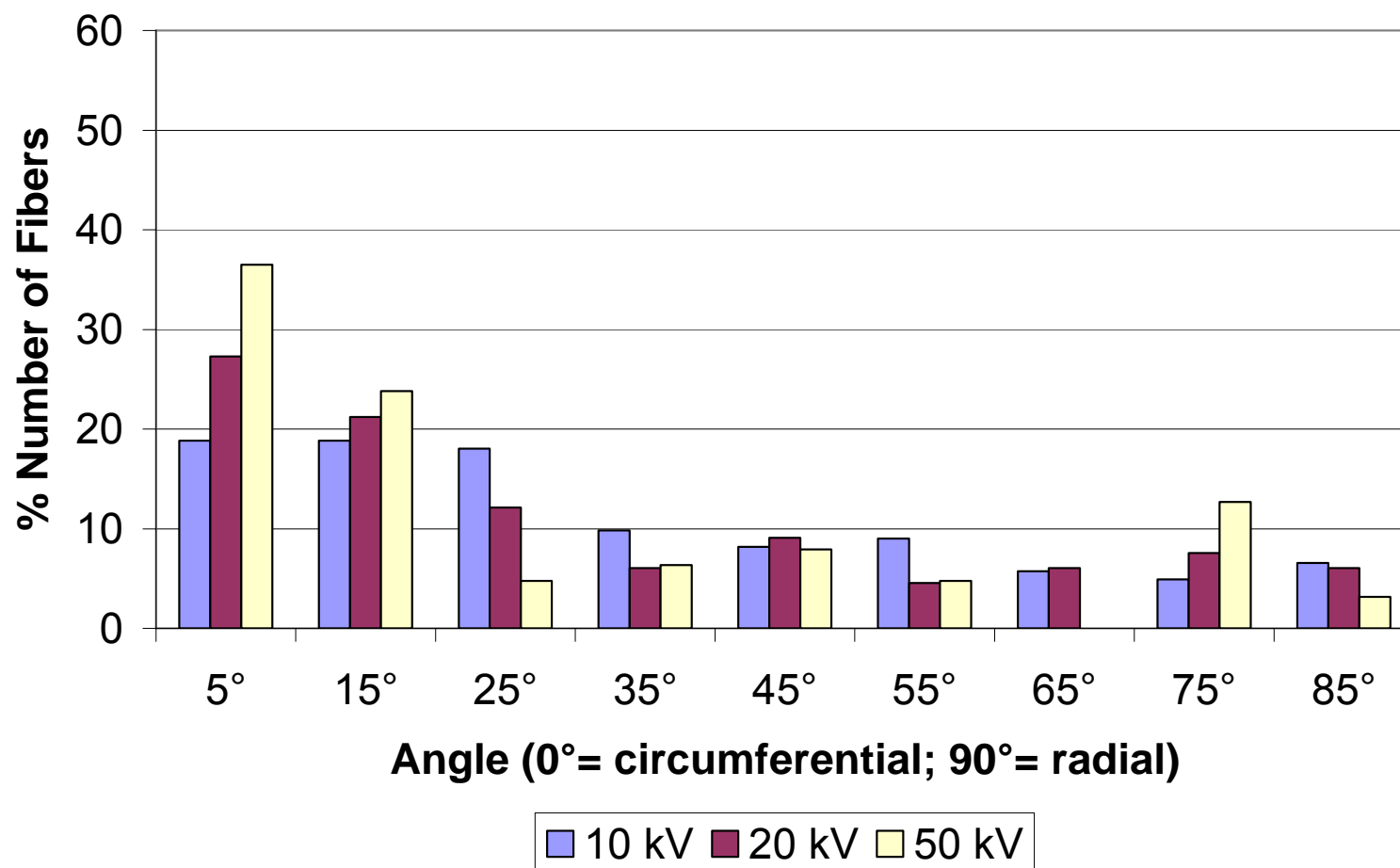


Figure 145: Distribution depending on potential at 13rpm disc speed / 20cm electrode distance / 4.76mm lay-down rod

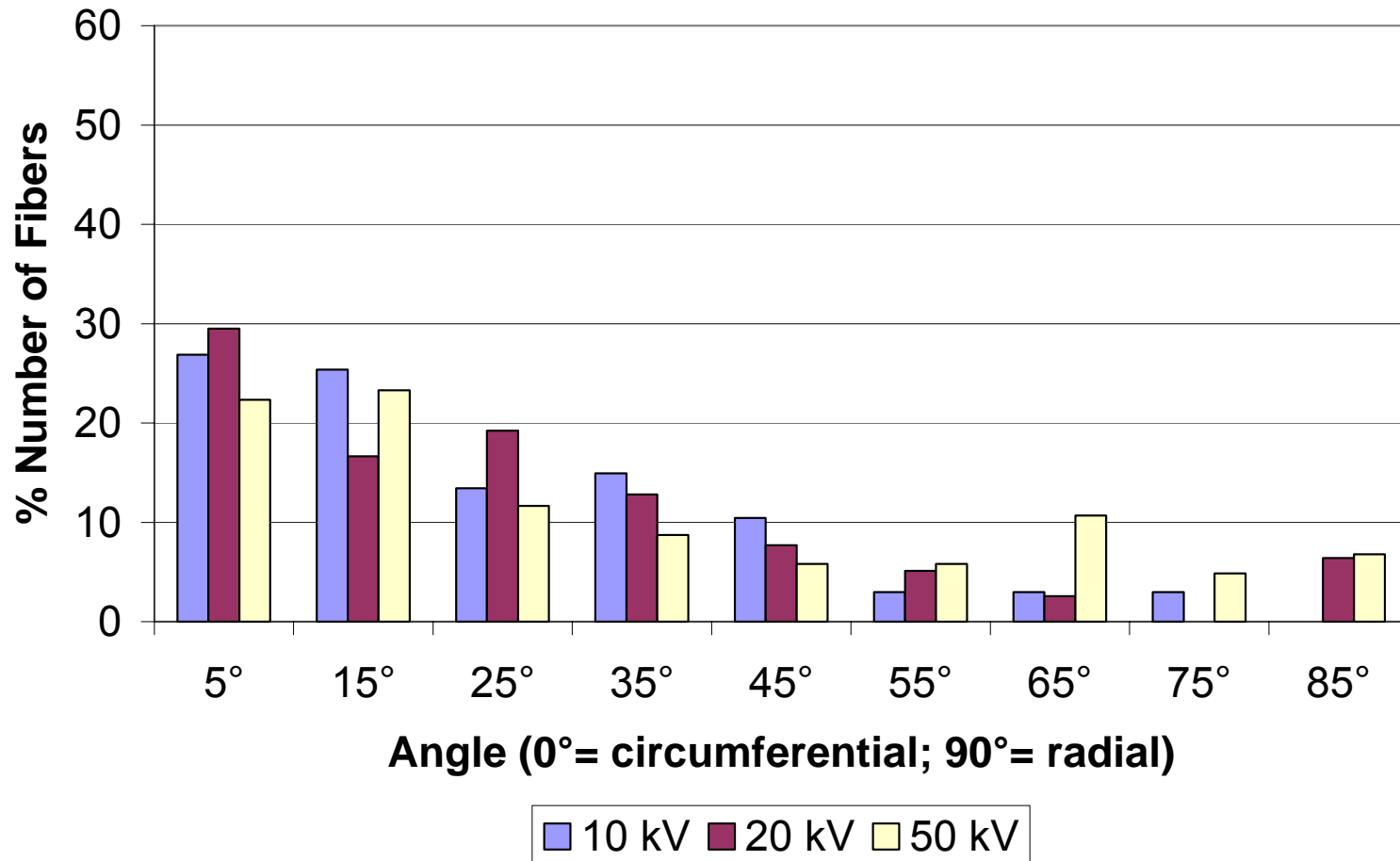


Figure 146: Distribution depending on potential at 23.5rpm disc speed / 20cm electrode distance / 4.76mm lay-down rod

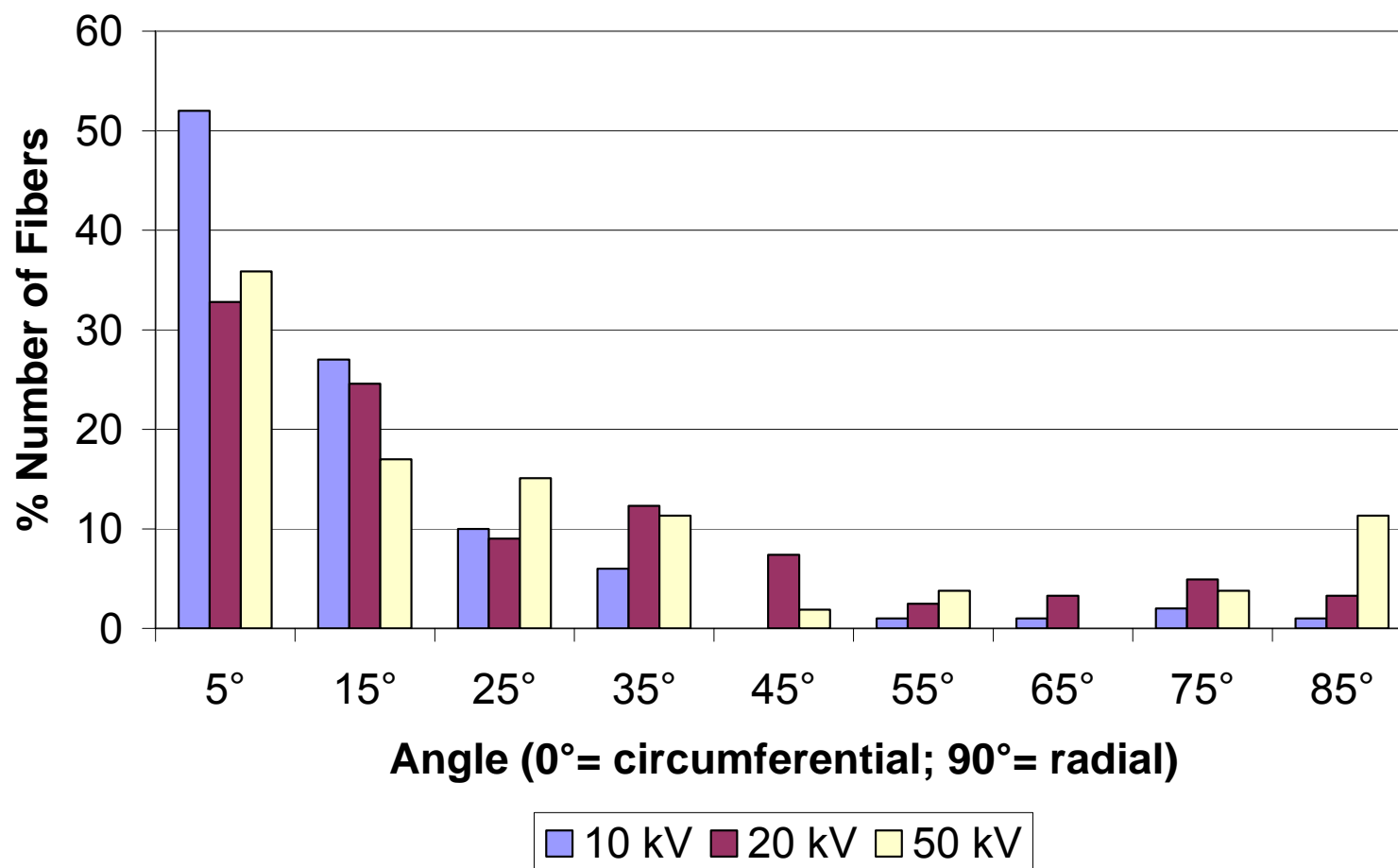


Figure 147: Distribution depending on potential at 50rpm disc speed / 20cm electrode distance / 4.76mm lay-down rod

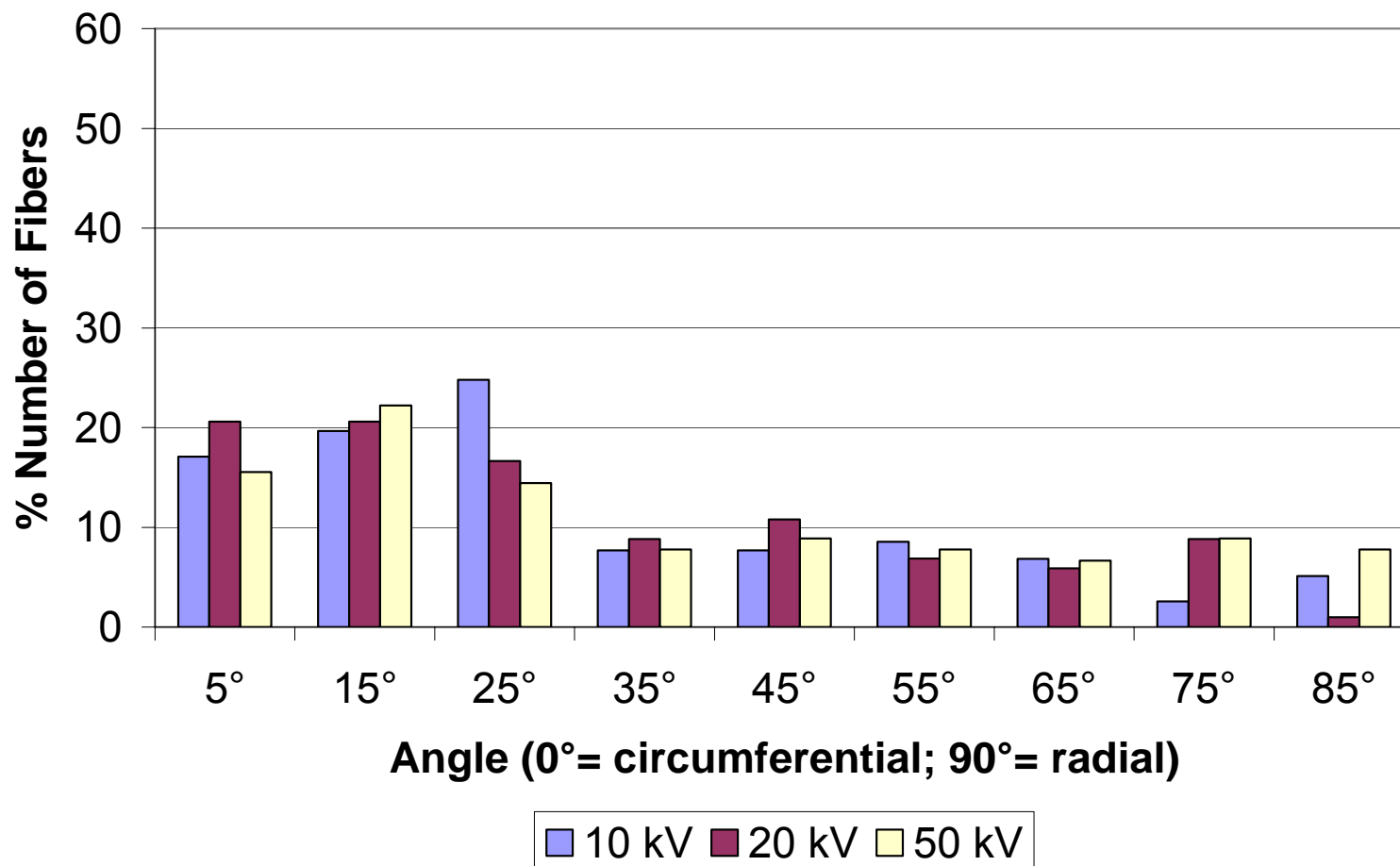


Figure 148: Distribution depending on potential at 13rpm disc speed / 30cm electrode distance / 4.76mm lay-down rod

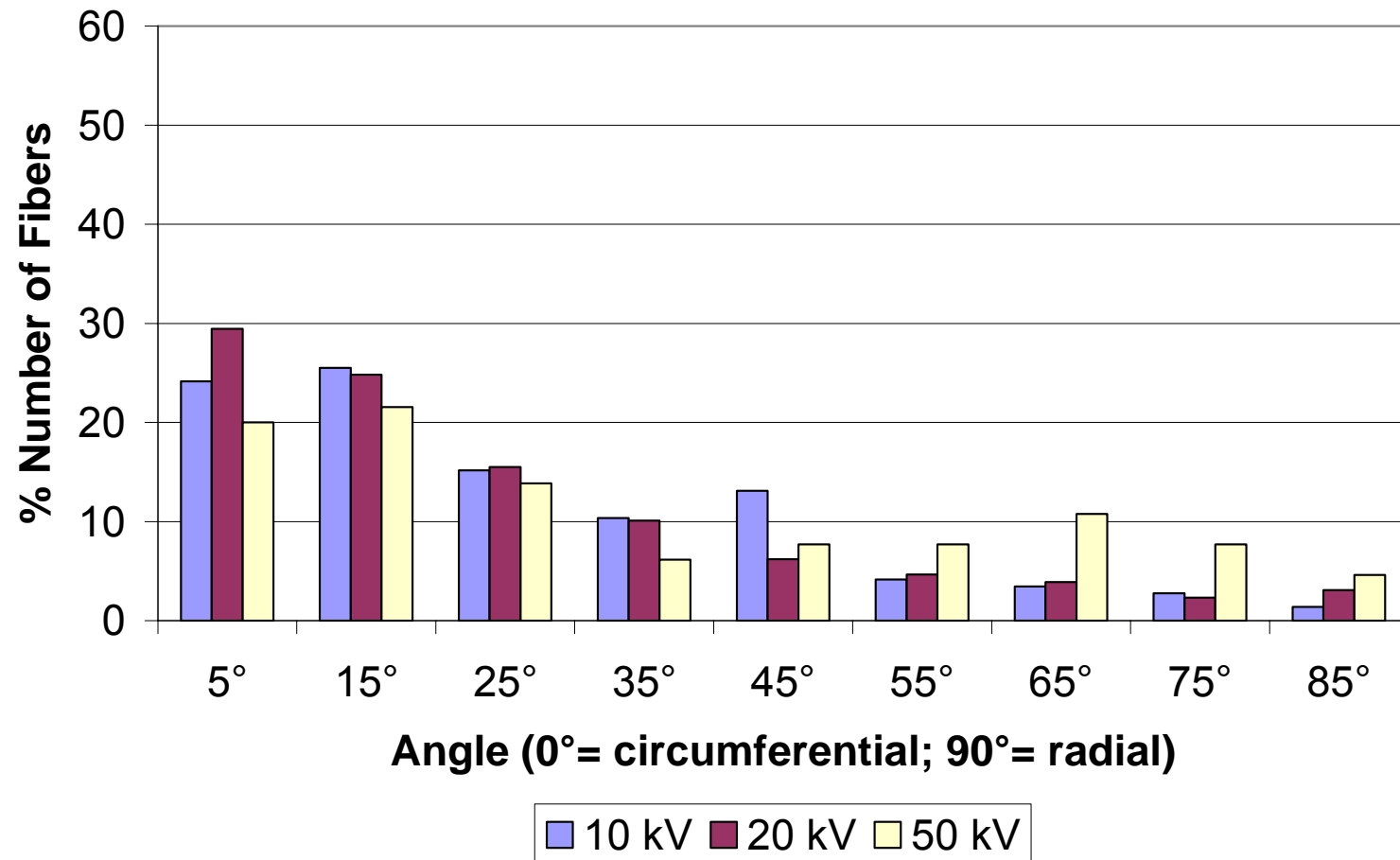


Figure 149: Distribution depending on potential at 23.5rpm disc speed / 30cm electrode distance / 4.76mm lay-down rod

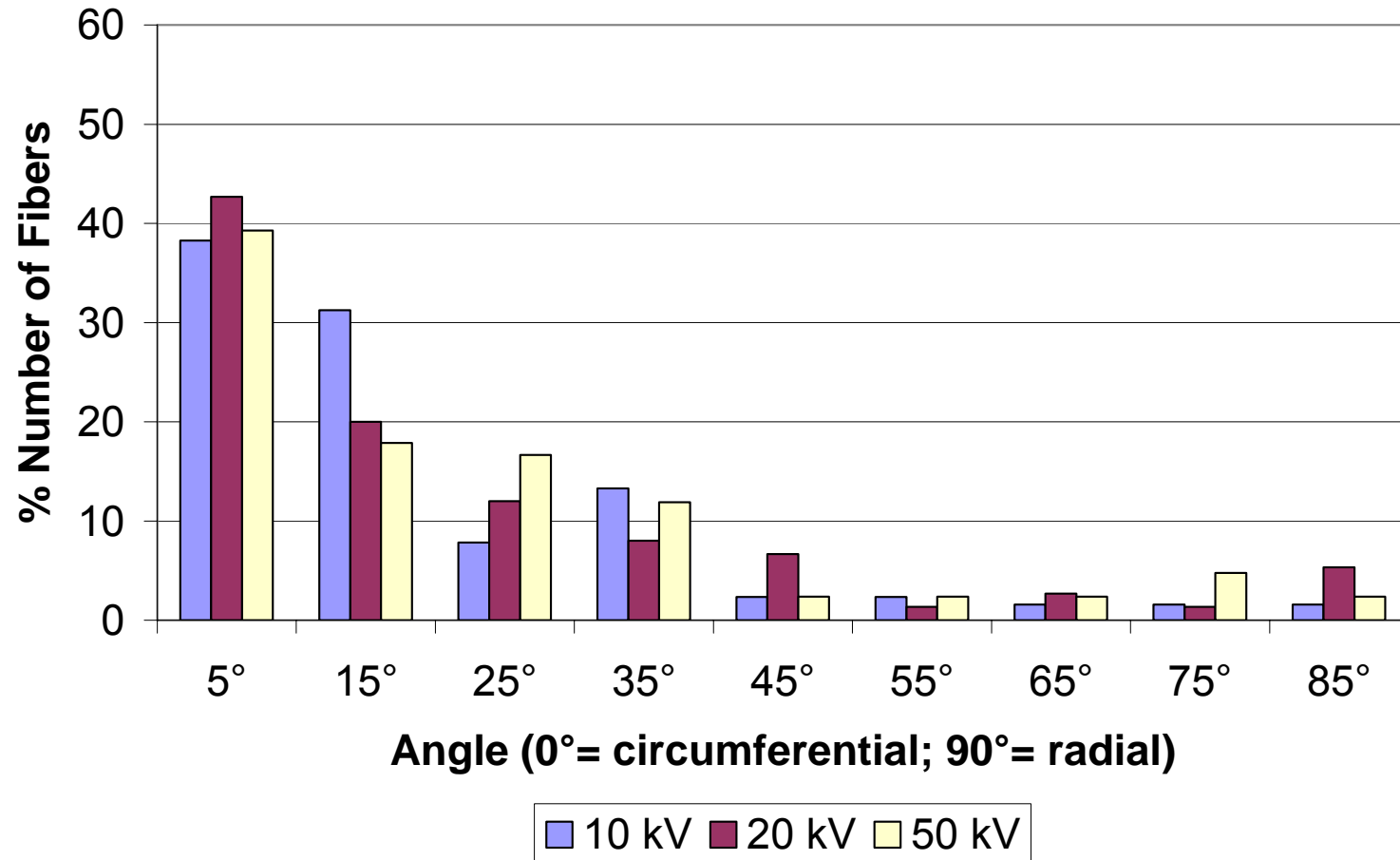


Figure 150: Distribution depending on potential at 50rpm disc speed / 30cm electrode distance / 4.76mm lay-down rod

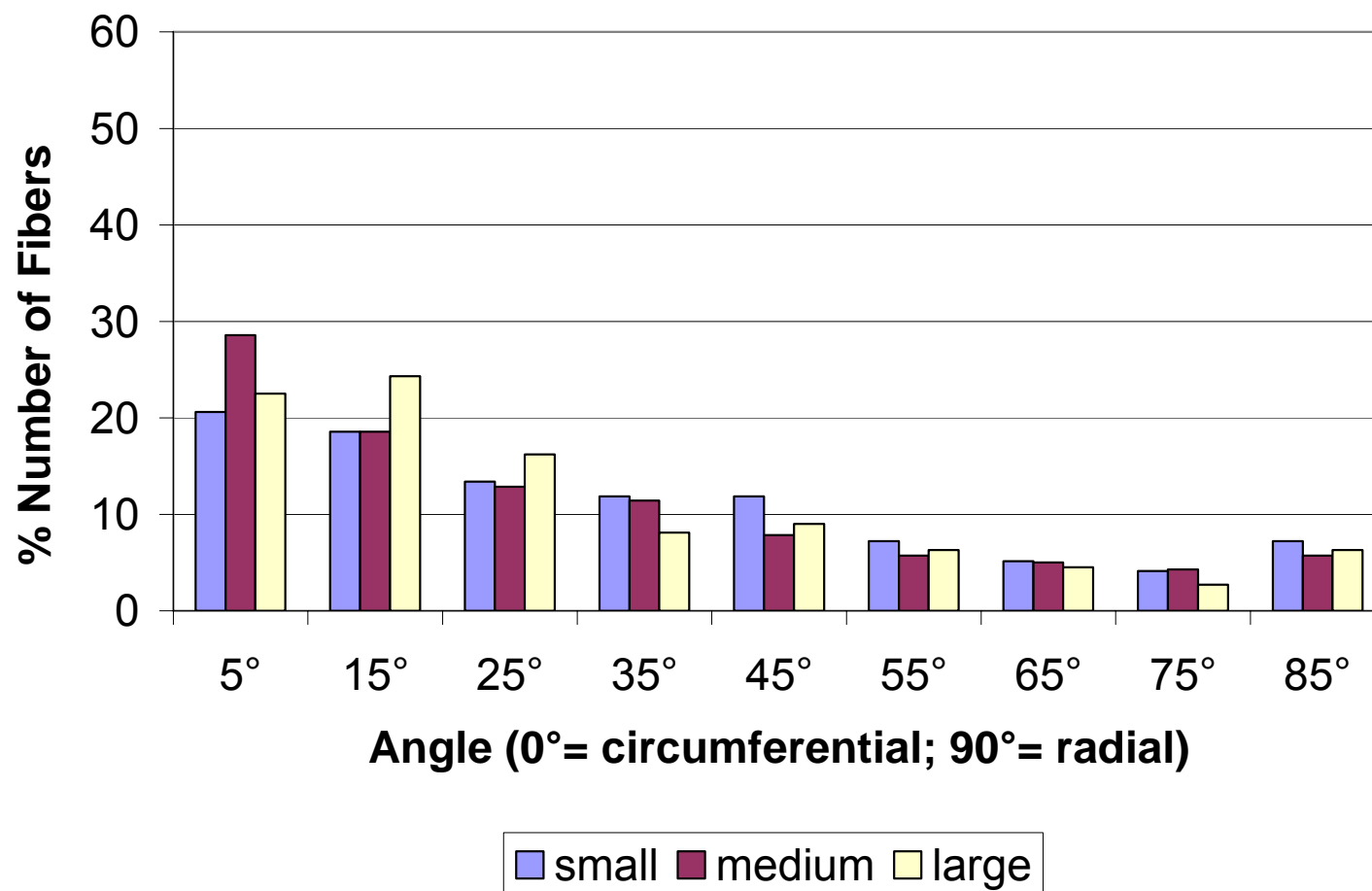


Figure 151: Distribution depending on rod diameter at 10cm electrode distance / 10kV electrostatic potential / 13rpm disc speed

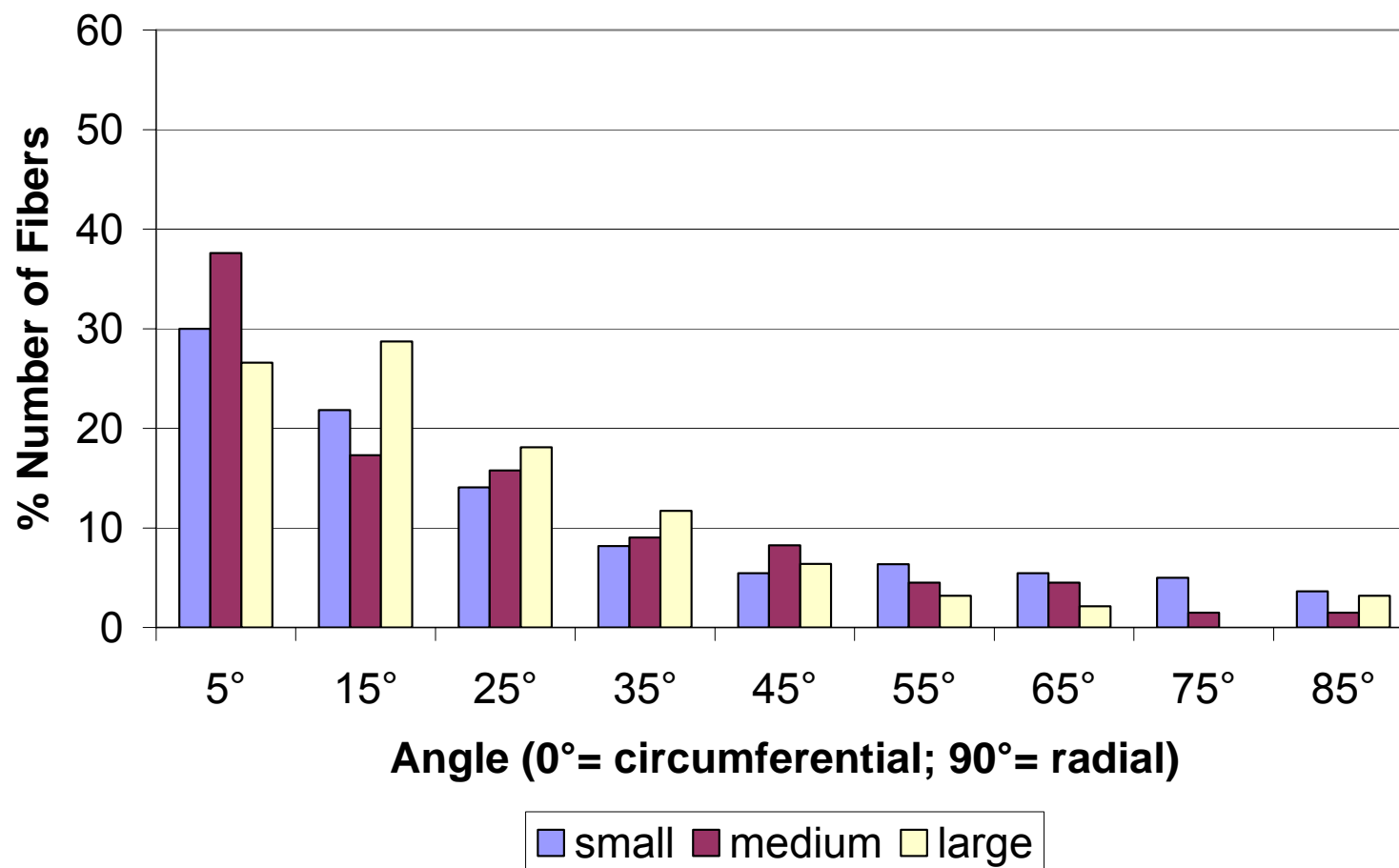


Figure 152: Distribution depending on rod diameter at 10cm electrode distance / 10kV electrostatic potential / 23.5rpm disc speed

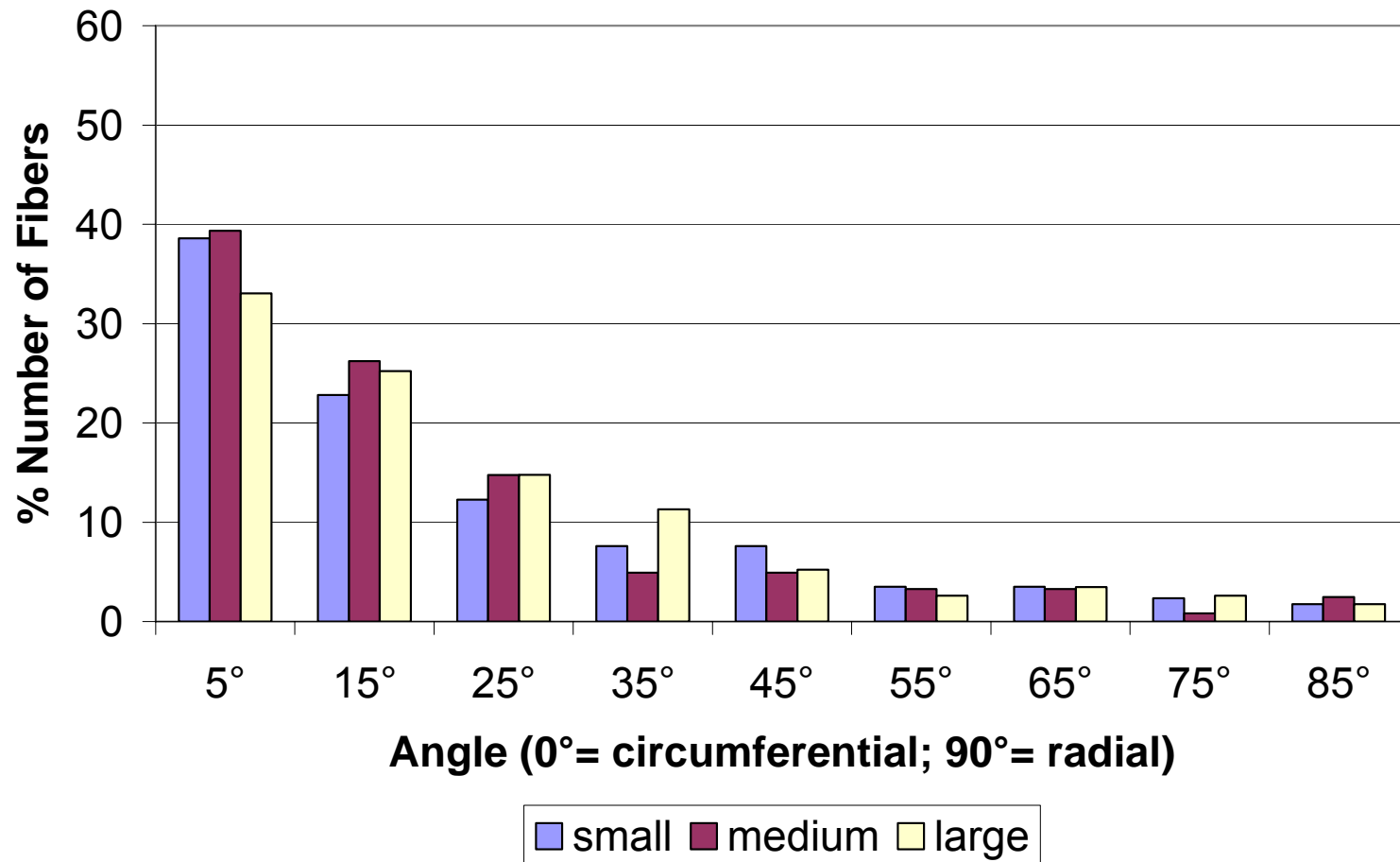


Figure 153: Distribution depending on rod diameter at 10cm electrode distance / 10kV electrostatic potential / 50rpm disc speed

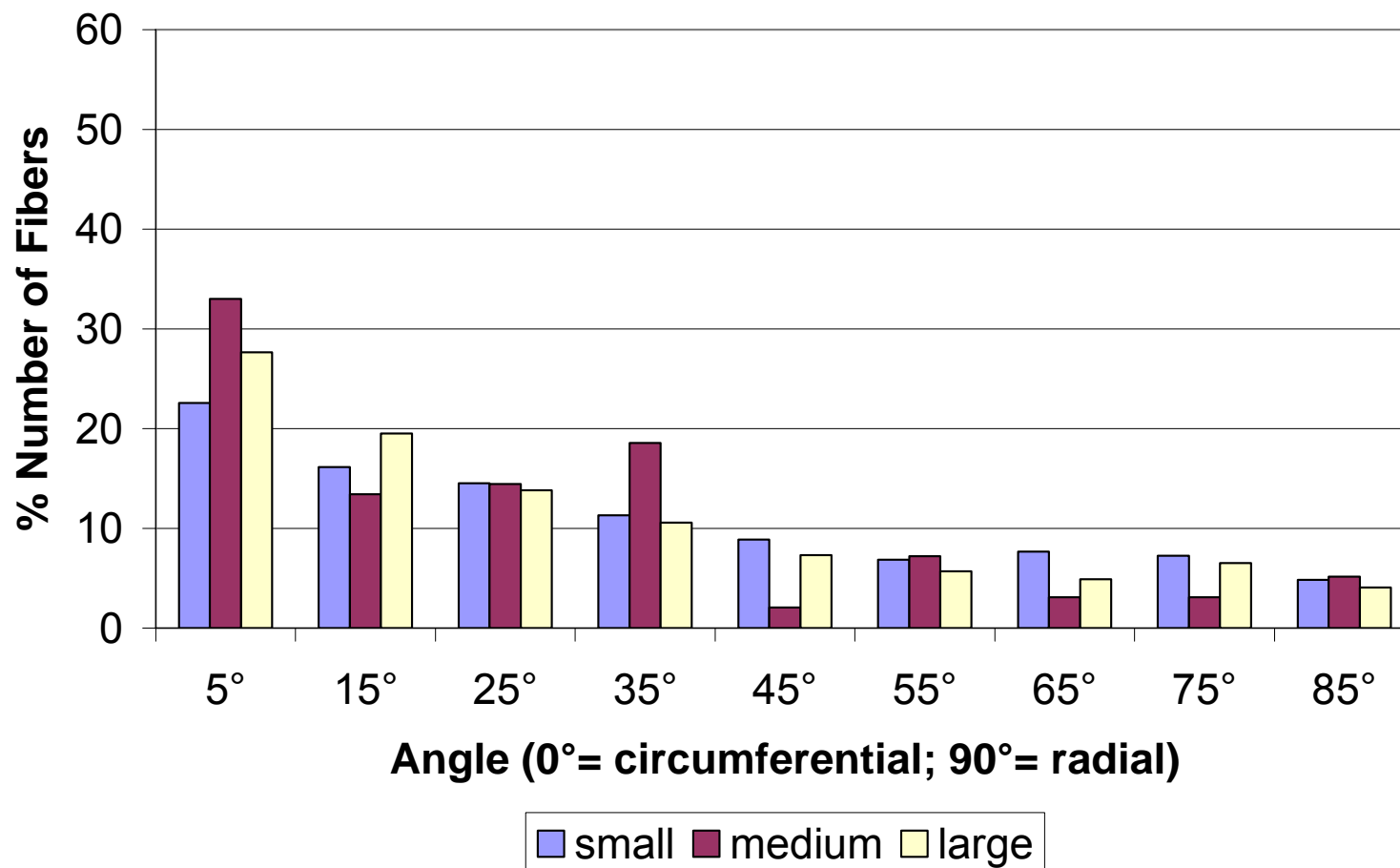


Figure 154: Distribution depending on rod diameter at 10cm electrode distance / 20kV electrostatic potential / 13rpm disc speed

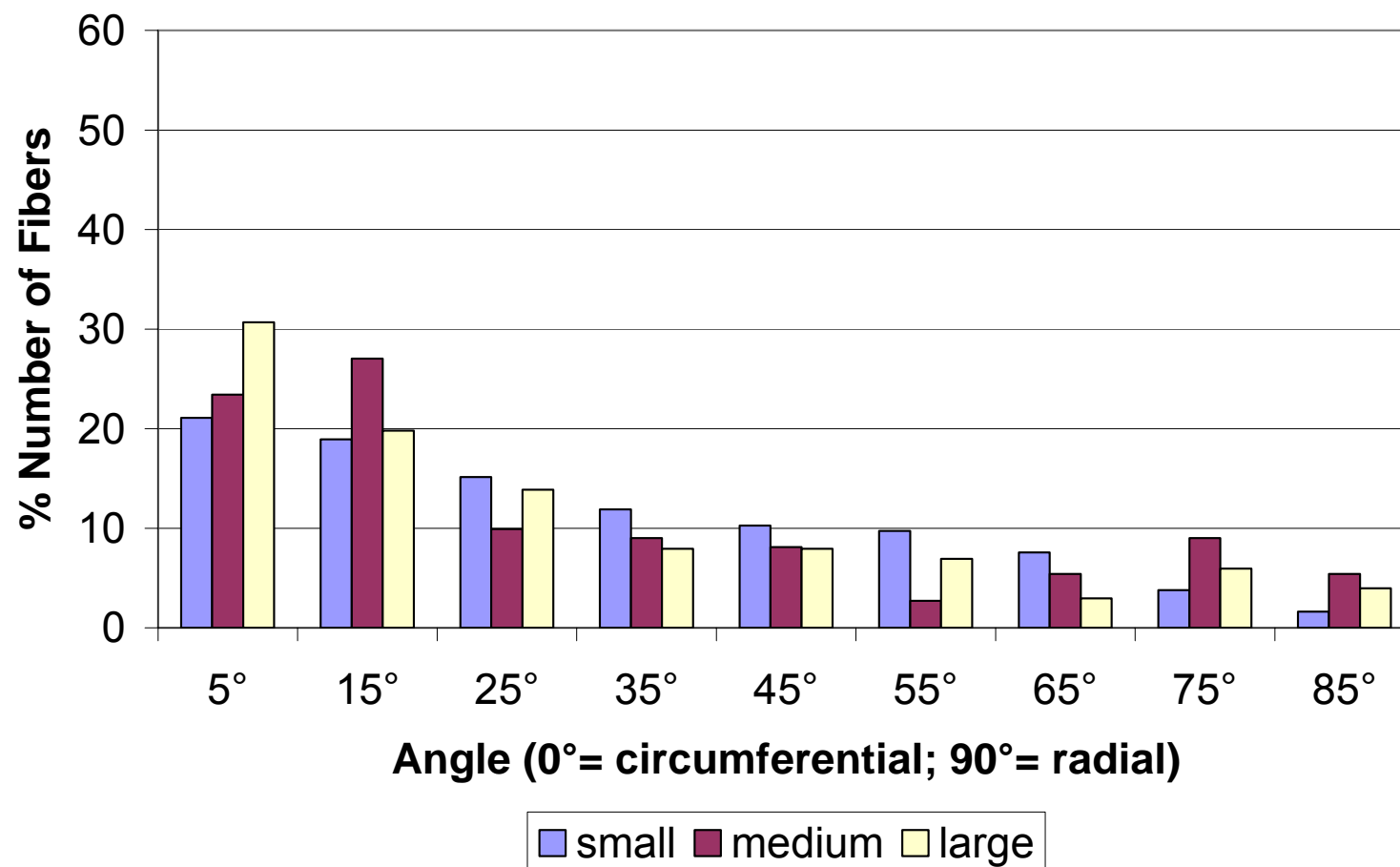


Figure 155: Distribution depending on rod diameter at 10cm electrode distance / 20kV electrostatic potential / 23.5rpm disc speed

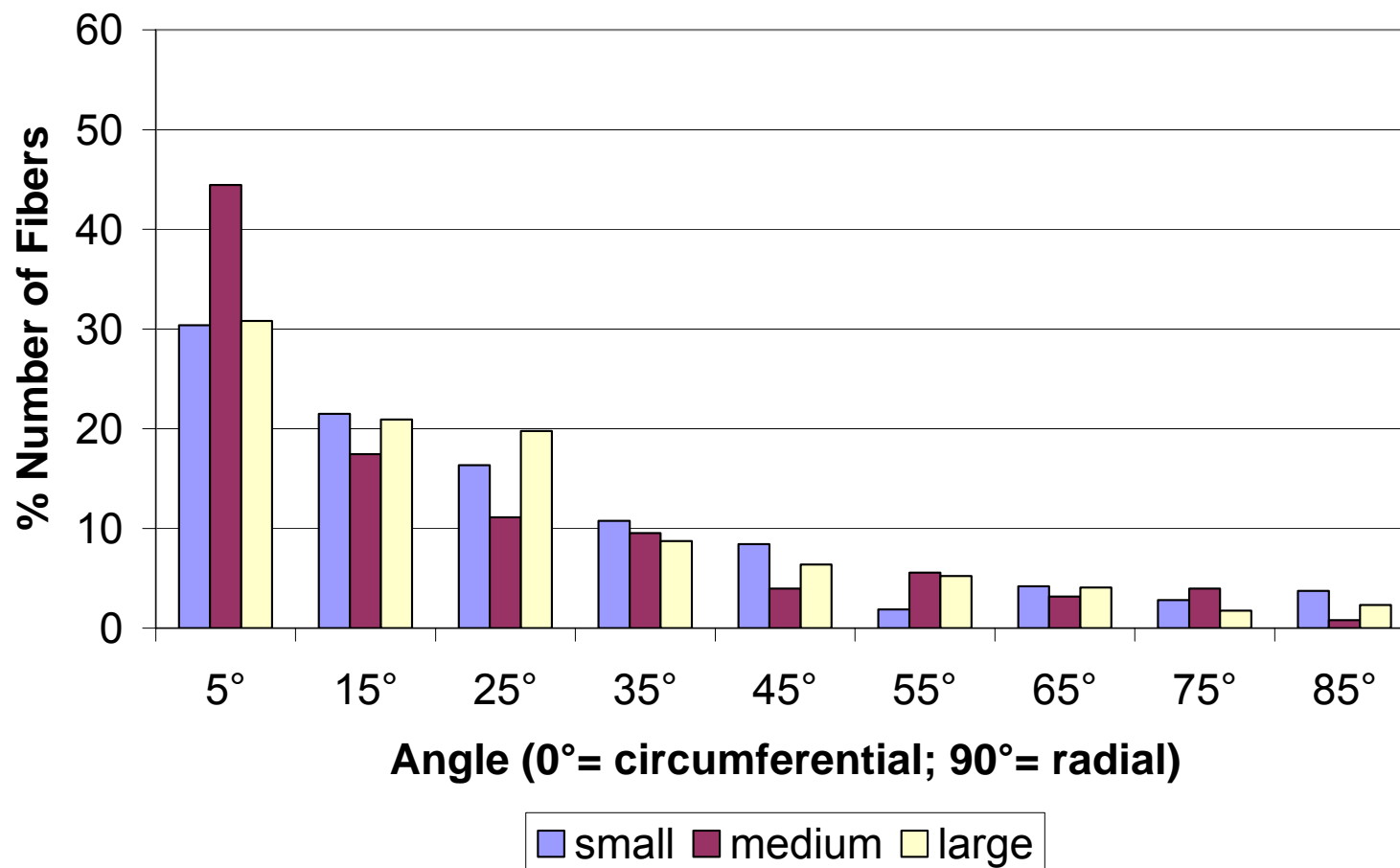


Figure 156: Distribution depending on rod diameter at 10cm electrode distance / 20kV electrostatic potential / 50rpm disc speed

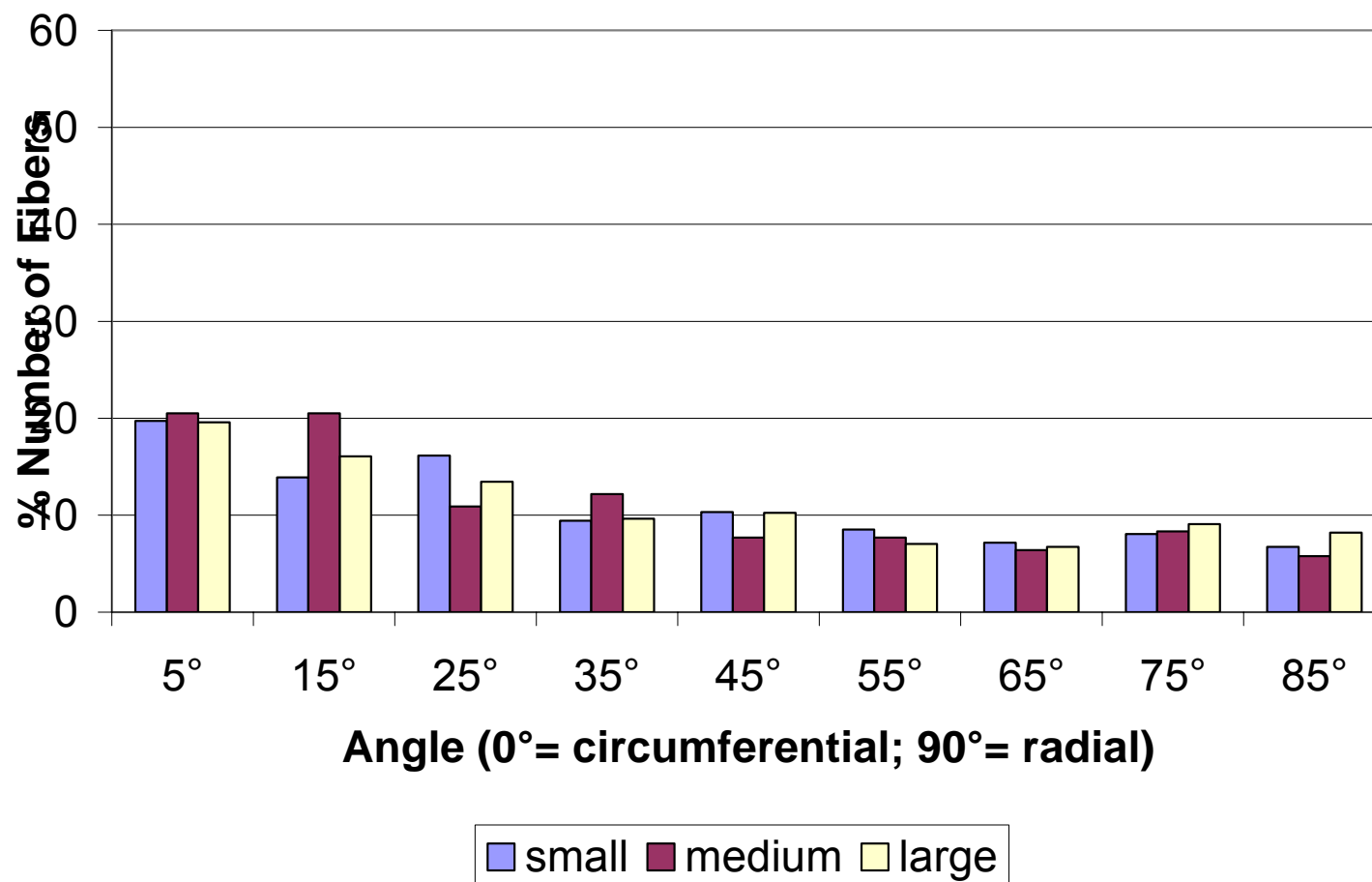


Figure 157: Distribution depending on rod diameter at 10cm electrode distance / 50kV electrostatic potential / 13rpm disc speed

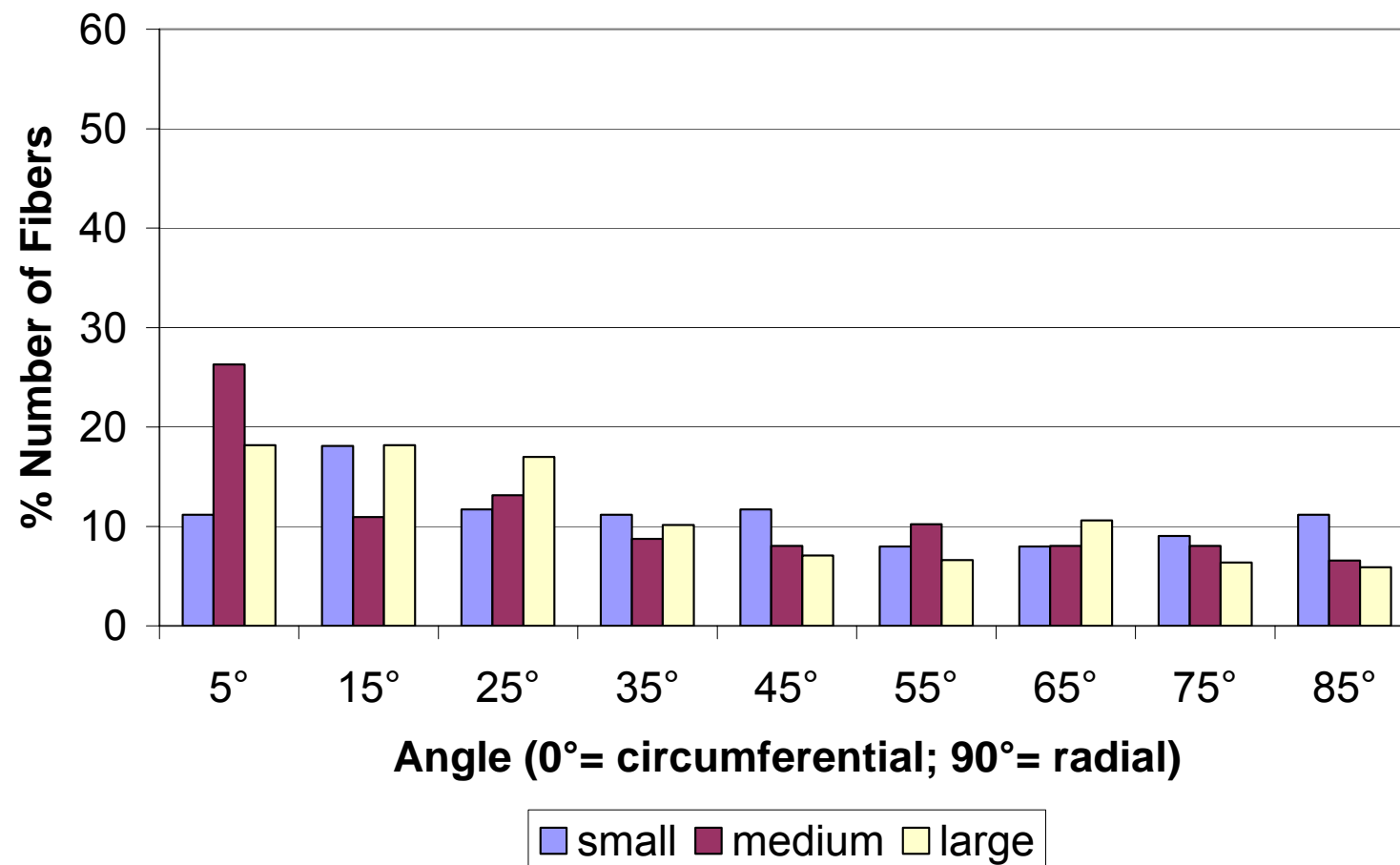


Figure 158: Distribution depending on rod diameter at 10cm electrode distance / 50kV electrostatic potential / 23.5rpm disc speed

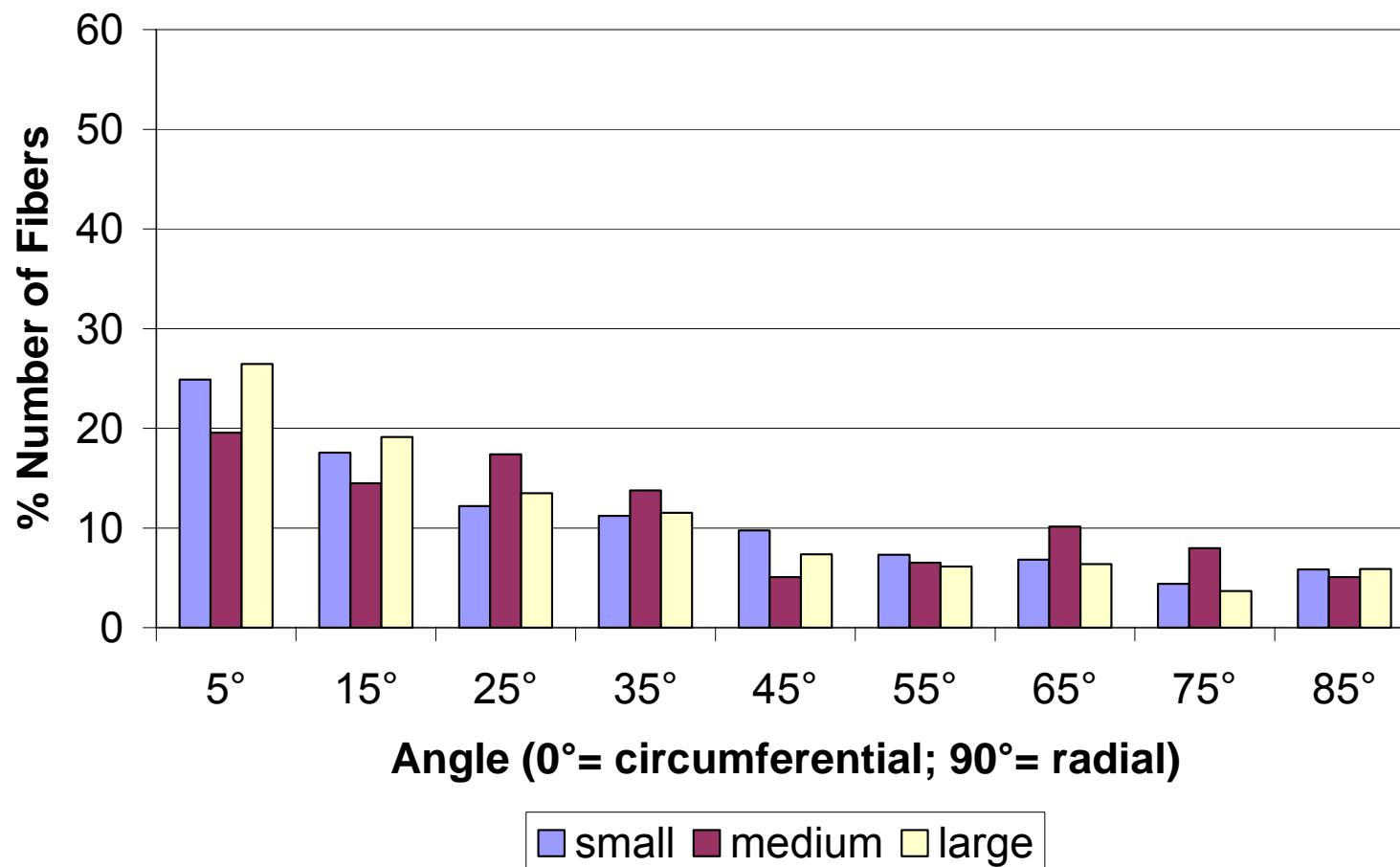


Figure 159: Distribution depending on rod diameter at 10cm electrode distance / 50kV electrostatic potential / 50rpm disc speed

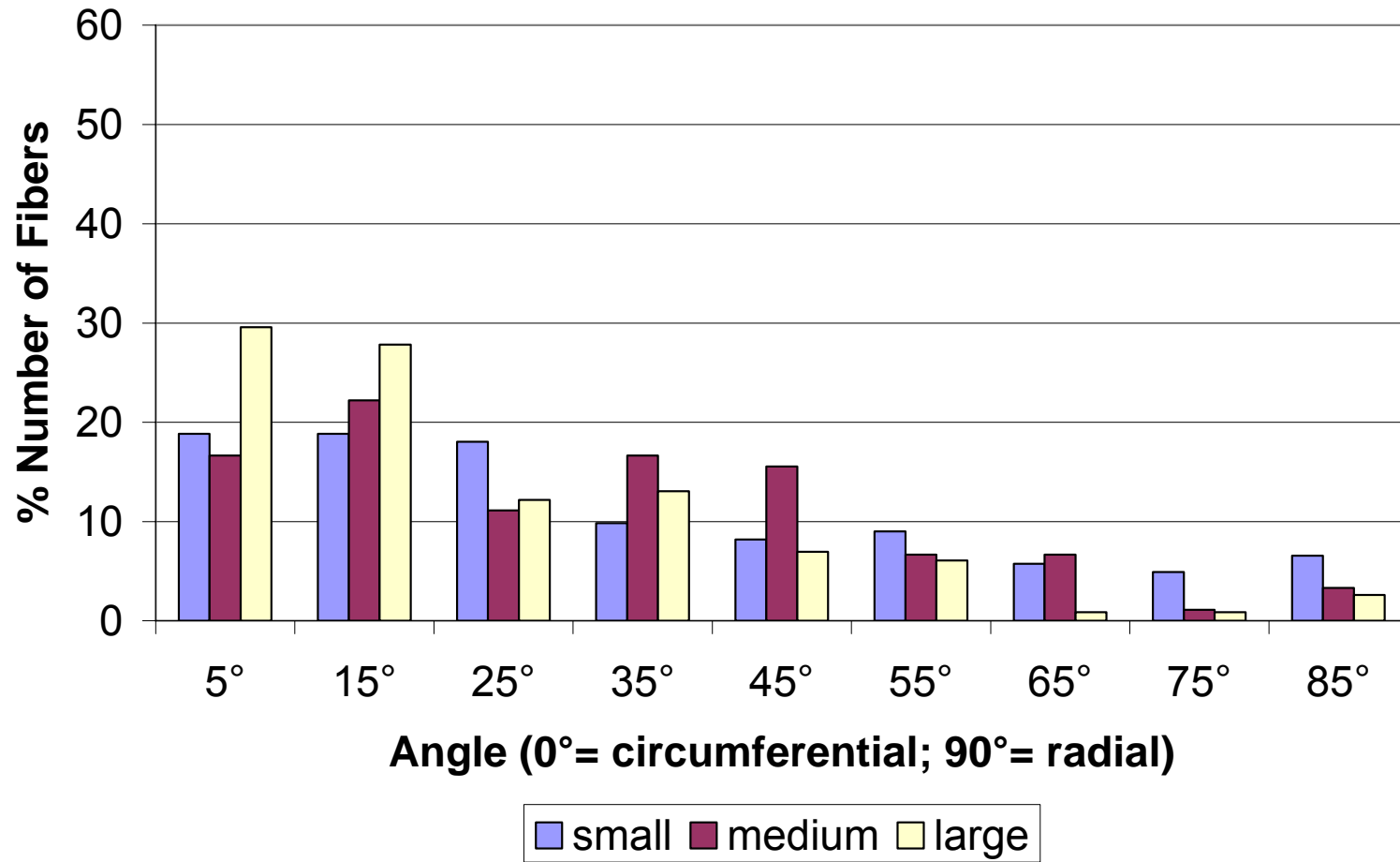


Figure 160: Distribution depending on rod diameter at 20cm electrode distance / 10kV electrostatic potential / 13rpm disc speed

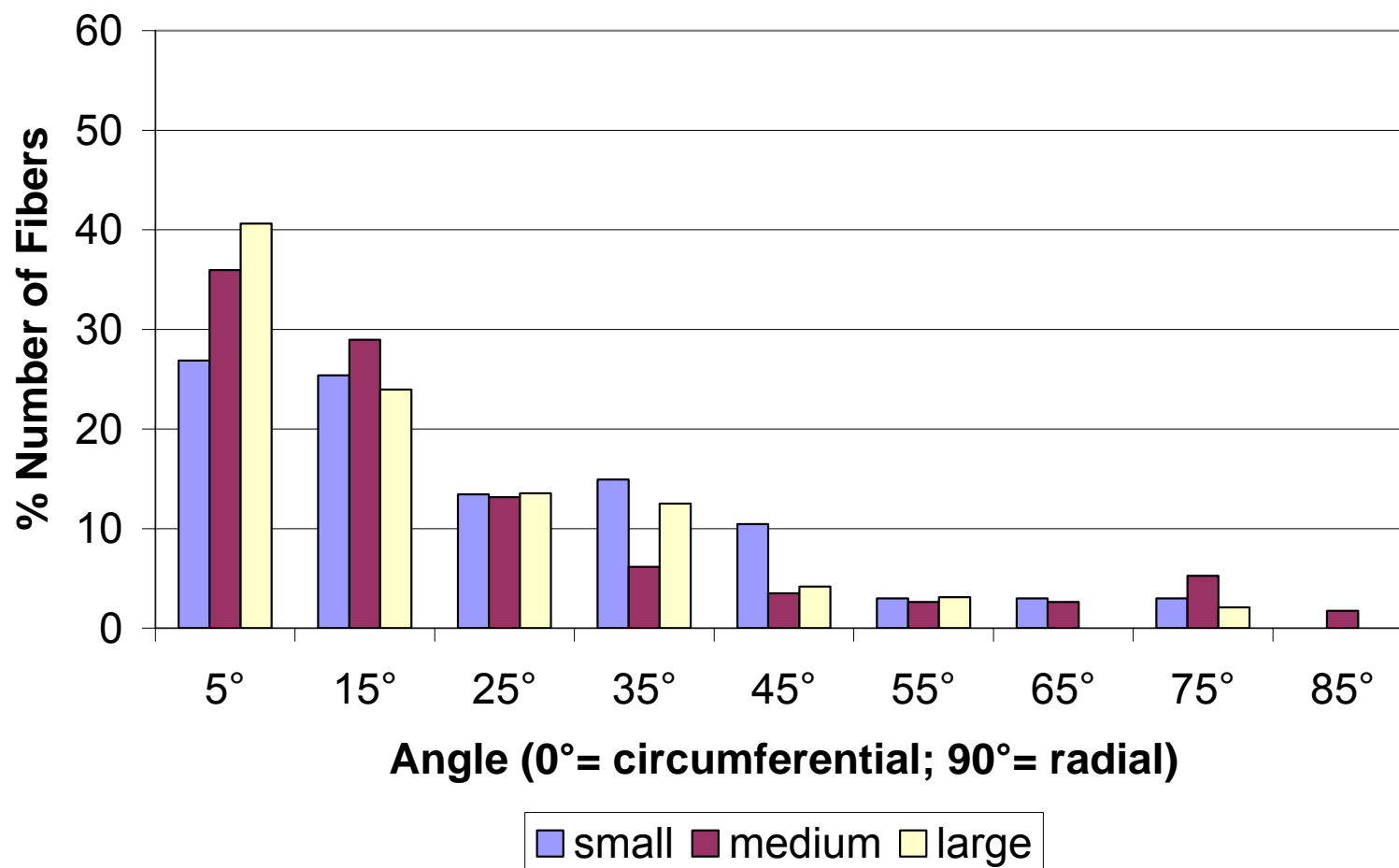


Figure 161: Distribution depending on rod diameter at 20cm electrode distance / 10kV electrostatic potential / 23.5rpm disc speed

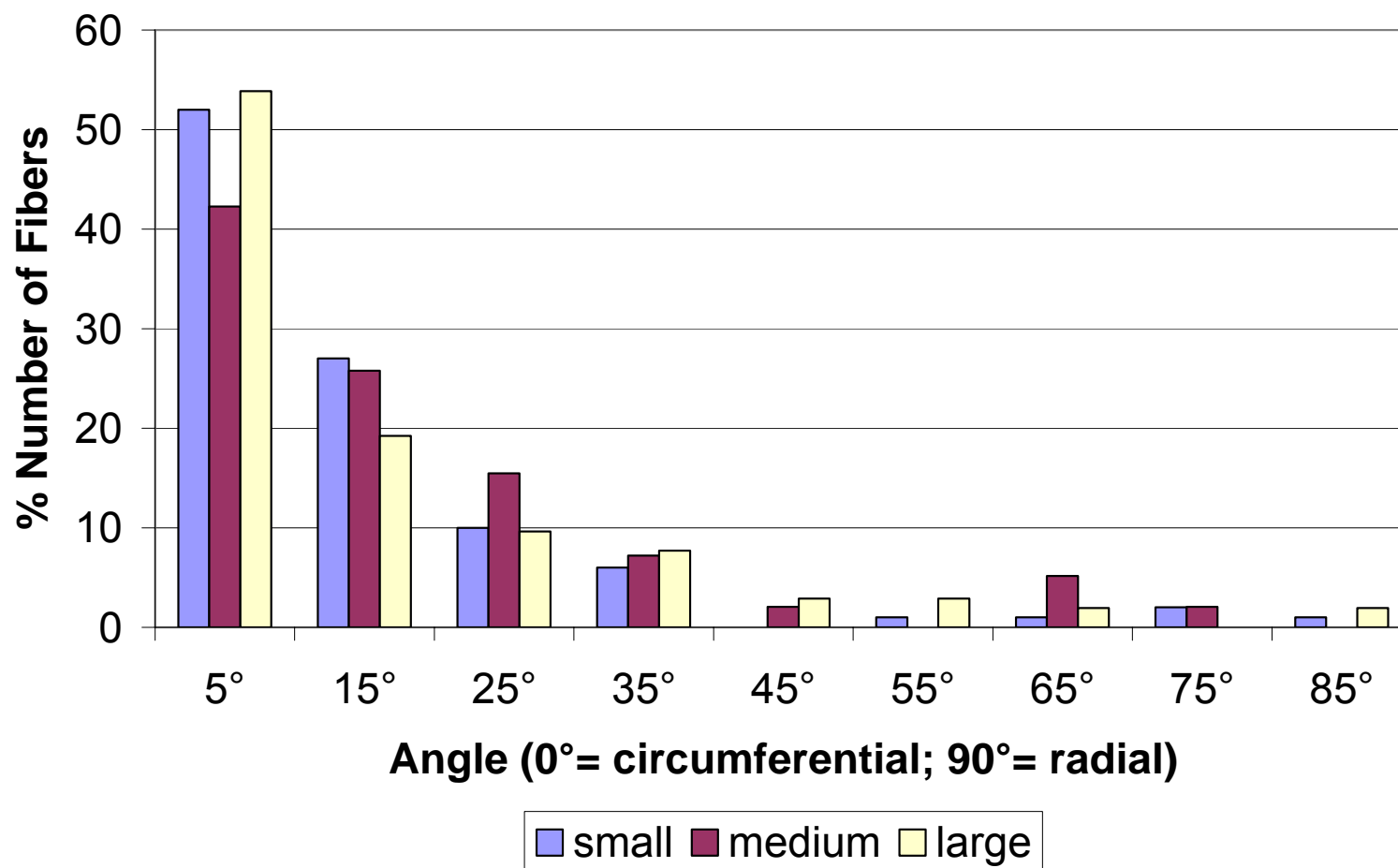


Figure 162: Distribution depending on rod diameter at 20cm electrode distance / 10kV electrostatic potential / 50rpm disc speed

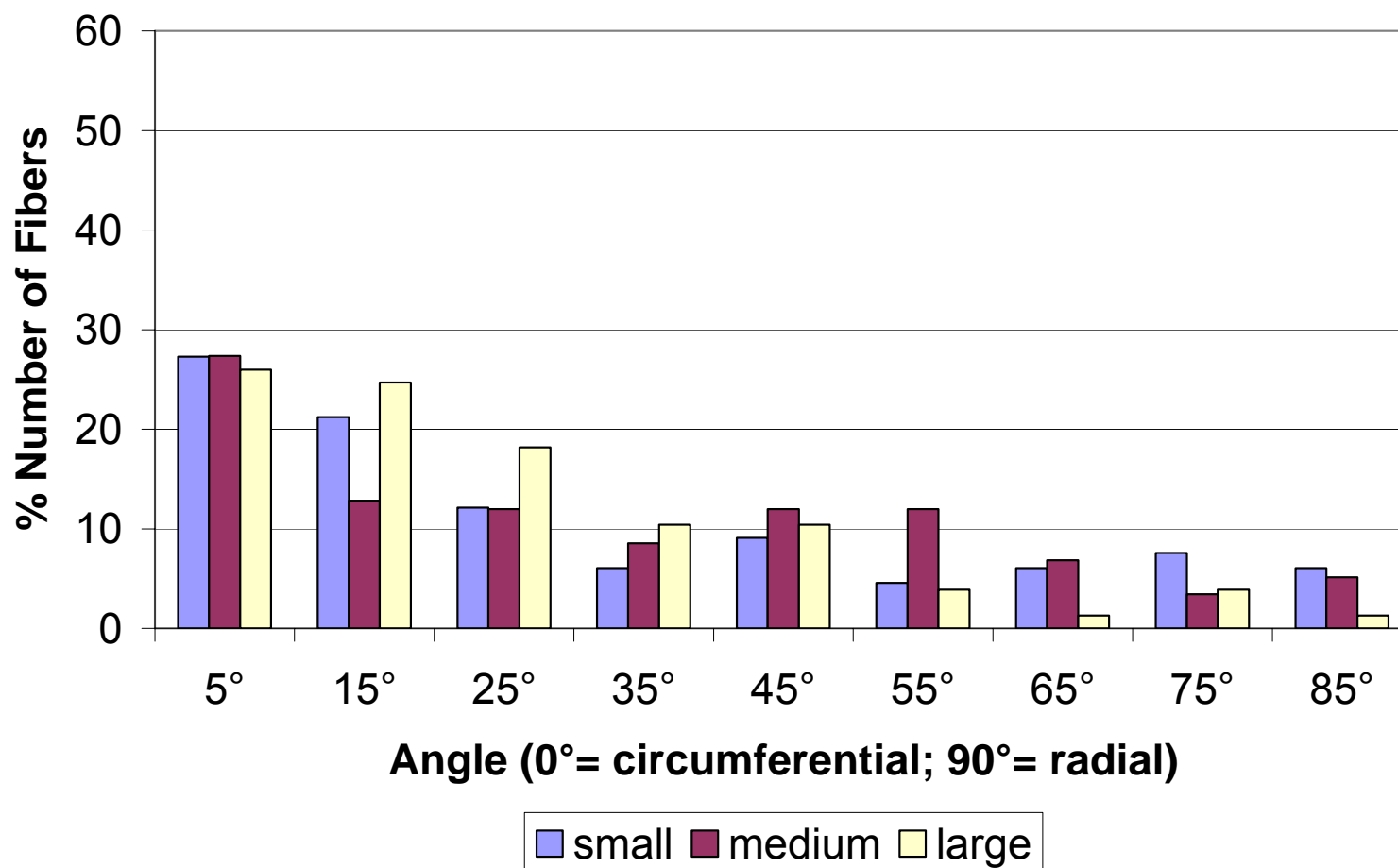


Figure 163: Distribution depending on rod diameter at 20cm electrode distance / 20kV electrostatic potential / 13rpm disc speed

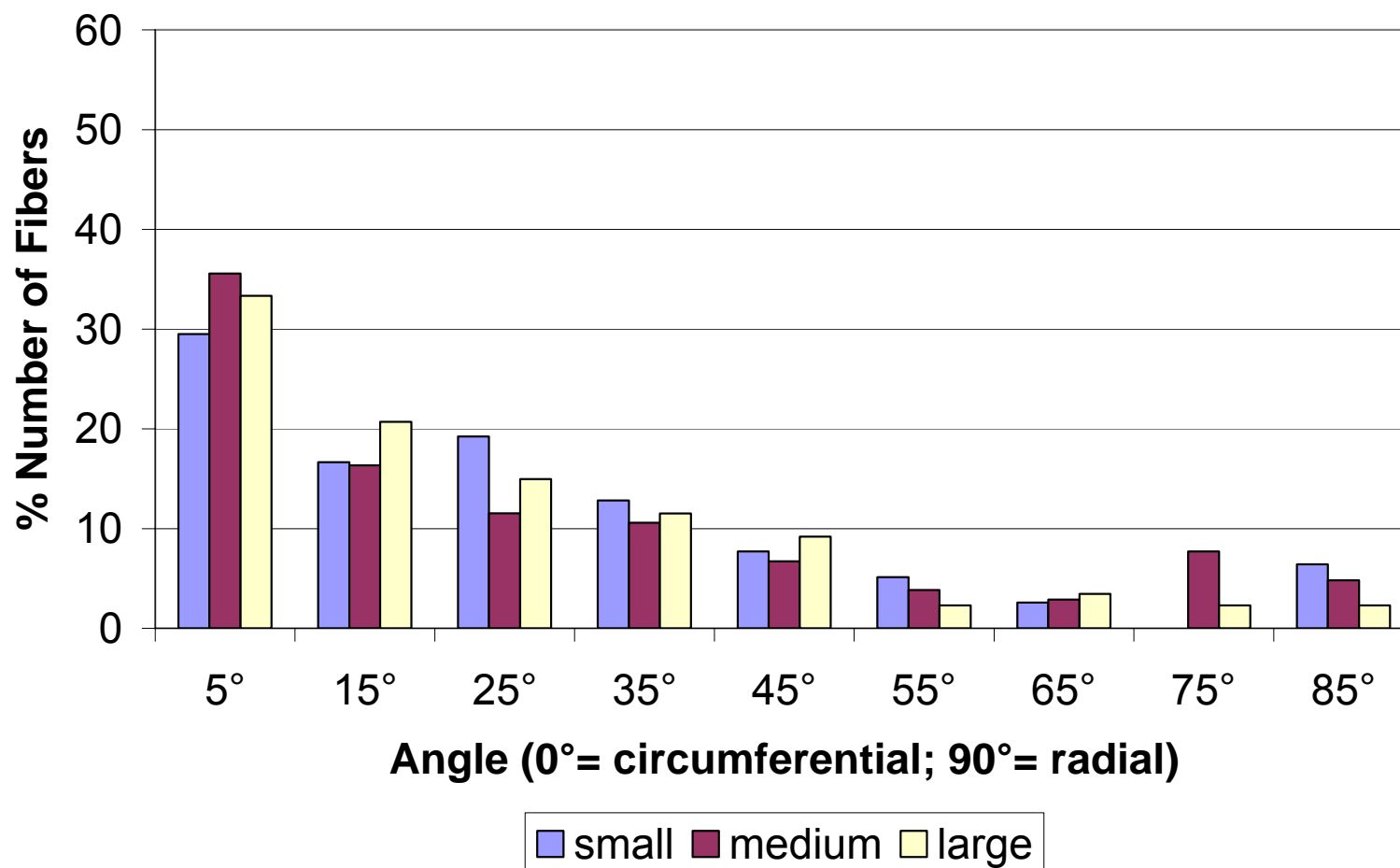


Figure 164: Distribution depending on rod diameter at 20cm electrode distance / 20kV electrostatic potential / 23.5rpm disc speed

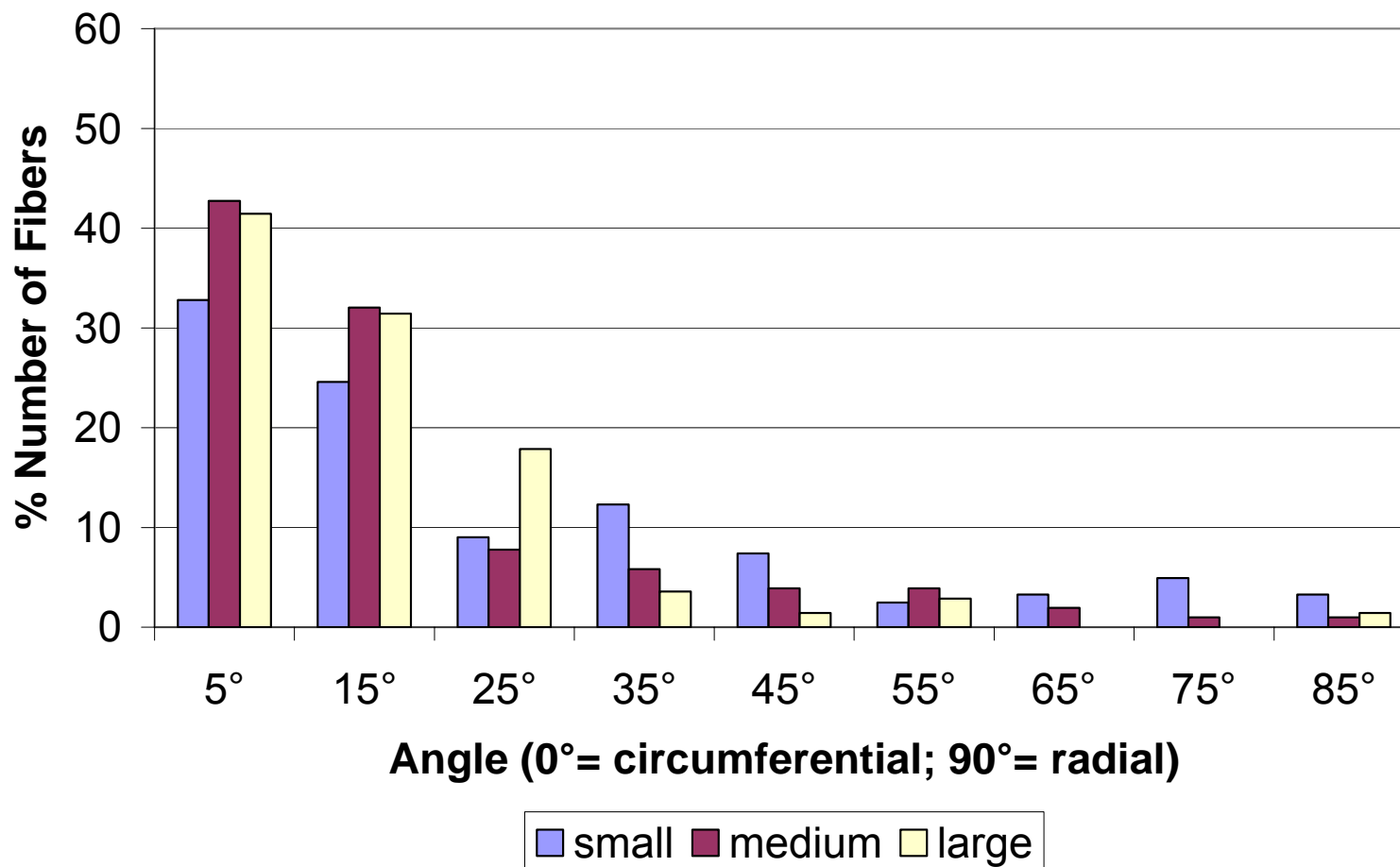


Figure 165: Distribution depending on rod diameter at 20cm electrode distance / 20kV electrostatic potential / 50rpm disc speed

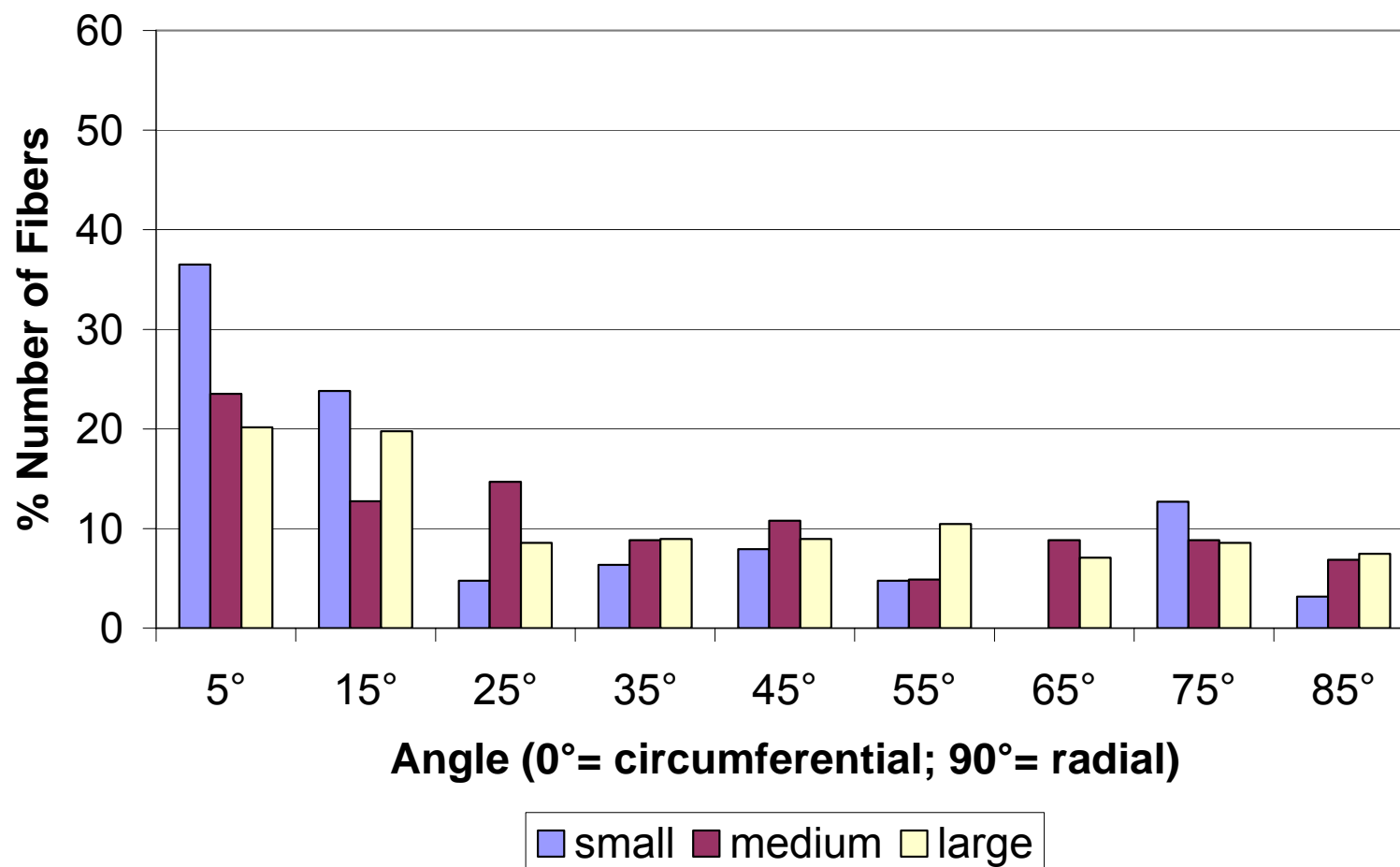


Figure 166: Distribution depending on rod diameter at 20cm electrode distance / 50kV electrostatic potential / 13rpm disc speed

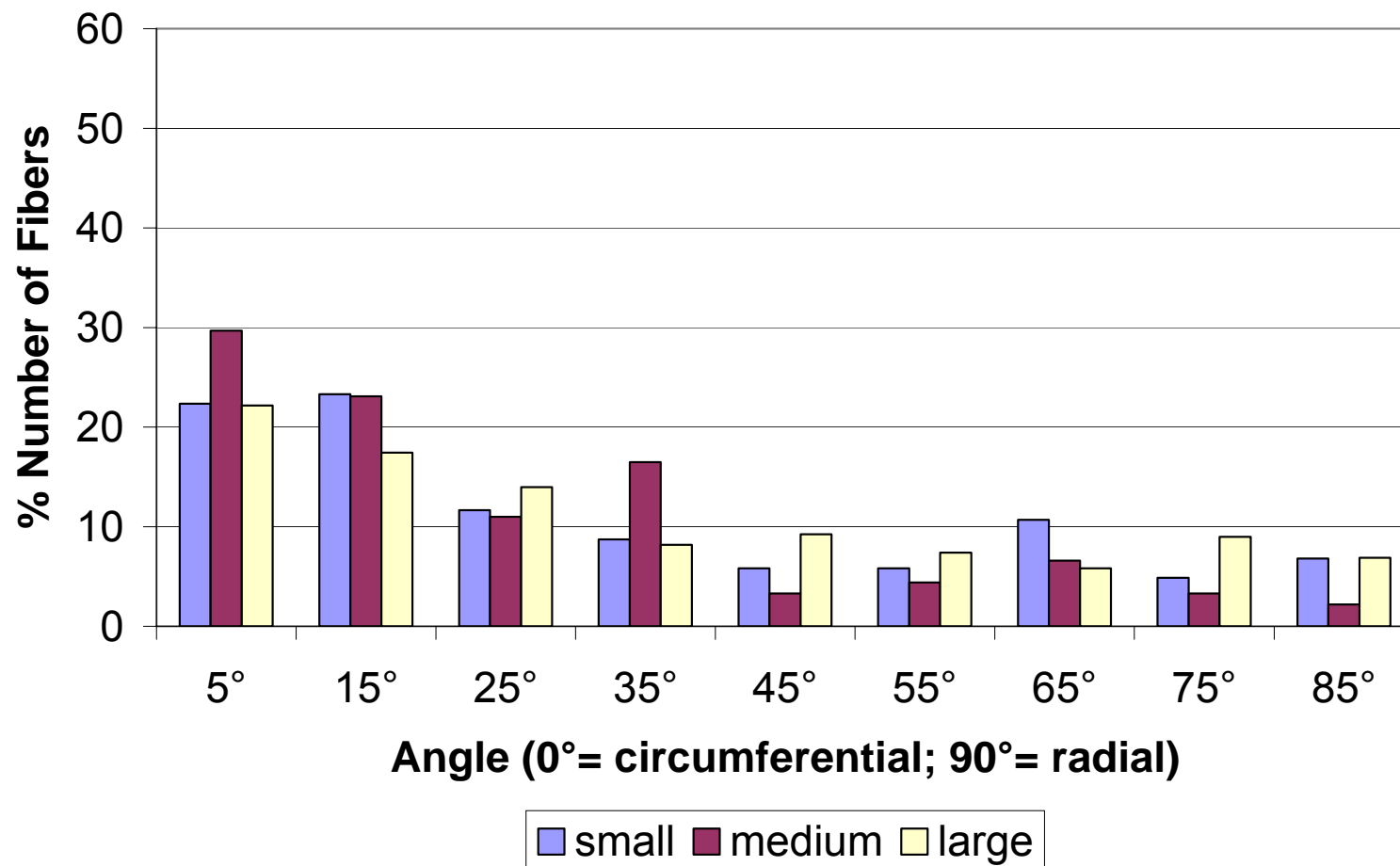


Figure 167: Distribution depending on rod diameter at 20cm electrode distance / 50kV electrostatic potential / 23.5rpm disc speed

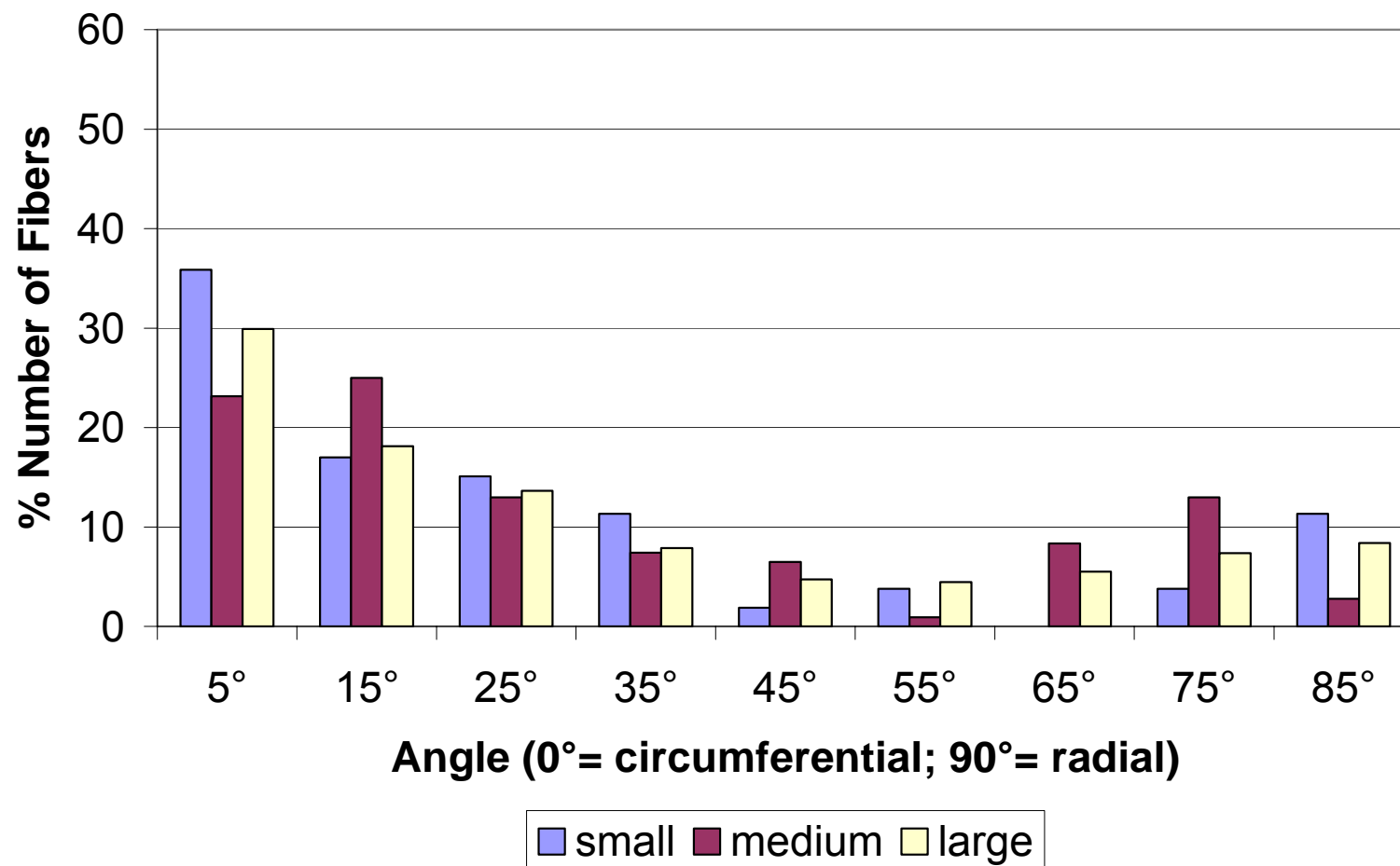


Figure 168: Distribution depending on rod diameter at 20cm electrode distance / 50kV electrostatic potential / 50rpm disc speed

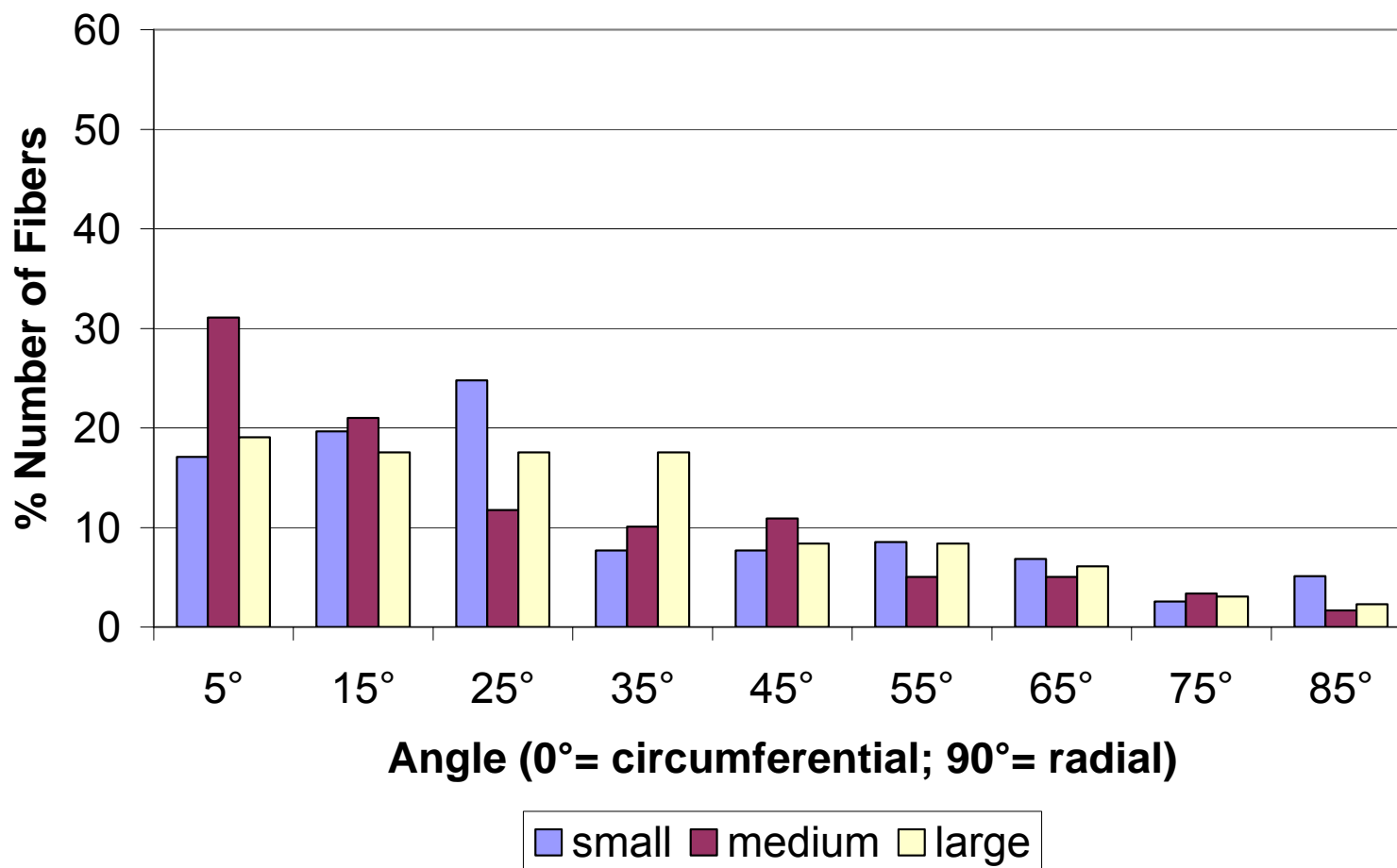


Figure 169: Distribution depending on rod diameter at 30cm electrode distance / 10kV electrostatic potential / 13rpm disc speed

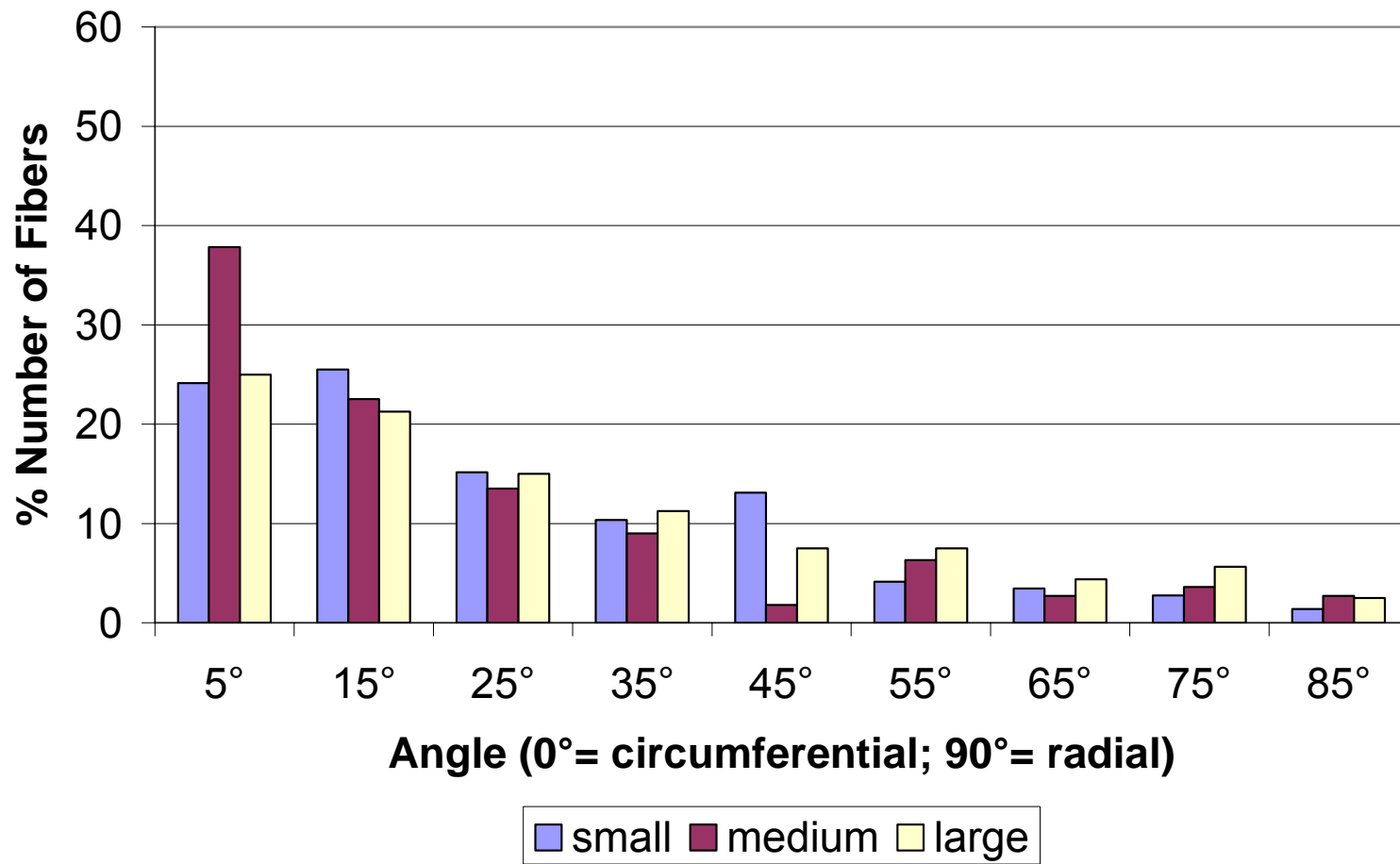


Figure 170: Distribution depending on rod diameter at 30cm electrode distance / 10kV electrostatic potential / 23.5rpm disc speed

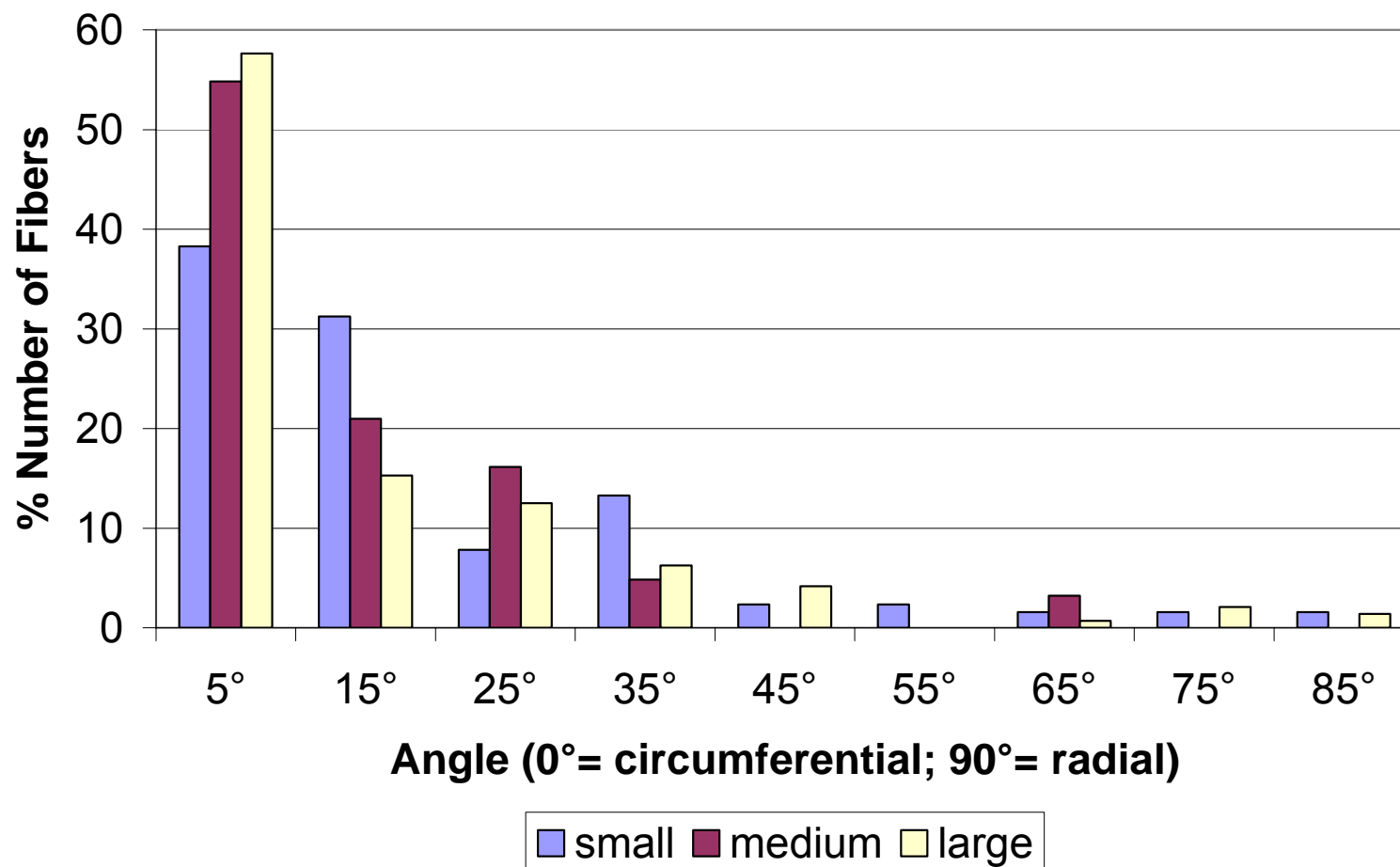


Figure 171: Distribution depending on rod diameter at 30cm electrode distance / 10kV electrostatic potential / 50rpm disc speed

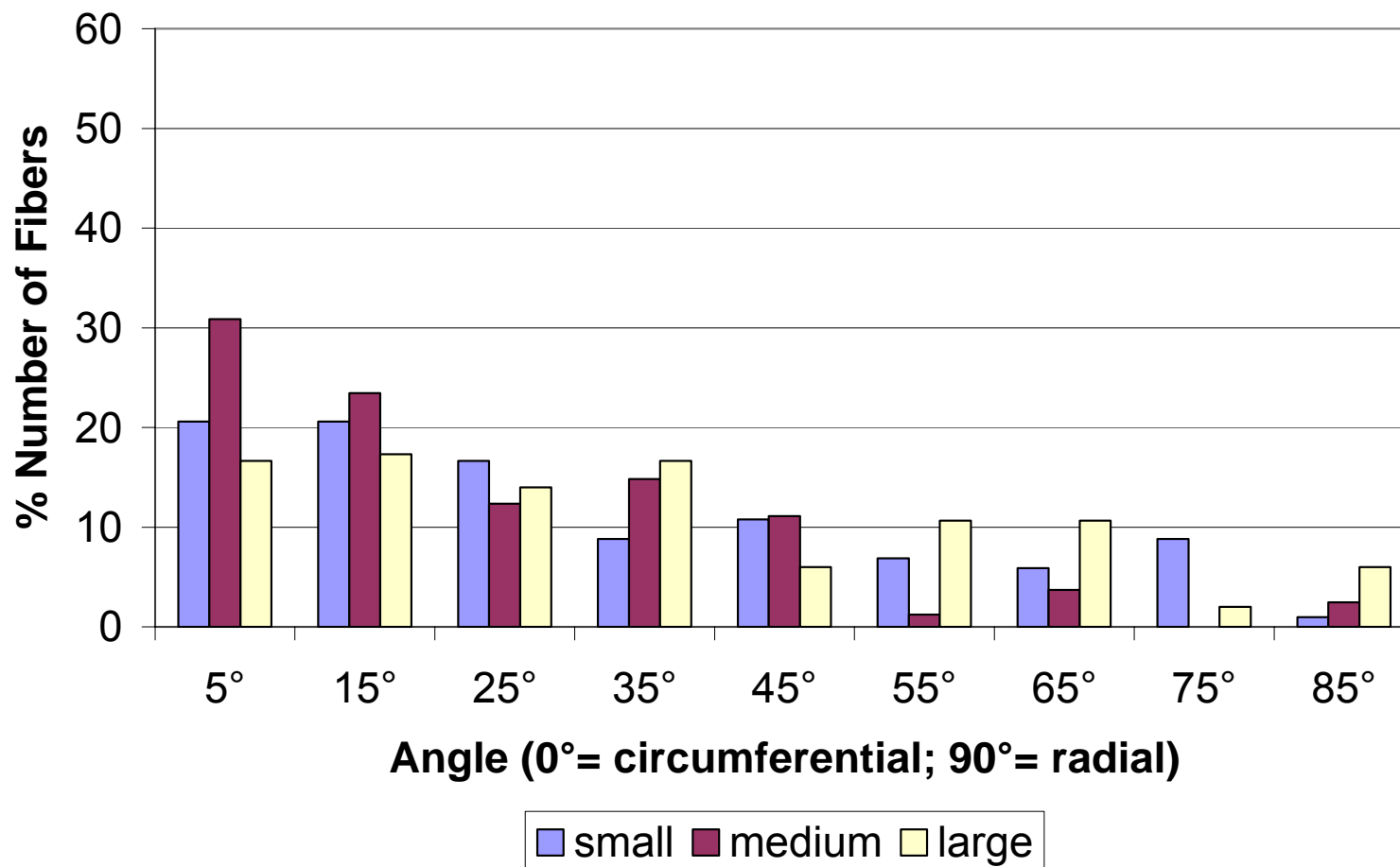


Figure 172: Distribution depending on rod diameter at 30cm electrode distance / 20kV electrostatic potential / 13rpm disc speed

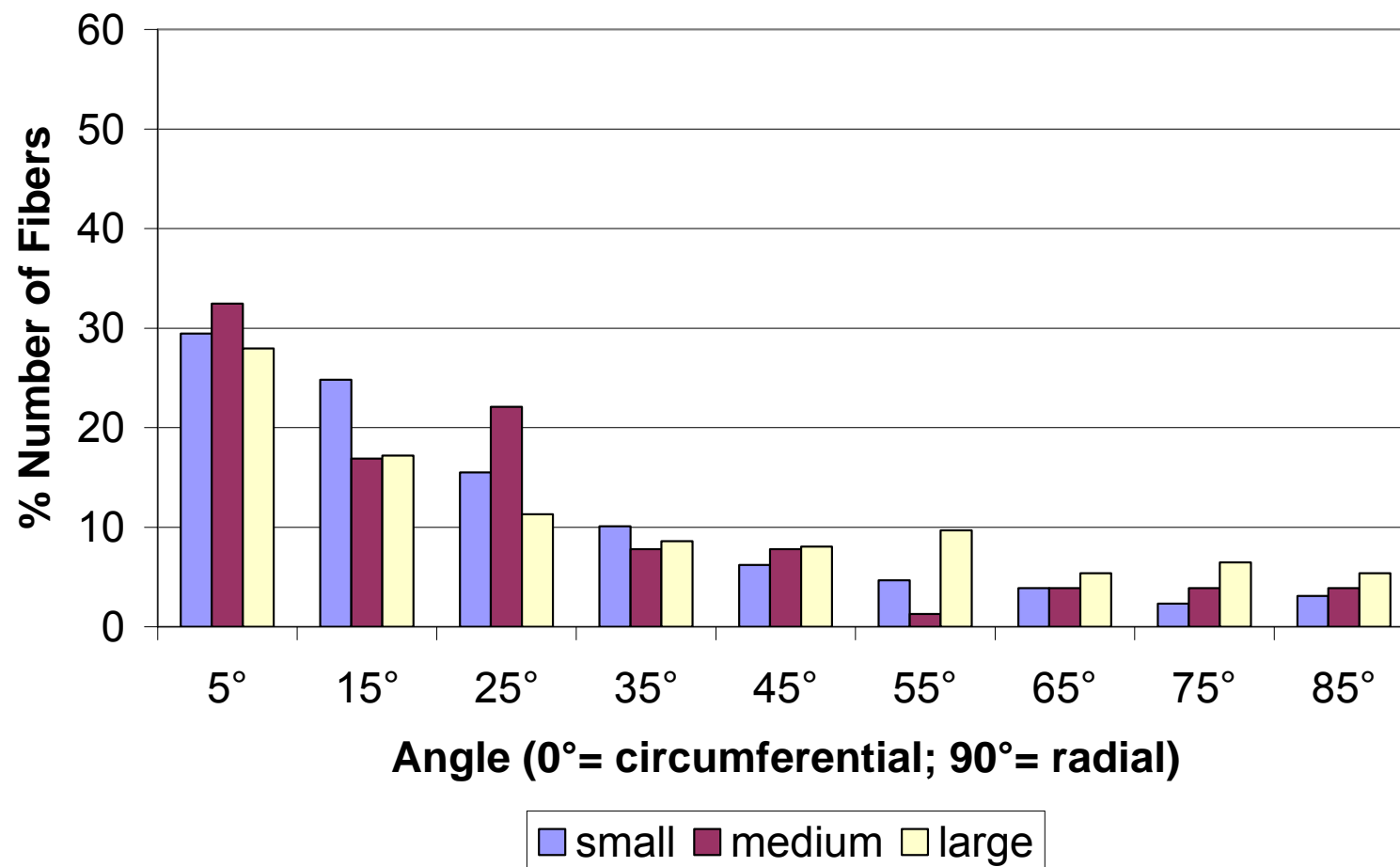


Figure 173: Distribution depending on rod diameter at 30cm electrode distance / 20kV electrostatic potential / 23.5rpm disc speed

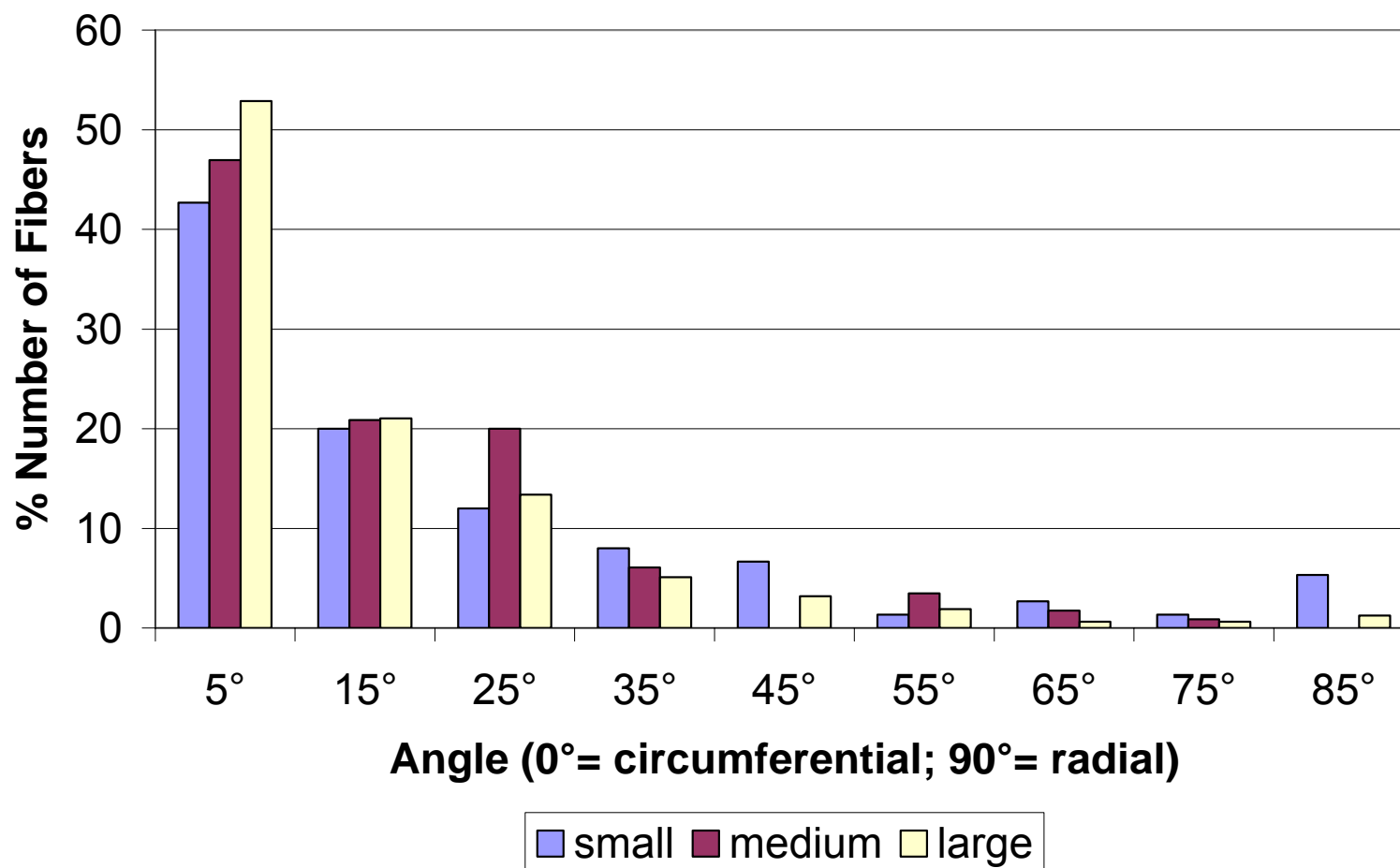


Figure 174: Distribution depending on rod diameter at 30cm electrode distance / 20kV electrostatic potential / 50rpm disc speed

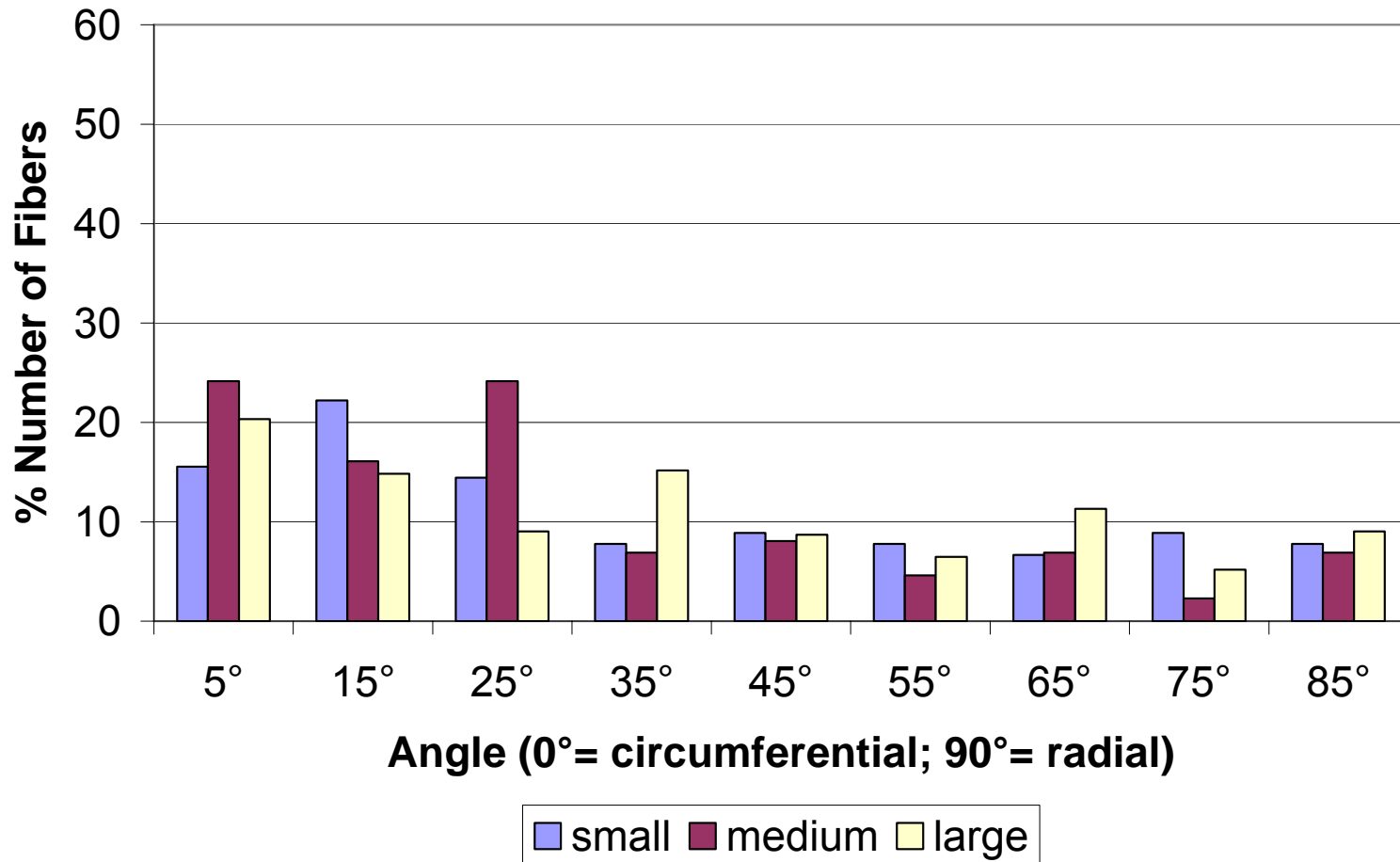


Figure 175: Distribution depending on rod diameter at 30cm electrode distance / 50kV electrostatic potential / 13rpm disc speed

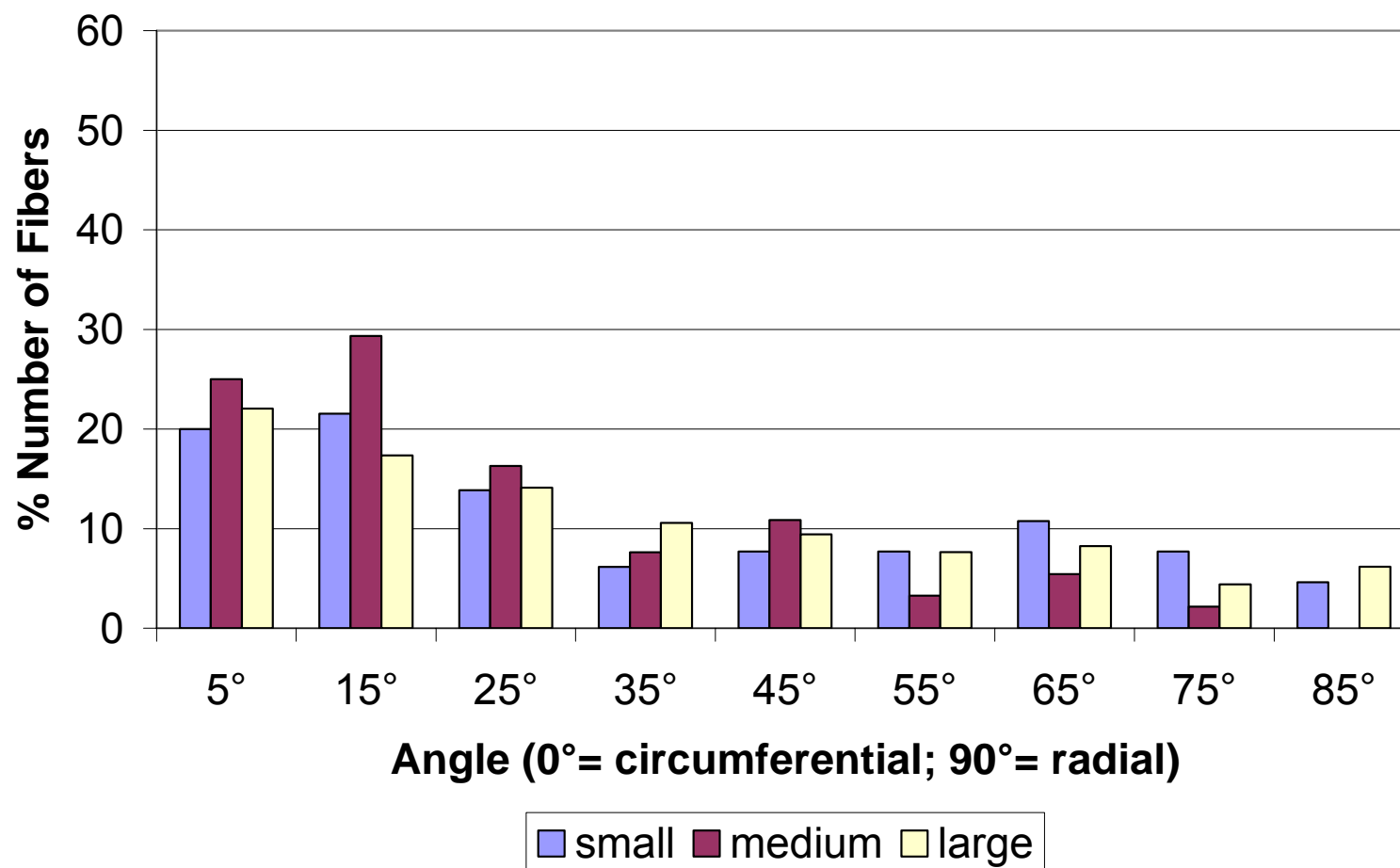


Figure 176: Distribution depending on rod diameter at 30cm electrode distance / 50kV electrostatic potential / 23.5rpm disc speed

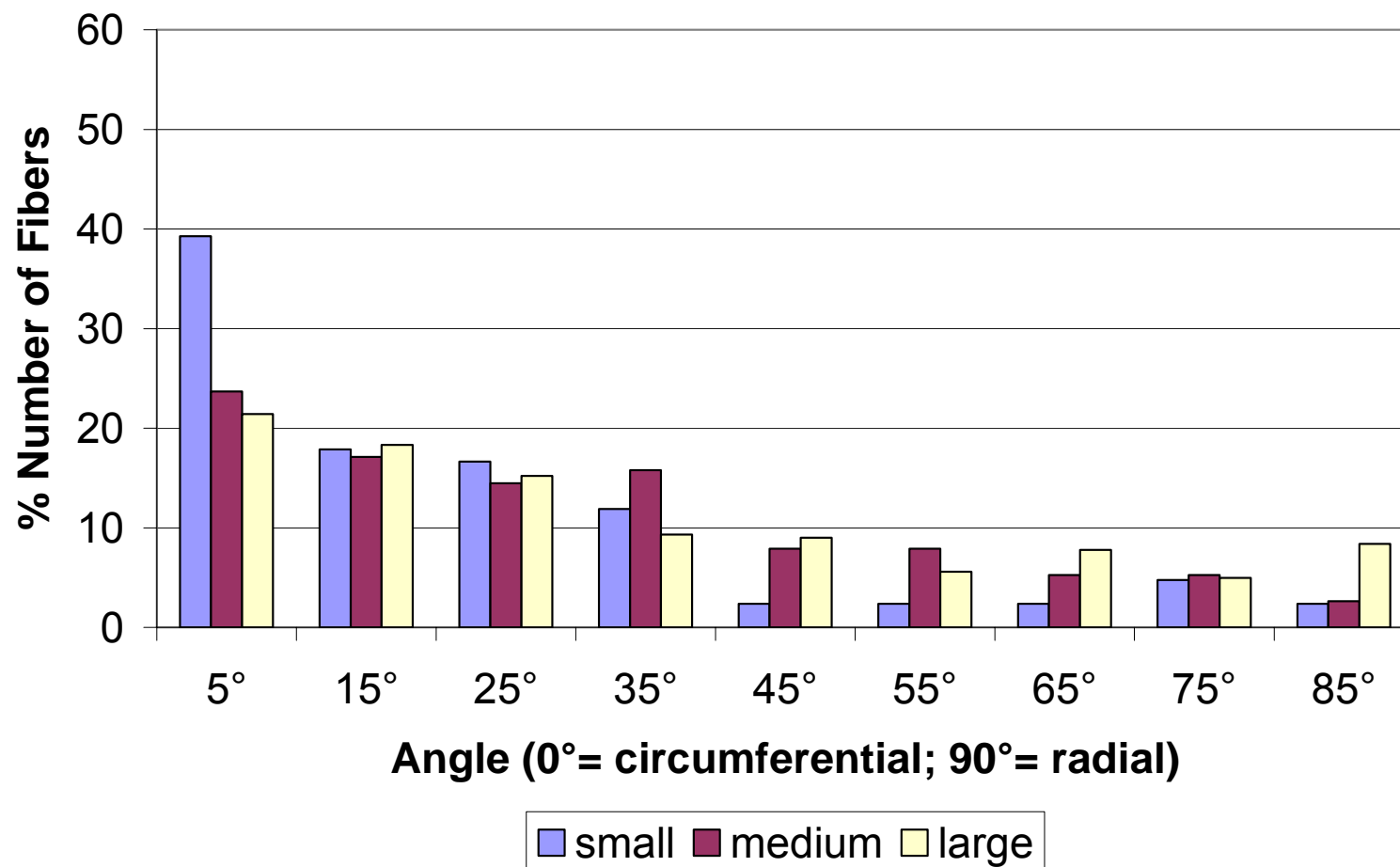


Figure 177: Distribution depending on rod diameter at 30cm electrode distance / 50kV electrostatic potential / 50rpm disc speed

### Appendix III: First Order Interaction Graphs

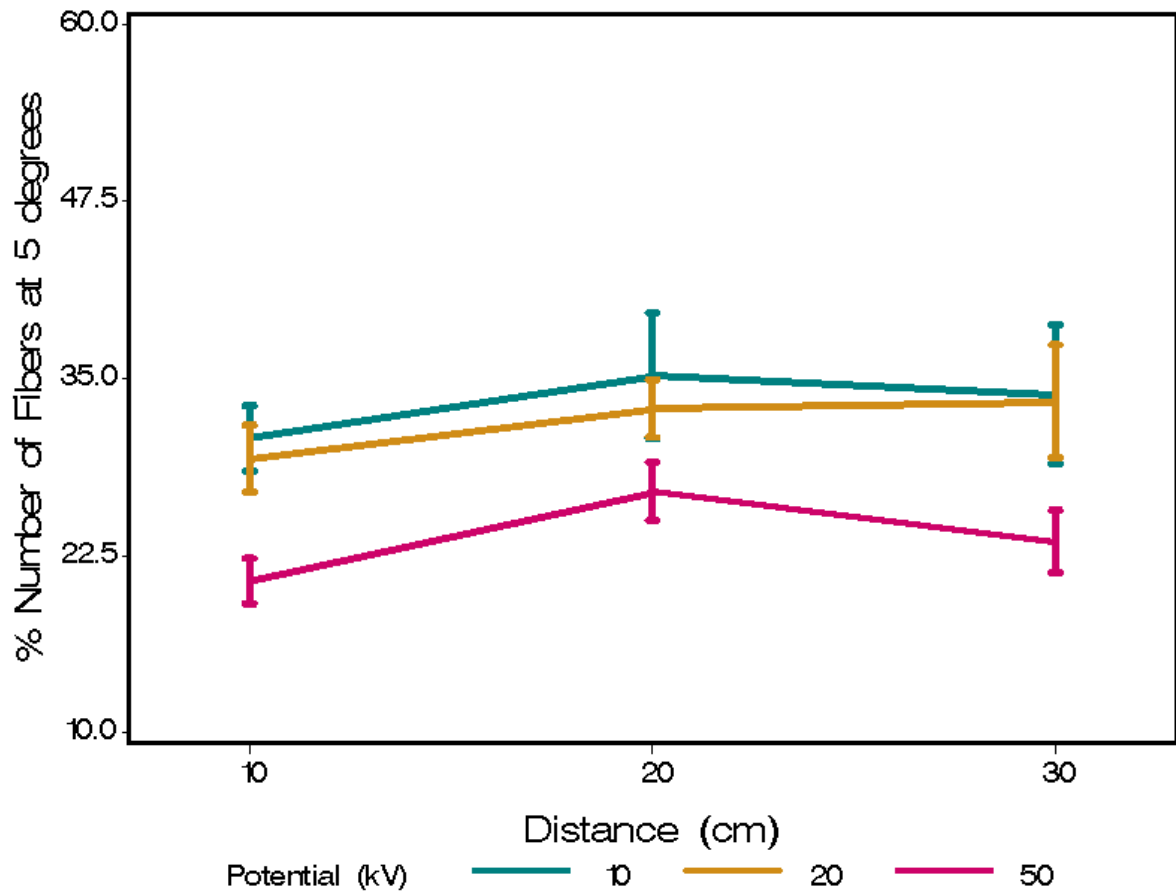


Figure 178: Percent number of fibers at 5° corresponding to the interaction of distance and potential

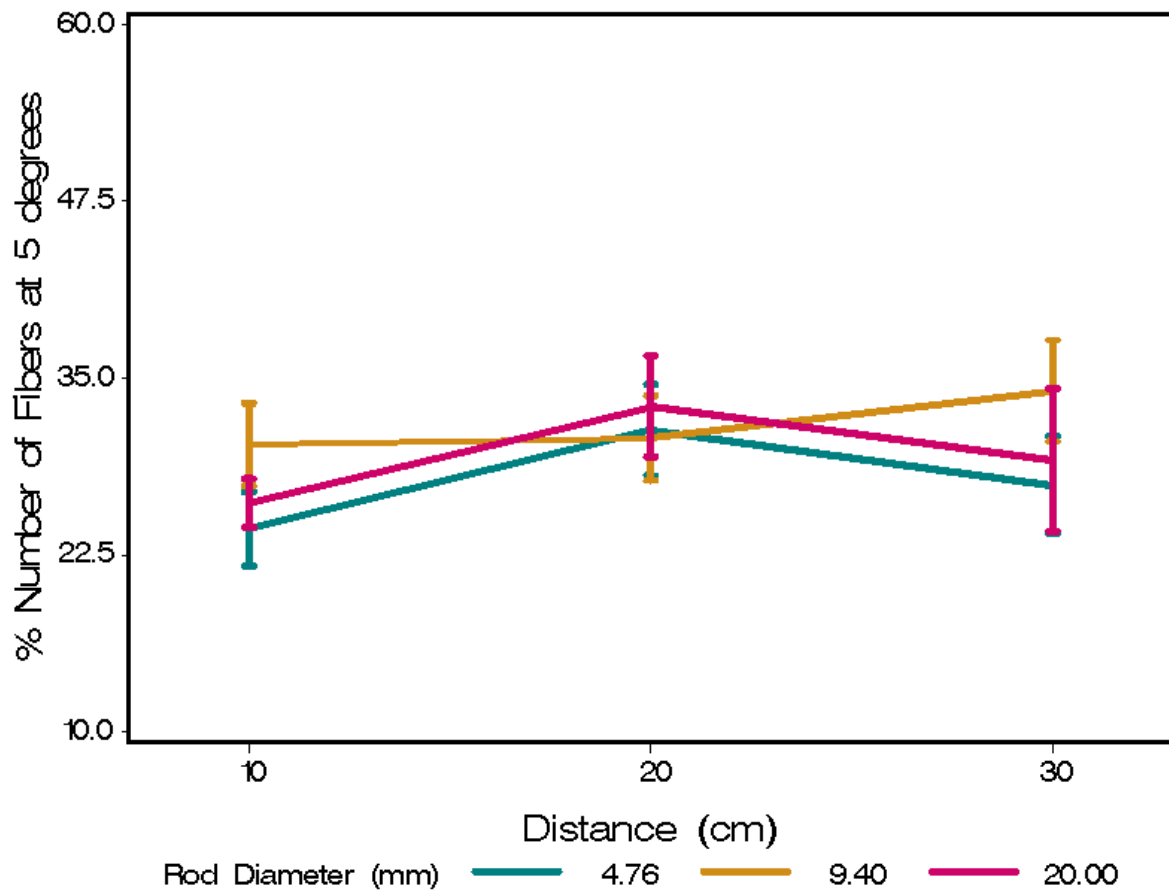


Figure 179: Percent number of fibers at 5° corresponding to the interaction of distance and rod diameter

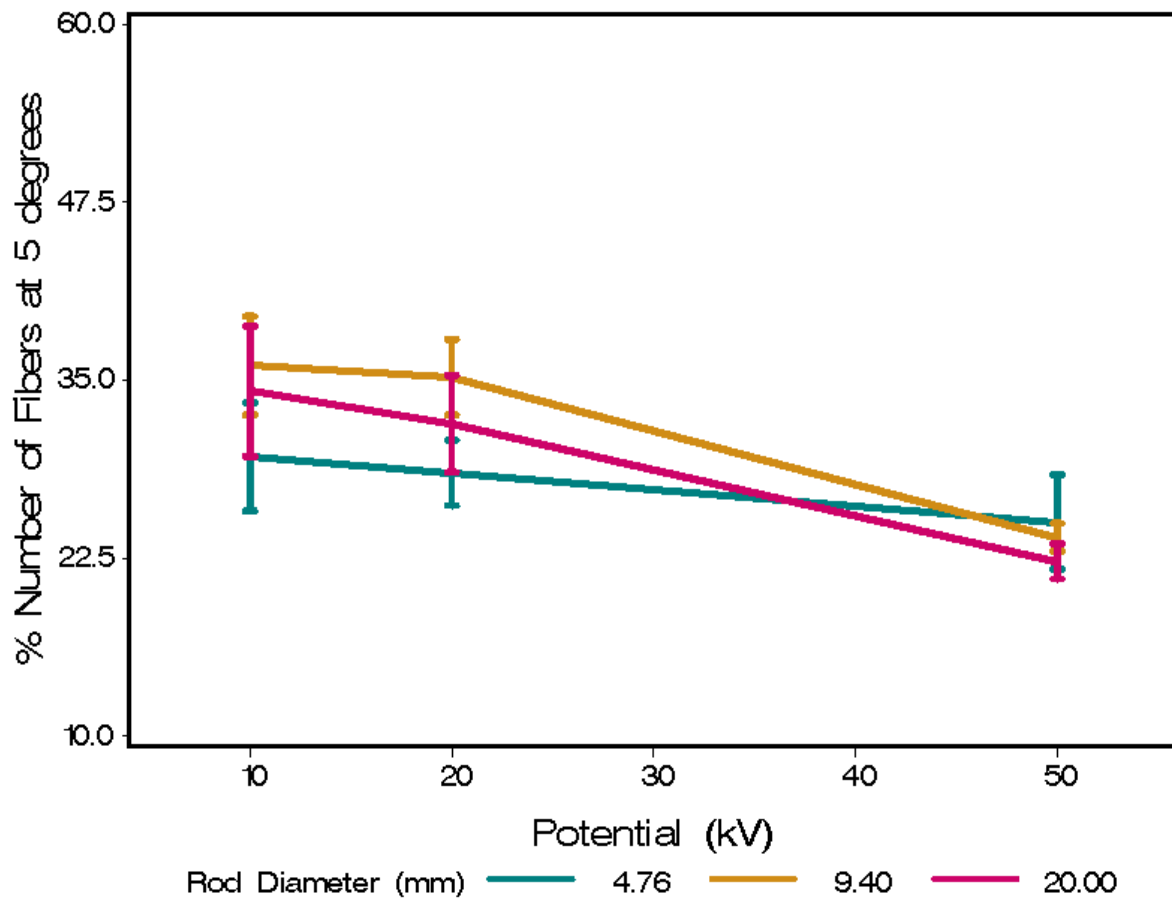


Figure 180: Percent number of fibers at 5° corresponding to the interaction of potential and rod diameter

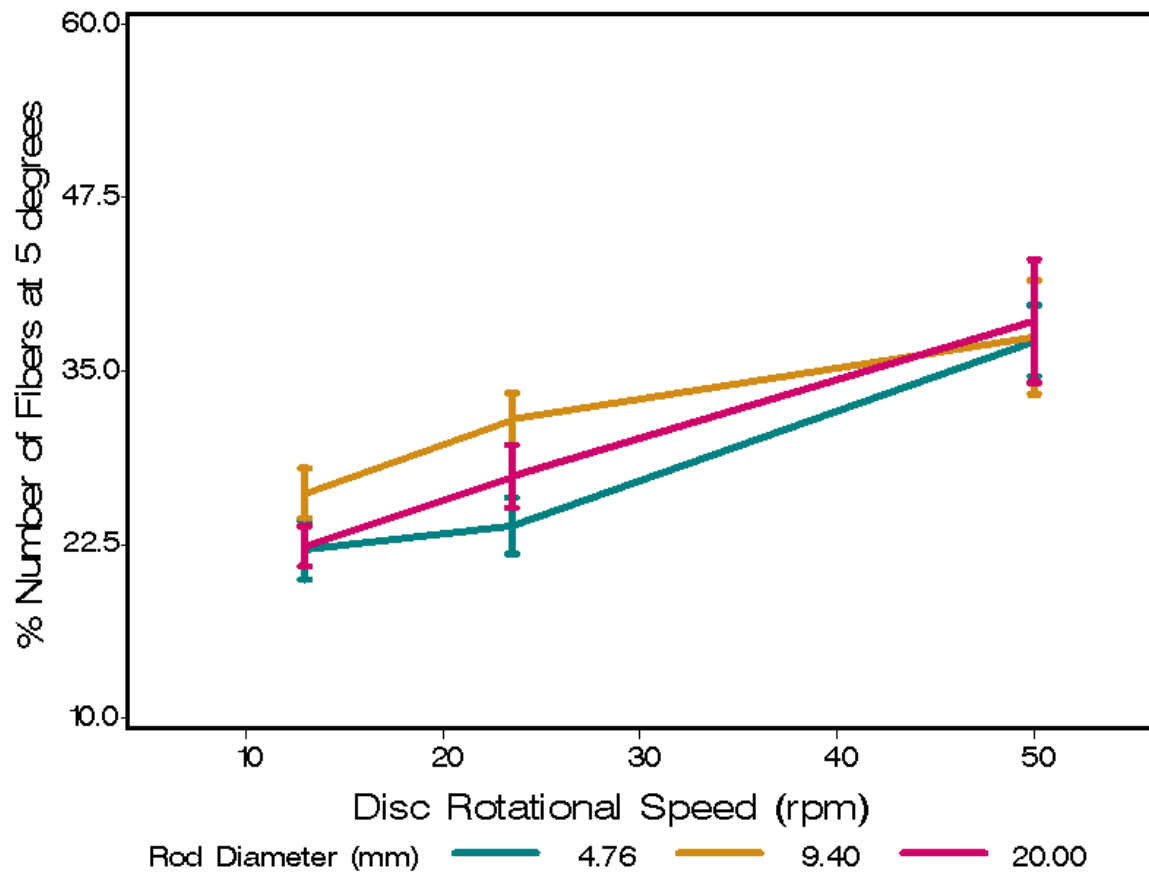


Figure 181: Percent number of fibers at 5° corresponding to the interaction of disc rotational speed and rod diameter